金属表面上の分子吸着と電荷移動
Design of Chemical Reactions at Interfaces

森川 良忠

Yoshitada Morikawa

Computational Physics Laboratory,
Department of Precision Engineering,
Grad. Sch. Engineering, Osaka University

http://www-cp.prec.eng.osaka-u.ac.jp/index_e.html
morikawa@prec.eng.osaka-u.ac.jp

大阪大学

3E-trilemma

- **Economy**
- **Energy**
- **Environment**

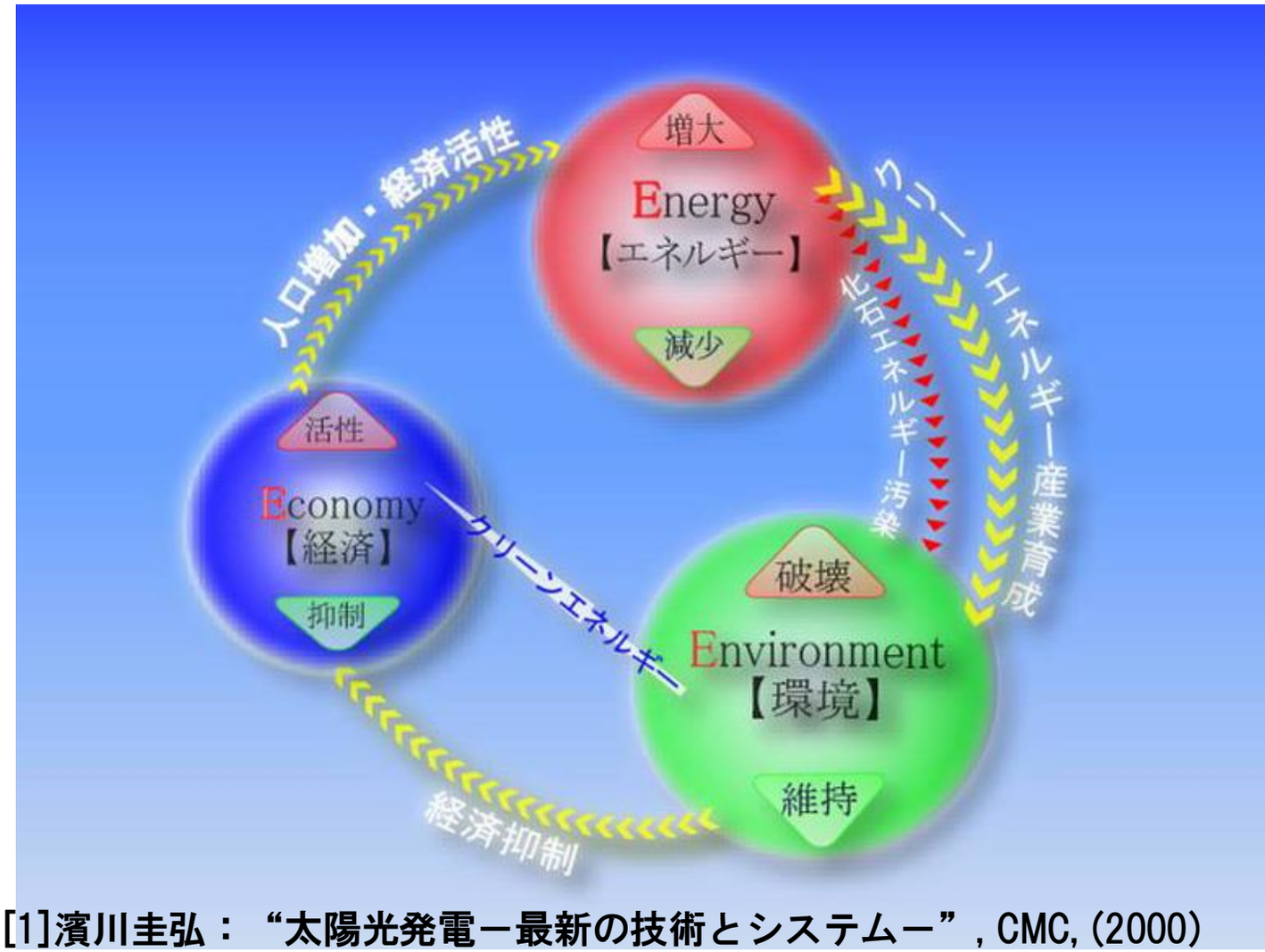

[1]濱川圭弘：“太陽光発電－最新の技術とシステム－”, CMC, (2000)

Solving the trilemma using Quantum Simulations.

Important roles of Interfaces

Nano-scale Interface Determines the performances of Devices

Organic Devices

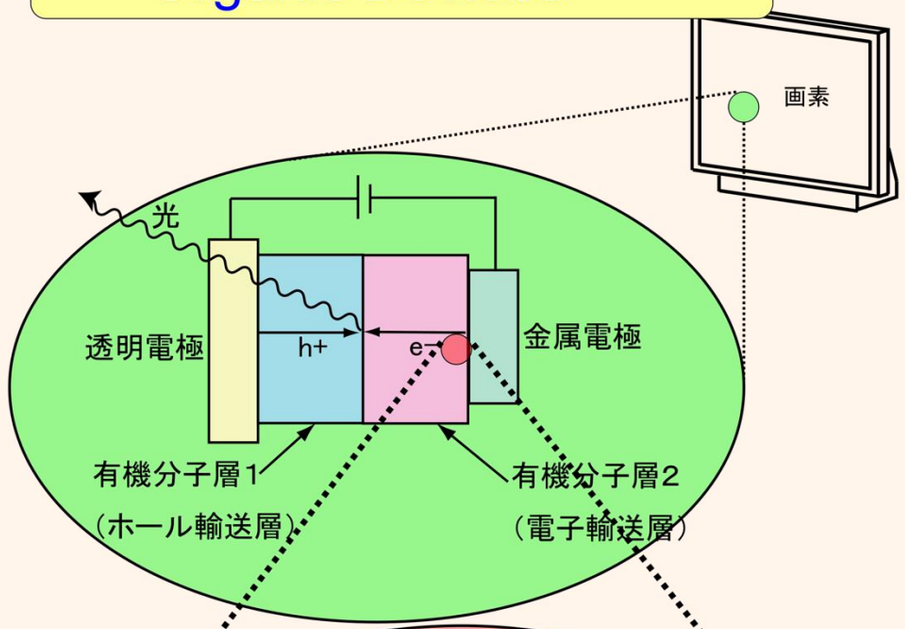

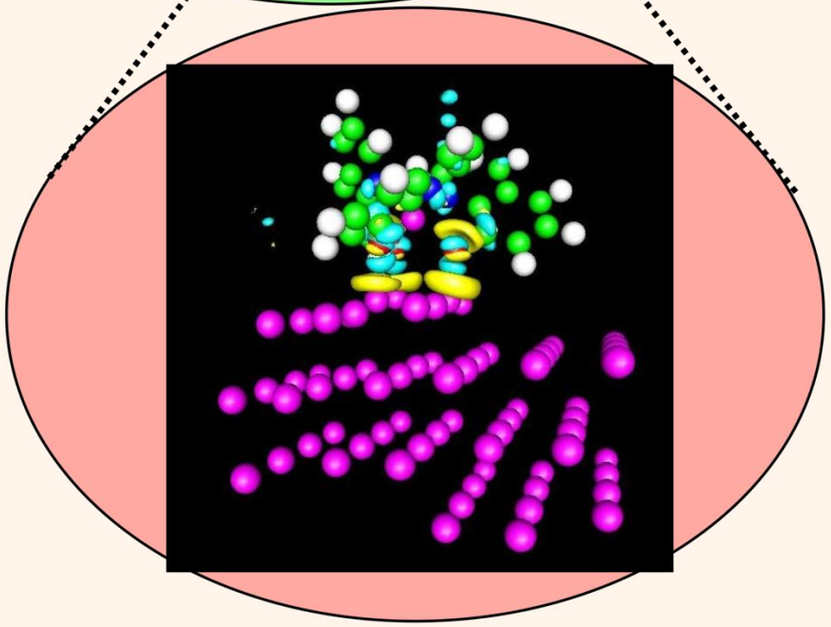

Fuel Cells

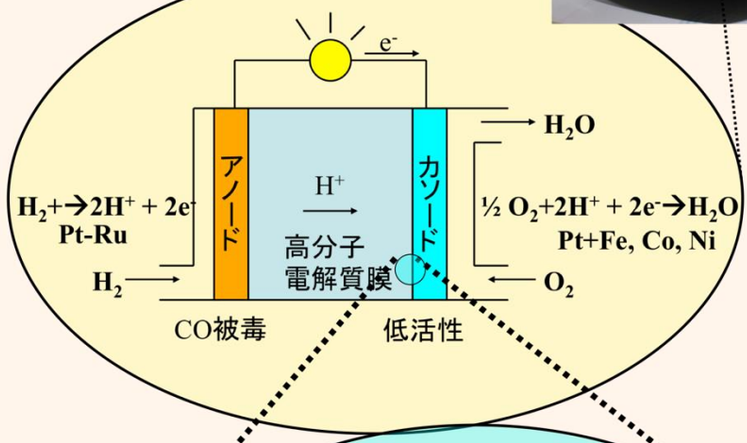

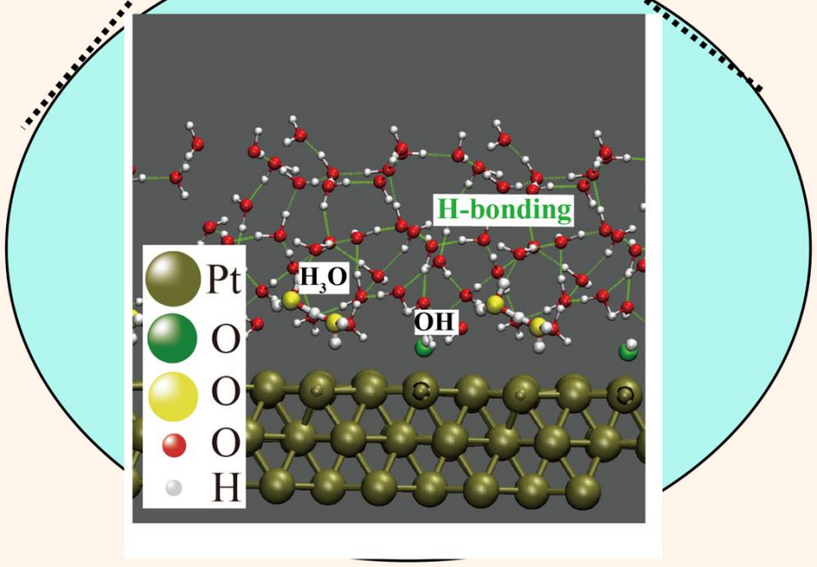

Quantum Simulations can clarify important factors determining the efficiency of reactions

Organic/Metal Interfaces

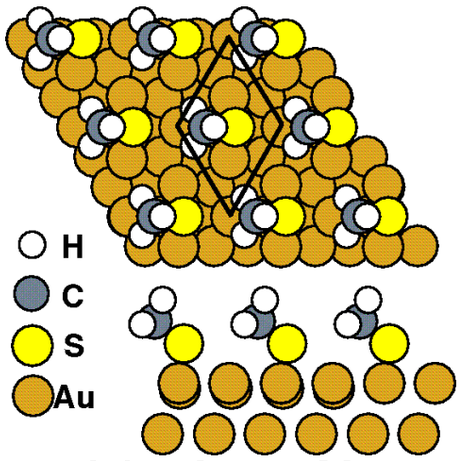

(a)Bridge Site
Most Stable

Thiol/Au surface
T. Hayashi *et al.*,
J. Chem. Phys.(2001)

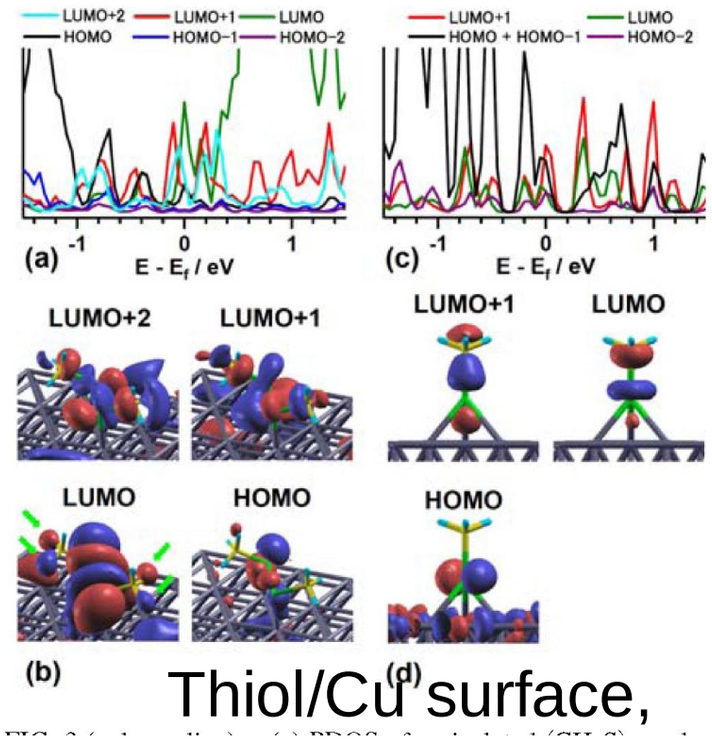

Thiol/Cu surface,
M. Ohara *et al.*,
Phys. Rev. Lett. (2008).

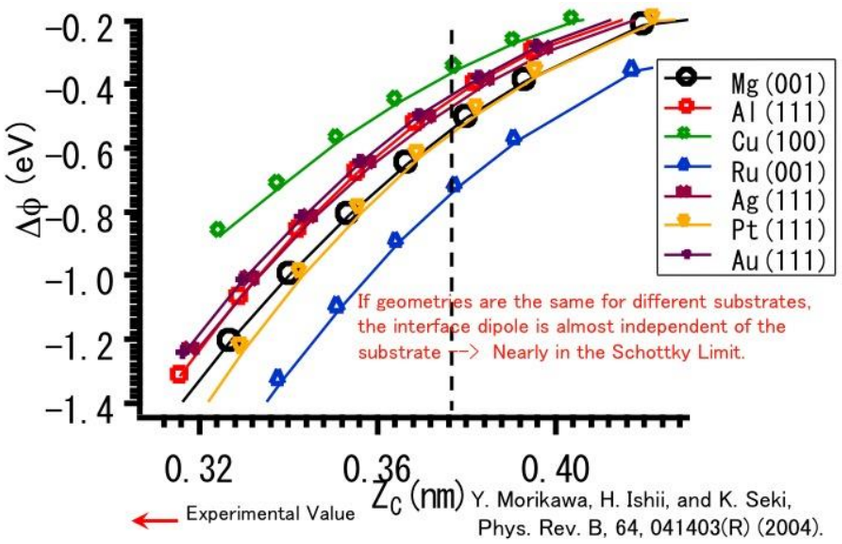

n-alkane/metal Y. Morikawa *et al.*,
Phys. Rev. B (2004)

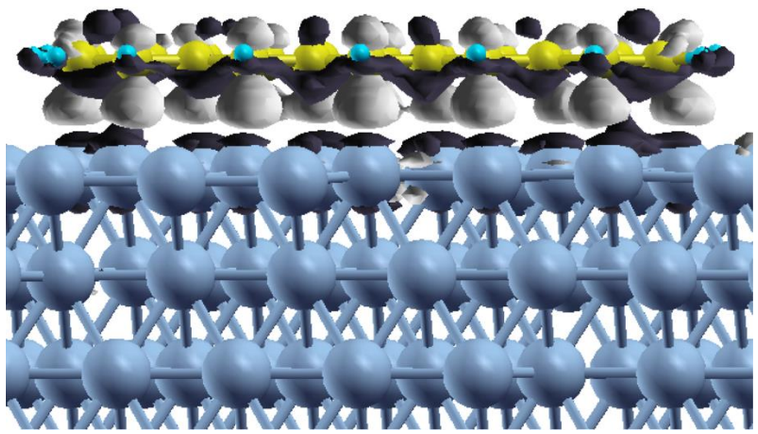

Pentacene/Metals, K. Toyoda *et al.*,
PRB (2007), ***JCP*** (2010), ***JPCC***, (2011).

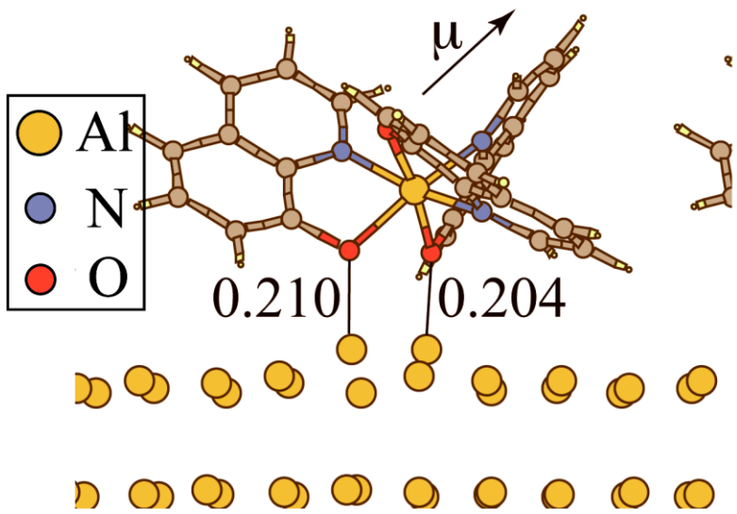

Alq_3/Metals, S. Yanagisawa *et al.*,
JCP (2008) ***PRB*** (2011).

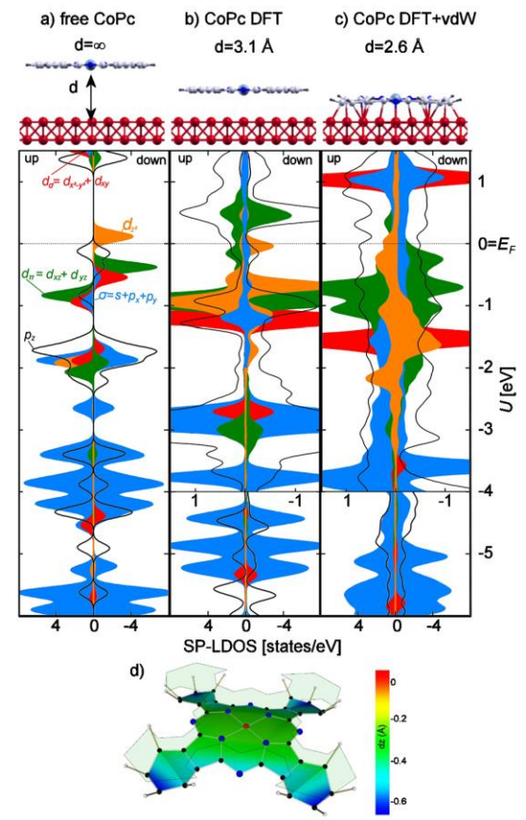

CoPc/Cu surface, J. Brede *et al*.,
Phys. Rev. Lett., (2010).

Heterogeneous Catalyst & Surface Reactions

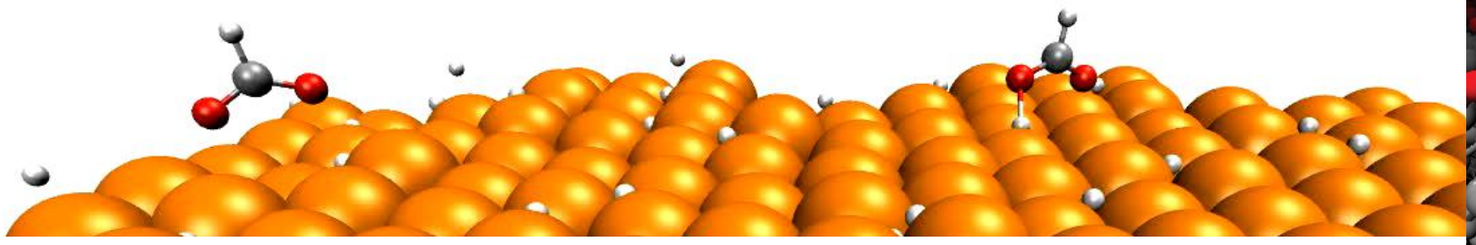

CO_2 hydrogenation on Cu surfaces
Fahdzi Muttaqien, *et al.*, ***J. Chem. Phys.*** (2014),
J. Chem. Phys. (2017) , ***Chem. Comm***. (2017),
Nature Chem. (2019).

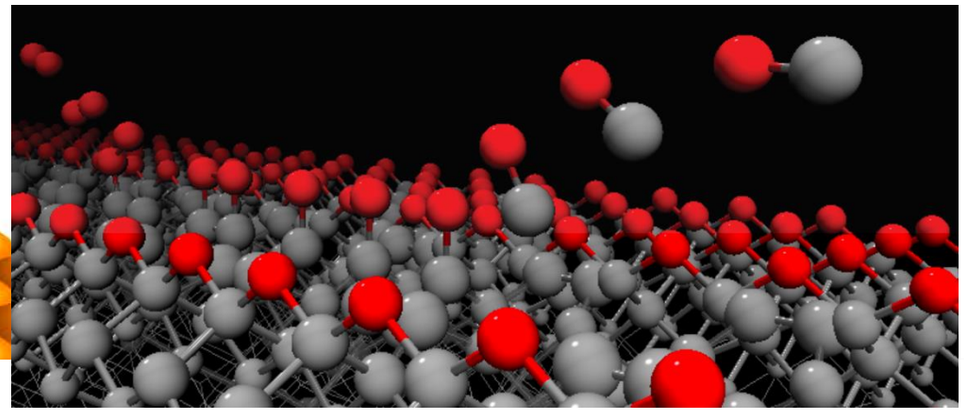

Oxidation of Diamond (100)
J.I. Erinquez *et al.*, ***Carbon*** (2021).

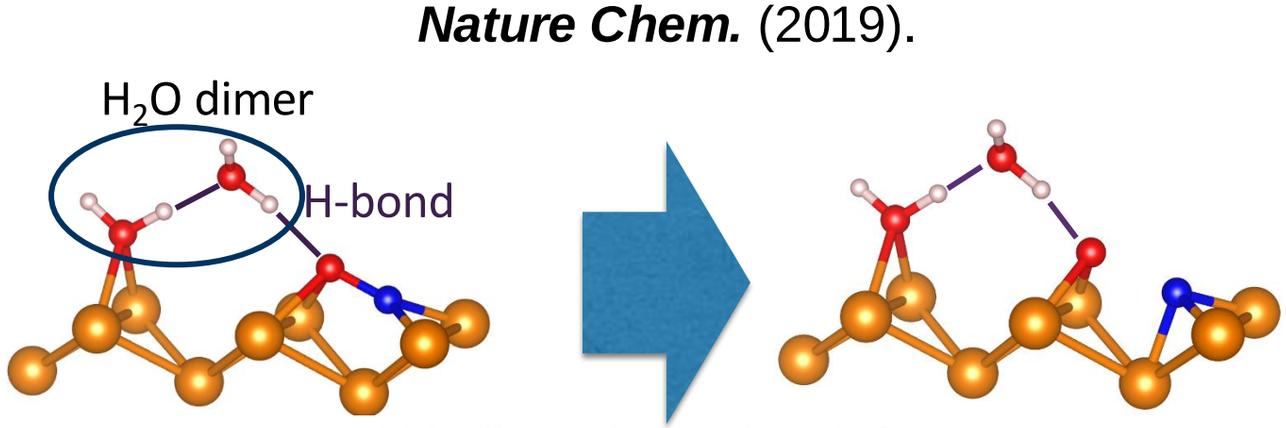

NO dissociation by H_2O
Thanh Ngoc Pham *et al.*,***JPhysChemC.***(2018).

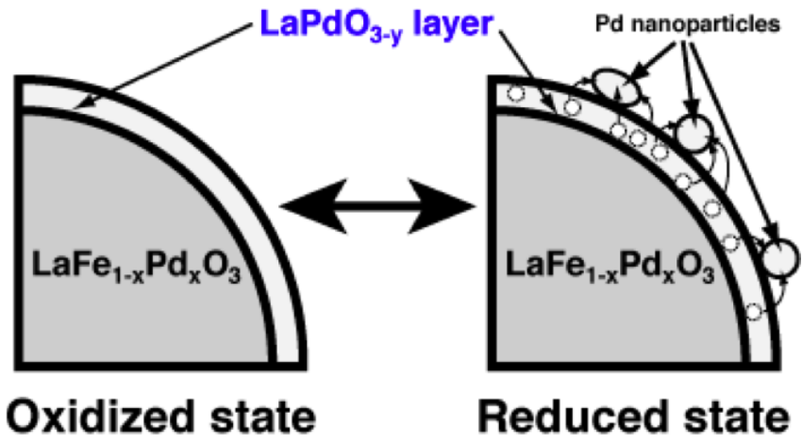

Suppression of Pd Sintering
I. Hamada *et al.*, ***J. Am. Chem. Soc.,*** (2011).

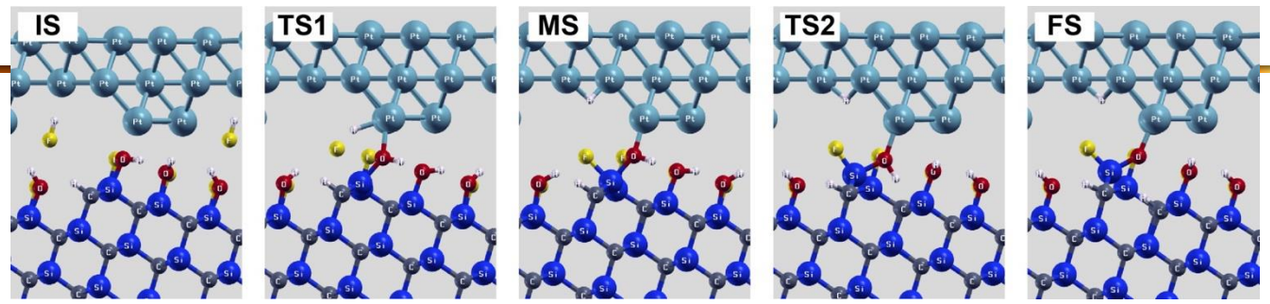

Etching of SiC by Pt catalyst
Bui Van Pho *et al.*,***Appl. Phys. Lett.***, (2015)
J.J.Appl.Phys (2018).

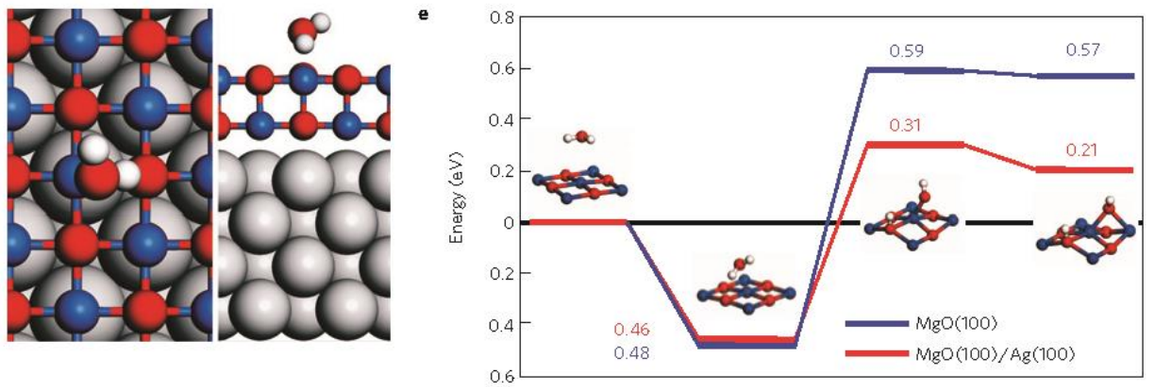

H_2O dissociation on MgO/Ag,
H.-J. Shin et al., ***Nature Materials*** (2010).

Chemical Reactions at Water/Solid Interfaces

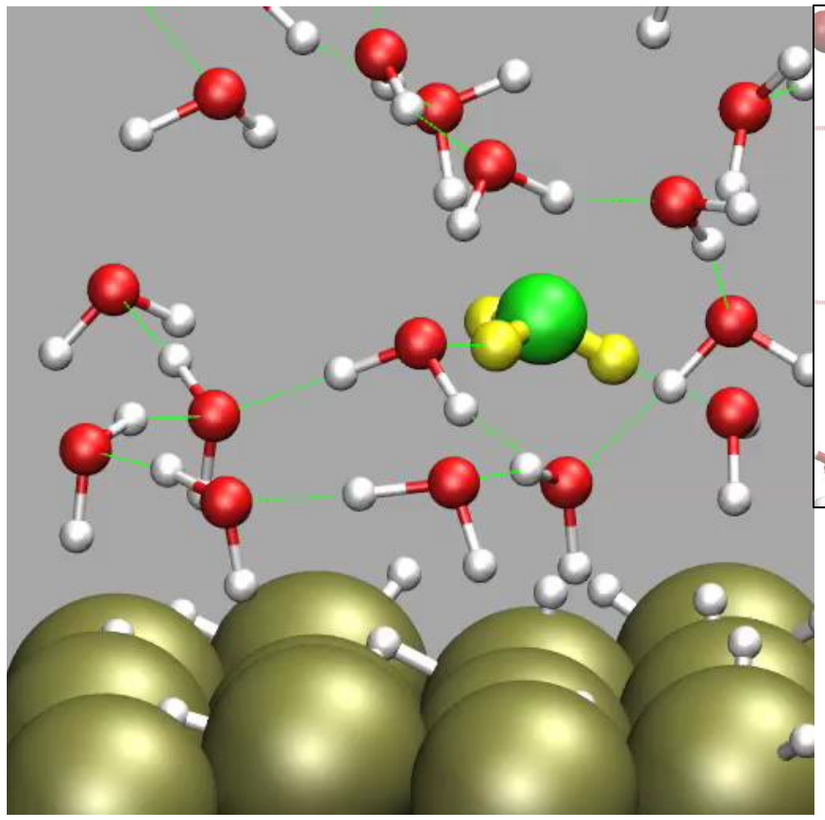

Hydrogen Evolution Reaction
M. Otani *et al*., ***J. Phys. Soc. Jpn*** (2008).
PCCP (2008), ***JPCC*** (2008).

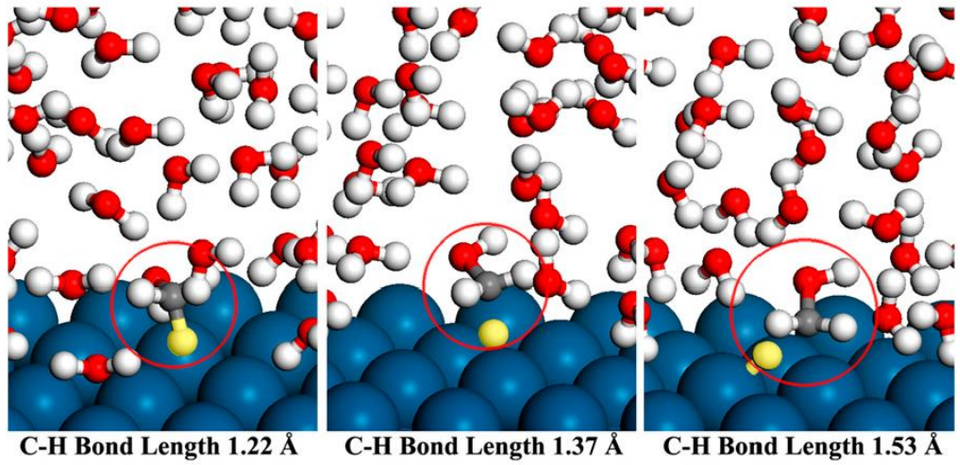

Methanol Oxidation on Pt Electrode
J. Herron *et al.*, ***PNAS USA*** (2016).

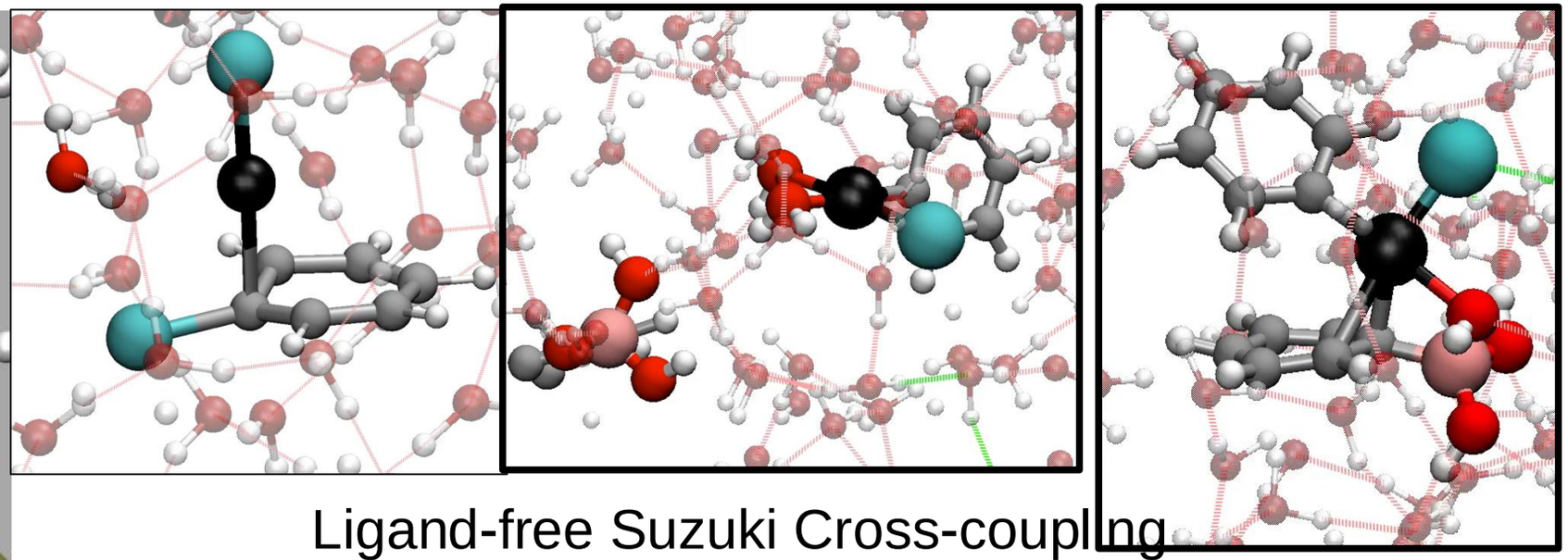

Ligand-free Suzuki Cross-coupling
T. Hirakawa et al., ***J. Chem. Phys. B*** (2017)
T. Hirakawa et al., ***J. Chem. Phys. C*** (2017)

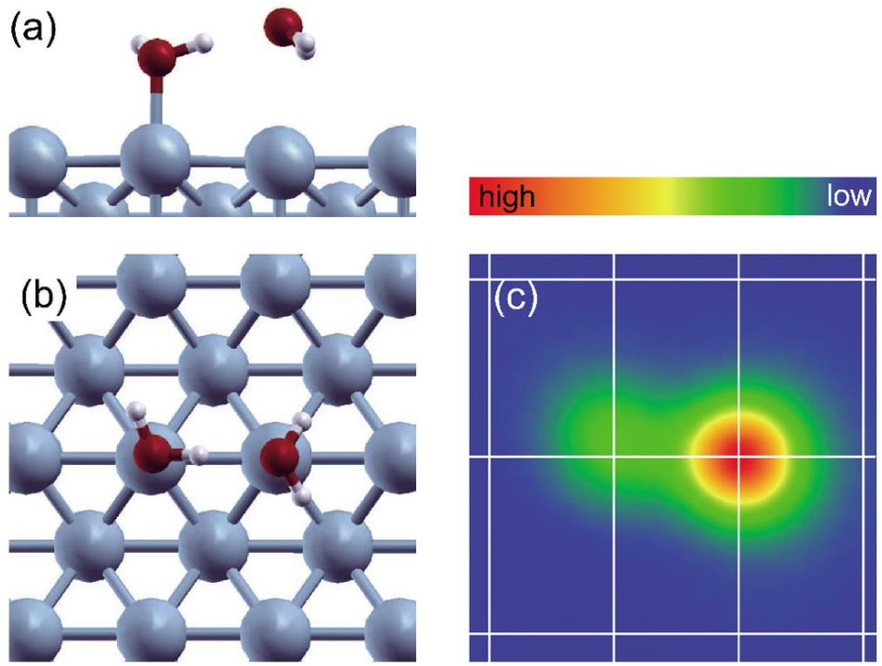

Water Dimer / Cu(110)
T. Kumagai *et al.*,
Phys. Rev. Lett., (2008),
Phys. Rev. B (2009).

Catalysis

- A catalyst accelerates chemical reactions by reducing the activation barriers but does not itself change before or after the chemical reactions.

A + B → AB

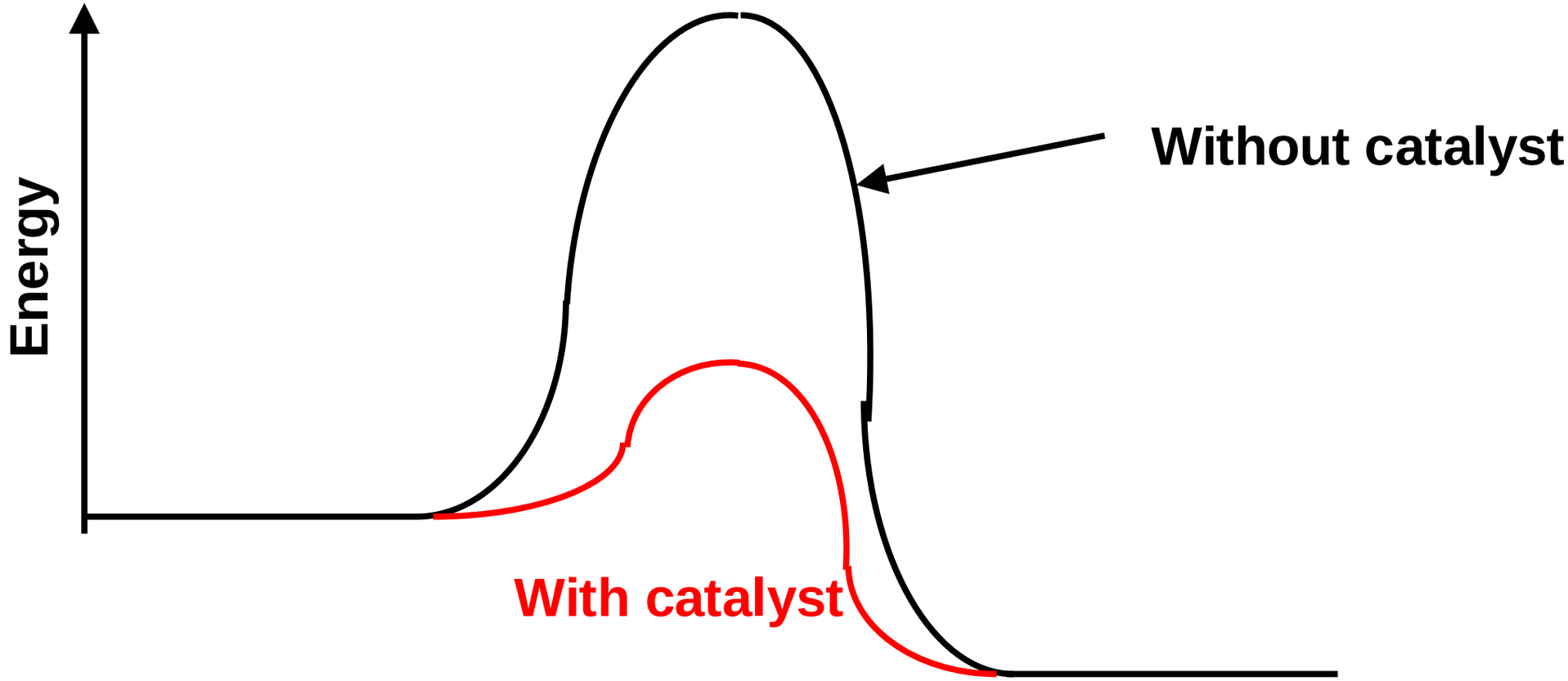

Ammonia synthesis

Fritz Haber
The Nobel Prize in Chemistry 1918

Carl Bosch
The Nobel Prize in Chemistry 1931

- Haber–Bosch process

$$N_2 + 3H_2 \Leftrightarrow NH_3 + 46.1\ kJ/mol$$

- Iron promoted with K_2O and Al_2O_3（Fe_3O_4・Al_2O_3・K_2O）
- First manufactured using the Haber process at an industrial scale in 1913 in Germany
- → 80% Fertilizer, plastics, fibers, explosives

Suzuki-Miyaura cross coupling

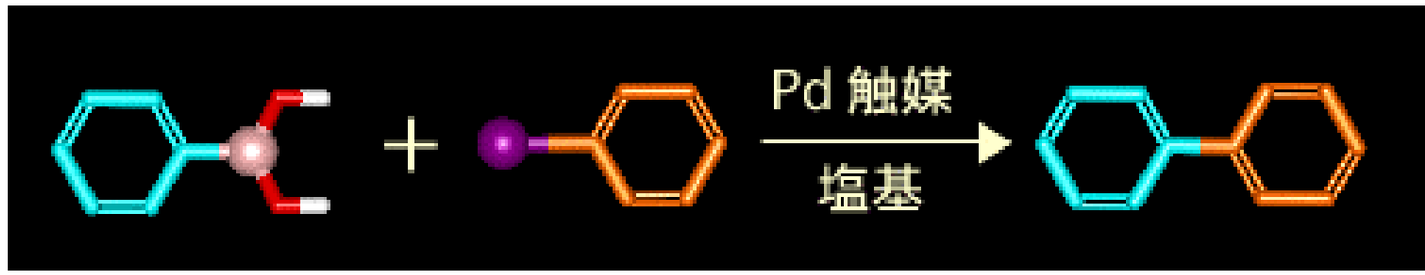

Phenylboronic acid + Bromobenzene→Biphenyl

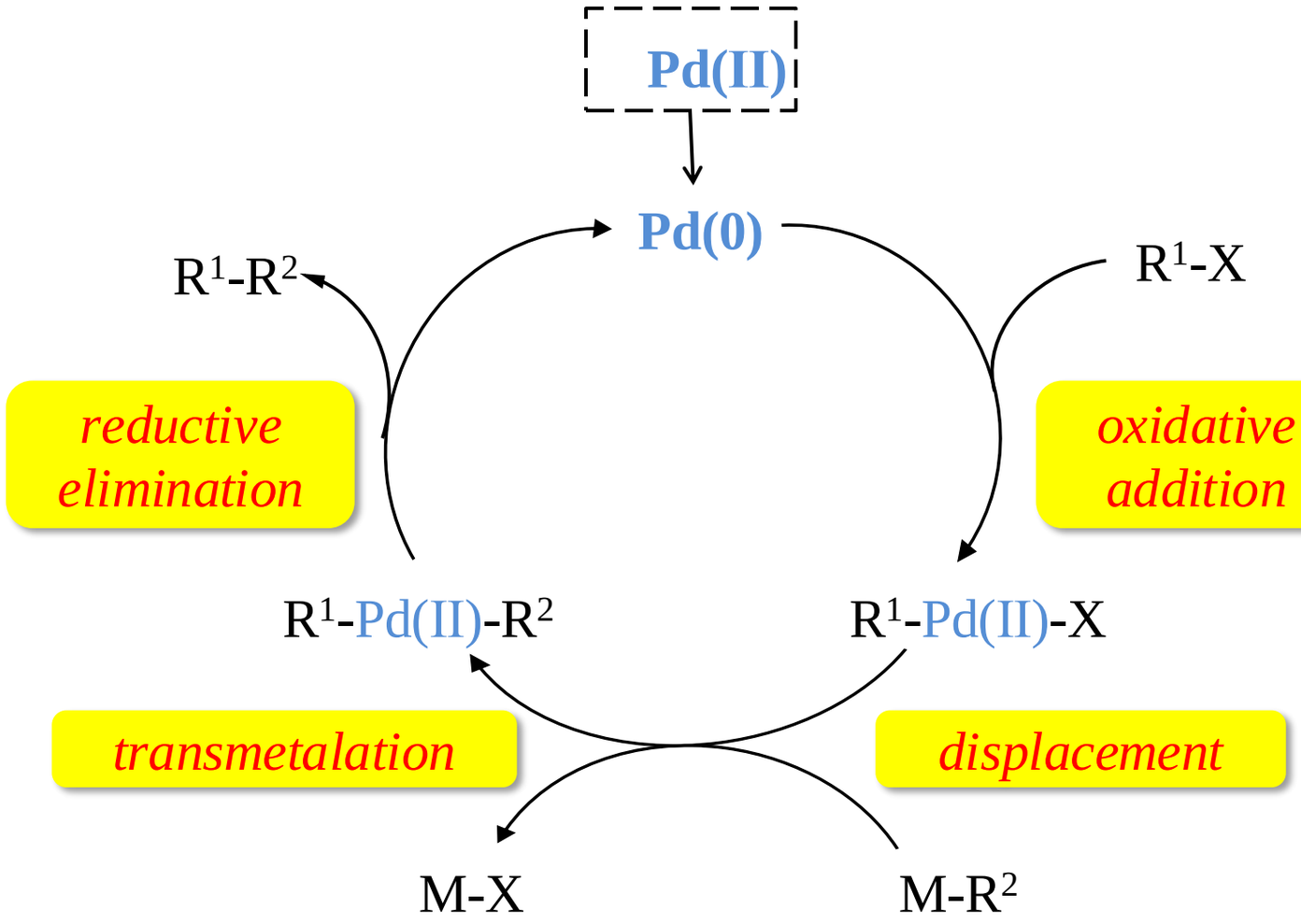

- Important in synthesizing molecules for liquid crystal display, organic electro-luminescent devices, and drugs.

R^1,R^2 = 芳香族化合物
X = ハロゲン

Three-way catalyst for Automobil Exhaust Gas

- Convert the following three emission gases.

$$CO + O_2 \rightarrow CO_2$$

$$NO + CO \rightarrow CO_2 + N_2$$

$$HC + O_2 \rightarrow CO_2 + H_2O$$

- 三元触媒（Three-Way Catalyst）
- Pt･Rh(10:1)，　Pt･Pd･Rh，　Pd･Rh，　Pd etc.
- Rhは資源的に厳しい。
- Pt: South Africa 74%, Russia 14%
- Pd: South Africa 25%, Russia 70%
- Rh: South Africa 67%, Russia 17%

Fuel Cell

Polymer Electrolyte Membrane Fuel Cell

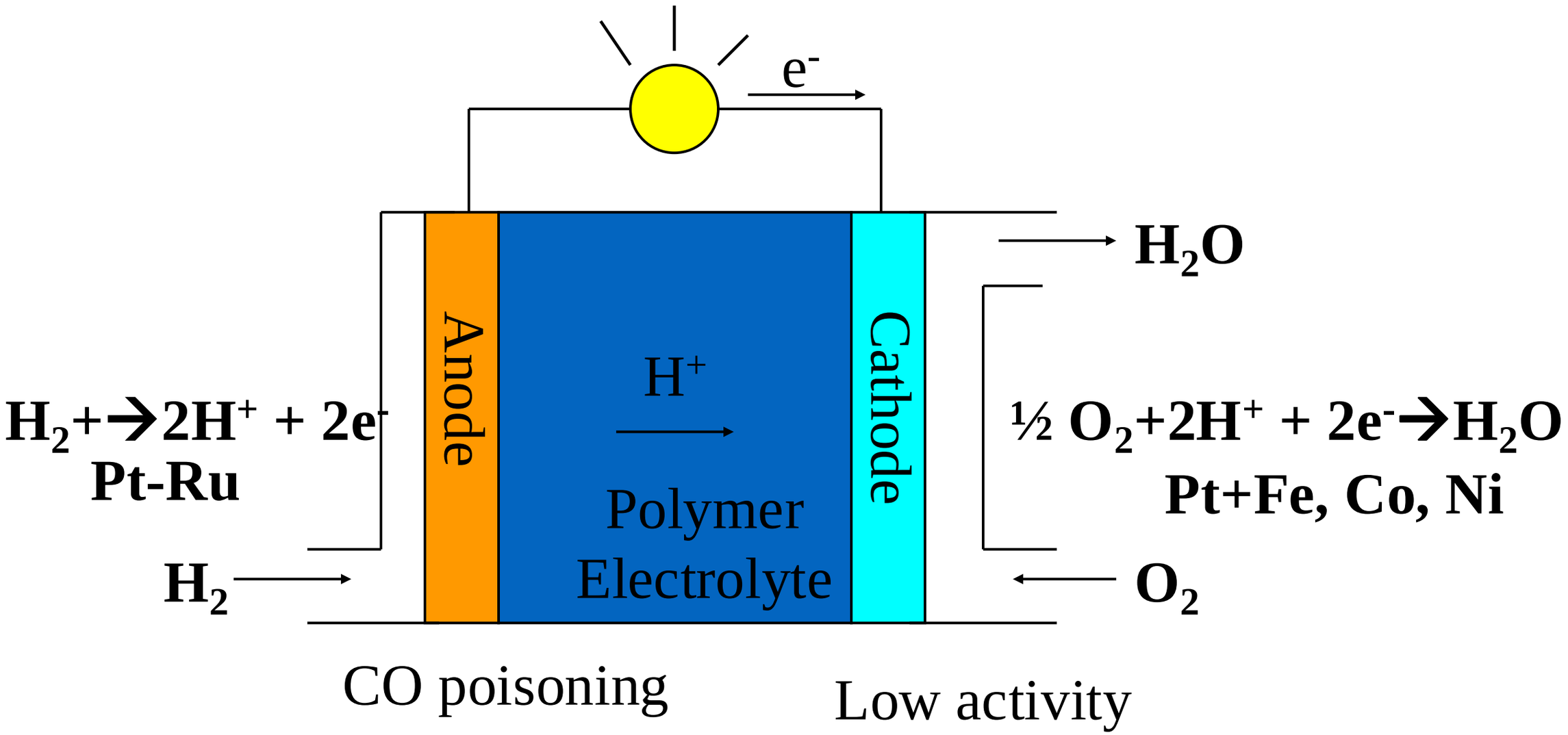

反応の触媒金属依存性

Catalysis

- Catalysts are important in not only industries but also in energy problems and environmental problems.

→ It is necessary to design catalysts with abundant elements.

→ By elucidating reaction mechanisms, it will be possible to design new catalysts theoretically.

It is possible to clarify mechanisms of chemical reactions from first-principles simulations.

MD simulation of electrode/water interface

- Total MD simulation time: 3.2 ps
- Added electrons: 0.25–0.40
- 353 K

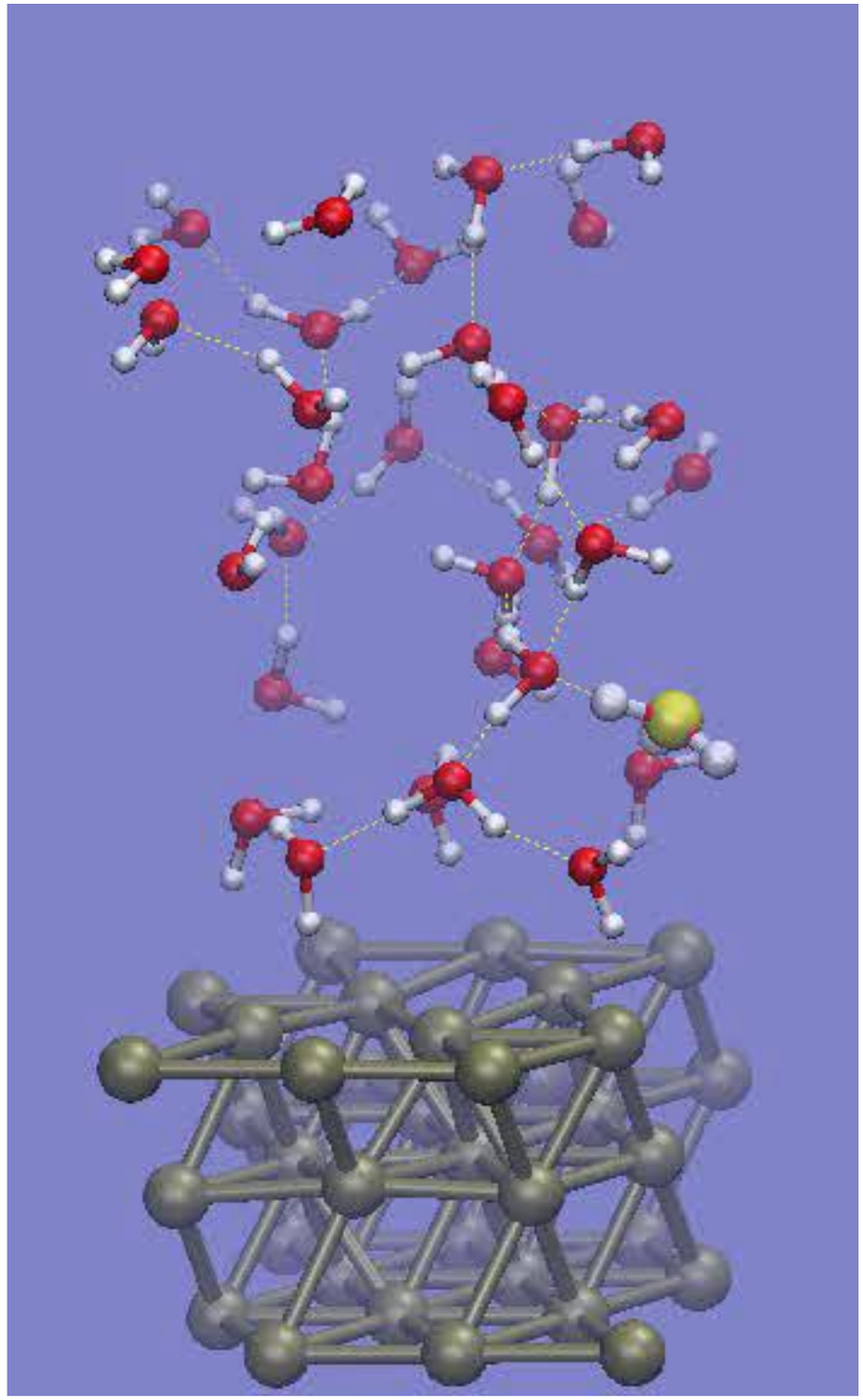

Time Scale 10^{-12} s.→1s.

Spacial Scale 10^{-9}m → 10^{-1}m

Super High-Resolution Microscopy

分子吸着エネルギー：基板金属依存性

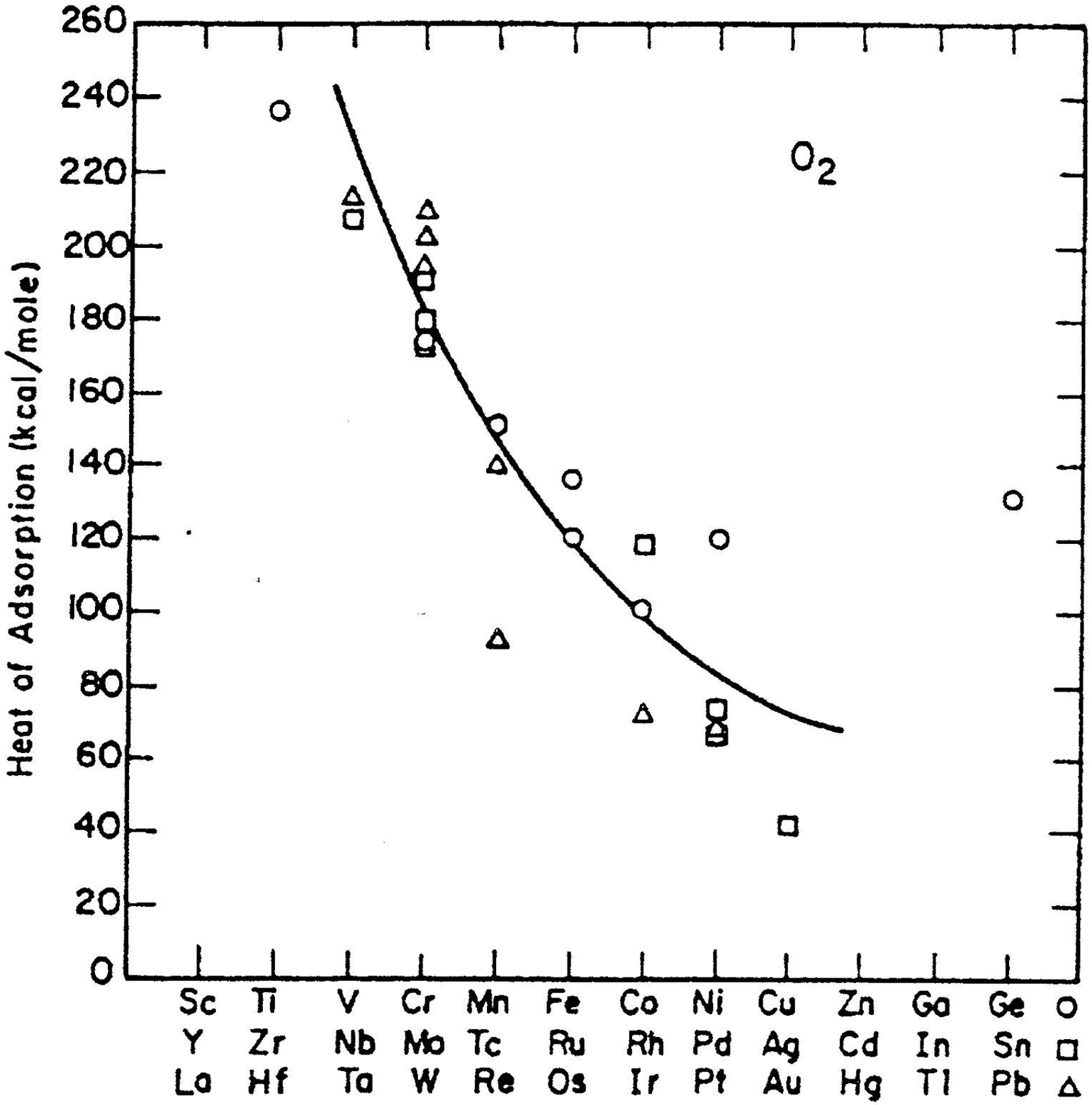

I. Toyoshima and G.A. Somorjai, Catal. Rev. Sci. Eng. **19**, 105 (1979).

CO分子吸着エネルギー：基板金属依存性

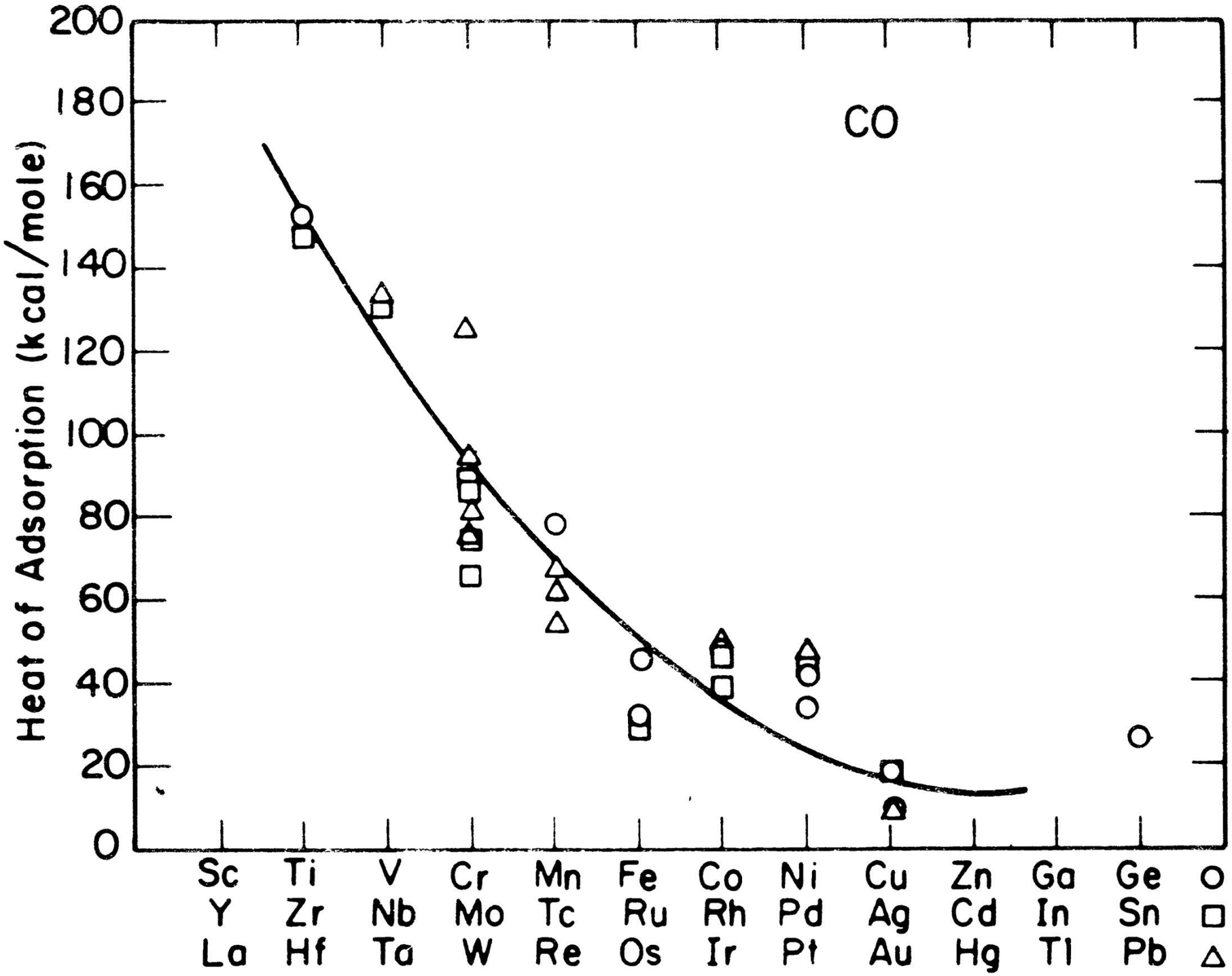

CO分子吸着状態：基板金属依存性

CO

IIIB	IVB	VB	VIB	VIIB	VIII	VIII	VIII	IB
Sc	Ti D	V	Cr	Mn	Fe D	Co	Ni M	Cu
Y	Zr	Nb	Mo D	Tc	Ru M	Rh	Pd M	Ag
La	Hf	Ta	W D,M	Re	Os	Ir M	Pt M	Au

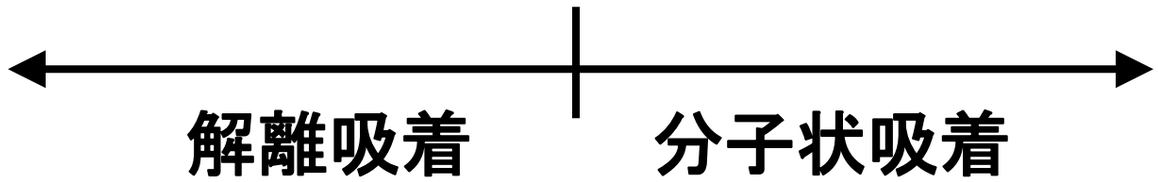

G. Borden, T.N. Rhodin, C. Brukner, R. Benbow, and Z. Hurysh, Surf. Sci. **59**, 593 (1976).

触媒活性:基板金属依存性

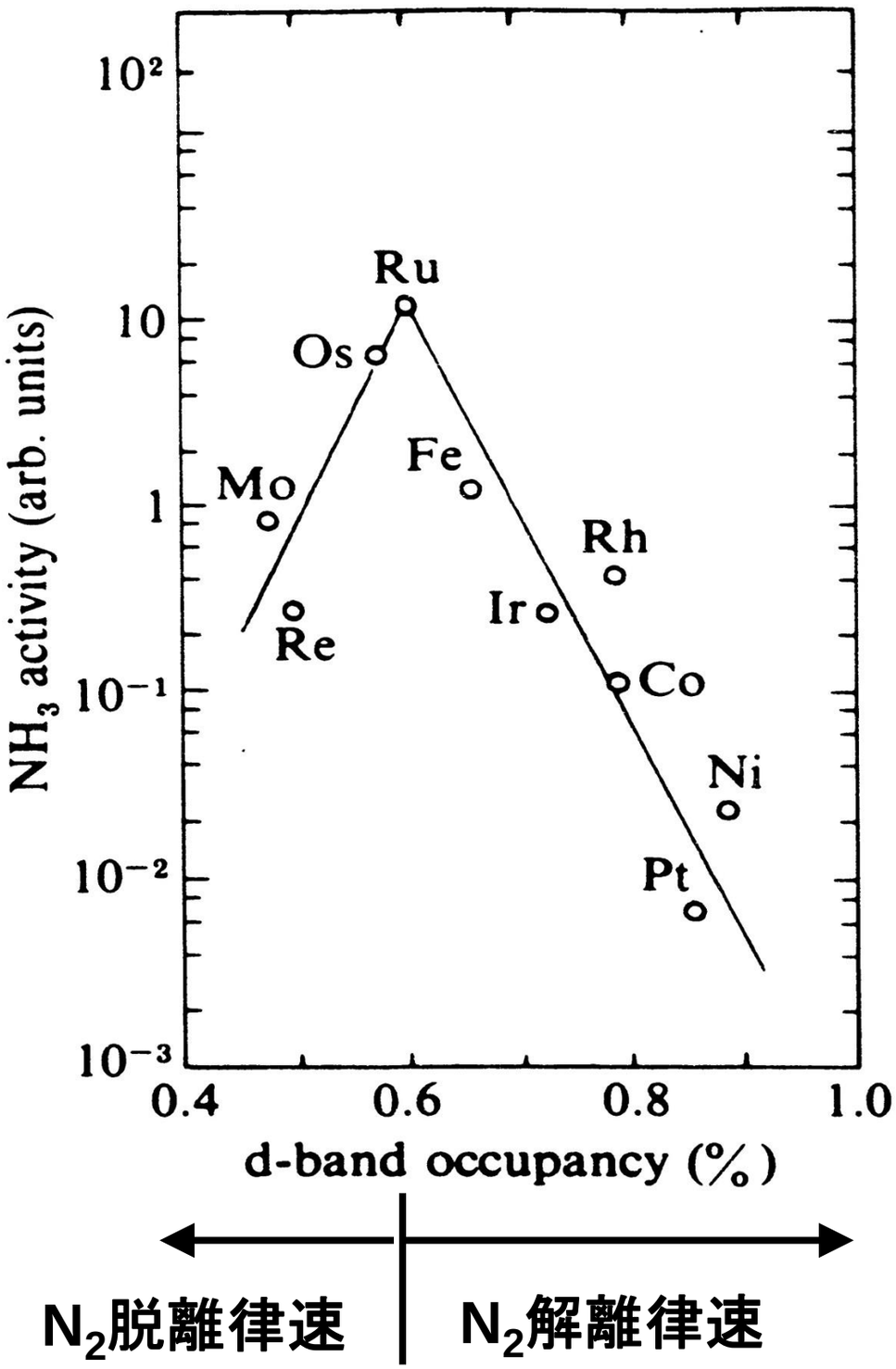

$$N_2 + 3H_2 \rightarrow 2NH_3$$

$$N_2 + 2^* \rightarrow 2N_{(a)}$$

$$H_2 + 2^* \rightarrow 2H_{(a)}$$

$$N_{(a)} + 3H_{(a)} \rightarrow NH_{3(a)}$$

$$NH_{3(a)} \rightarrow NH_3\uparrow$$

Ni(001)

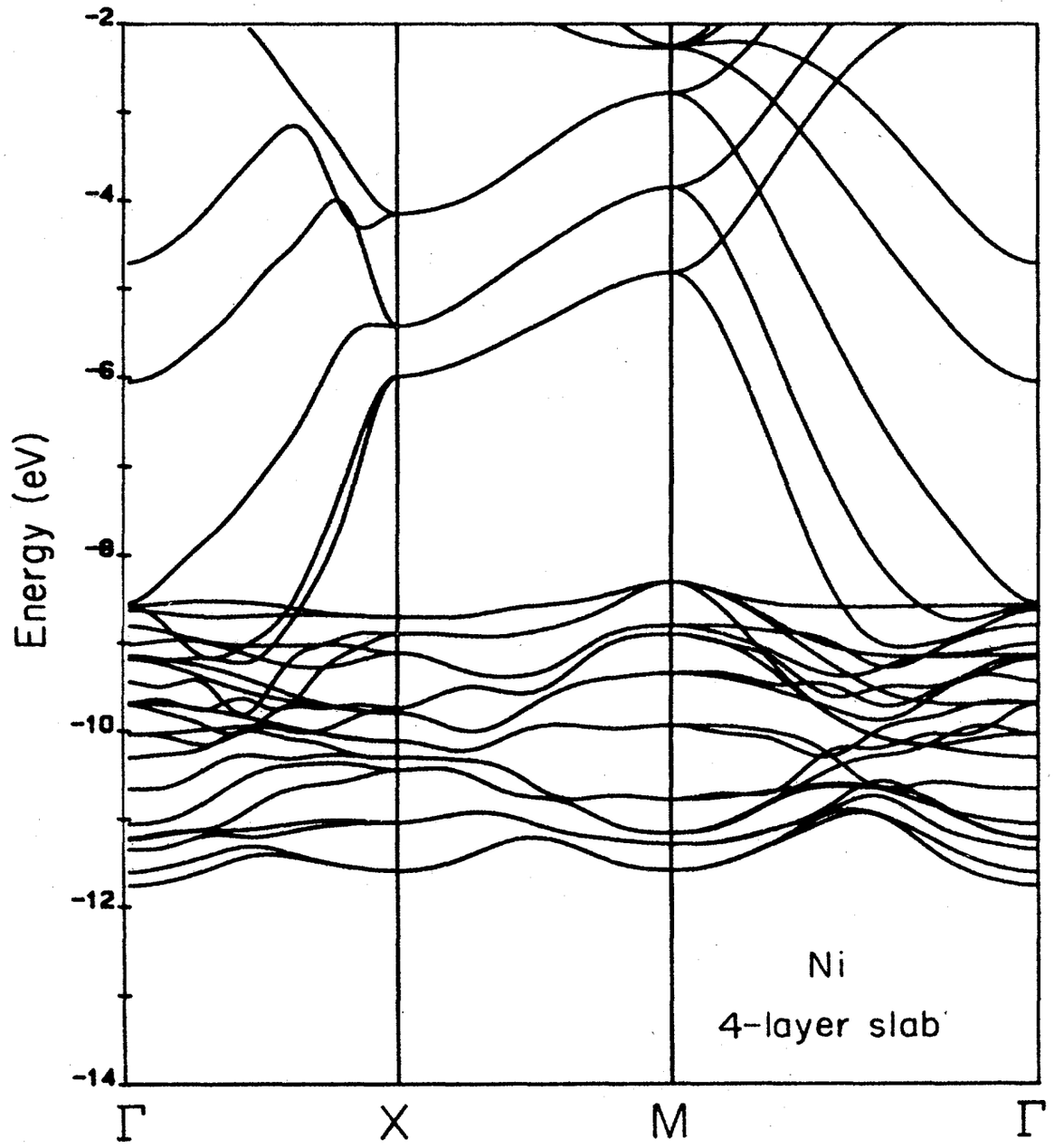

FIG. 2. The band structure of a four-layer Ni slab that serves as a model for a Ni(100) surface. The flat bands are derived from Ni 3*d*, the more highly dispersed ones above these are 4*s*,4*p*.

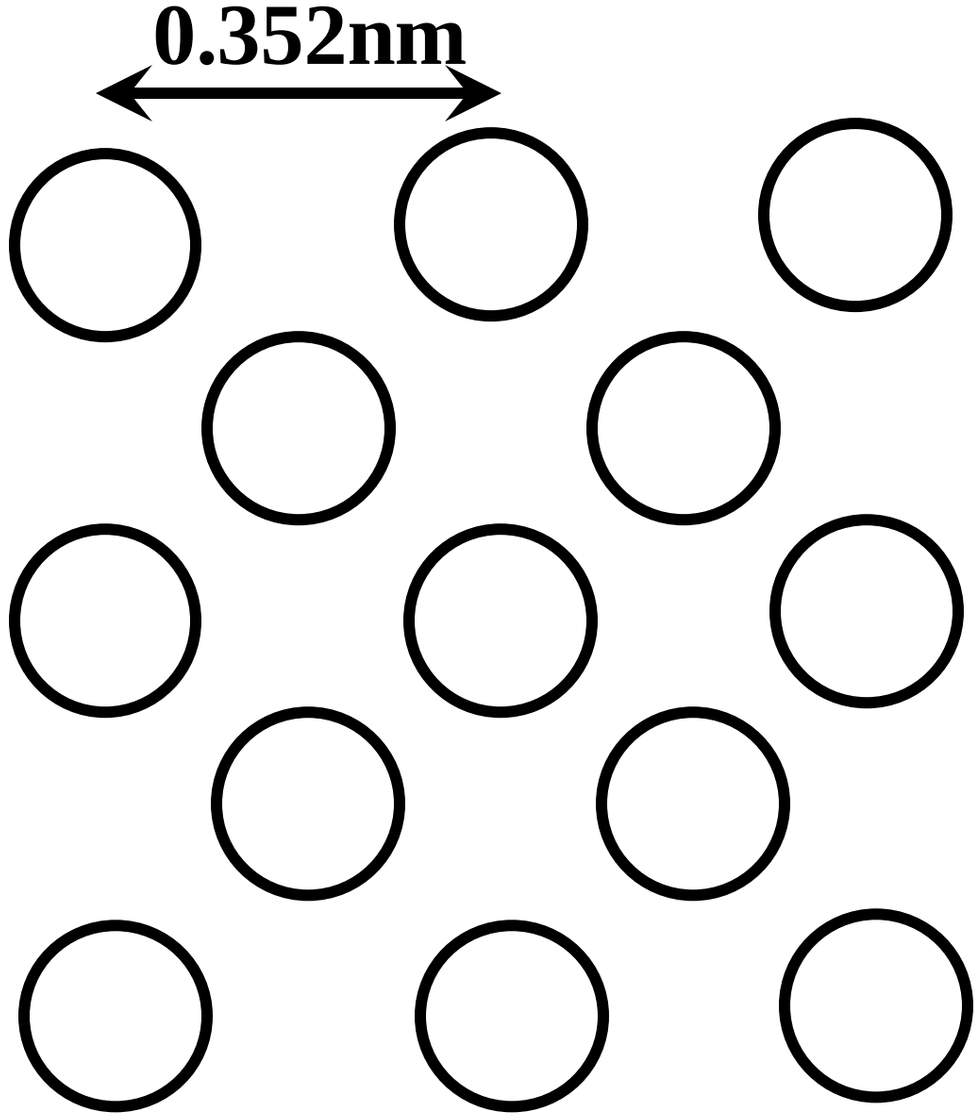

- Ni(001) fcc
- A=0.352 nm

CO、N_2分子軌道

	N_2		CO	
2π ($1\pi_g$)	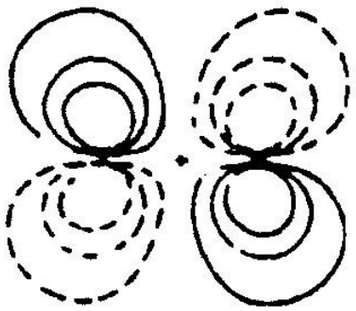	2π	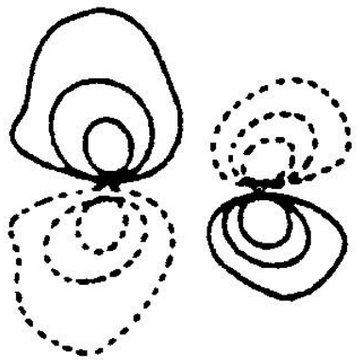	LUMO
5σ ($3\sigma_g$)	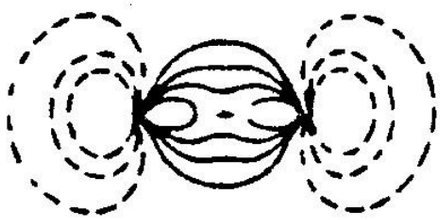	5σ	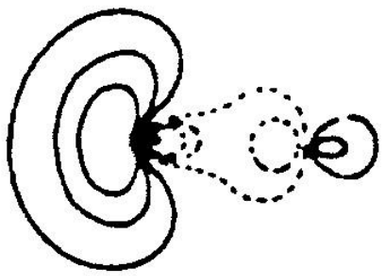	HOMO
1π ($1\pi_u$)	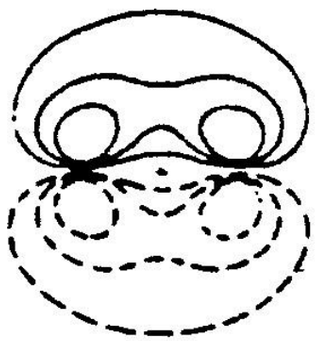	1π	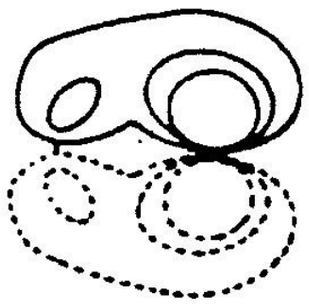	
4σ ($2\sigma_u$)	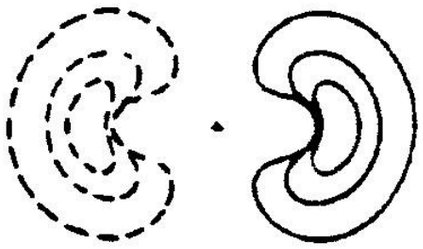	4σ	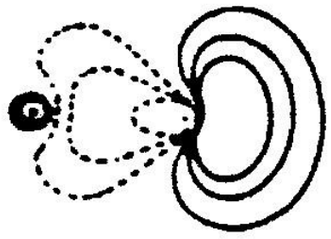	

CO monolayer

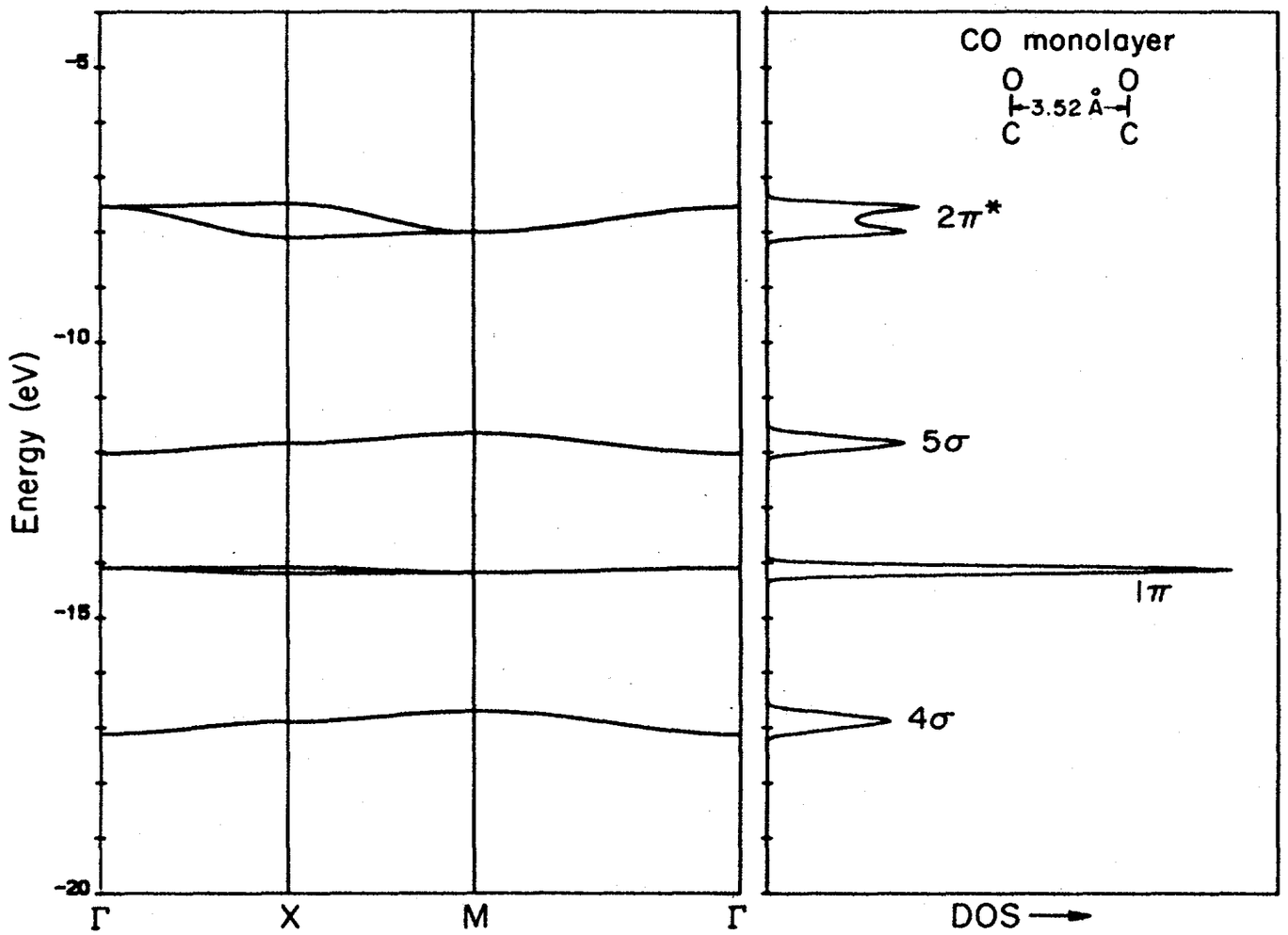

FIG. 3. The density of states (right) corresponding to the band structure (left) of a square monolayer of CO's, 3.52 Å apart.

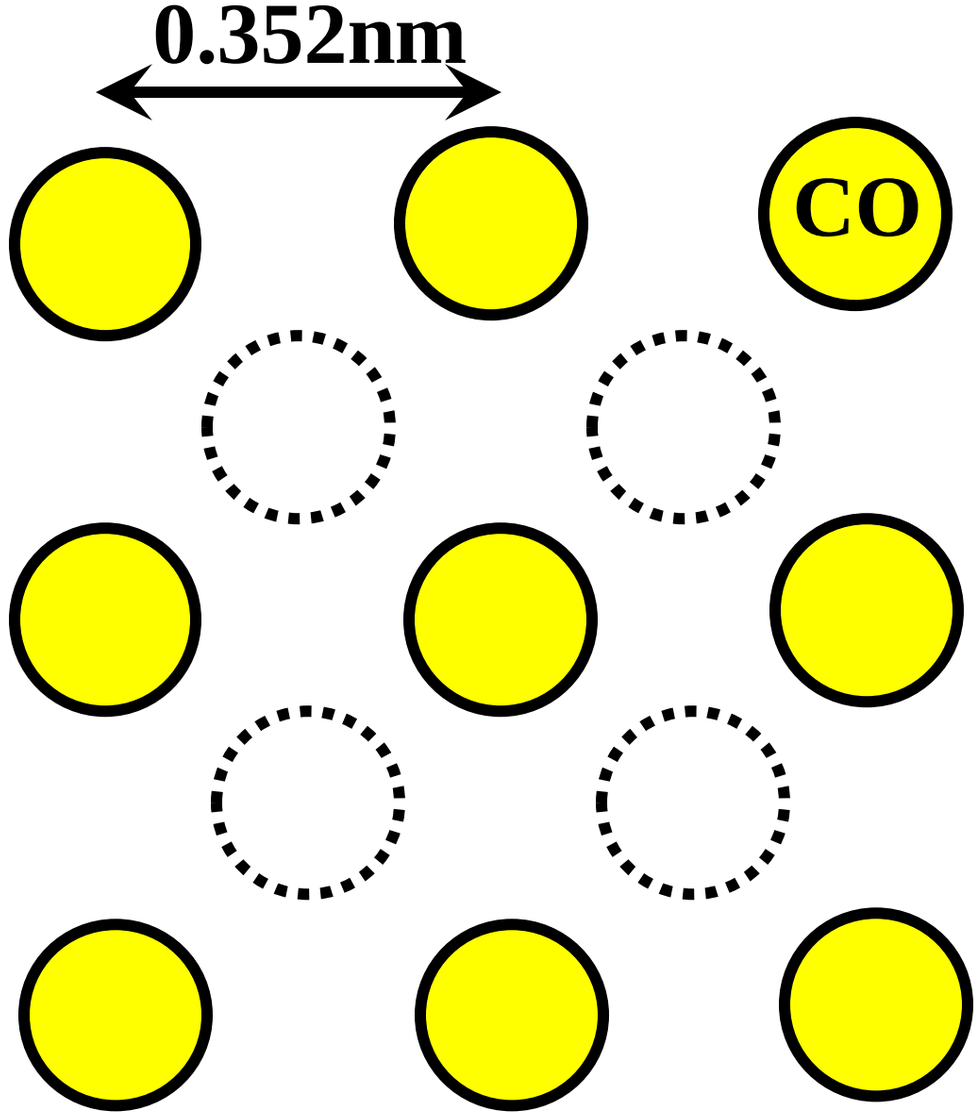

- CO
- A=0.352 nm

CO/Ni(001) c(2x2)

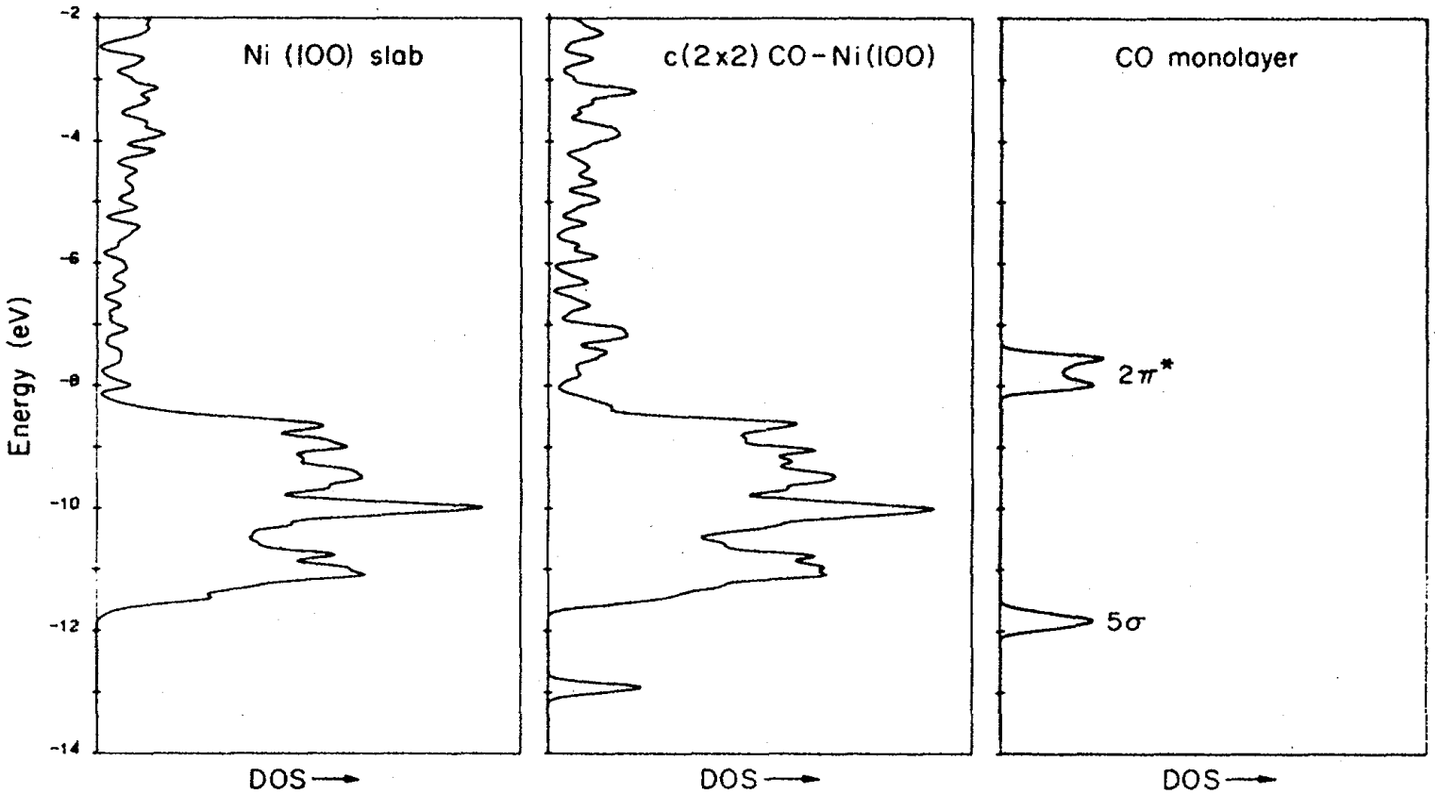

FIG. 4. The total density of states of a model $c(2\times2)$CO-Ni(100) system (center), compared to its isolated four-layer Ni slab (left) and CO monolayer components.

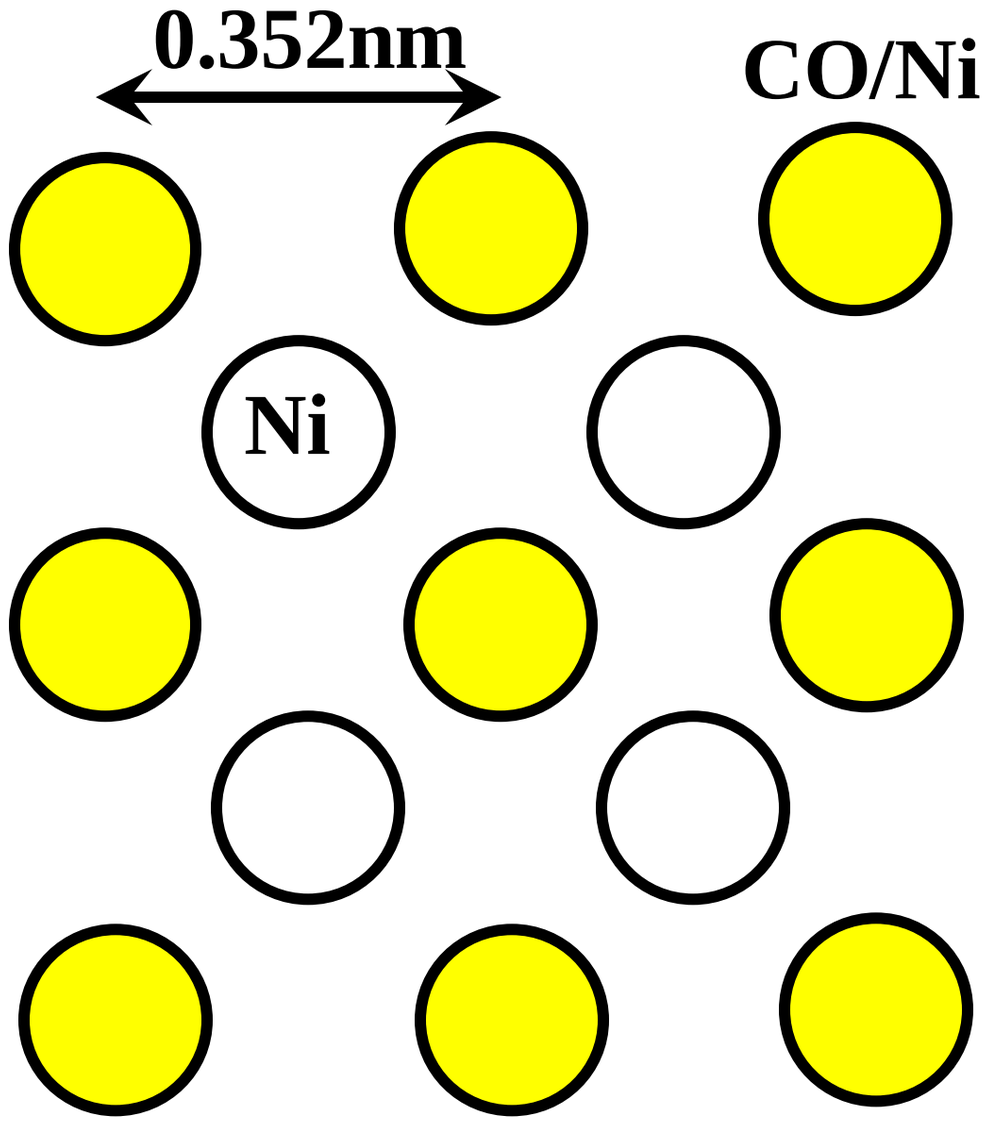

- CO
- A=0.352 nm

CO/Ni(001) c(2x2) Projected Density of States

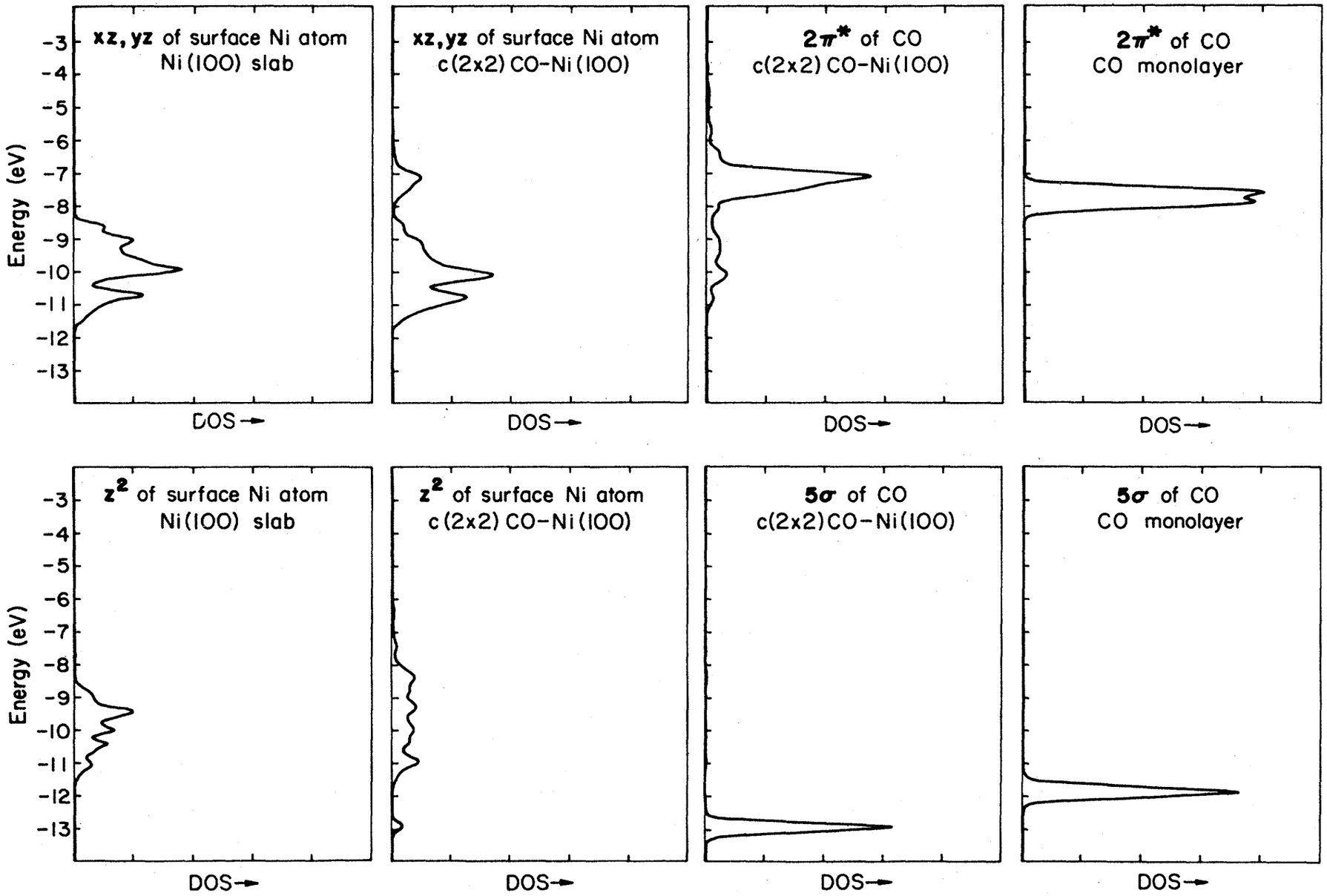

FIG. 6. "Interaction diagrams" for 5σ and $2\pi^*$ of $c(2\times2)$CO-Ni(100). The extreme left and right panels in each case show the contributions of the appropriate orbitals (z^2 for 5σ, xz,yz for $2\pi^*$) of a surface metal atom (left), and of the corresponding isolated CO monolayer MO. The middle two panels then show the contributions of the same fragment MO's to the DOS of the composite chemisorption system.

Where are the bonds?: Mulliken Overlap Population

$$y = c_1 c_1 + c_2 c_2,$$

$$\int y^2 dx = \int c_1 c_1 + c_2 c_2^2 dx$$

$$= c_1^2 + c_2^2 + \boxed{2c_1 c_2 S_{12}},$$

$$S_{12} = \int c_1 c_2 dx.$$

$2c_1c_2S_{12}$：正→同符号で重なり
結合性軌道

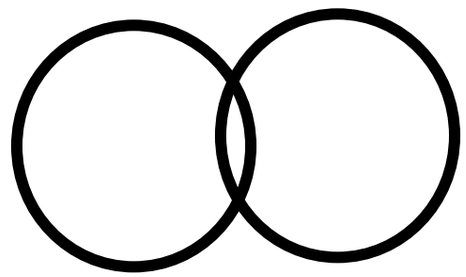

負→異符号で重なり
反結合性軌道

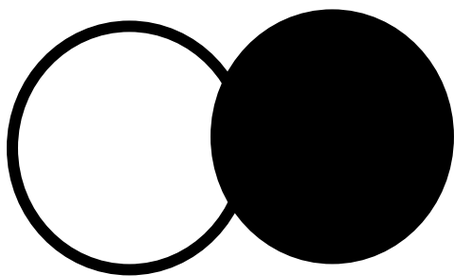

Mulliken Overlap Population

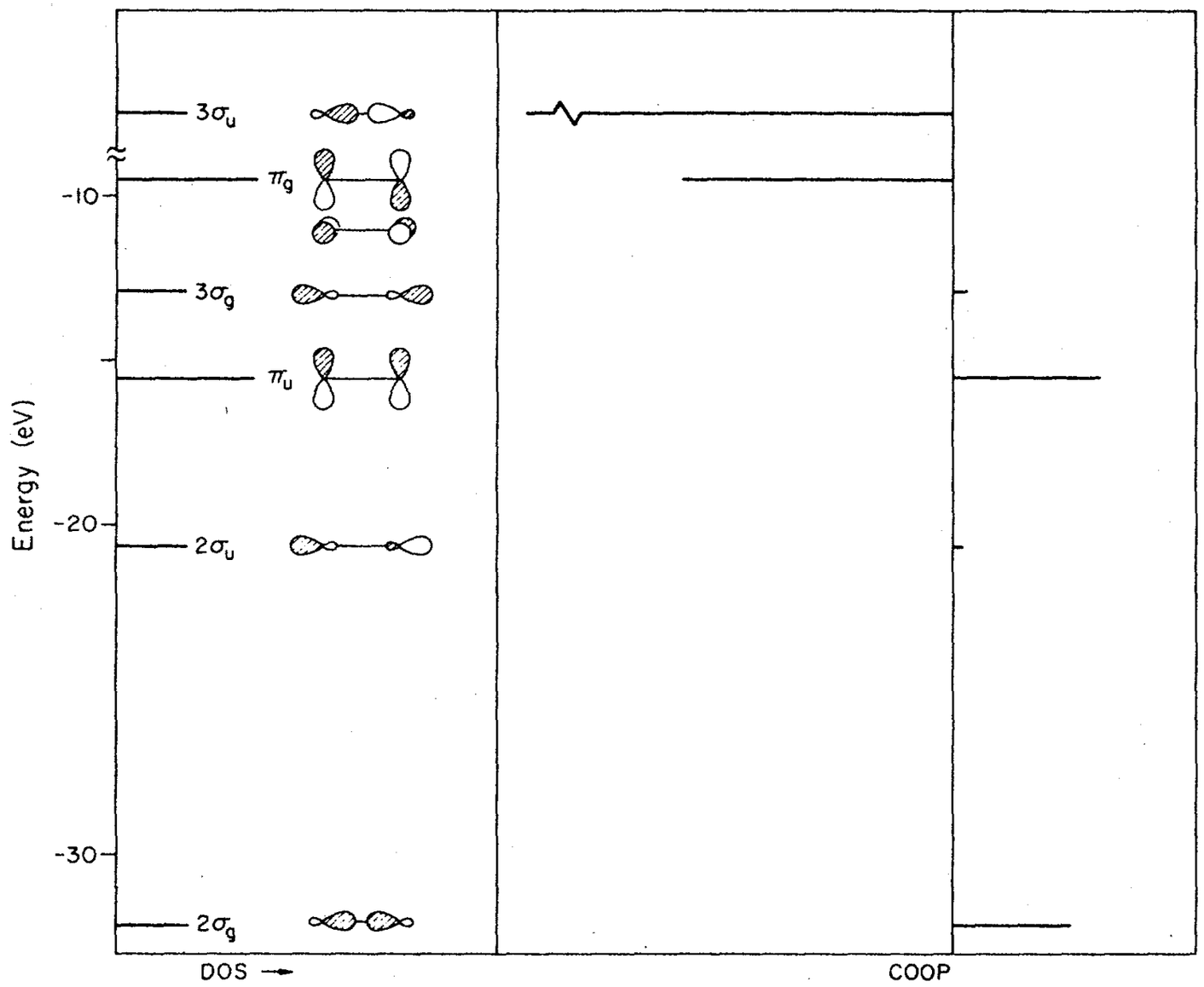

FIG. 9. The orbitals of N_2 (left) and a "solid-state way" to plot the density of states and crystal orbital overlap population curves for this molecule. The $1\sigma_g$ and $1\sigma_u$ orbitals are out of the range of this figure.

Crystal Orbital Orverlap Population: Extension of Mulliken Population to Solid.

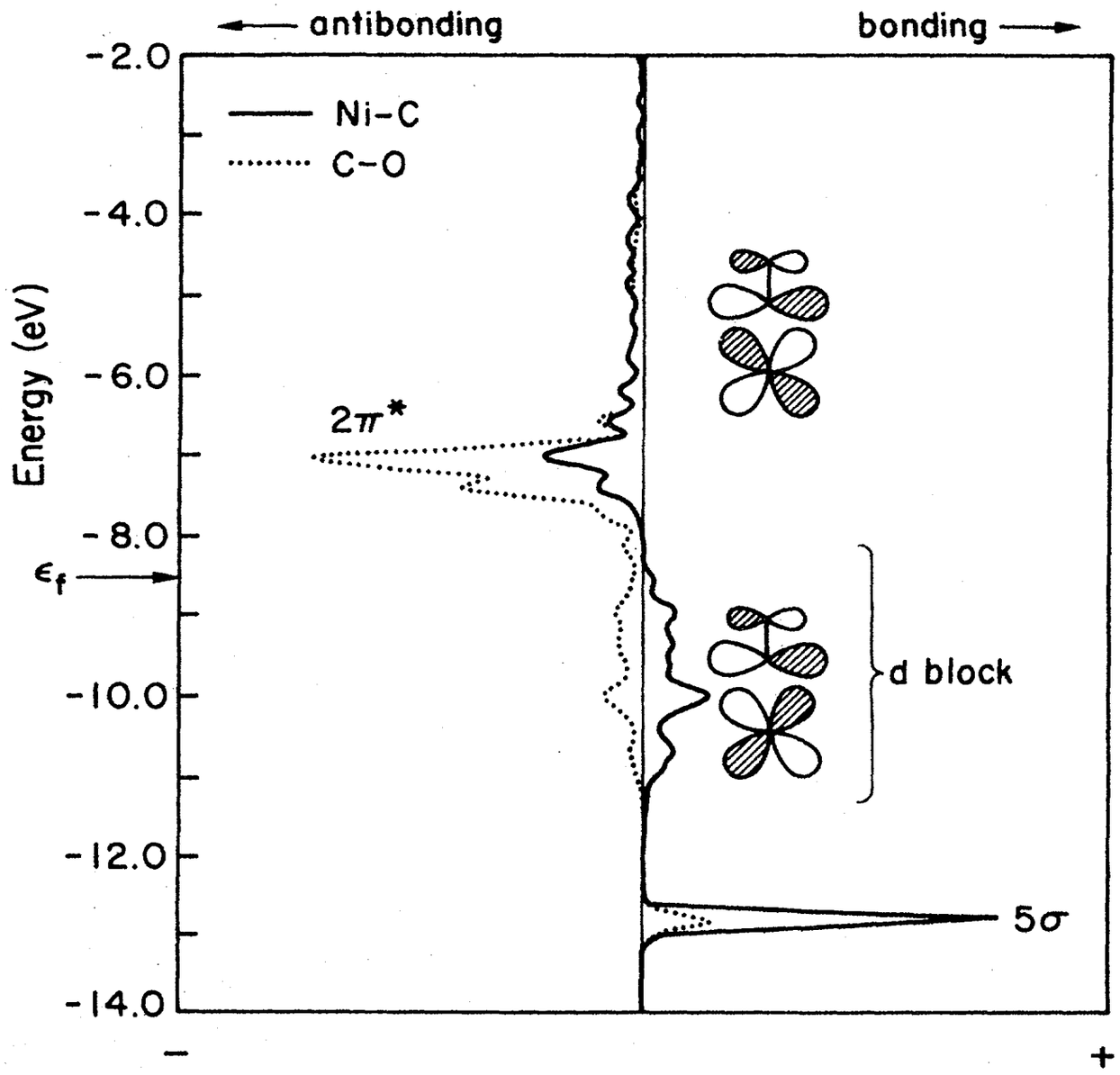

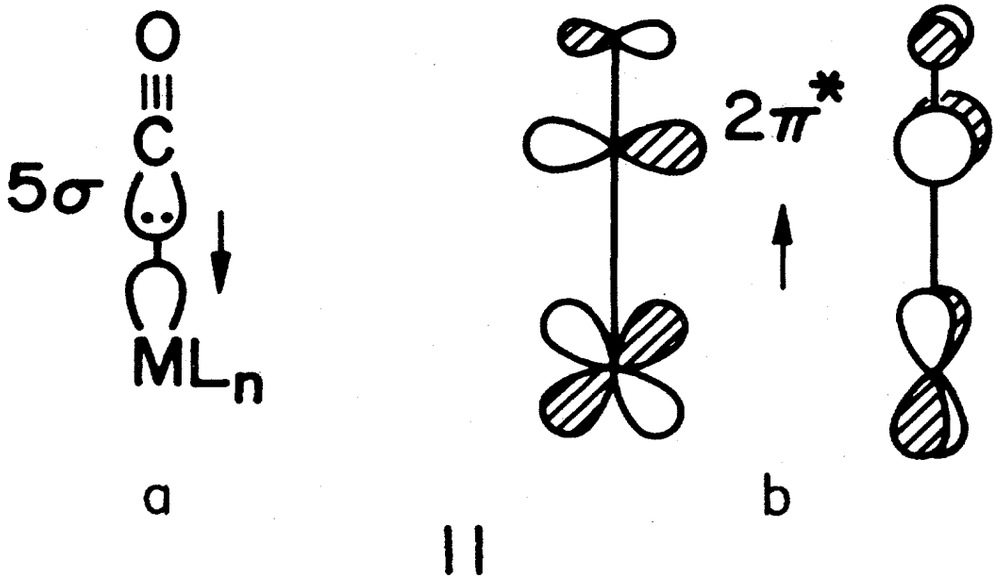

FIG. 10. Crystal orbital overlap population for CO, on top, in a $c(2\times2)$CO-Ni(100) model. Representative orbital combinations are drawn.

CO分子吸着エネルギー：基板金属依存性

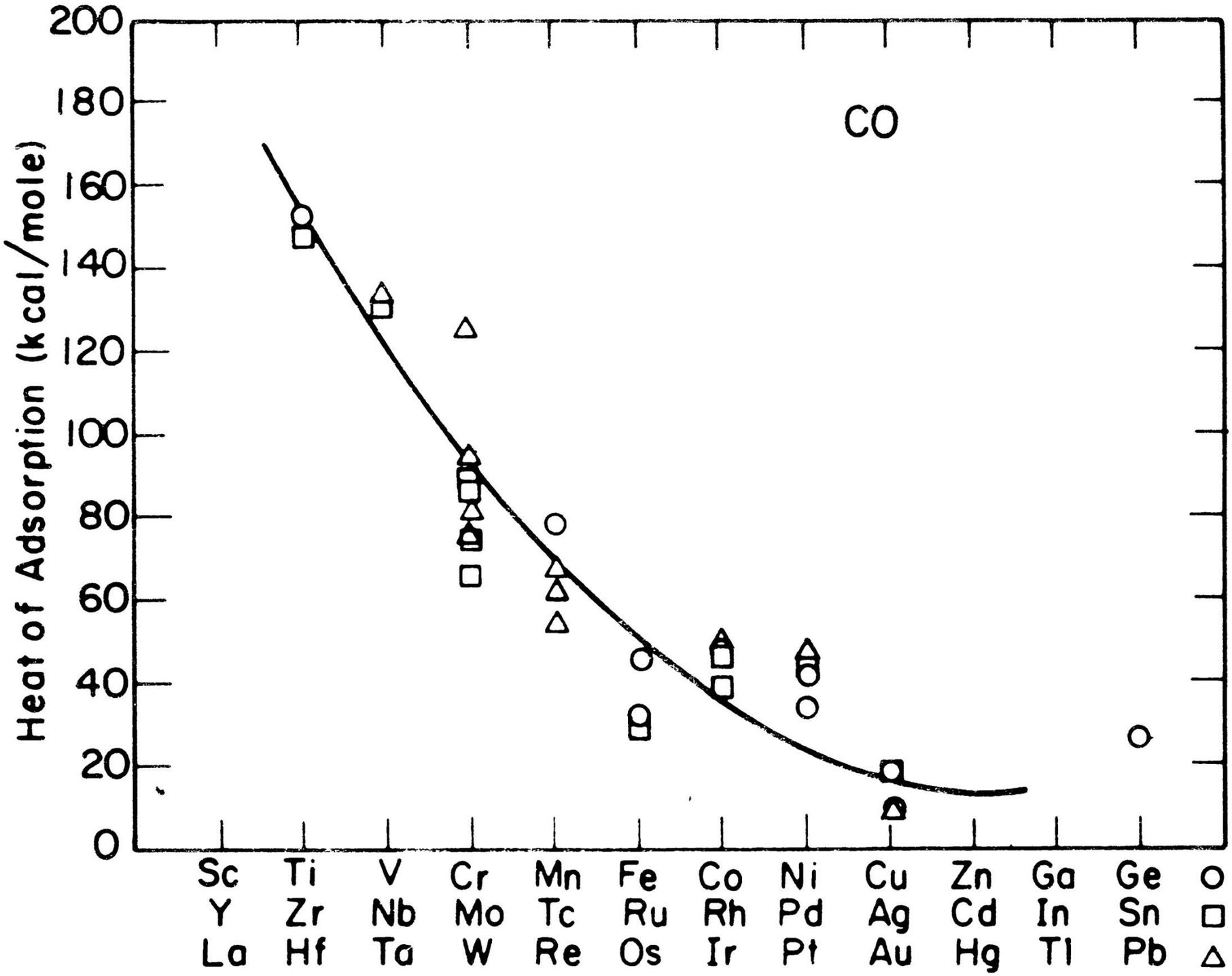

CO、N_2分子軌道

	N_2		CO	
2π ($1\pi_g$)	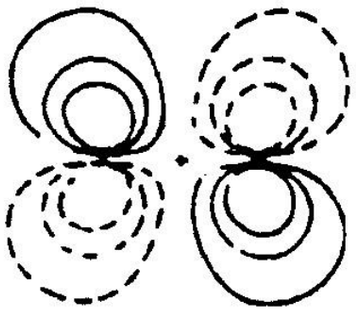	2π	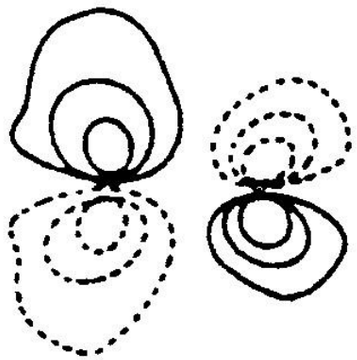	LUMO
5σ ($3\sigma_g$)	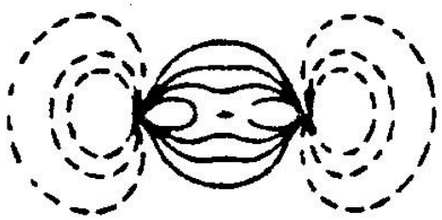	5σ	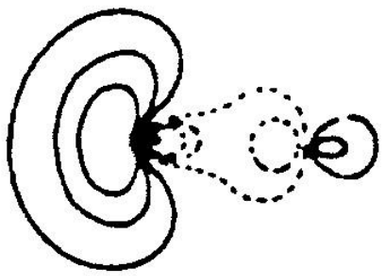	HOMO
1π ($1\pi_u$)	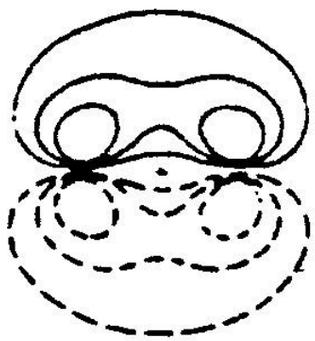	1π	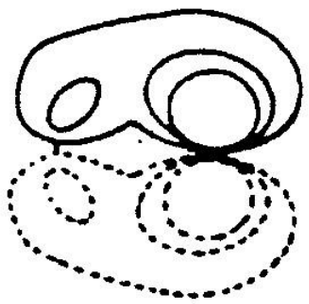	
4σ ($2\sigma_u$)	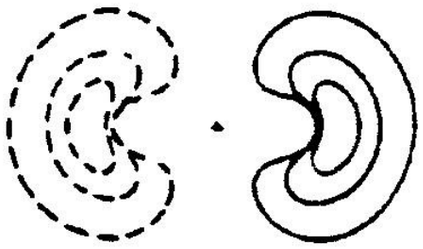	4σ	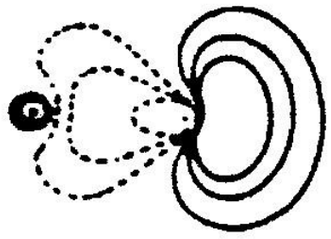	

吸着子とd電子との相互作用

- 吸着子とd電子との相互作用は一電子エネルギー補正（δE_{1el}）として取り入れられる。これを二準位モデルで取り入れる。

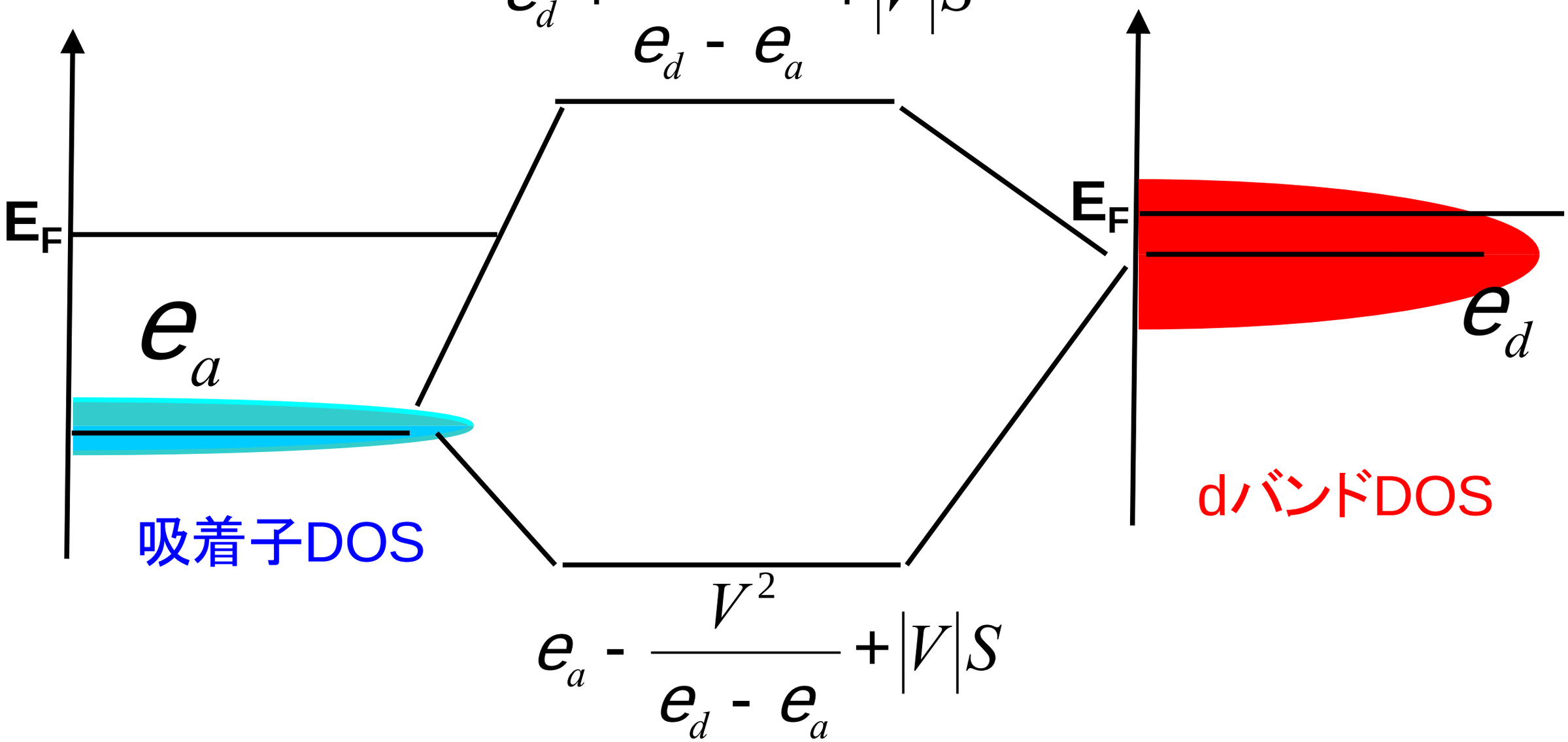

CO分子の吸着エネルギー

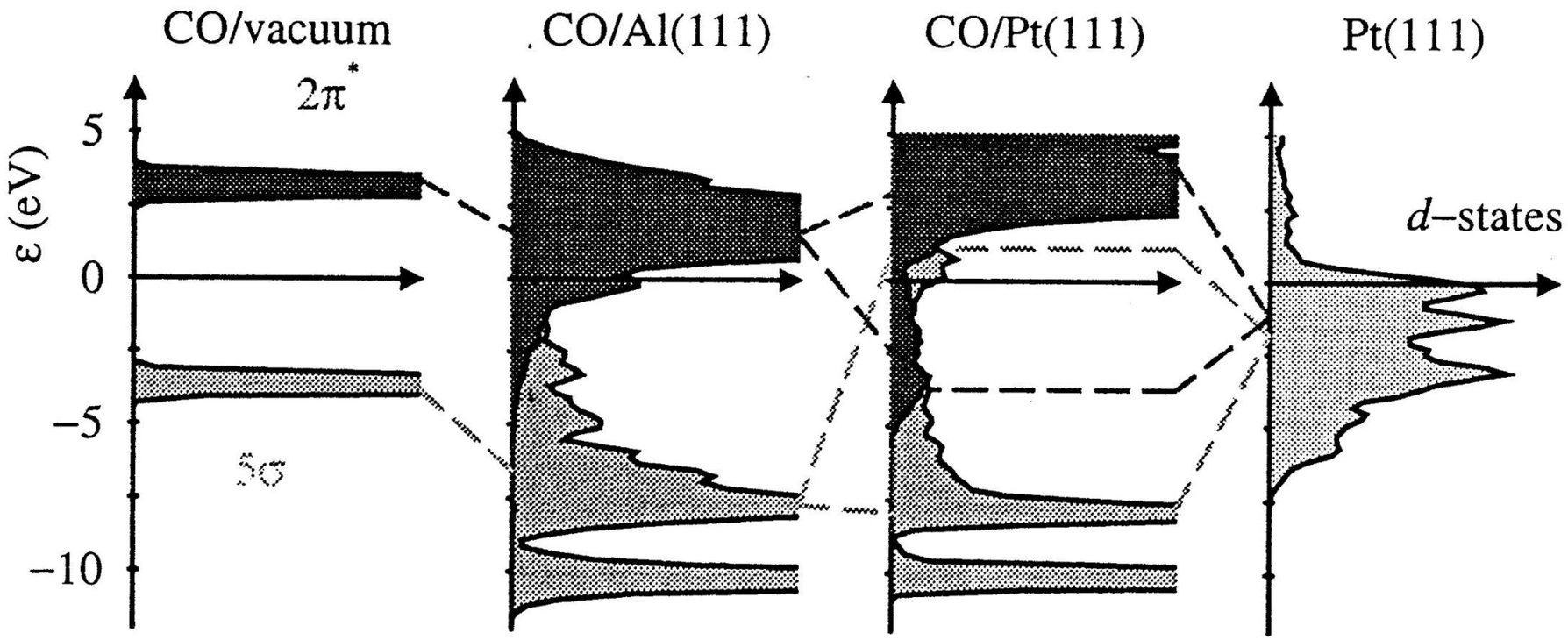

$$E_{d\text{-}hyb} \approx -4\left[f\frac{V_p^2}{e_{2p}-e_d} - fS_p|V_p|\right] - 2\left[(1-f)\frac{V_s^2}{e_d-e_s} - (1+f)S_s|V_s|\right]$$

CO分子の吸着エネルギー

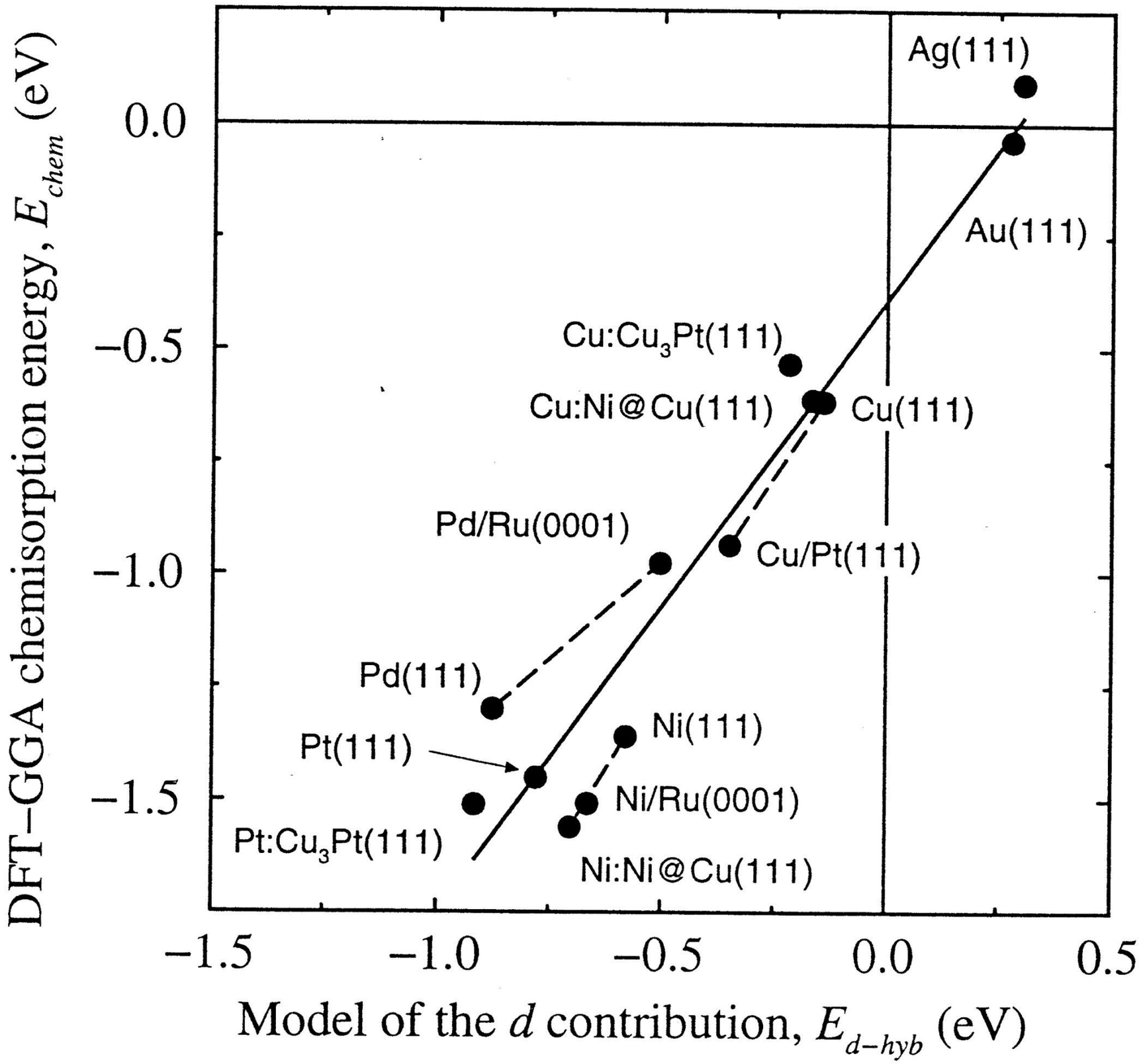

原子･分子の吸着エネルギー

$$E_{d-hyb} \approx -4\left[f\frac{V_p^2}{e_{2p}-e_d}+fS_p\left|V_p\right|\right]$$

$$-2\left[(1-f)\frac{V_s^2}{e_d-e_s}+(1+f)S_s\left|V_s\right|\right].$$

For late transition metals $(f \approx 1)$,

$$E_{d-hyb} \approx -4\left[f\frac{V_p^2}{e_{2p}-e_d}+fS_p\left|V_p\right|\right],$$

$$dE_{d-hyb} \approx -4f\frac{V_p^2}{(e_{2p}-e_d)^2}de_d.$$

吸着エネルギーとdバンド中心

Vを固定してε_dのみを変化させると

$$dE_{d\text{-}hyb} \approx -4f\frac{V_p^2}{(e_{2p}-e_d)^2}de_d.$$

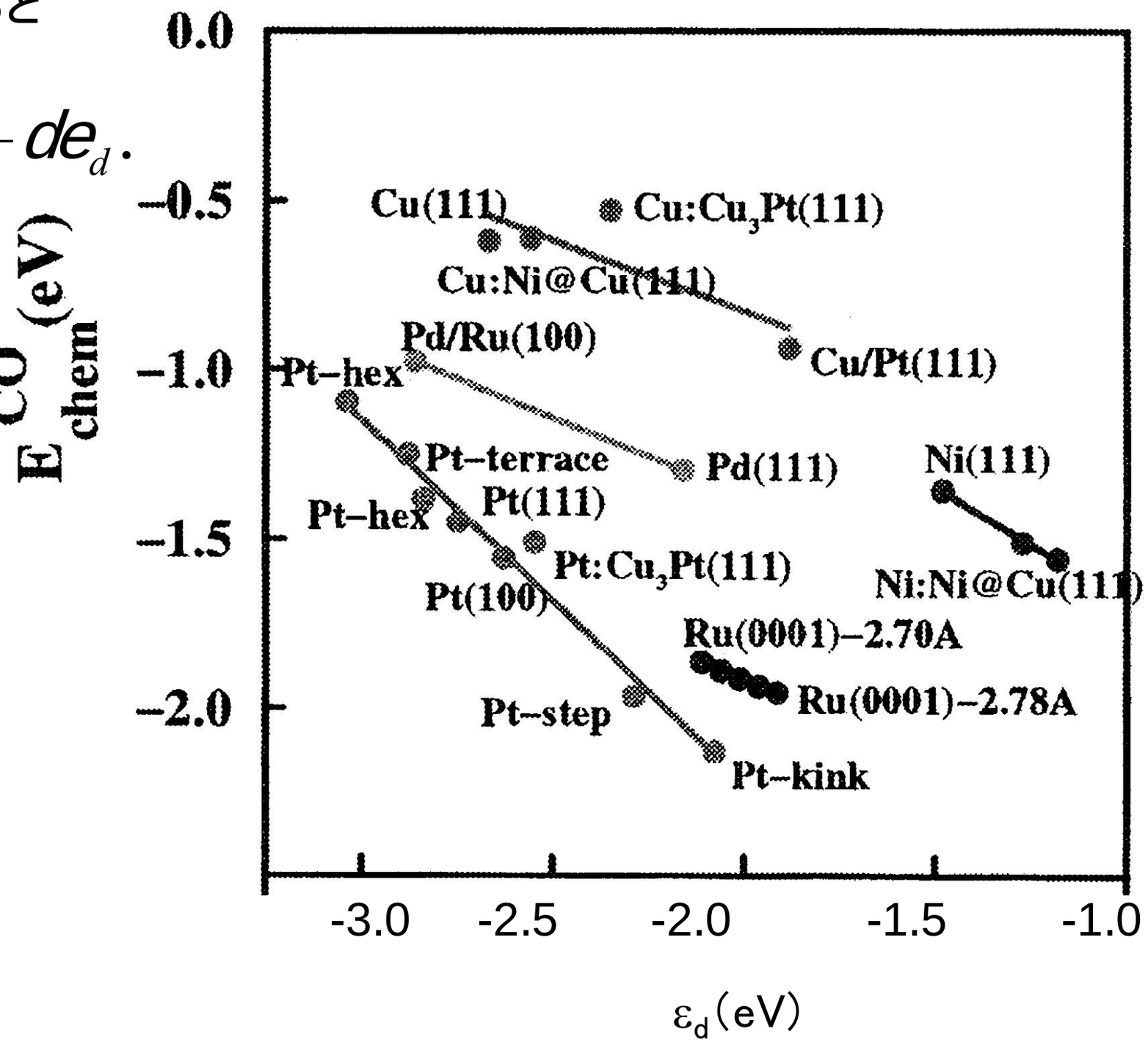

CO分子の解離吸着過程

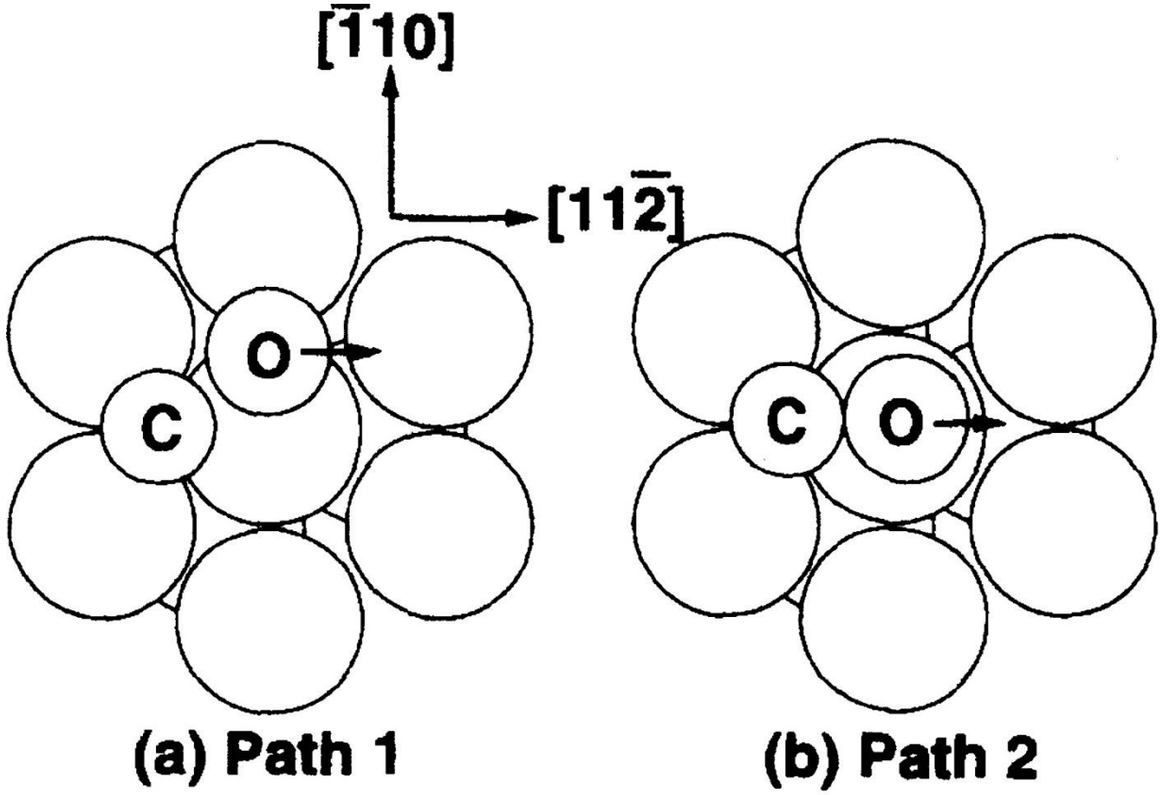

(a) Path 1　　(b) Path 2

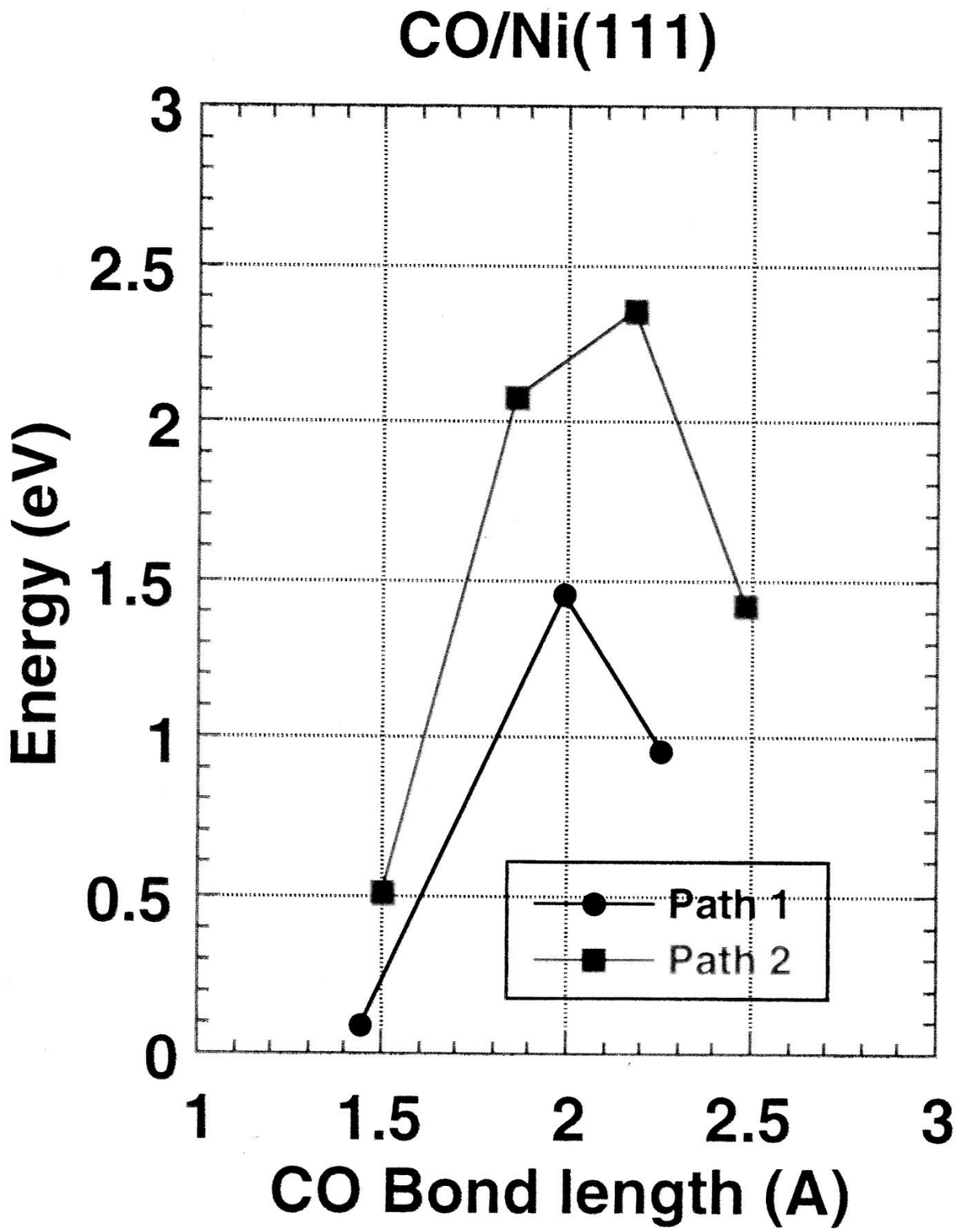

CO分子の解離吸着過程

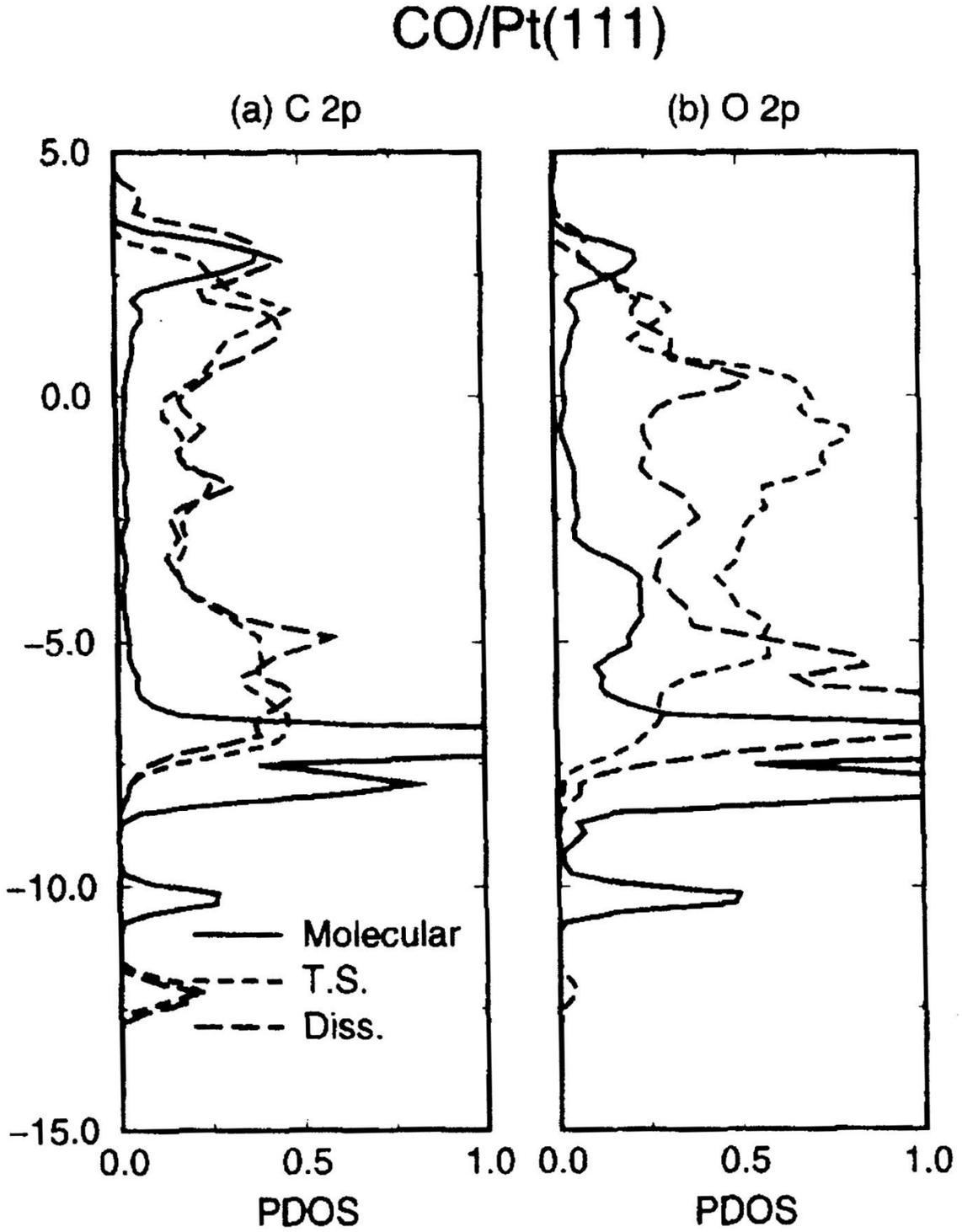

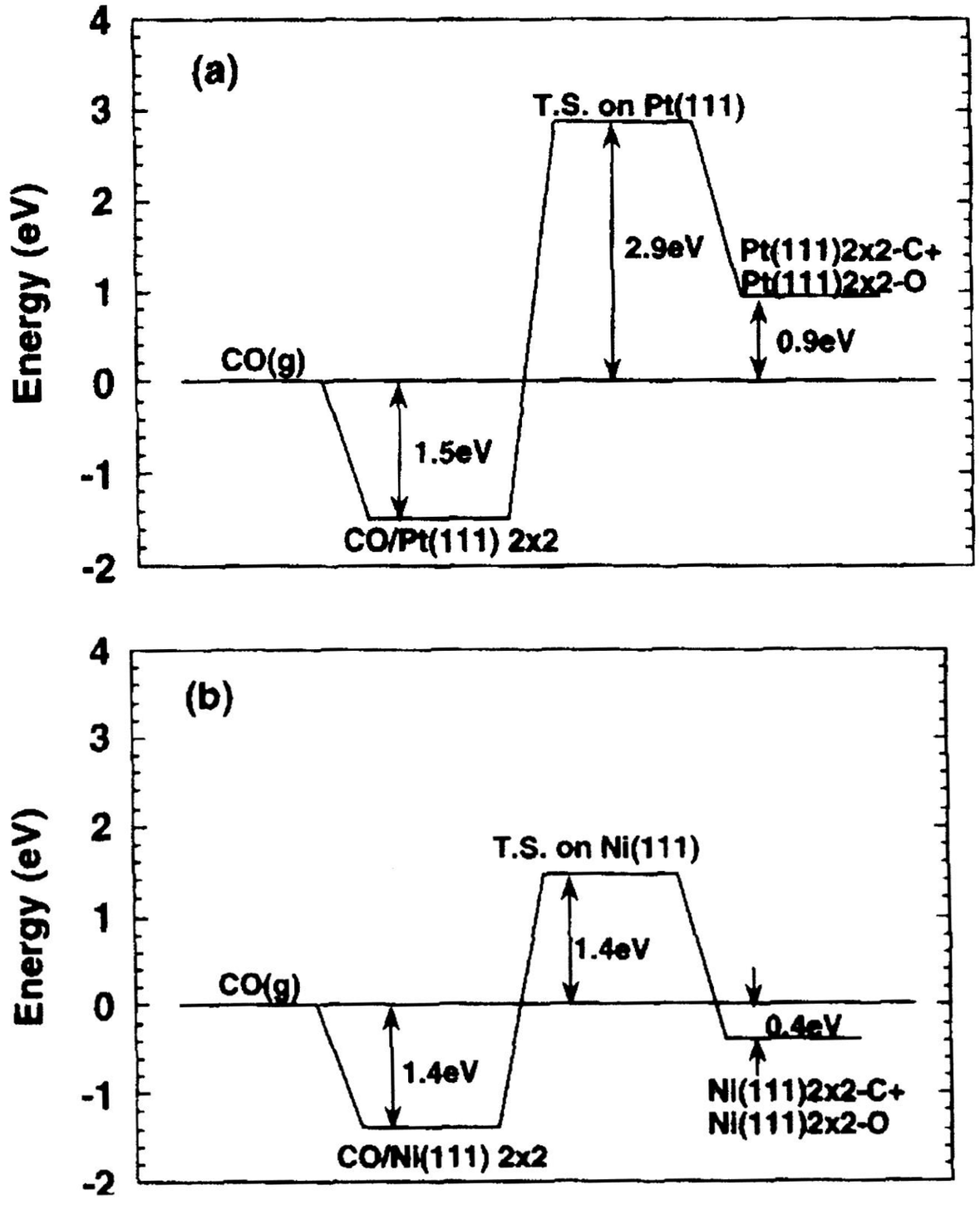

吸着エネルギーとdバンド中心

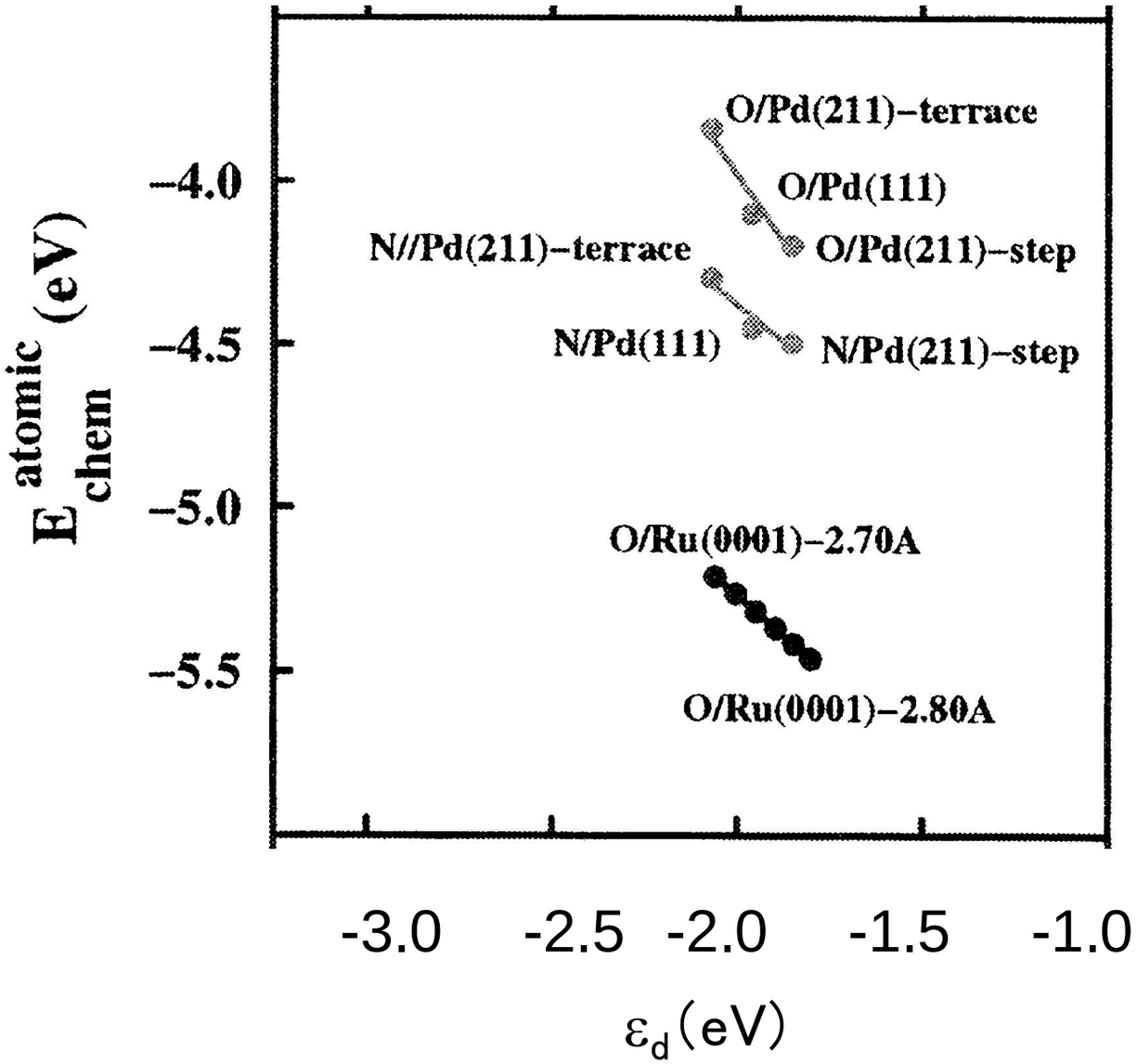

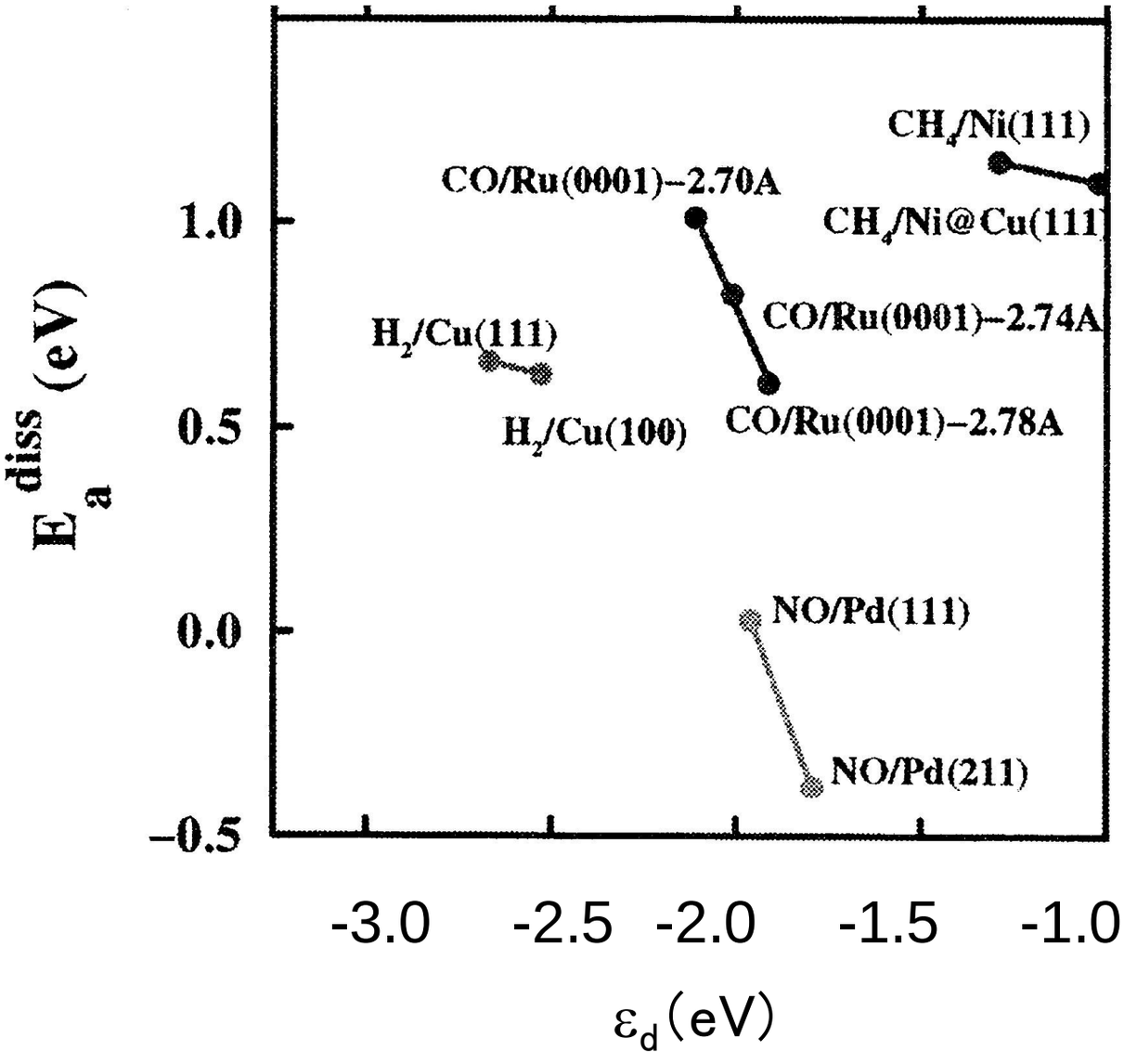

Universality in Heterogeneous Catalysis

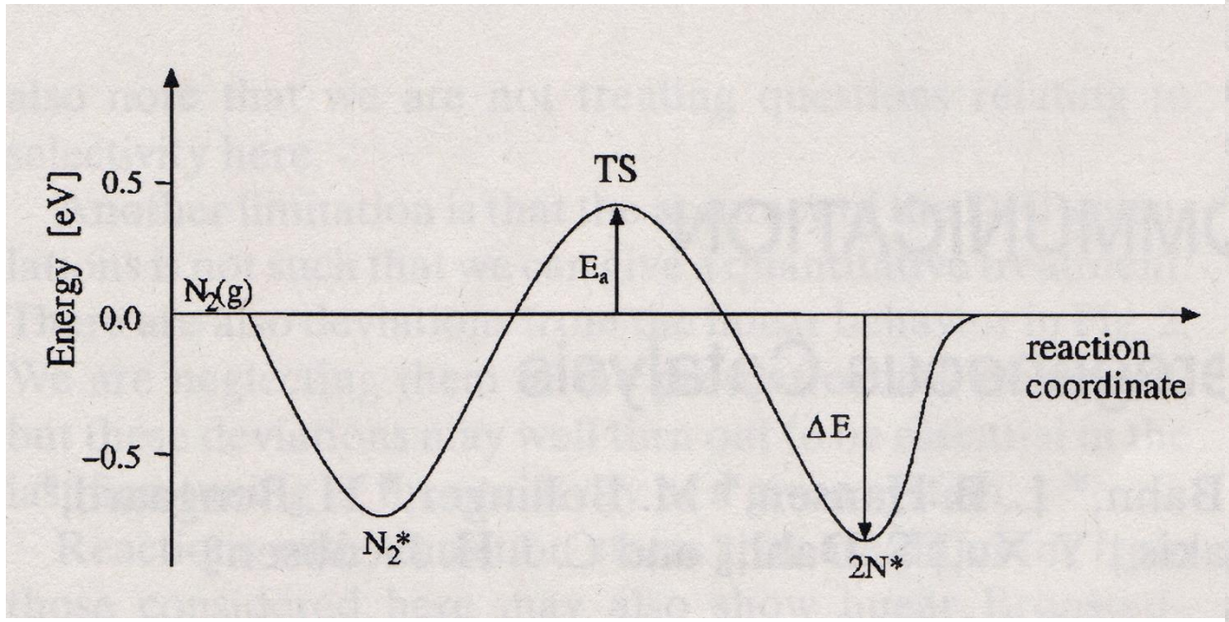

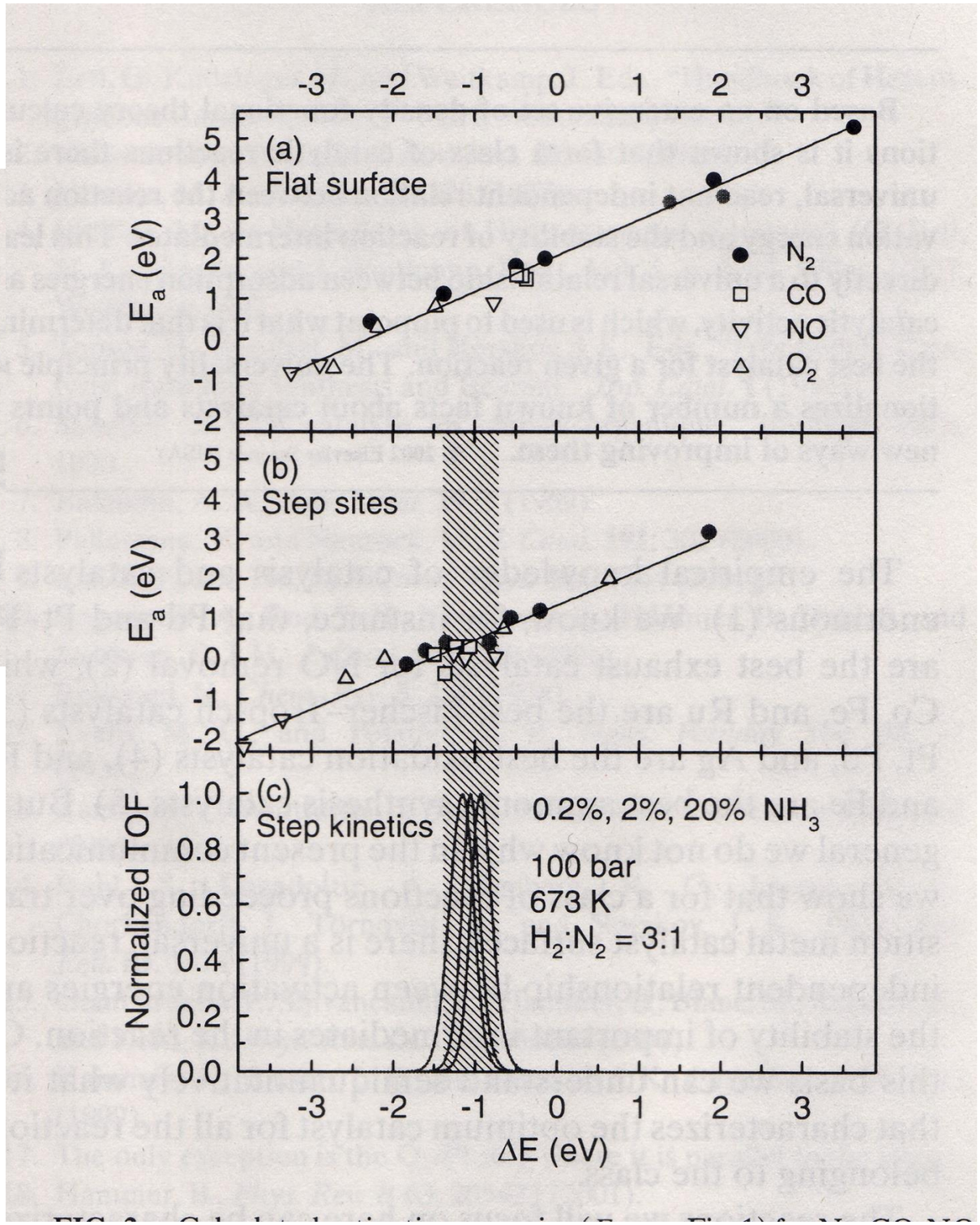

J.K. Norskov et al., *J. Catal.* 209, 275 (2002).

Hydrogen Evolution Reaction

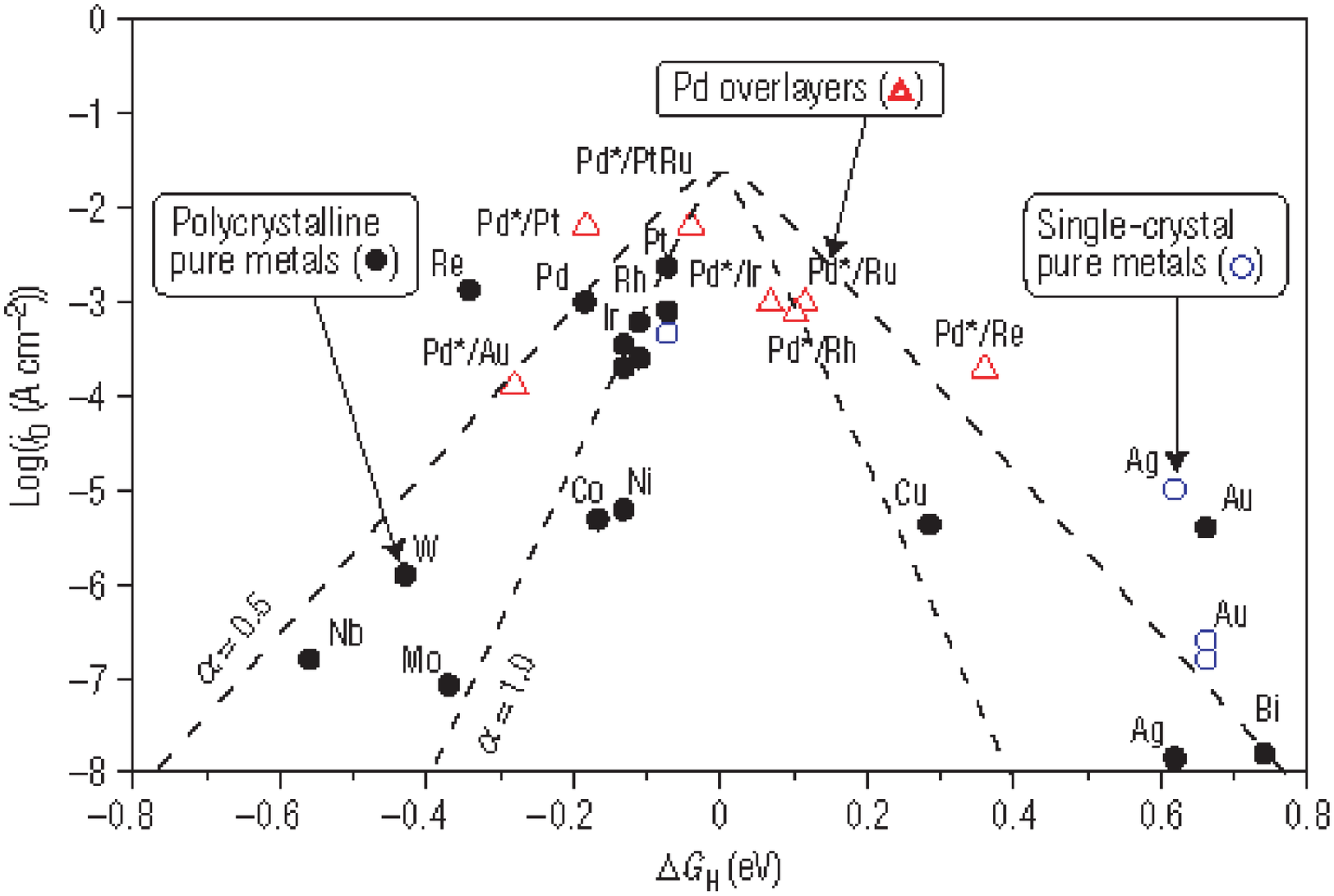

J. Greeley, T. F. Jaramillo, J. Bonde, I. Chorkendorff, and J.K. Norskov, Nature Materials, 5, 909 (2006).

Hydrogen Evolution Reaction

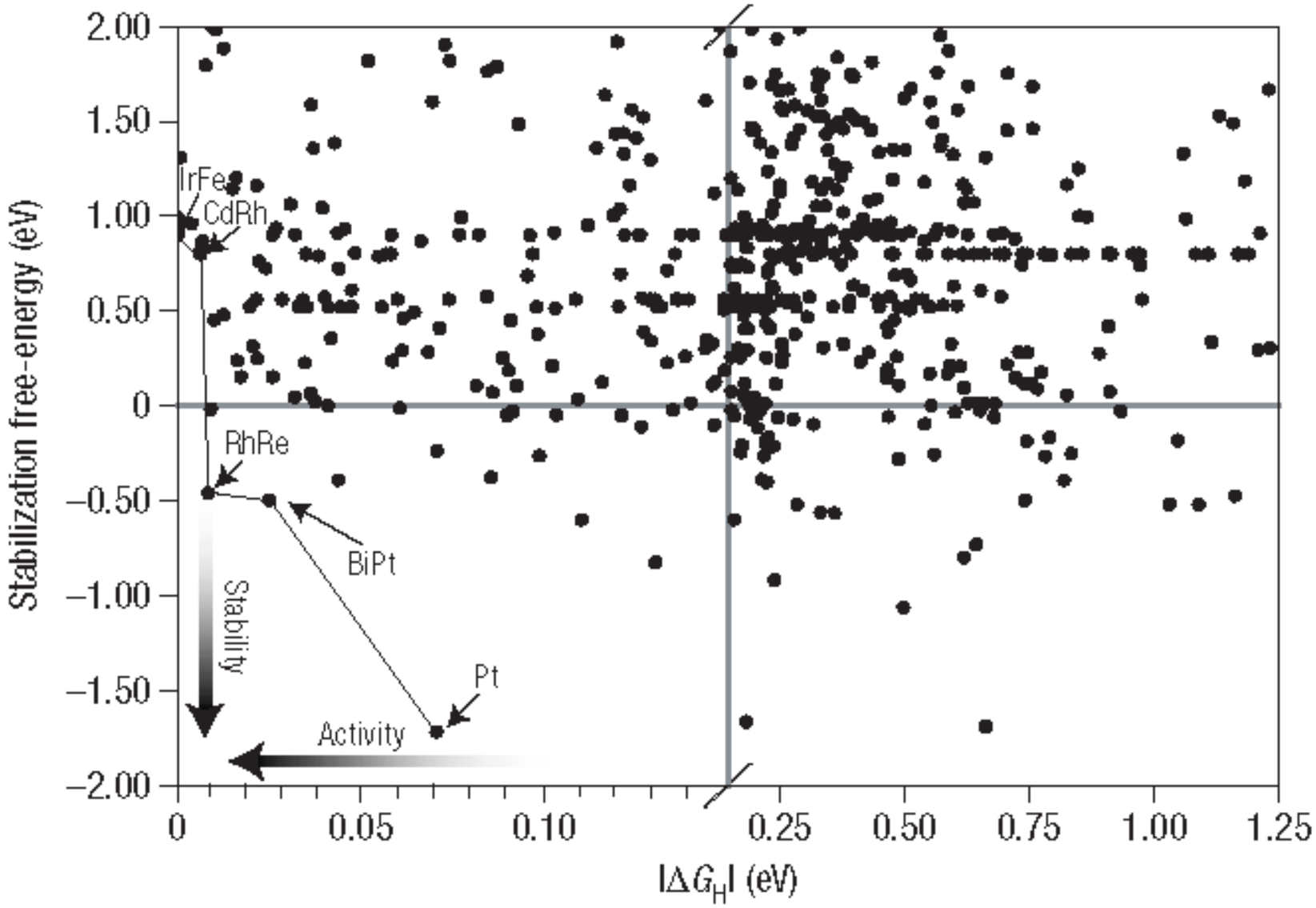

J. Greeley, T. F. Jaramillo, J. Bonde, I. Chorkendorff, and J.K. Norskov, Nature Materials, 5, 909 (2006).

Hydrogen Evolution Reaction

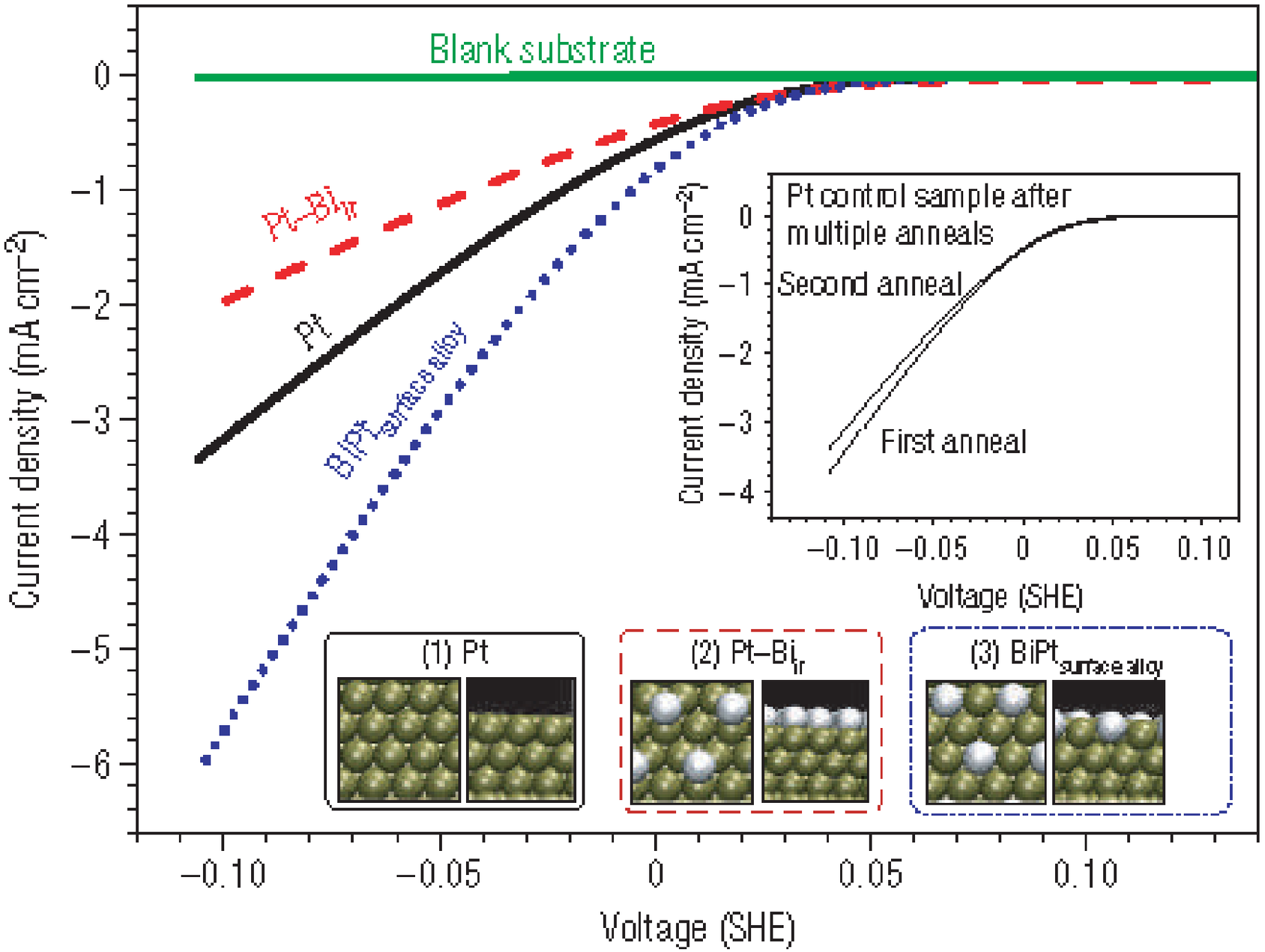

J. Greeley, T. F. Jaramillo, J. Bonde, I. Chorkendorff, and J.K. Norskov, Nature Materials, 5, 909 (2006).

Oxygen Reduction Reaction

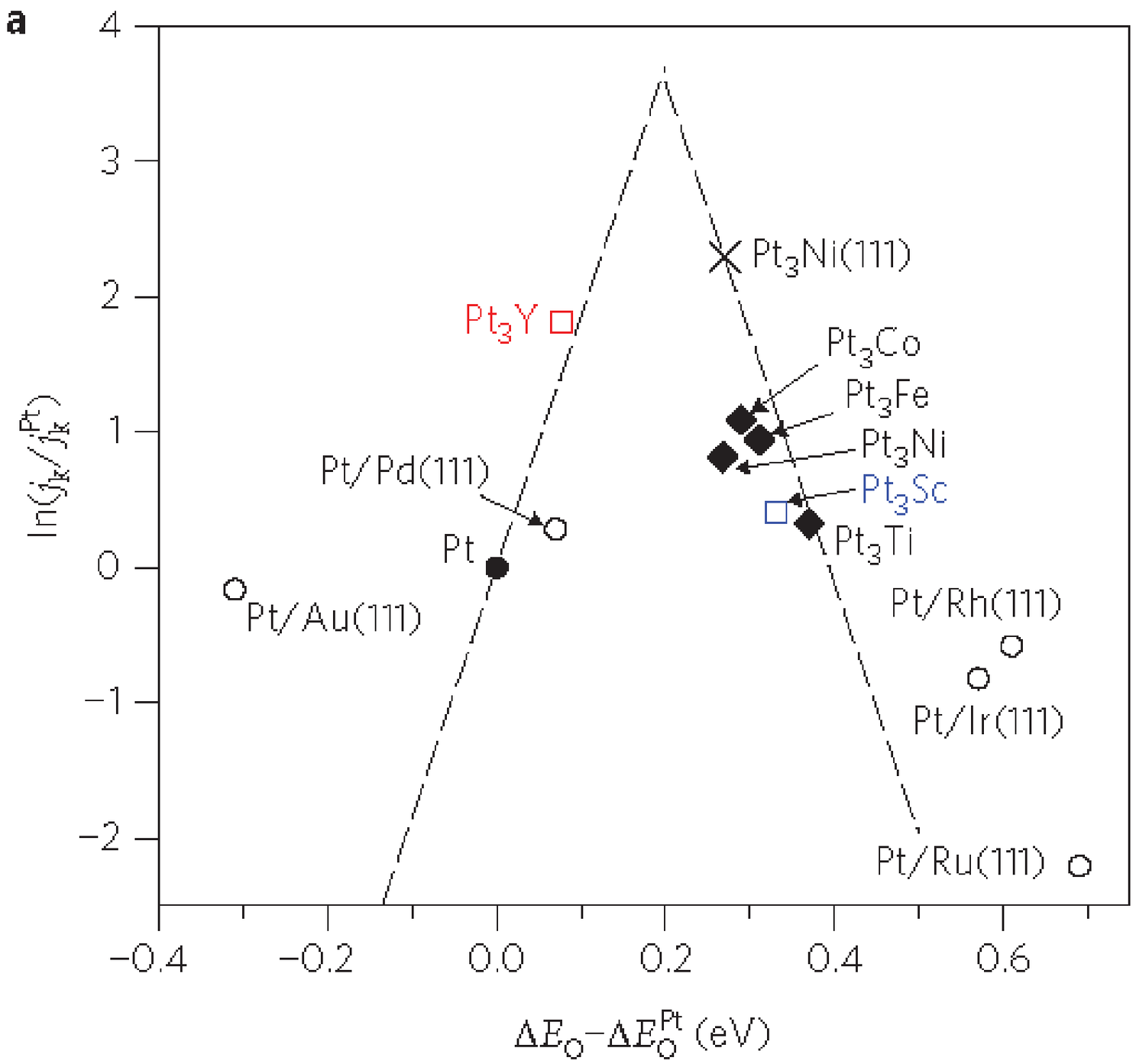

J. Greeley, I.E.L. Stephens, A.S. Bondarenko, T.P. Johansson, H.A. Hansen, T. F. Jaramillo, J. Rossmeisl, I. Chorkendorff, and J.K. Norskov, Nature Chemistry, 1, 552 (2009).

Oxygen Reduction Reaction

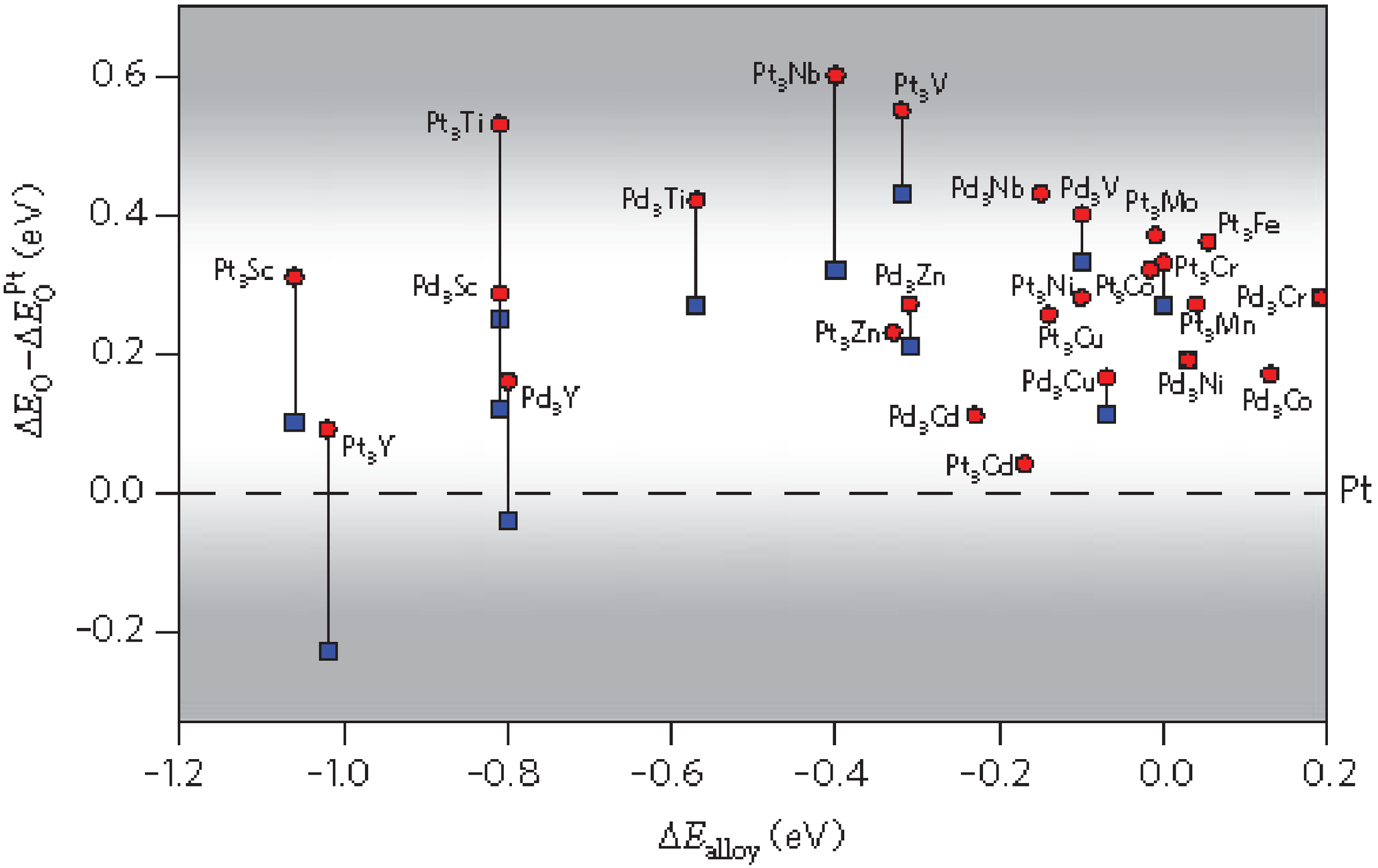

J. Greeley, I.E.L. Stephens, A.S. Bondarenko, T.P. Johansson, H.A. Hansen, T. F. Jaramillo, J. Rossmeisl, I. Chorkendorff, and J.K. Norskov, Nature Chemistry, 1, 552 (2009).

Oxygen Reduction Reaction

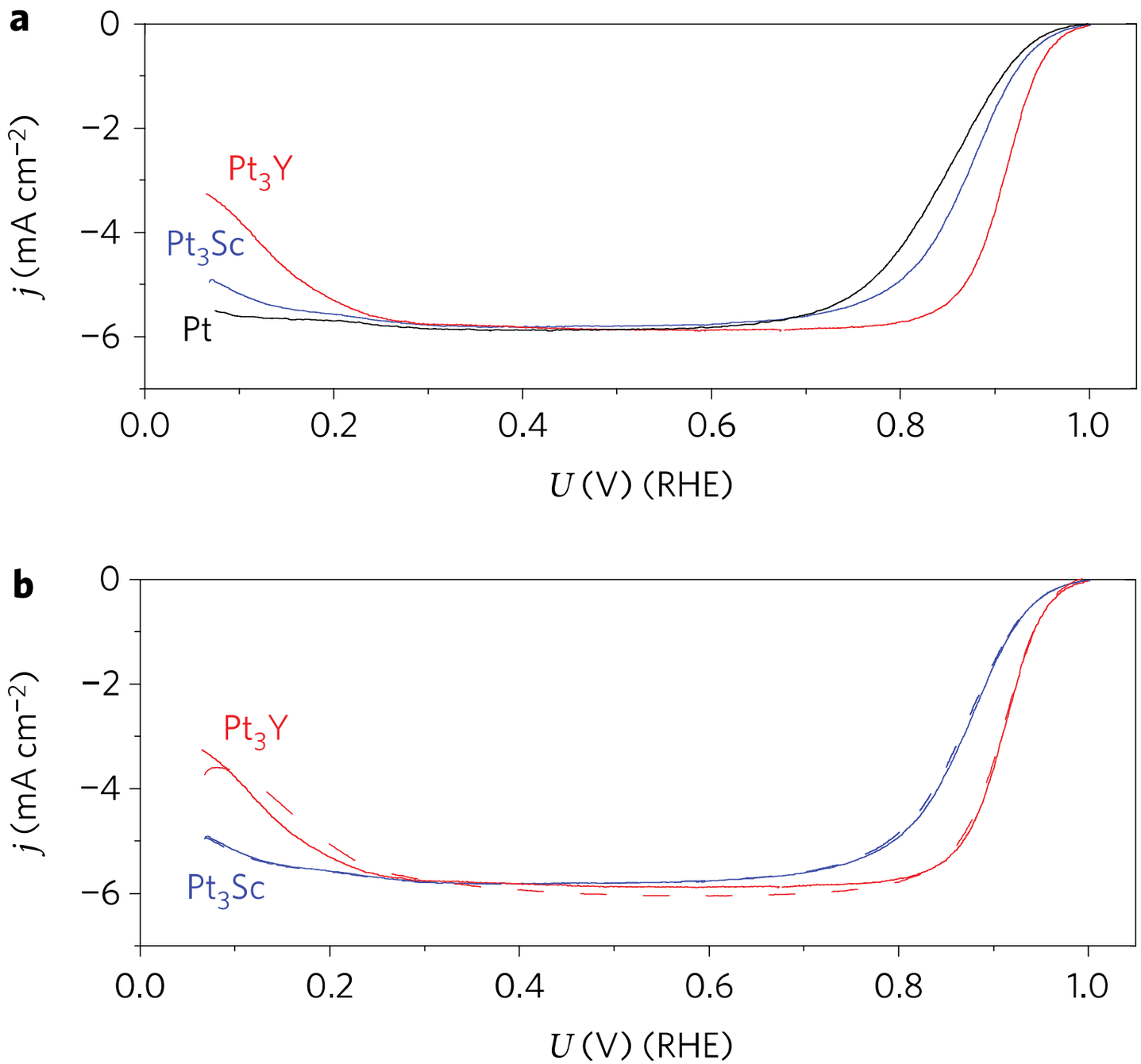

J. Greeley, I.E.L. Stephens, A.S. Bondarenko, T.P. Johansson, H.A. Hansen, T. F. Jaramillo, J. Rossmeisl, I. Chorkendorff, and J.K. Norskov, Nature Chemistry, 1, 552 (2009).

機械学習力場による不均一触媒の動的過程の研究

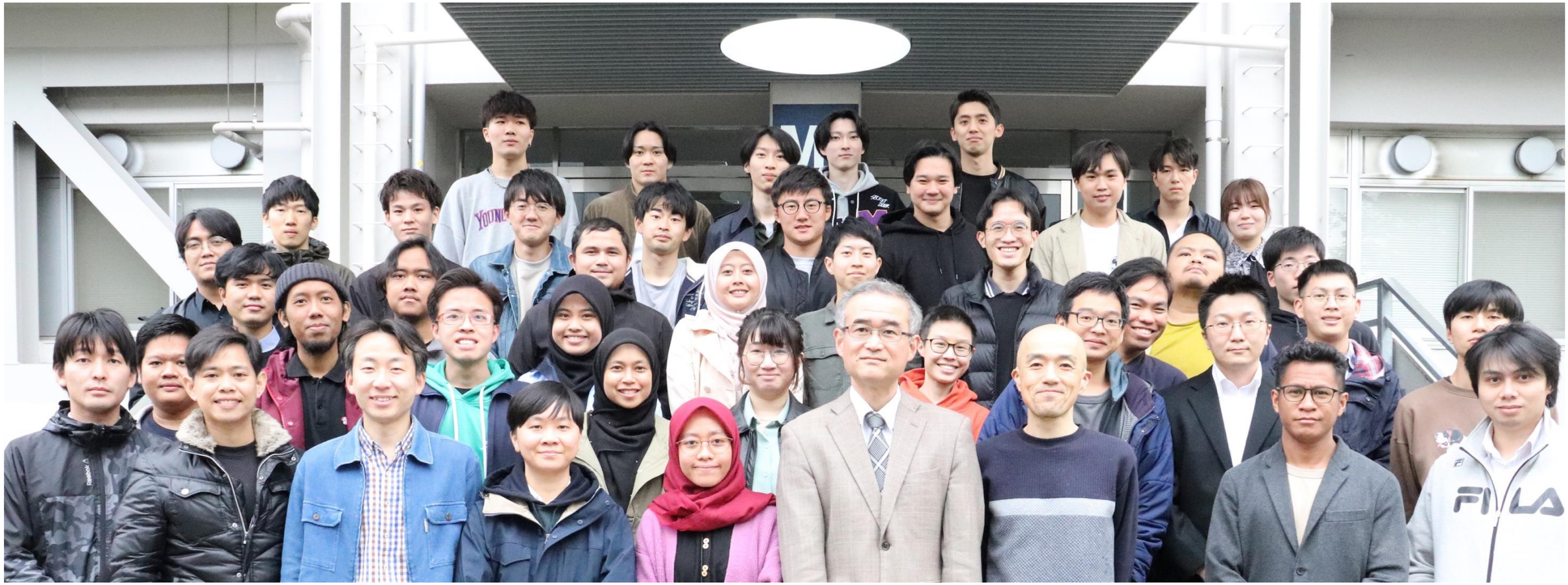

森川良忠

大阪大学 大学院工学研究科

Outline

1. Introduction

2. The Elucidation of Cu-Zn Surface Alloying on Cu(997) by Machine-Learning Molecular Dynamics

H.H. Halim and Y. M, *ACS Phys. Chem. Au*, 5, 430-447 (2022).

3. Machine Learning Molecular Dynamics Simulation of CO-driven Formation of Cu Clusters on Cu(111)

H.H. Halim, R. Ueda and YM, *J. Phys. Condensed Matter, Special Issue from the Speakers of Surface Science Discussions 2022 and 2023*, 35, 495001 (18pp) (2023).

Methanol Synthesis

$$CO_2 + 3H_2 \xrightarrow[250\ C,\ 5\ MPa]{Cu/ZnO} CH_3OH + H_2O$$

- ☑ **Hydrogenation of CO_2 to Formate**
  - **Slow reaction**
  - **Eley-Rideal mechanism[1,2]**

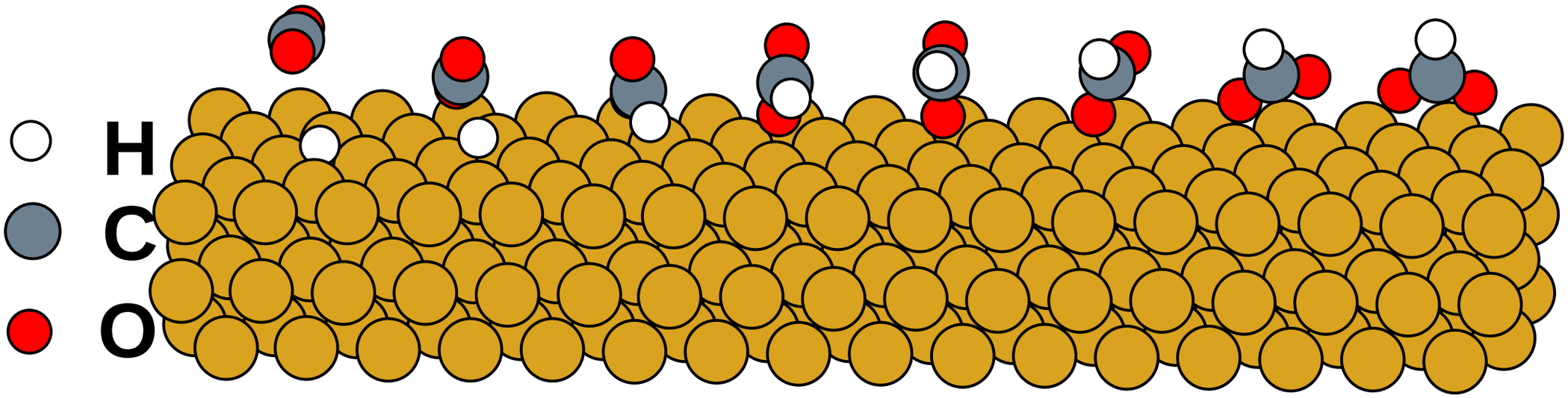

1.H. Nakano *et al.*, *J. Phys. Chem. B* **105**, 1355 (2001).
2.G. Wang, Y. Morikawa, J. Nakamura *J. Phys. Chem. B* **110**, 9 (2006).

Importance of Bending Mode

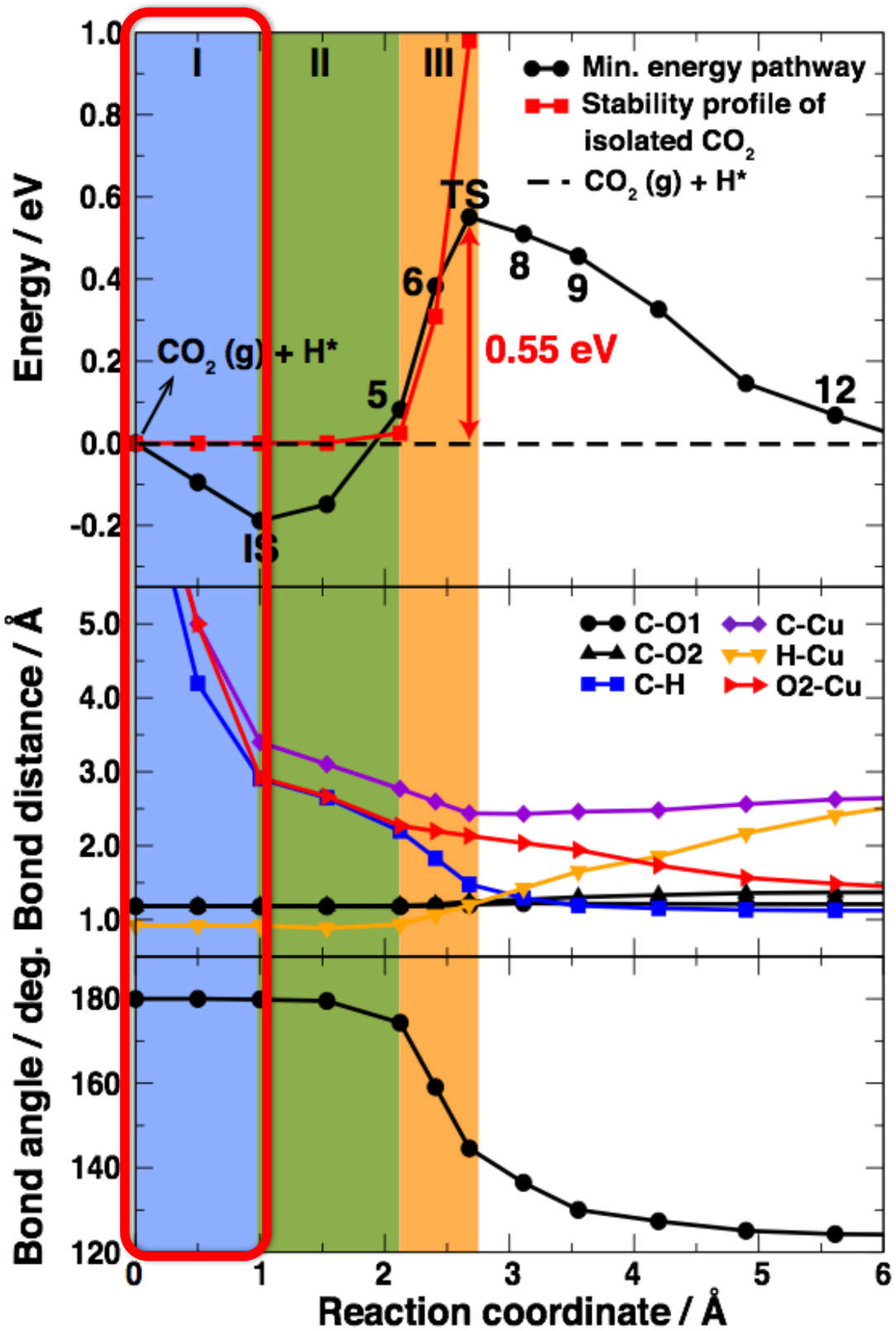

Region I : vdW attractive

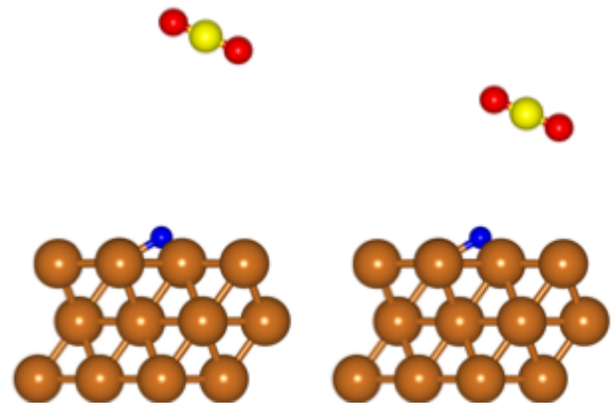

F. Muttaqien, YM *et al.*, ***Chem. Comm.***, 53, 9222(2017).

J. Quan, YM, J. Nakamura *et al.*, ***Nature Chem.***, 11, 722-729 (2019).

Importance of Bending Mode

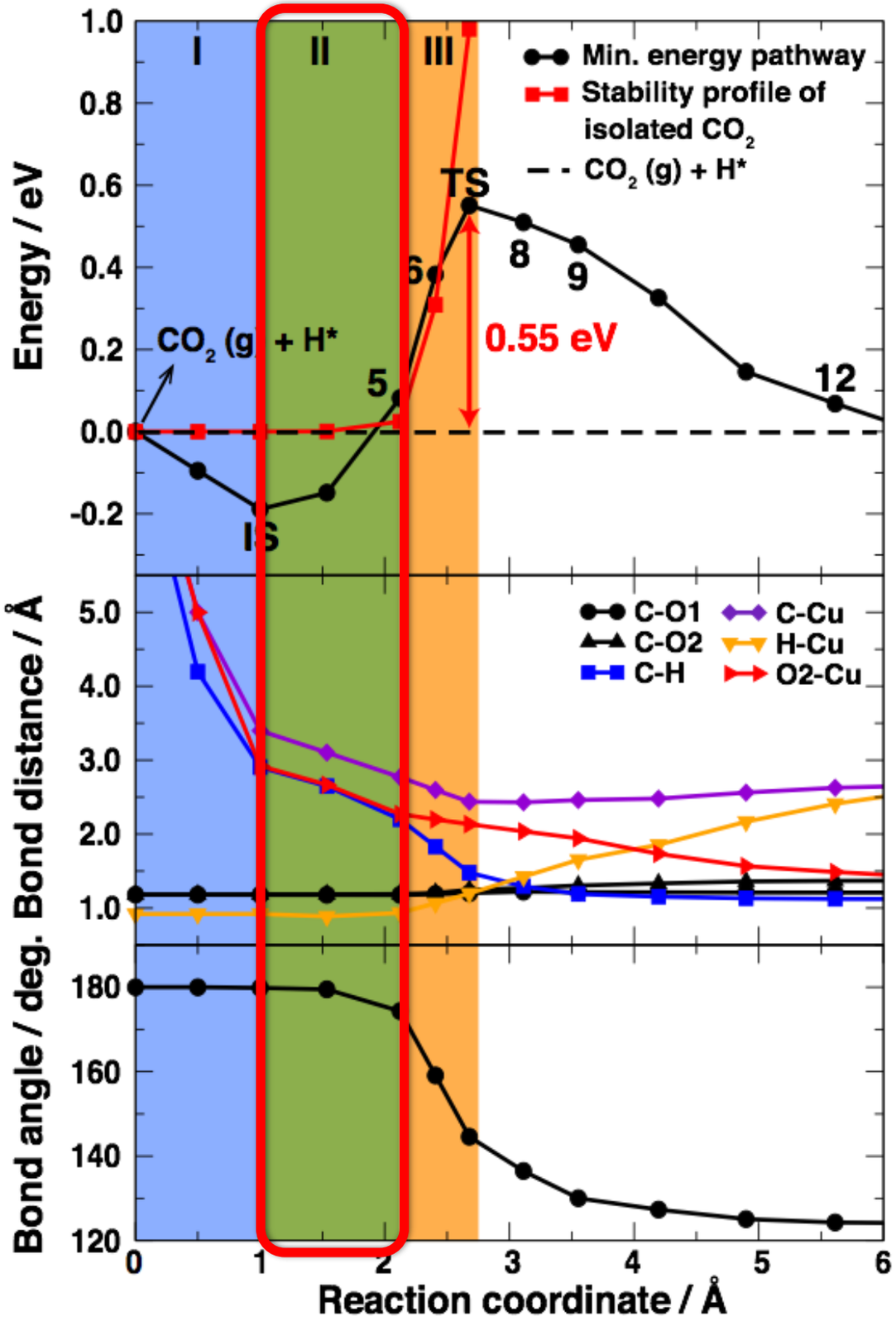

Region I : vdW attractive

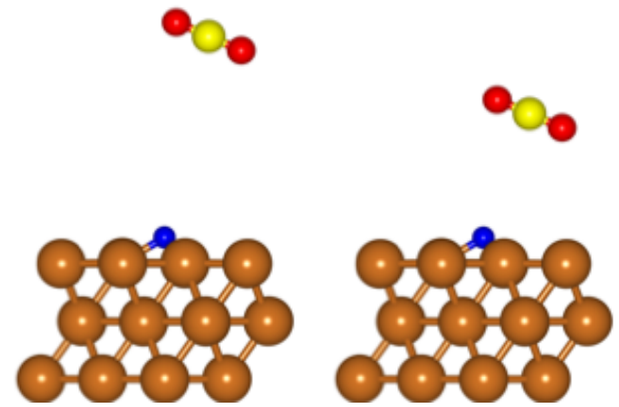

Region II : Pauli repulsion

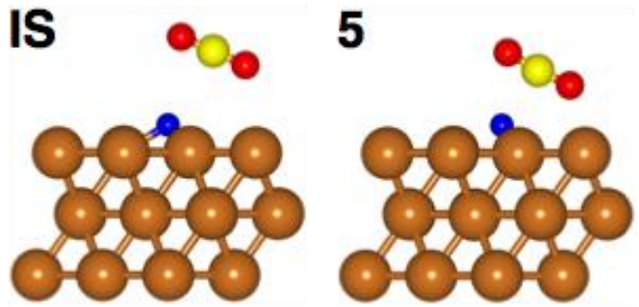

F. Muttaqien, YM *et al.*, ***Chem. Comm.***, 53, 9222(2017).
J. Quan, YM, J. Nakamura *et al.*, ***Nature Chem.***, 11, 722-729 (2019).

Importance of Bending Mode

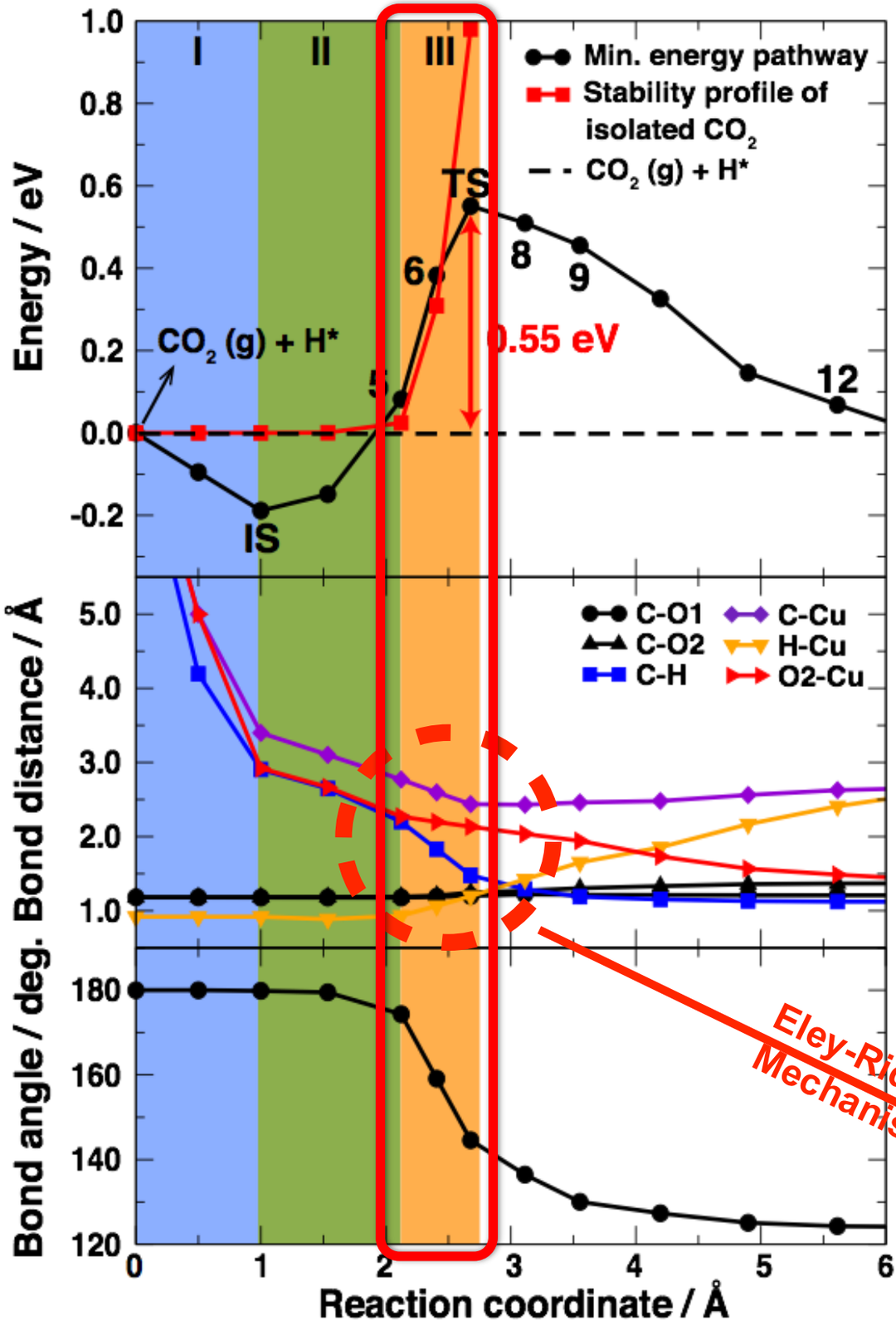

Region I : vdW attractive

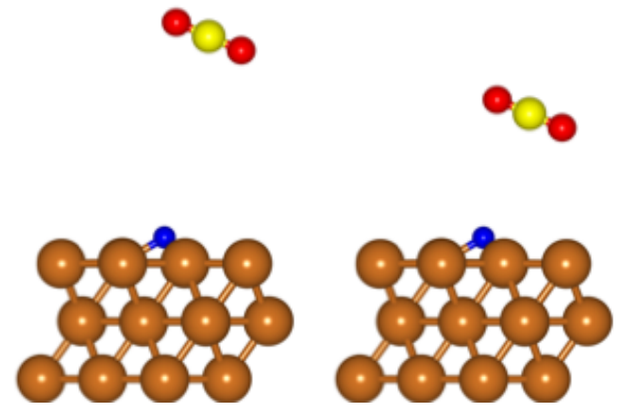

Region II : Pauli repulsion

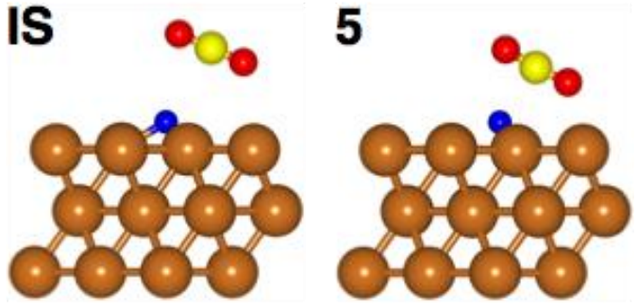

Region III : Bending mode induced reaction

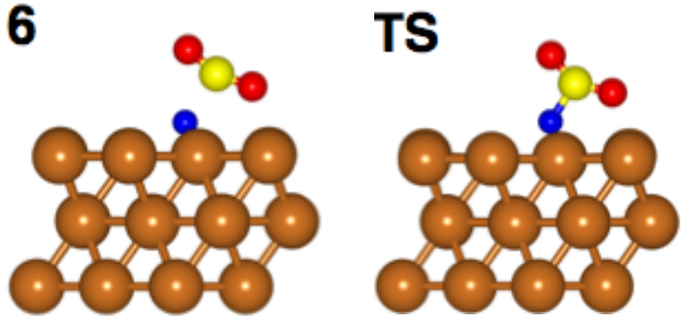

F. Muttaqien, YM *et al.*, ***Chem. Comm.***, 53, 9222(2017).
J. Quan, YM, J. Nakamura *et al.*, ***Nature Chem.***, 11, 722-729 (2019).

CO_2 hydrogenation on Cu(111)

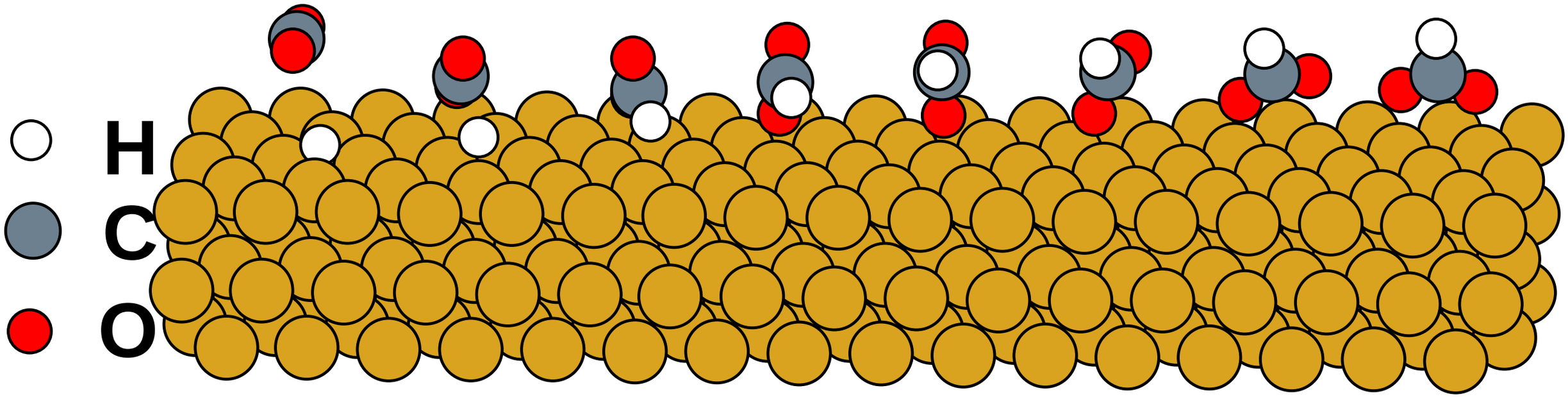

Exp. Activation Barrier = 0.59 ±0.05 eV

Reaction rate is slow:

➔ Insufficient excitation of O-C-O bending mode

✓Excite CO_2 bending mode

⇔ Enhance formate synthesis

Dynamical simulations are necessary to clarify the dependence of the reaction probability on the initial conditions of gas-phase molecules

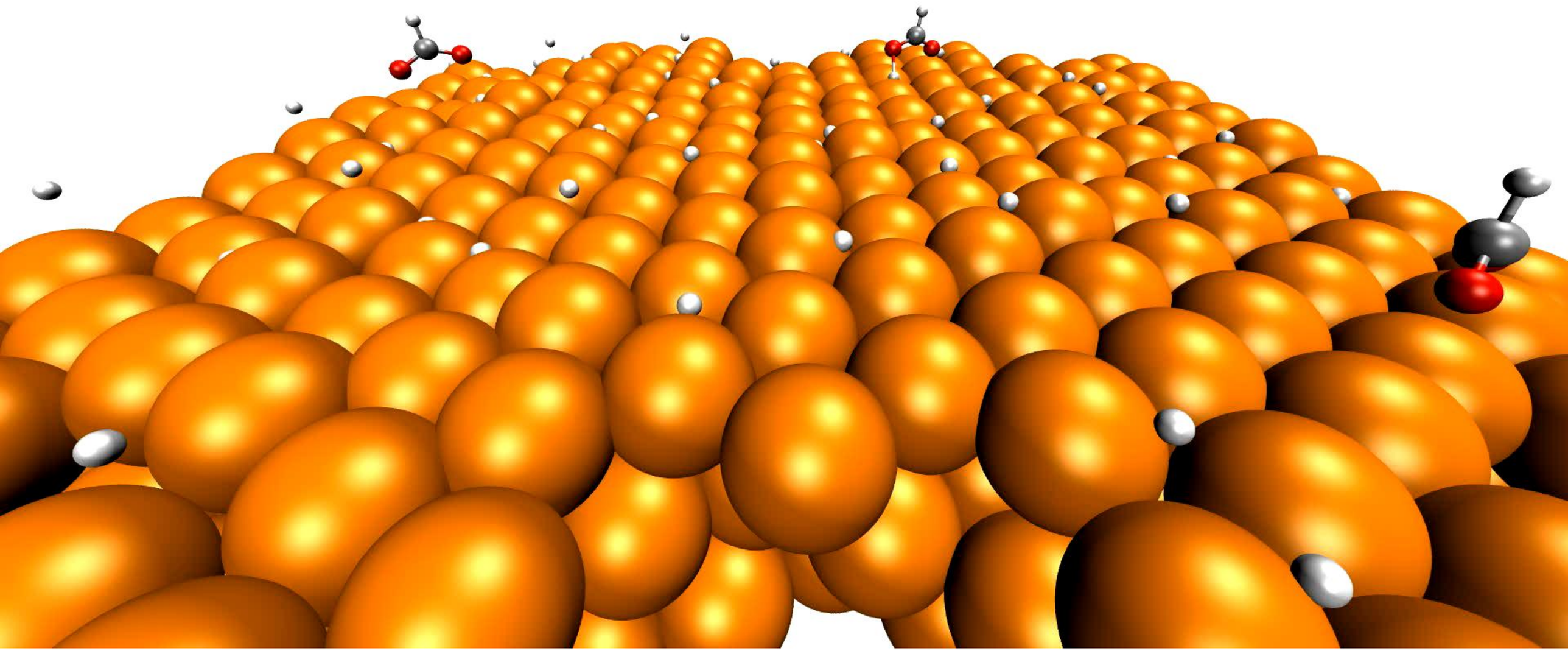

O-C-O bending mode excitation promotes

F. Muttaqien, YM *et al.*, ***Chem. Comm.***, 53, 9222(2017).
J. Quan, YM, J. Nakamura *et al.*, ***Nature Chem.***, 11, 722-729 (2019).

大阪大学

Promotional effect of Cu-Zn alloy

Fujitani, T., et al., *Surface Science*. **1997**, *121,122, 583-586.*

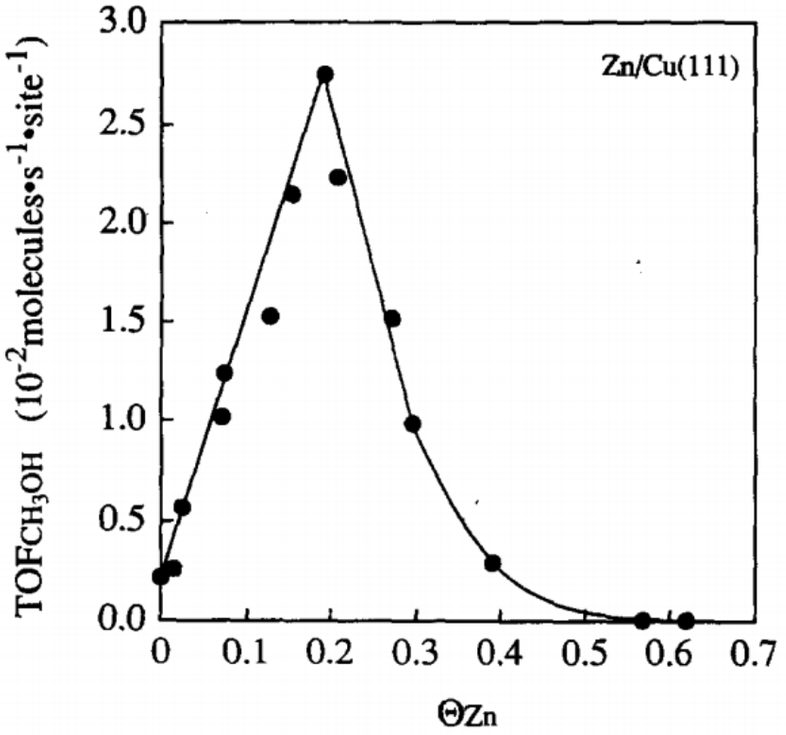

CuZn **increases TOF** by 13-fold at Θ_{Zn} = 0.19

Formation process of Cu-Zn surface

Sano, et.al. *J. Phys. Chem. B*, (2002),106, 31,7627-7633

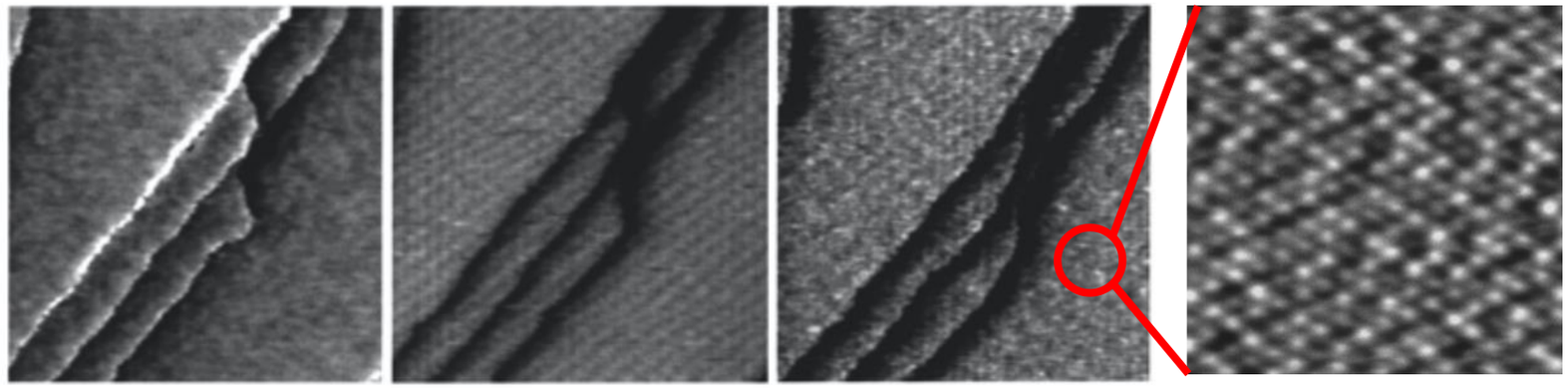

Annealing clean Cu-Zn alloy at 523 K leads to formation of **Zn^{sub}/Cu(111)**

What are the shape of the active sites ?

A	Cu(1 1 1)	Zn^{sub}/Cu(1 1 1)	Zn^{on}/Cu(1 1 1)
$E_f^{HCOO/A}$	−0.50	−0.43	−0.95
$E_f^{TS/A}$	+0.80	+0.88	+0.38
$E_f^{H_2COO/A}$	+0.06	+0.10	−0.28

Zn adatoms can promote the reaction for methanol synthesis

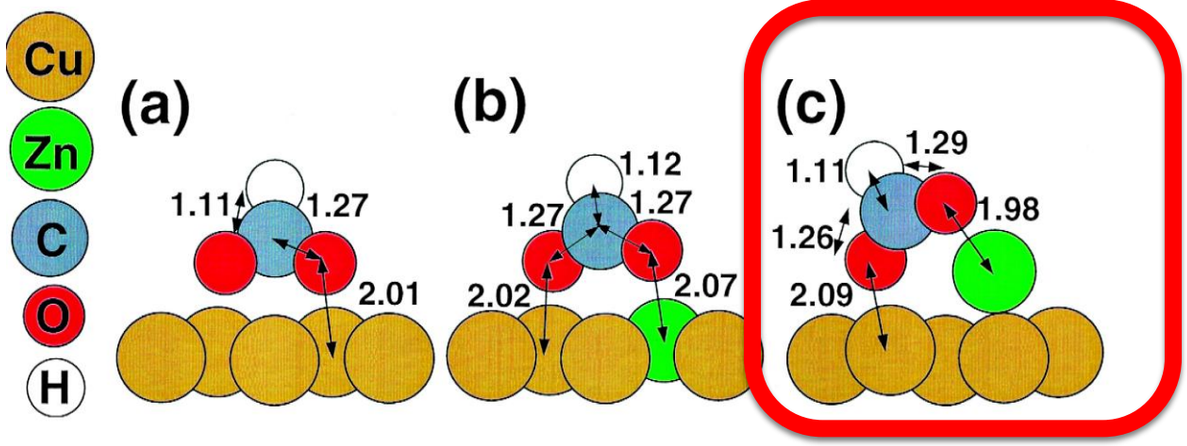

YM, *et al*., . Chem. Phys. Lett., **304**, 91 (1999)
Appl. Surf. Sci., **169–170** 11 (2001)

Cu-Zn stacking faults as active site

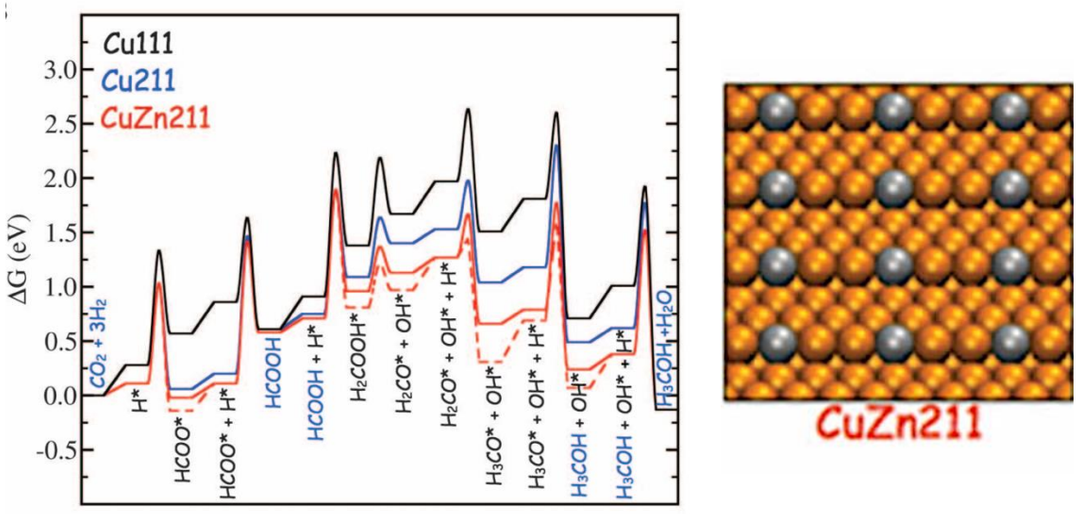

Methanol synthesis is promoted by
Zn atoms located at surface defects.

Behrens et al., *Science*, **336**, 893-897 (2012).

In situ observations are important.

How to elucidate the non-equilibrium states ?

Experimental Approach

➢ Scanning Tunneling Microscope (STM)

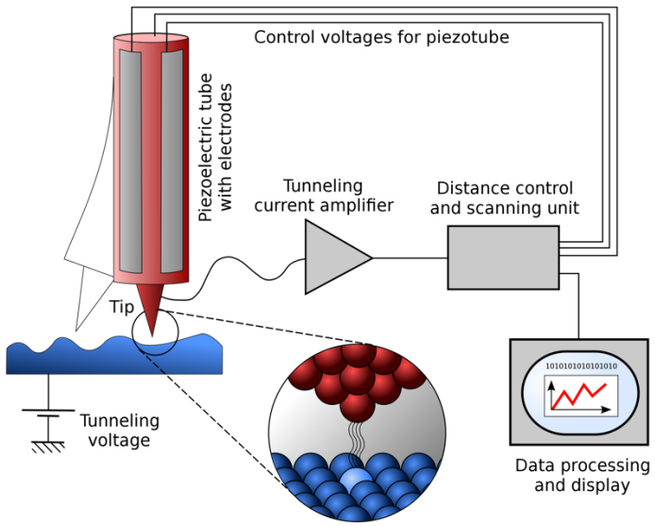

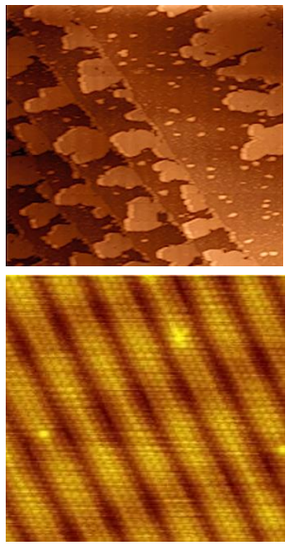

https://en.wikipedia.org/wiki/Scanning_tunneling_microscope

Experiment has difficulty to capture atomistic events

Computational Approach

➢ Single-scale simulations

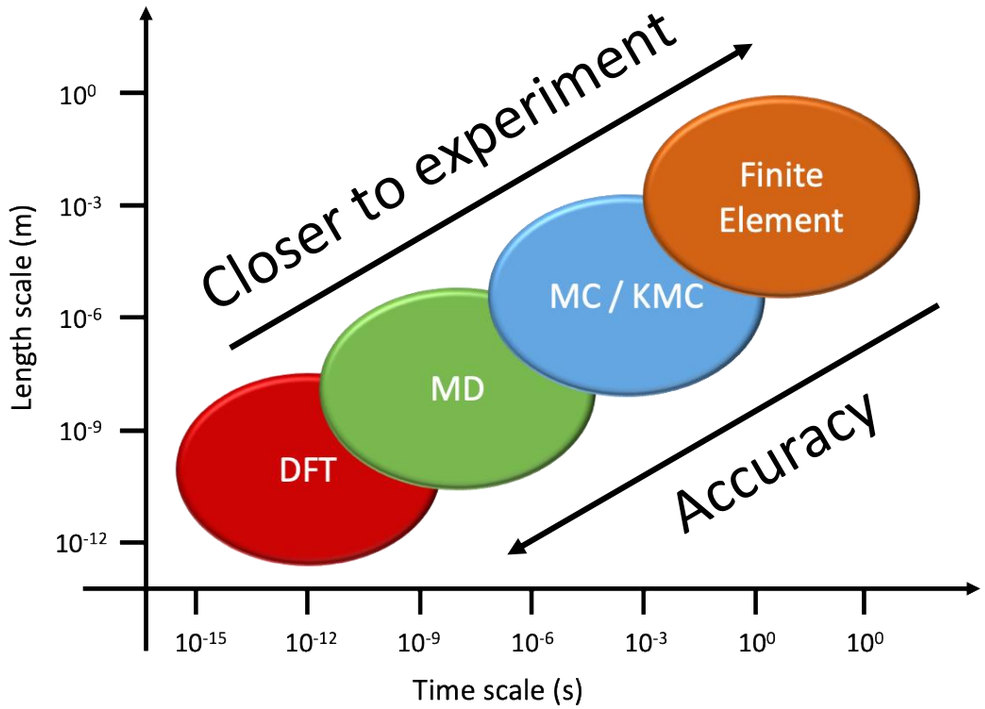

There is a trade-off between scale and accuracy

Multi-scale Simulation

DFT Calculation → “Bridge” → Molecular simulation

Machine learning force-field Molecular Dynamics

✓ Accurate for general chemical species

✓ Feasible for large system and long time scale

Outline

1. Introduction

2. The Elucidation of Cu-Zn Surface Alloying on Cu(997) by Machine-Learning Molecular Dynamics

   H.H. Halim and Y. M, *ACS Phys. Chem. Au*, 5, 430-447 (2022).

3. Machine Learning Molecular Dynamics Simulation of CO-driven Formation of Cu Clusters on Cu(111)

   H.H. Halim, R. Ueda and YM, *J. Phys. Condensed Matter, Special Issue from the Speakers of Surface Science Discussions 2022 and 2023*, in press.

The Elucidation of Cu-Zn Surface Alloying on Cu(997) by Machine-Learning Molecular Dynamics

Harry H. Halim (D3), Yoshitada Morikawa

Graduate School of Engineering

Osaka University

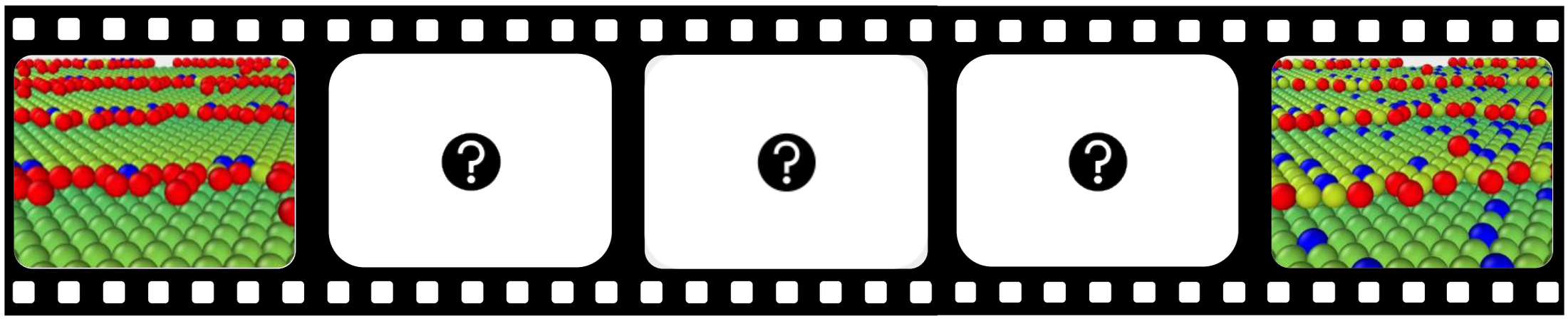

Harry H. Halim and Y. Morikawa, *ACS Phys. Chem. Au*, **5**, 430-447 (2022).

Methodology

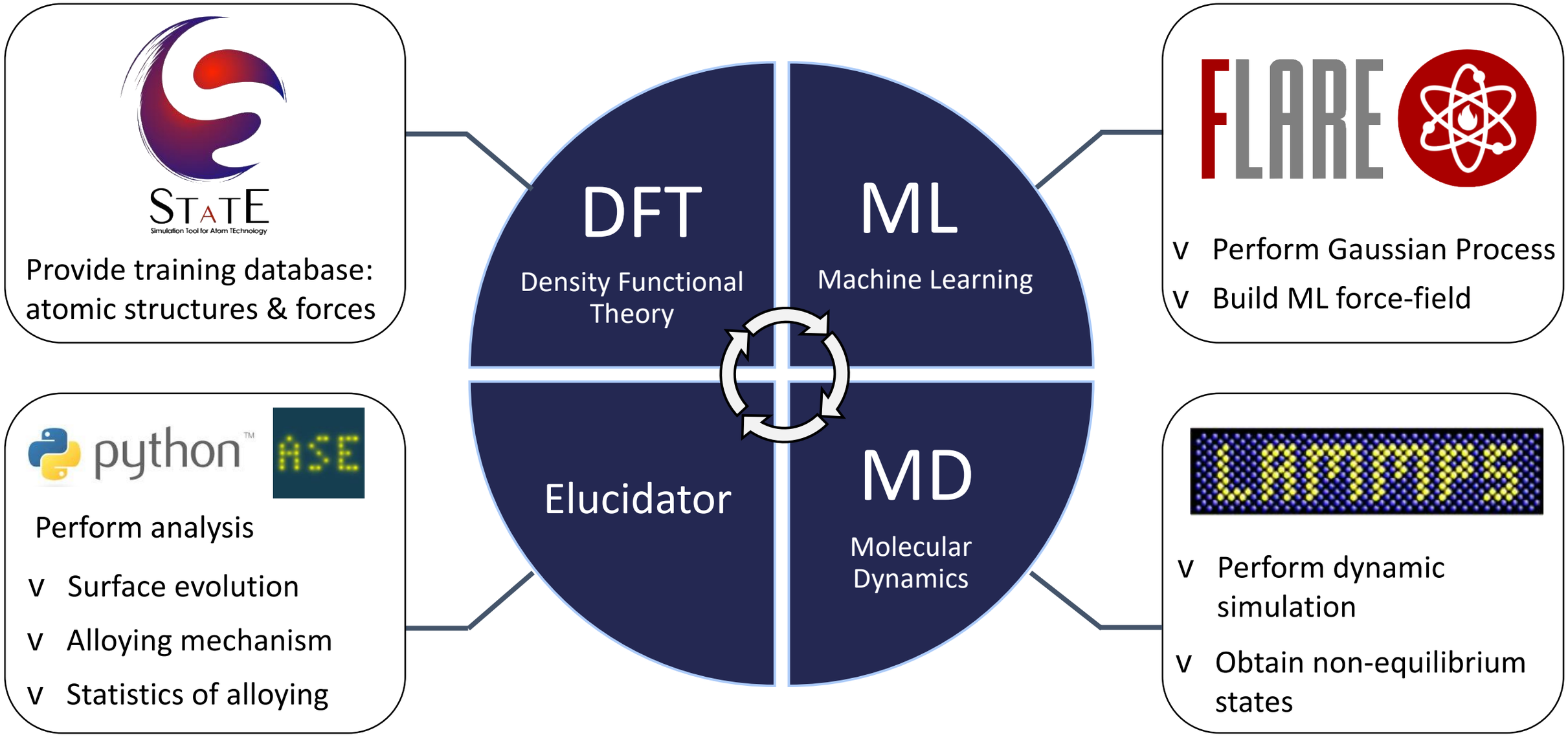

[STATE] Morikawa. Y., et.al, Appl. Sur. Sci 169-170, 11 (2001).

[FLARE] Vandermause. J., et.al, npj Comput Mater 6, 20 (2020).

[LAMMPS] Plimpton, S., J Comp Phys 117, 1-19 (1995).

[Elucidator] https://github.com/hhlim12 (under development)

Gaussian Process Force Field

Vandermause. J., et.al, npj Comput Mater 6, 20 (2020).

Simplifying assumption:

E_i (i.e., local energy of atom i) only depends on small clusters in local environment (ρ_i).

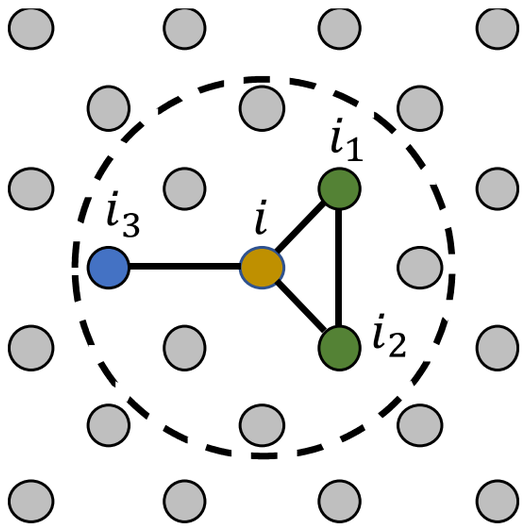

2-body cluster

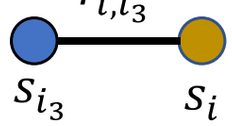

3-body cluster

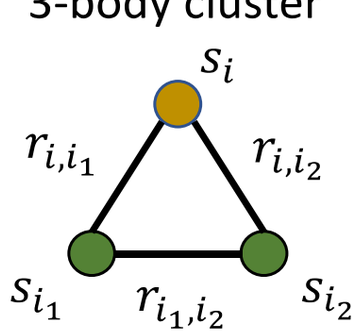

$$E_i = \sum_{n=2}^{\text{max body}} \sum_{i \in \rho_i^{(n)}} \varepsilon_{\boldsymbol{s}_{i,i_1,\ldots,i_{n-1}}}(\boldsymbol{d}_{i,i_1,\ldots,i_{n-1}})$$

$\boldsymbol{s}_{i,i_1,\ldots,i_{n-1}}$: **atomic elements** in the cluster

$\boldsymbol{d}_{i,i_1,\ldots,i_{n-1}}$: **atomic distances** in the cluster

Local energy kernel

$$k(\rho_i, \rho_j) = \sum_{n=2}^{\text{max body}} \sum_{\substack{i \in \rho_i^{(n)} \\ j \in \rho_j^{(n)}}} \sum_{\boldsymbol{P}_n} \delta_{\boldsymbol{s}_{i,i_1,\ldots,i_{n-1}}, \boldsymbol{P}_n \boldsymbol{s}_{\boldsymbol{j},j_1,\ldots,j_{n-1}}} k_n$$

2 and 3 body kernels

$$k_2(r_{i,i_1}, r_{j,j_1}) = \sigma_{s,2}^2 \exp\left(-\frac{(r_{i,i_1} - r_{j,j_1})^2}{2\ell_2^2}\right) f_{\text{cut}}$$

$$k_3(\mathbf{d}_{i,i_1,i_2}, \mathbf{d}_{j,j_1,j_2}) = \sigma_{s,3}^2 \exp\left(-\frac{||\mathbf{d}_{i,i_1,i_2} - \mathbf{d}_{j,j_1,j_2}||^2}{2\ell_3^2}\right) f_{\text{cut}}$$

Force kernel

$$k_{\alpha,\beta}(\rho_i, \rho_j) = \frac{\partial^2 k(\rho_i, \rho_j)}{\partial r_{i,\alpha} \partial r_{j,\beta}}$$

Force prediction

$$f_{i\alpha} = k_{i\alpha}^{-T}(K + \sigma_n^2 I)^{-1}\bar{y}$$

Uncertainty of force prediction

$$\sigma_{i\alpha}^2 = k_{\alpha,\alpha}(\rho_i, \rho_i) - \bar{k}_{i\alpha}^{T}\left(K + \sigma_n^2 I\right)^{-1}\bar{k}_{i\alpha}$$

大阪大学

Active and On-the-fly Learning

Vandermause. J., et.al, npj Comput Mater 6, 20 (2020).

Initial structure
"parent structure"

Do DFT calculation

Data : $\{(\rho_i, \mathbf{F}_i)\}$

GP force-field
$\overline{f_{i\alpha}^*} = \mathbf{k}_{i\alpha}^{*\mathrm{T}}(\mathbf{K} + \sigma^2\mathbf{I})^{-1}\mathbf{t}$

Fast

MD simulation

Fast

Updated structure

Calculate GP force and uncertainty

$\overline{f_{i\alpha}^*} = \mathbf{k}_{i\alpha}^{*\mathrm{T}}(\mathbf{K} + \sigma^2\mathbf{I})^{-1}\mathbf{t}$

$\sigma_{i\alpha}^2 = k_{\alpha,\alpha}(\rho_i, \rho_i) - \mathbf{k}_{i\alpha}^{*\mathrm{T}}(\mathbf{K} + \sigma^2\mathbf{I})^{-1}\mathbf{k}_{i\alpha}^*$

Is GP uncertainty < threshold ?

Yes

Keep GP force
(use old force-field)

No

Discard GP force

Slow

Do DFT calculation

Data : $\{(\rho_i, F_i)\}$

Update GP force-field &
Train hyperparameters

Only data with high uncertainty are included

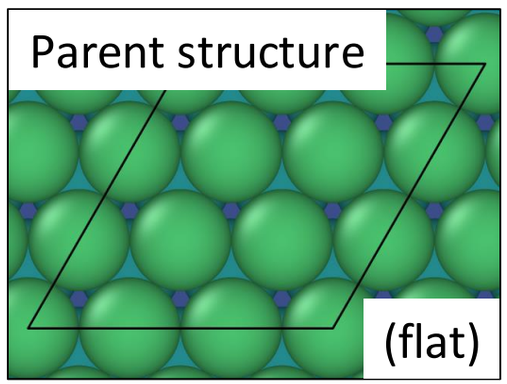

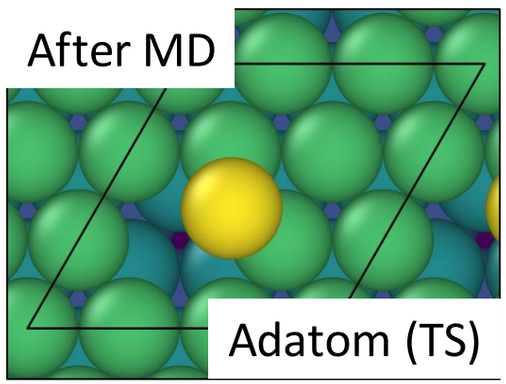

High
Uncertainty

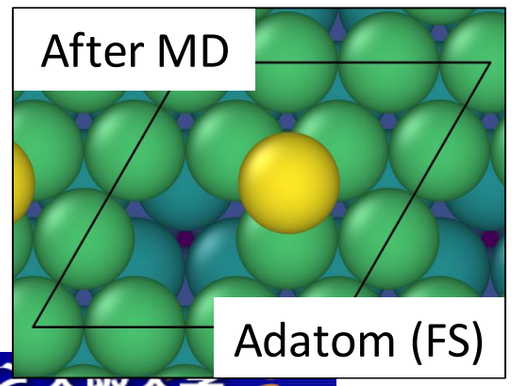

Database

Remarks of the on-the-fly learning:

- The data is still affected by parent structure
- It is a serial process, bottle-necked by DFT

Database & Validation of Force-field

- ❖ The database is built using *active and on the fly* learning.
- ❖ Important surfaces features are included in the database.

STATE
Simulation Tool for Atom TEchnology

FLARE

List of Surface Features

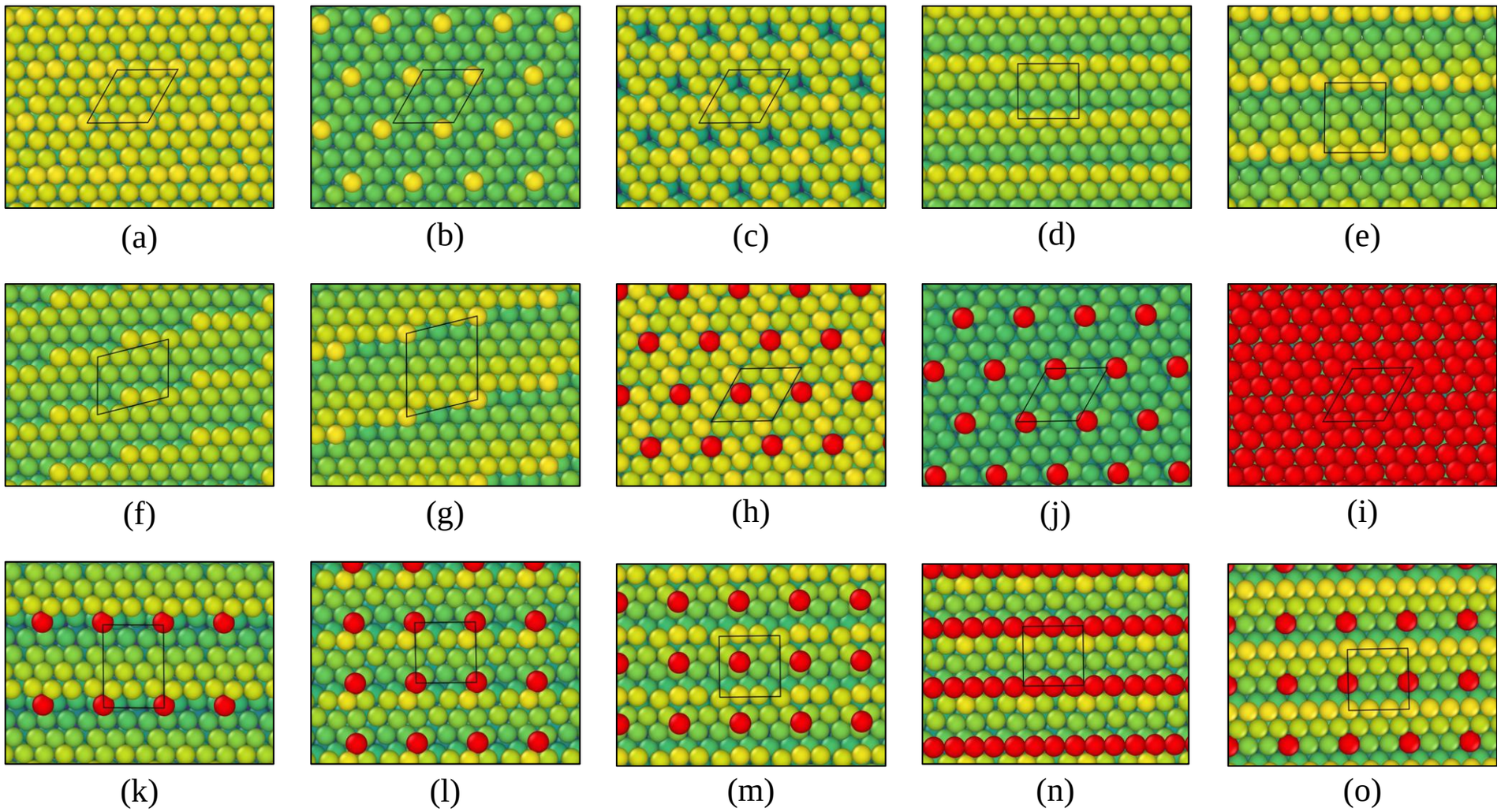

Final database : 326 atomic envs.

大阪大学

Validation of *force-field*

Cu activation energies

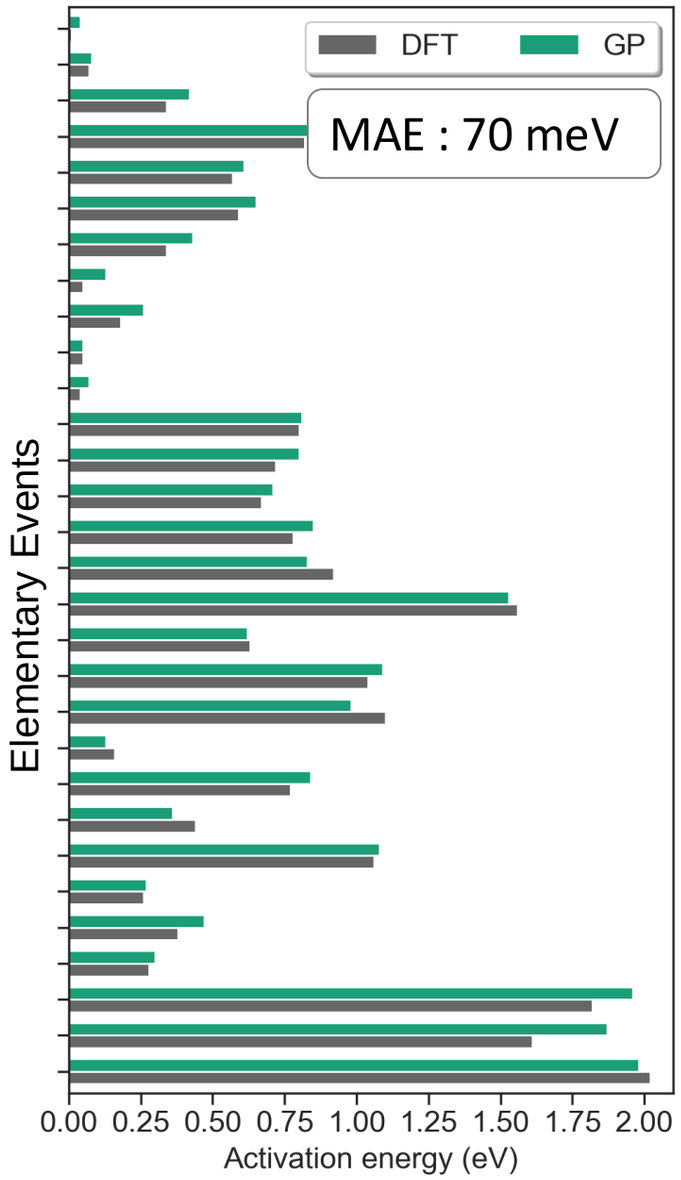

Zn activation energies

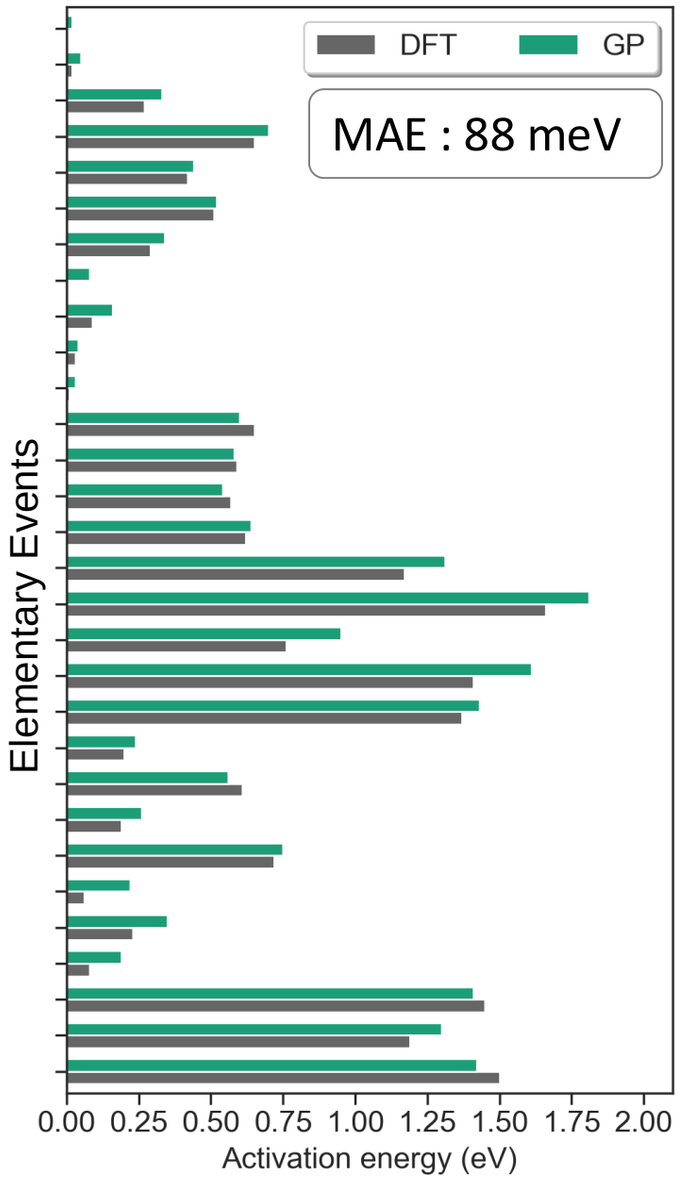

Force components

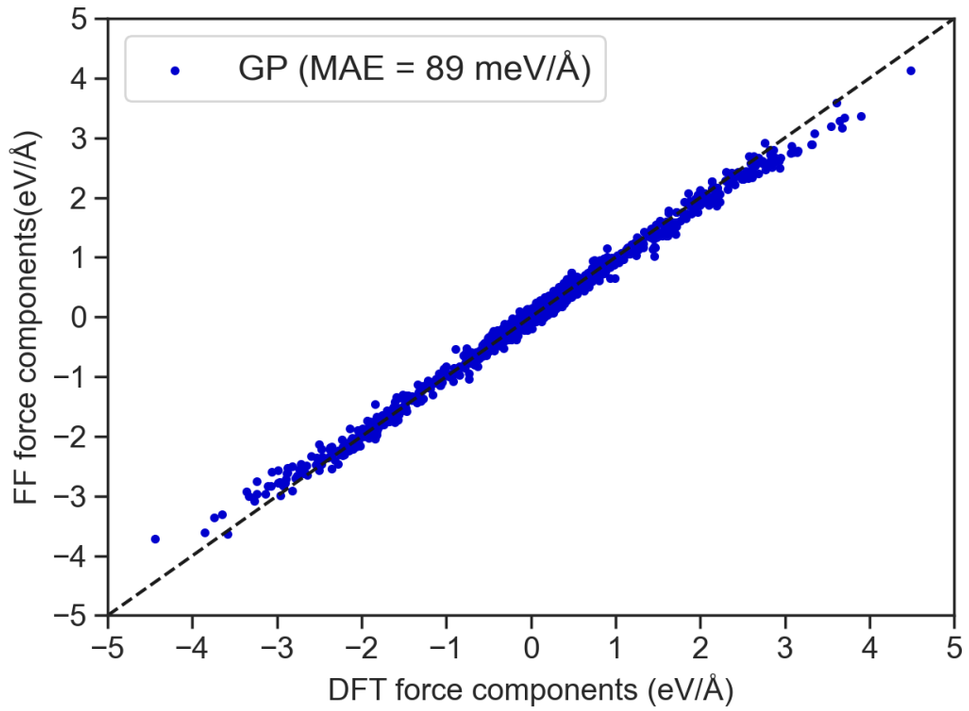

Test set to validate forces consists of **357 highest uncertainty envs.** during 2 μs MD simulation.

The test set to validate activation energy consists of **94 elementary events** involving Cu and Zn atoms.

MD Preparations

Definitions used in surface model (Cu(997) – Zn alloy)

Cu $Zn^{(ad)}$ $Zn^{(sub)}$

Side View

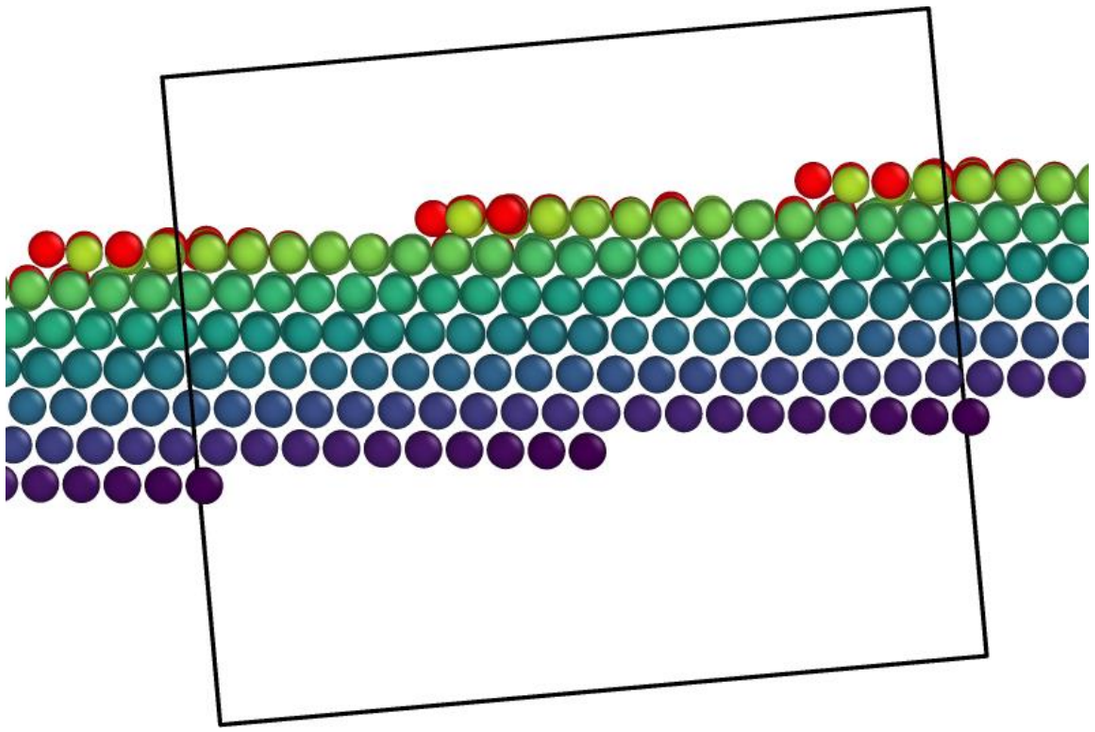

20 rows x 20 columns = 400 atoms / layer

Top View

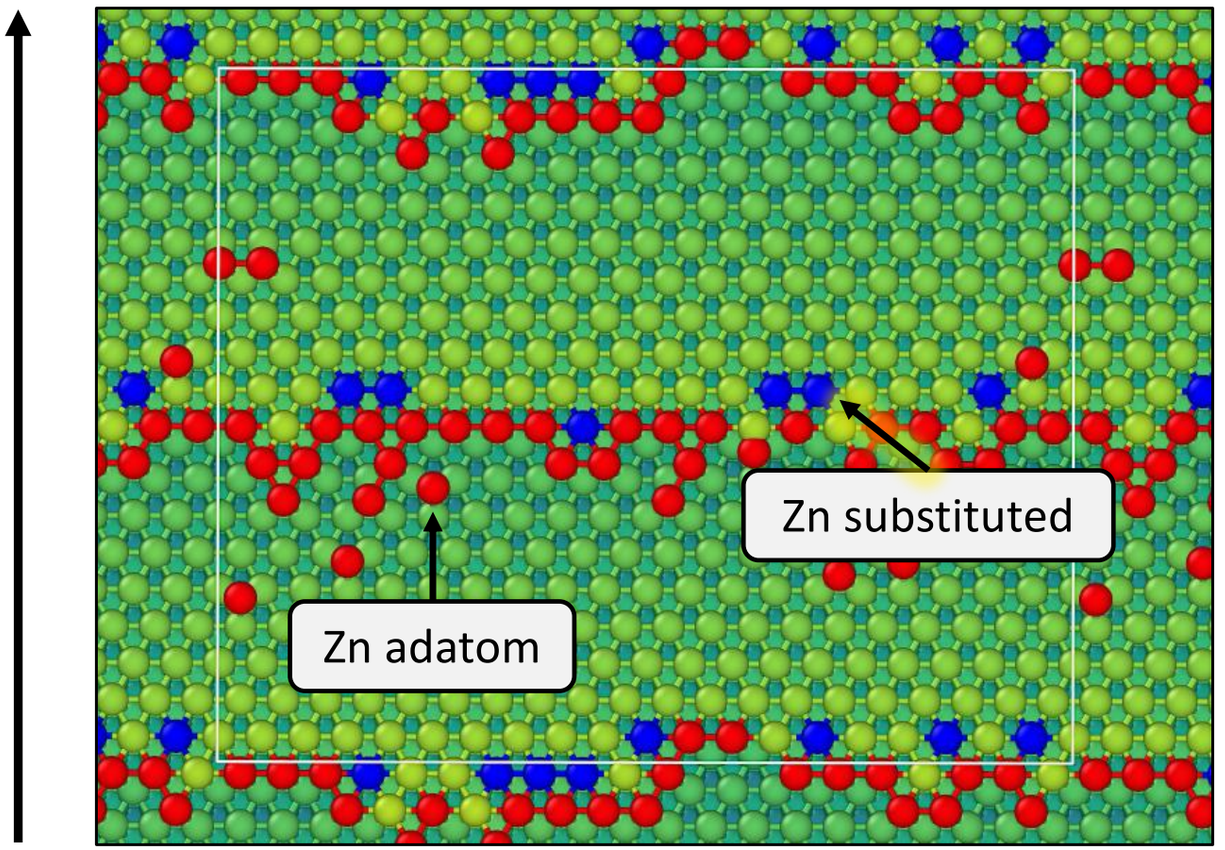

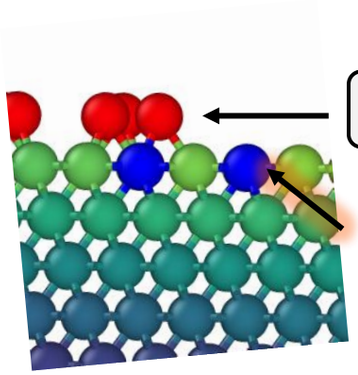

Results and Discussion

Evolution of Zn Atoms on Cu(997) at 700 K

Cu $Zn^{(ad)}$ $Zn^{(sub)}$

MLMD Observation on Formation of Cu-Zn Surface

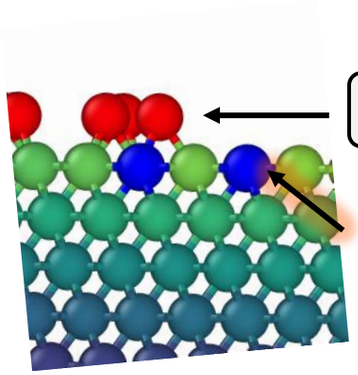

Zn adatom CN < 9

Zn substituted CN ≥ 9

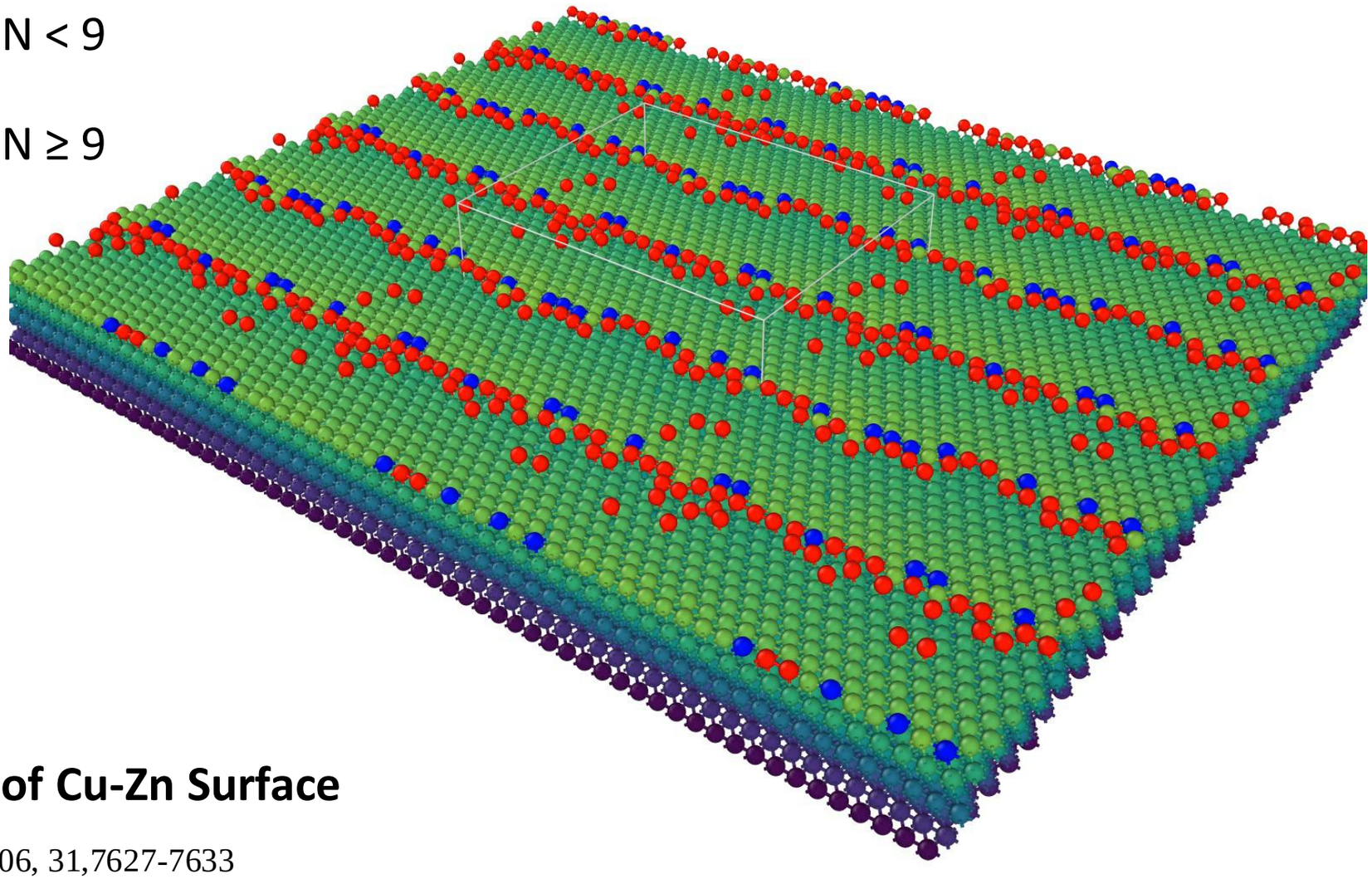

STM Observation on Formation of Cu-Zn Surface

Sano, et.al. *J. Phys. Chem. B,* (2002),106, 31,7627-7633

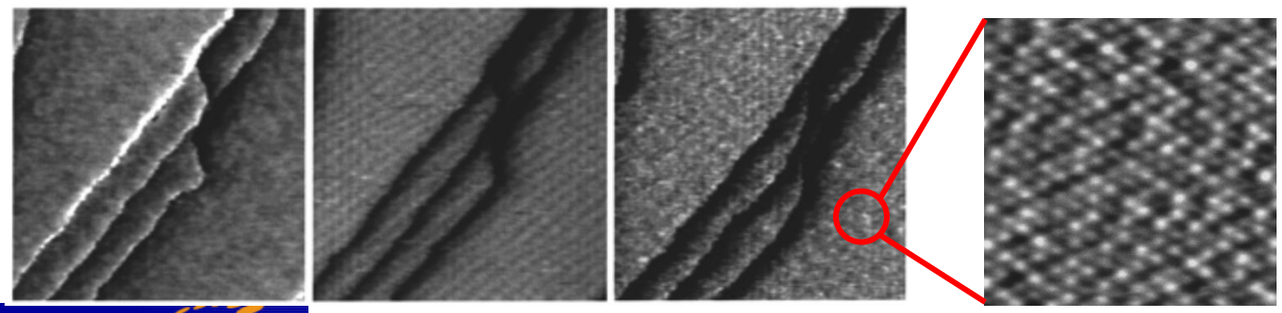

The MLMD and STM show Zn alloyed from the **step edge** to **middle terrace**.

大阪大学

Results and Discussion

Evolution of Zn Atoms on Cu(997) at 700 K $\Delta t = 5\ fs$

Cu $Zn^{(ad)}$ $Zn^{(sub)}$

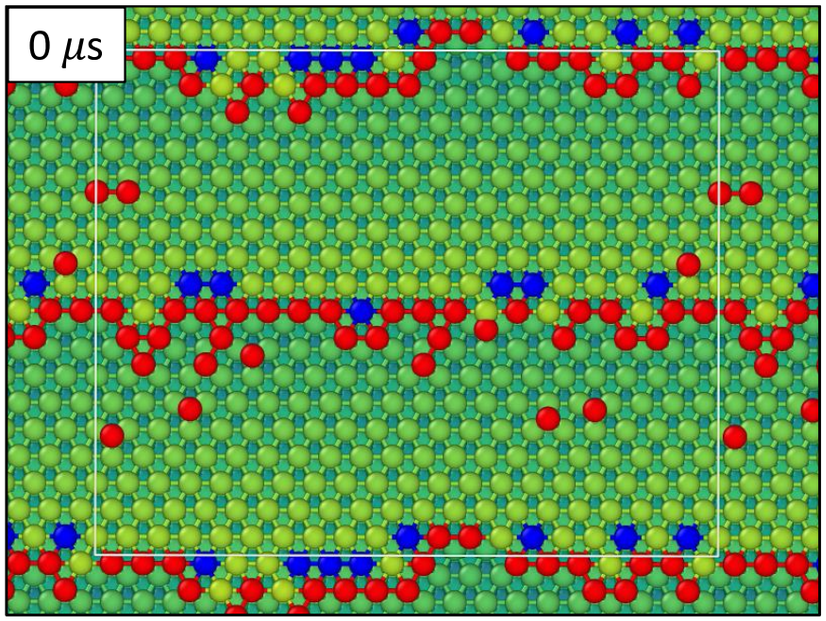

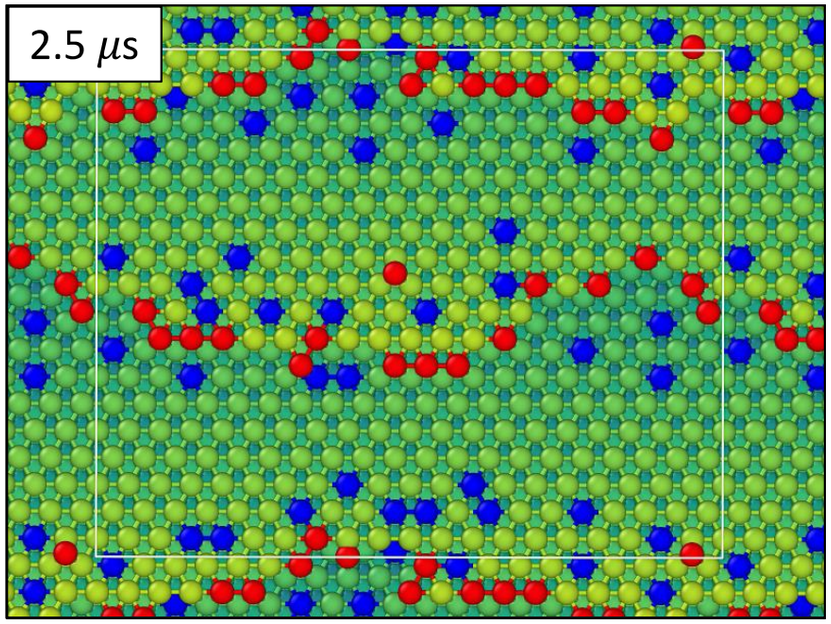

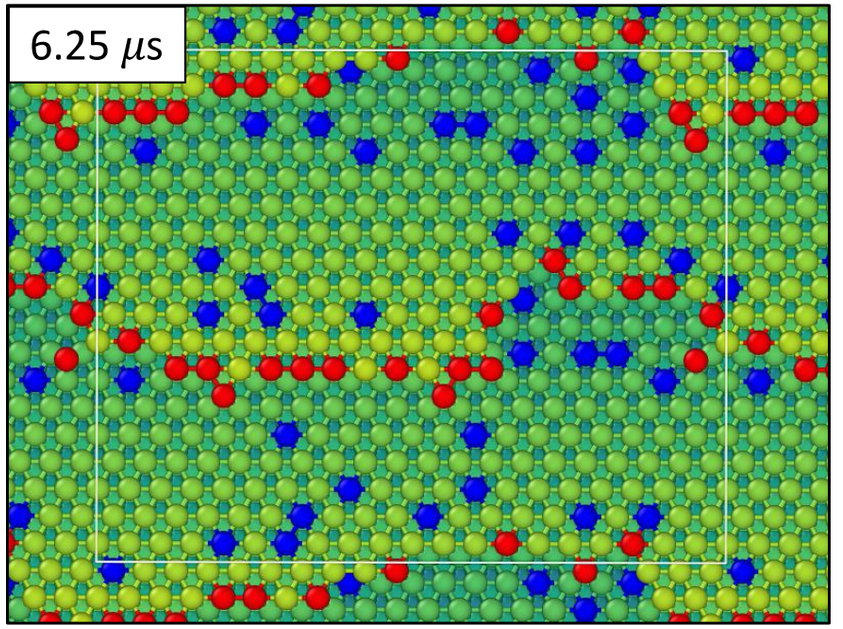

Initially most of the Zn attach to the step edge

Zn incorporate the upper and lower terrace

Some Zn atoms are incorporated at middle terrace

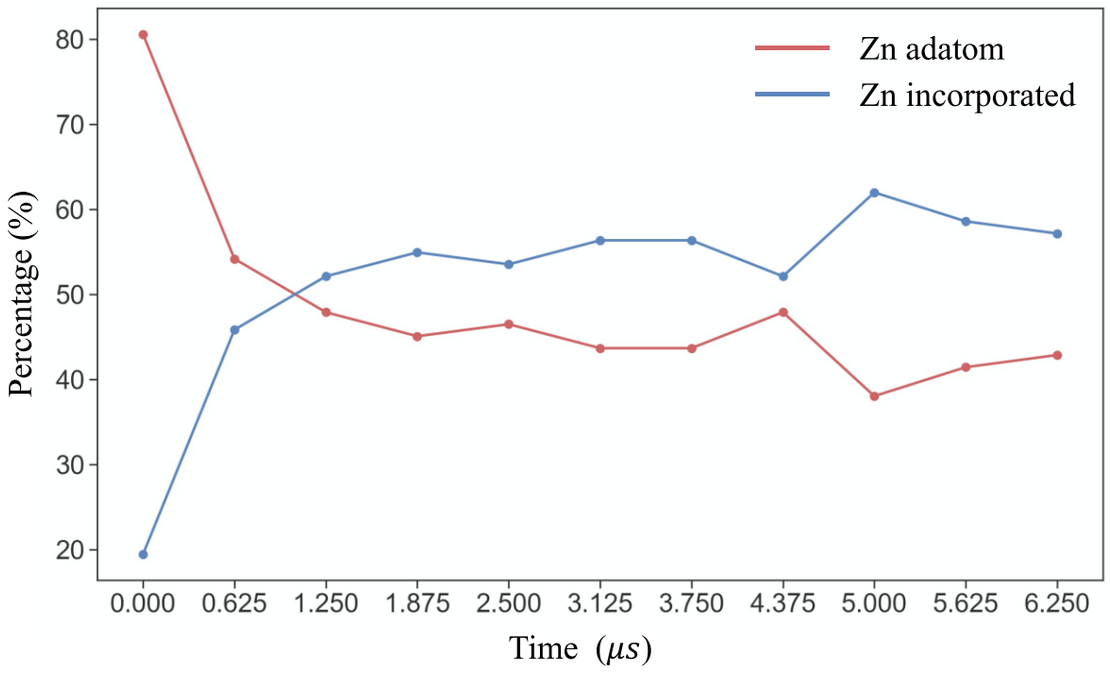

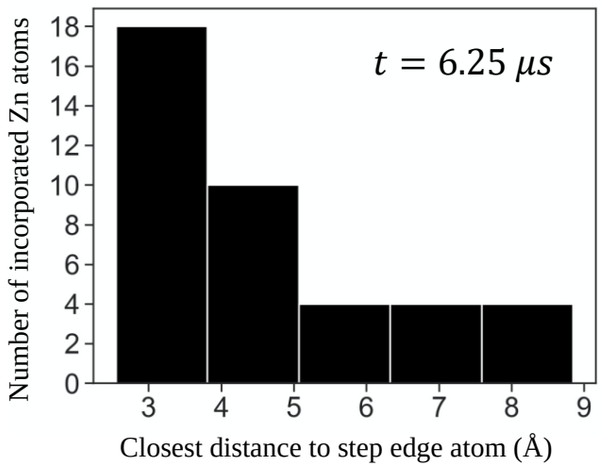

Zn mostly incorporate region near step edge.

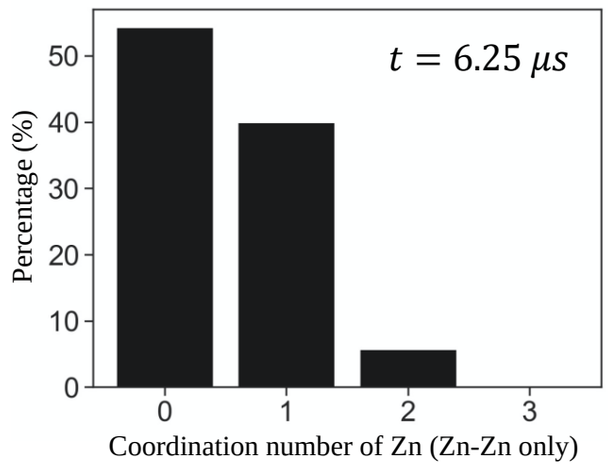

No significant Zn-Zn interaction in the alloy.

大阪大学

A. Dominant Alloying mechanisms at **Upper Terrace**

A.1 Confinement by other step adatoms (75 alloying events)

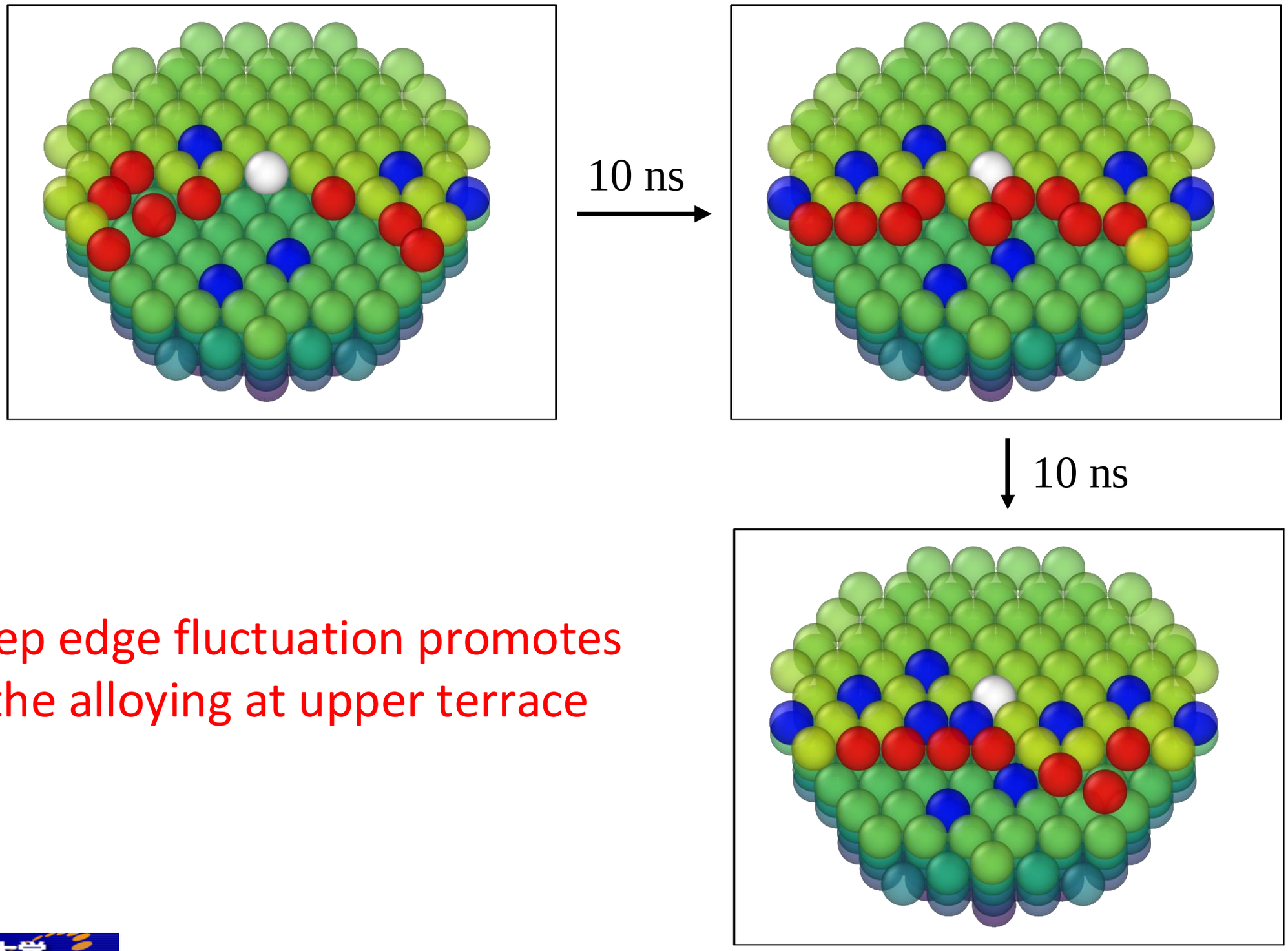

Step edge fluctuation promotes the alloying at upper terrace

B. Dominant alloying mechanisms at **Lower terrace**

B.1 Step-assisted direct exchange (45 alloying events)

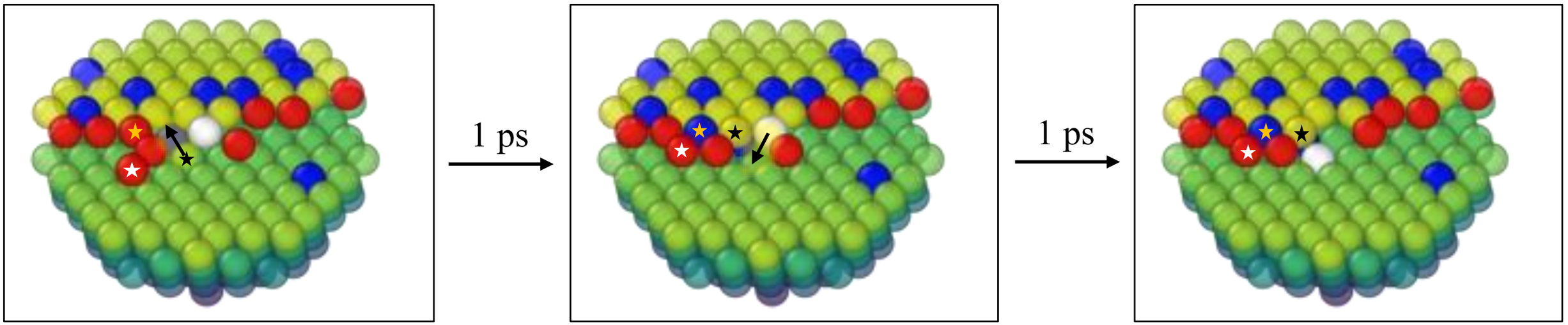

Energy barrier of direct exchange process

	Initial state		Final state		Energy barrier (eV)
	Zn	Cu	Zn	Cu	
Without step edge	Adatom on terrace	Terrace-atom	Terrace-atom	Adatom on terrace	1.37
With step edge	Adatom on terrace	Lower terrace	Lower terrace	Adatom at step edge	0.76

Steps and kinks promote atom kick out process.

C. Dominant alloying mechanisms at **Middle terrace**

C.1. Wave deposition (18 alloying events)

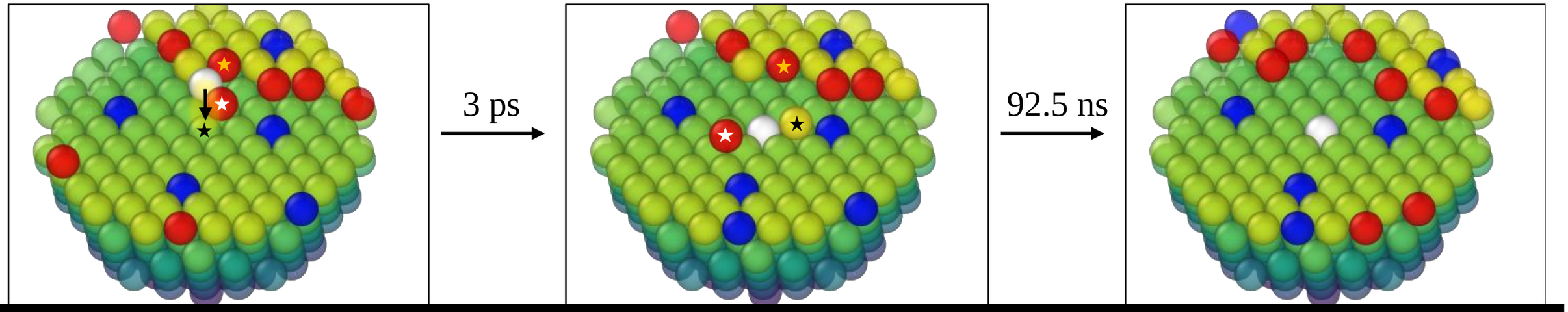

Steps help transporting Zn atoms to middle terrace

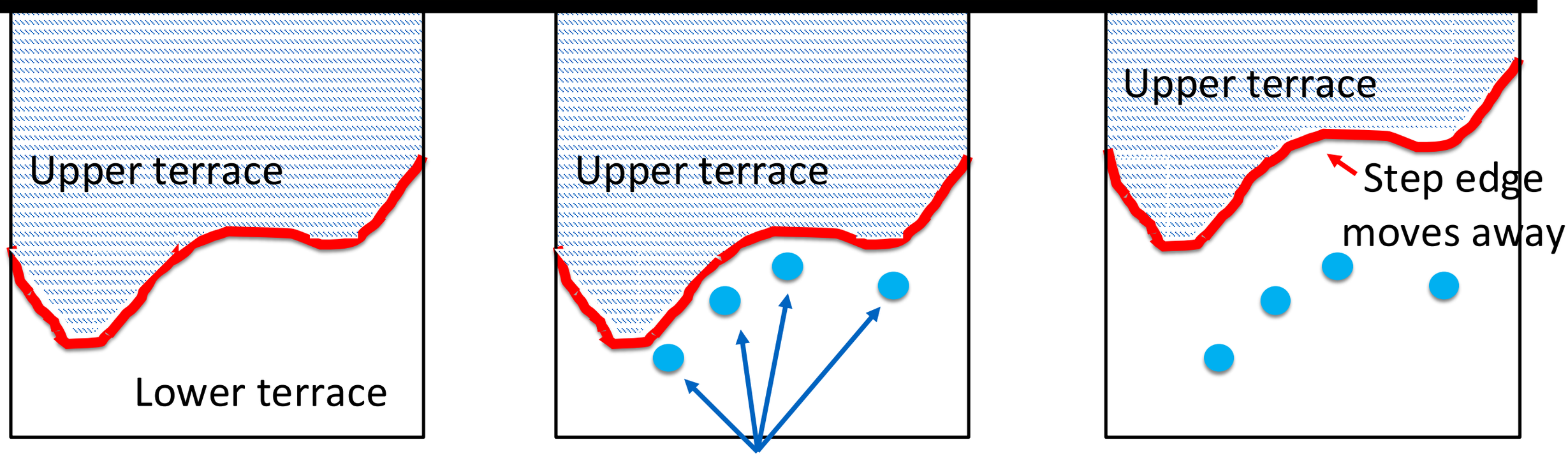

C. Classification of the alloying mechanisms (**Middle terrace**)

C.2 Confinement by other step adatoms (15 alloying events)

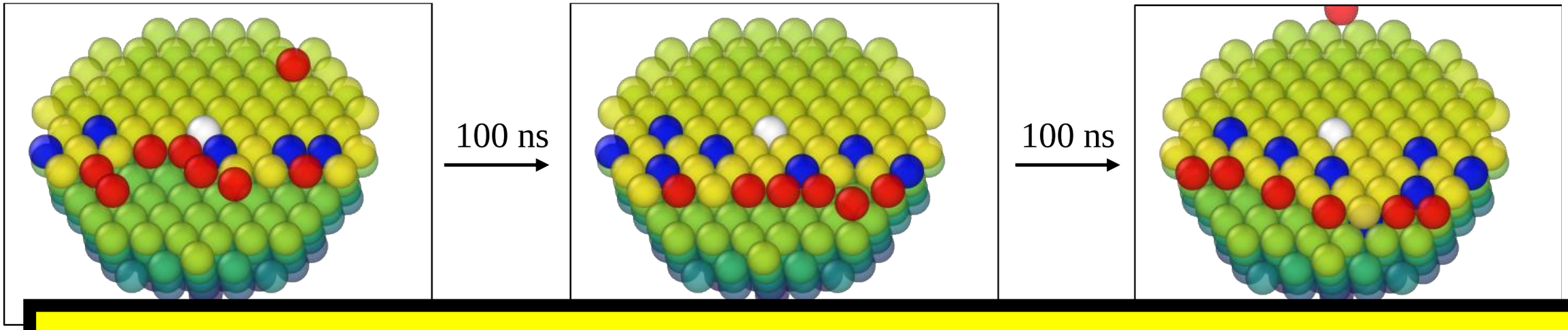

Even at middle terrace, steps play an important role in the formation of Cu-Zn alloy

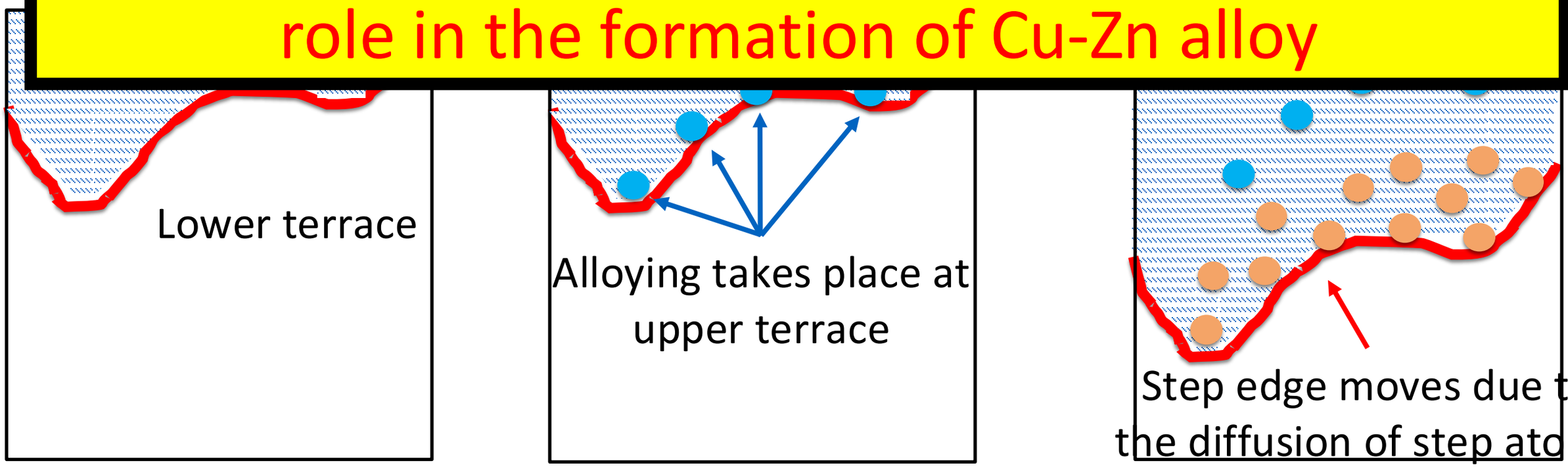

Summary and Conclusions of the first topic

- The alloying process of Cu-Zn surface were investigated **by machine-learning molecular dynamics**.

- The surface alloying is initiated at **upper and lower terraces** near the step edge.

- The rationalization of alloying behavior are performed.

Surface Region	Dominant Mechanism
Upper Terrace	**Confinement of Zn step adatom**
Lower Terrace	**Step-assisted Direct Exchange**
Middle Terrace	**Deep confinement** and **Wave deposition**

- Step edge contributes to the surface alloying in all surface region: **upper terrace**, **lower terrace**, and **middle terrace**.

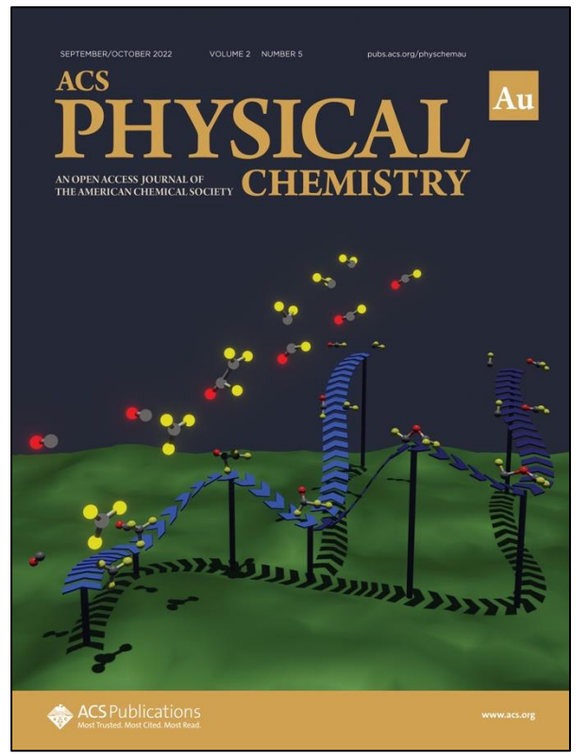

H. H. Halim and Y. Morikawa. ***ACS Phys. Chem Au,*** 2022, 2, 5, 430–447.

Outline

1. Introduction

2. The Elucidation of Cu-Zn Surface Alloying on Cu(997) by Machine-Learning Molecular Dynamics

H.H. Halim and Y. M, *ACS Phys. Chem. Au*, 5, 430-447 (2022).

3. Machine Learning Molecular Dynamics Simulation of CO-driven Formation of Cu Clusters on Cu(111)

H.H. Halim, R. Ueda and YM, ***J. Phys. Condensed Matter, Special Issue from the Speakers of Surface Science Discussions 2022 and 2023*****, 35, 495001 (18pp) (2023).**

Machine Learning Molecular Dynamics Simulation of CO-driven Formation of Cu Clusters on Cu(111)

Harry H. Halim (D3), Ryo Ueda, Yoshitada Morikawa

Graduate School of Engineering
Osaka University

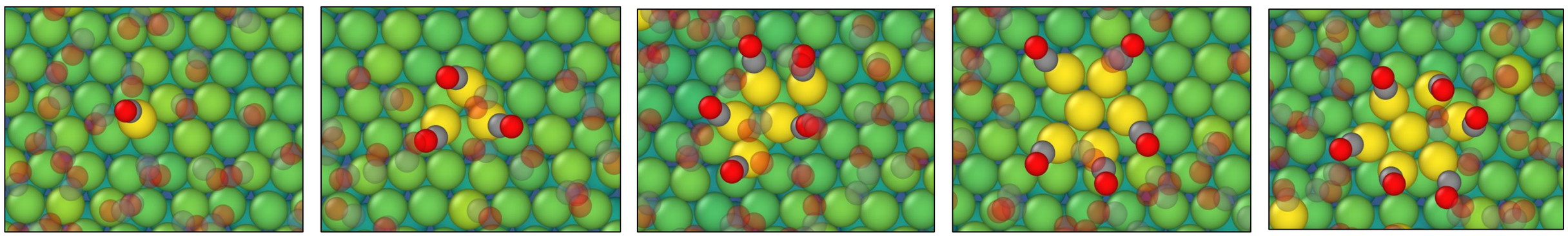

H.H. Halim, R. Ueda and YM, J. *Phys. Condensed Matter, Special Issue from the Speakers of Surface Science Discussions 2022 and 2023*, **35**, 495001 (2023).

Introduction

The role of CO in methanol synthesis

Synthetic Gas (CO / CO_2 / H_2) —$Cu/ZnO/Al_2O_3$, $200^oC – 300^oC$→ Methanol + Water

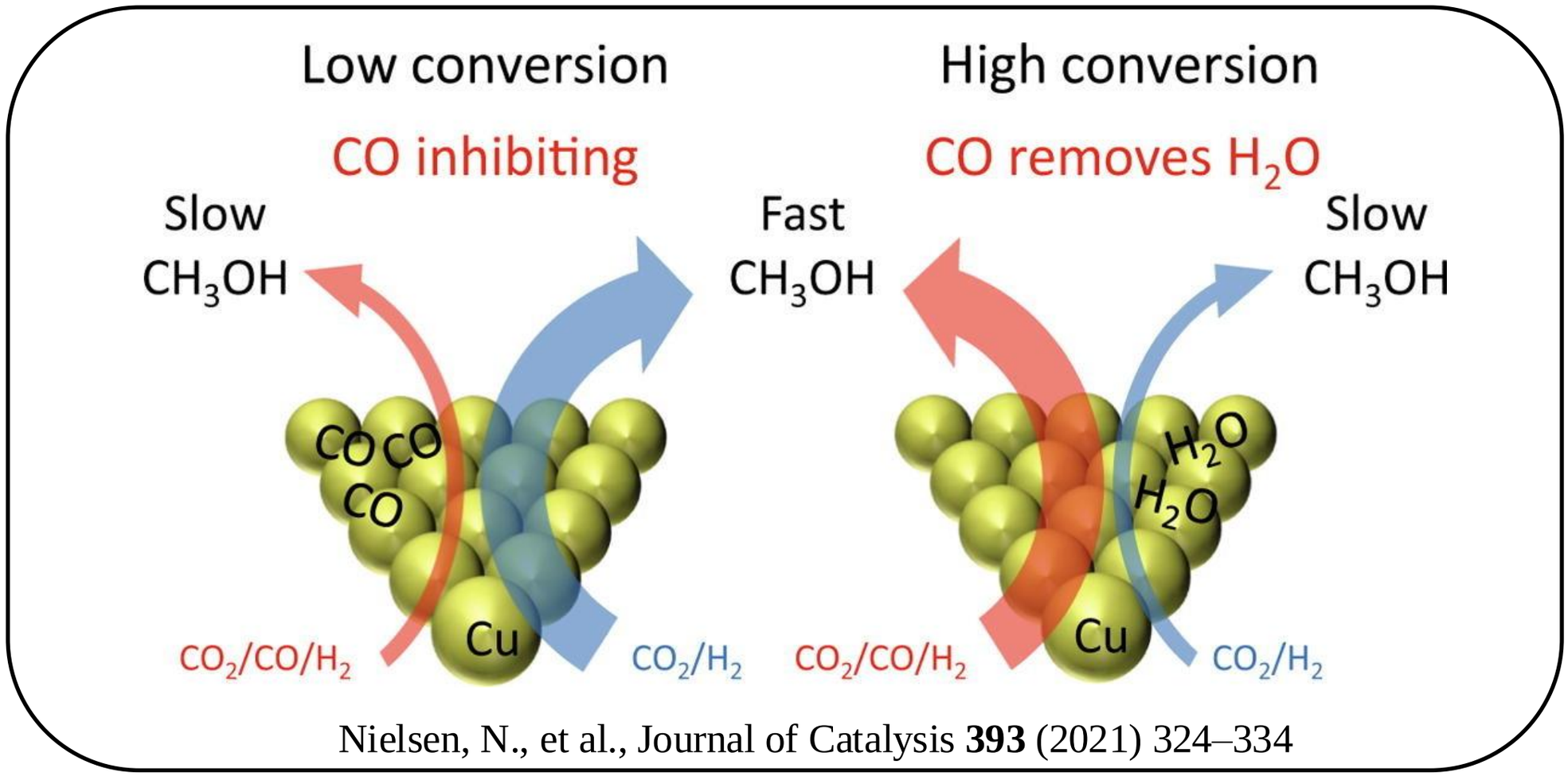

Nielsen, N., et al., Journal of Catalysis **393** (2021) 324–334

- ❖ CO becomes **inhibitor** during **low conversion** of methanol synthesis
- ❖ CO becomes **promoter** during **high conversion** of methanol synthesis

Origin of the promotion effect of CO

CO-induced formation of Cu clusters on Cu surfaces

Eren, B. *et al*., Science, **351** (2016), 475-478.

CO Pressure

0 ML 0.06 ML 0.09 ML > 1 ML

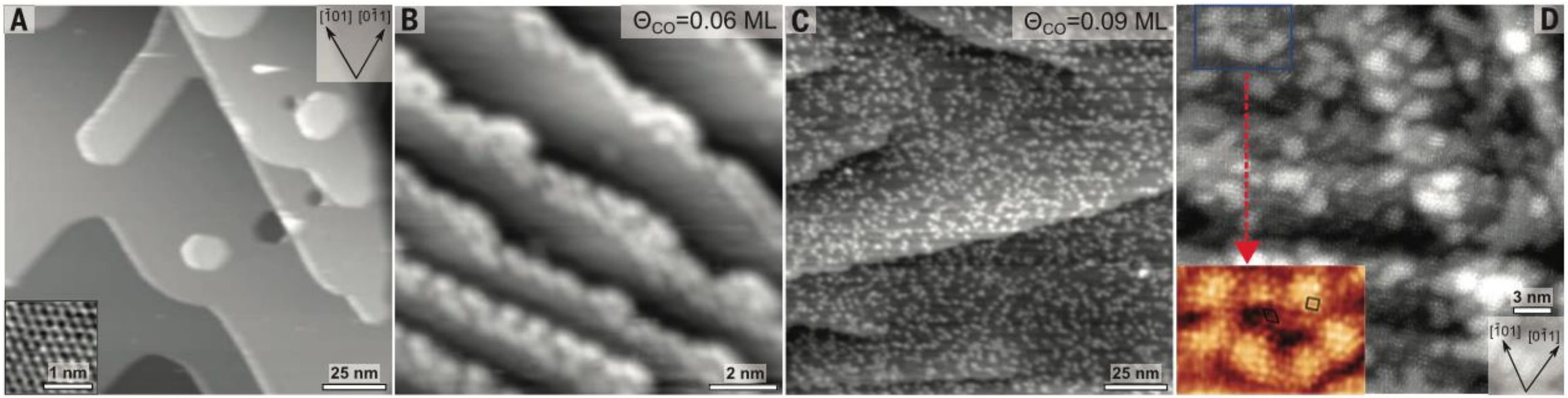

❖ Cu stepped surface decomposes into **clusters** when exposed to CO

❖ Cu clusters are active for water dissociation in RWGS reaction

❖ CO might affect the catalysis by transforming the Cu surface.

Methodology

- ❖ CO and Cu dynamics are indispensable in the description of catalysis
- ❖ MLMD can be used to capture the accurate dynamics efficiently

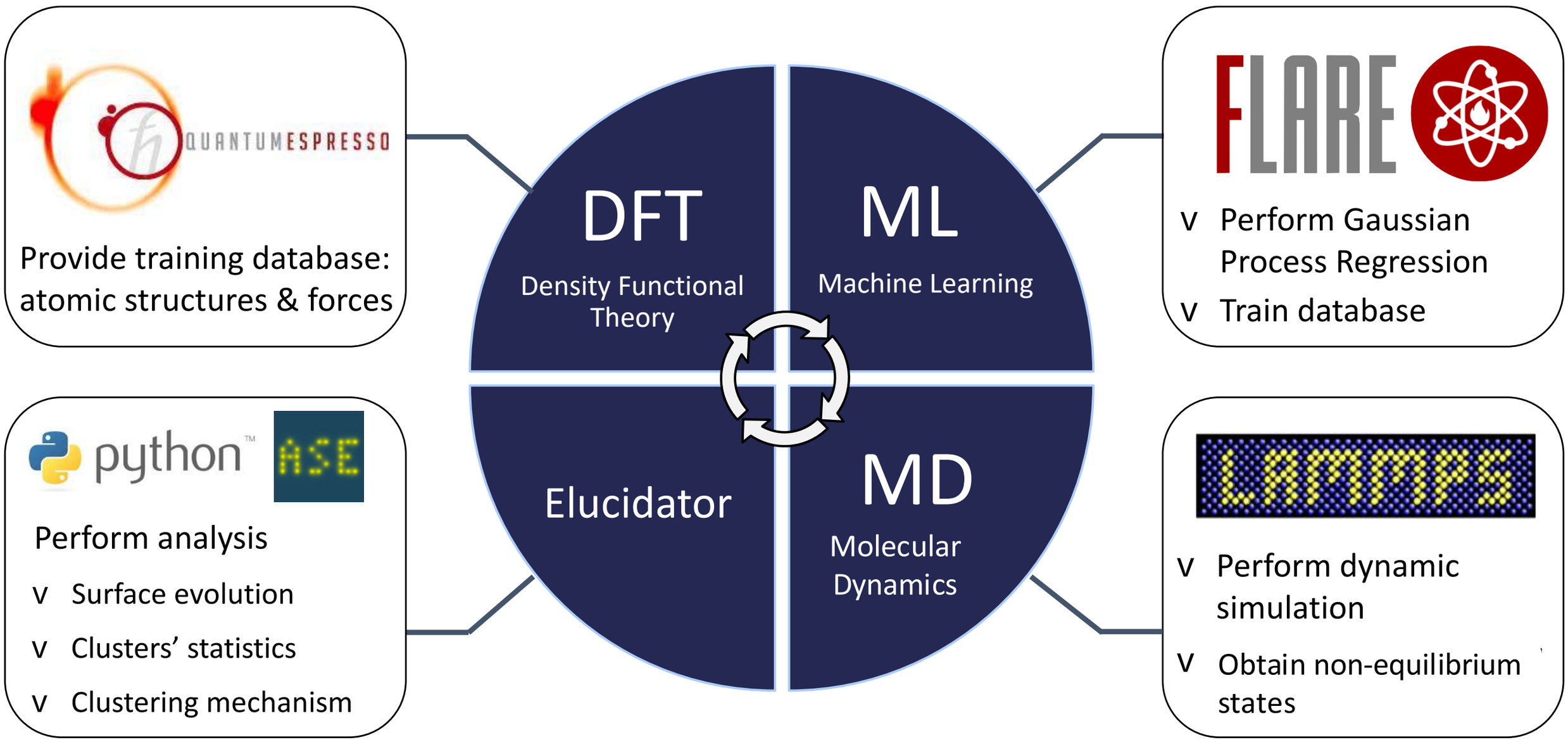

[QE] P. Giannozzi., et.al, J. Phys. Condens. Matter 21 39550 (2009).

[ASE] Ask Hjorth Larsen, et al., J. Phys.: Condens. Matter Vol. **29** 273002, 2017

[FLARE] Vandermause. J., et.al, npj Comput Mater 6, 20 (2020).

[LAMMPS] Plimpton, S., J Comp Phys, 117, 1-19 (1995).

Methodology
Generate the database

❖ Training is done by active and on-the-fly learning

List of surface features

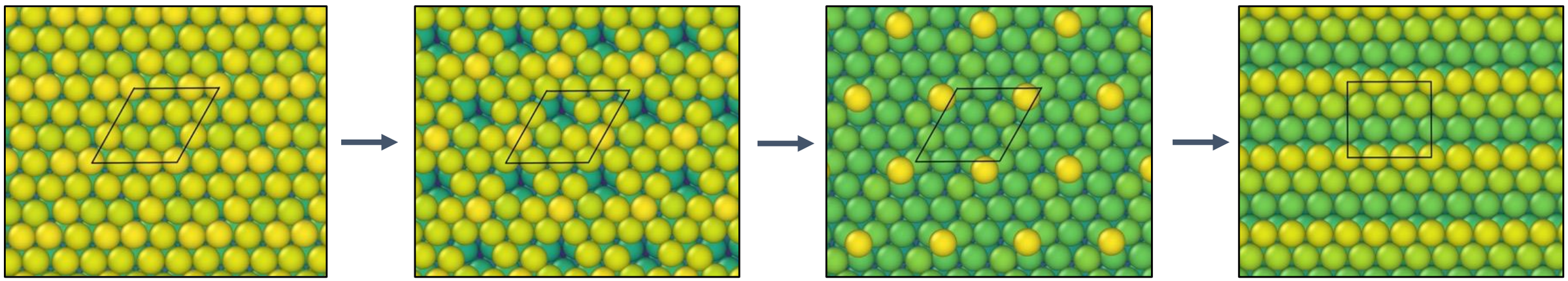

Cu flat | Cu vacancy | Cu + Cu-clusters | Cu stepped

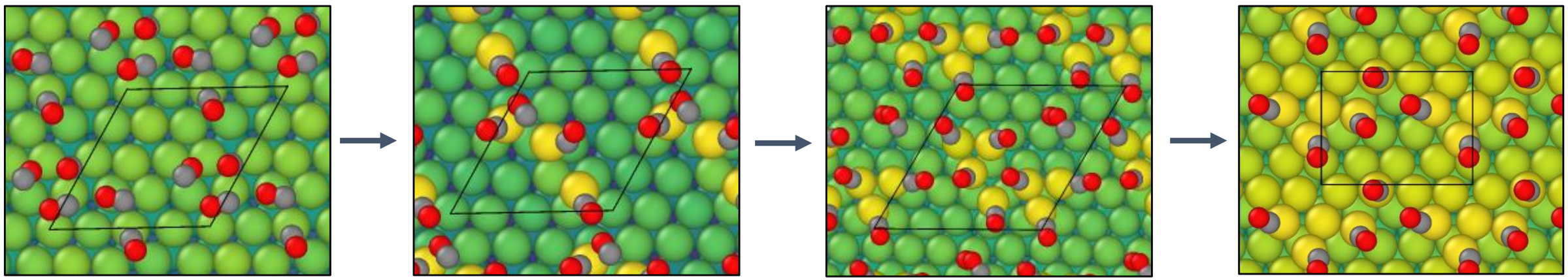

Cu flat + CO | Cu adatoms + CO | Cu-clusters + CO | Cu stepped + CO

❖ Final dataset consists of 3,000 local environments

Methodology
Validation of ML model (MAE and uncertainty)

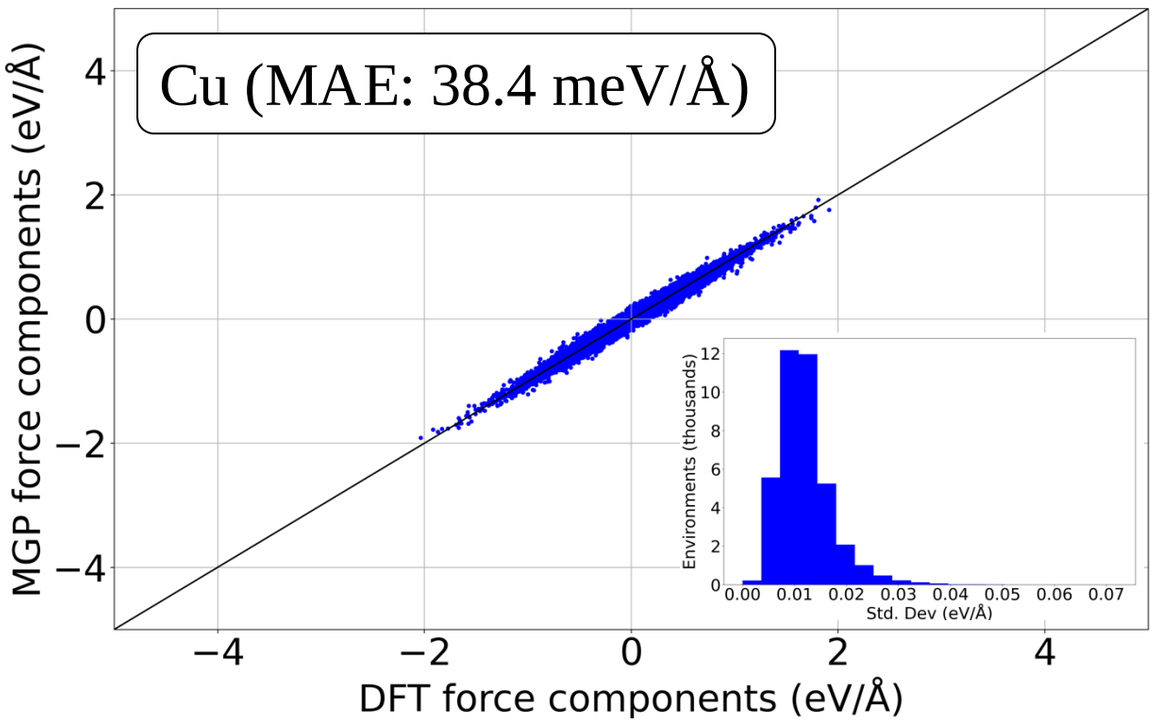

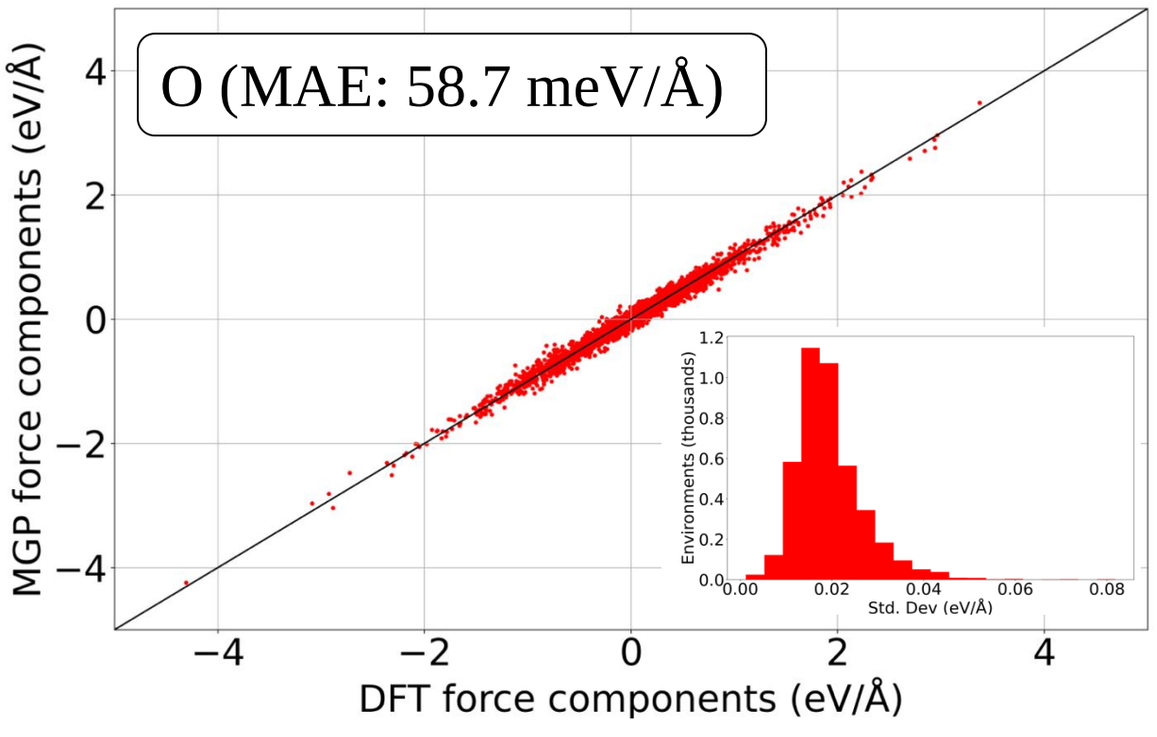

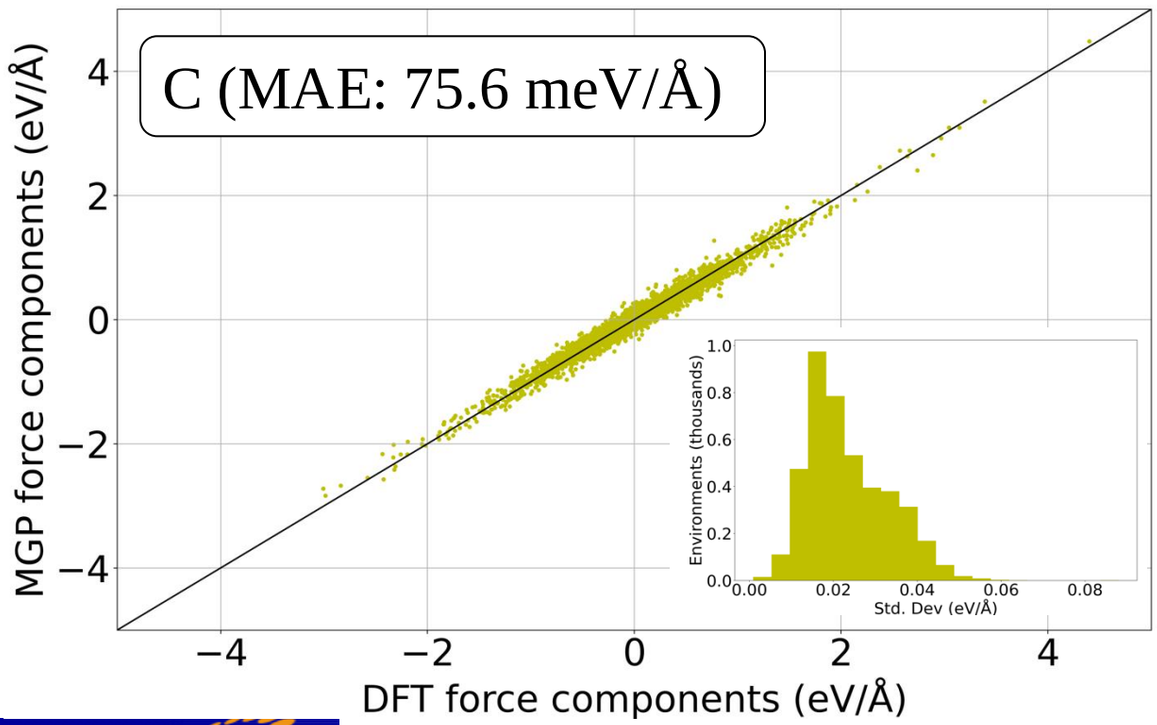

- Validation set contains 144 structures (snapshots) sampled from MD trajectories
- MAE (in force predictions) for each elements is below < 100 meV/Å
- Uncertainty (in terms of std. deviation) for each element is < 88 meV/Å

Methodology
Validation of ML model (desorption energy)

The rate of desorption can be measured from MLMD, from which desorption energy is obtained.

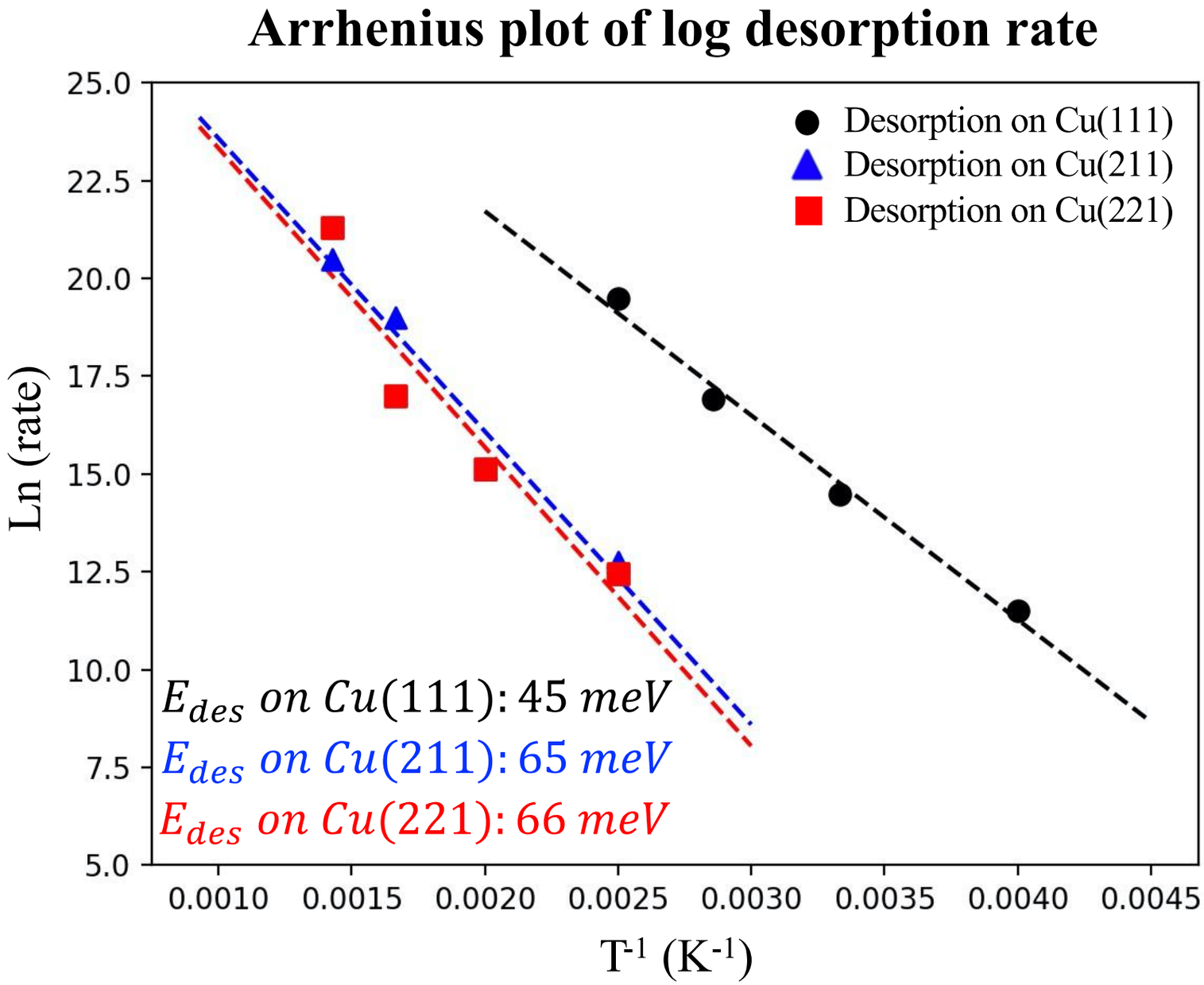

Arrhenius equation

$$\ln(rate) = \ln \nu - \frac{E_{des}}{RT}$$

Surface	Desorption Energy (eV)	
	Exp.[1]	MLMD
Cu(111)	0.49	0.45
Cu(221)	0.60	0.66
Cu(211)	0.61	0.65

[1] Vollmer, S. *Catal. Lett.* 2001, *77(1)*, 97-101.

❖ MLMD can well reproduce the desorption rate of CO on Cu surfaces

Methodology
Initial structures in MD simulation

Cu-island is deposited on Cu(111) (2341 atoms / unit cell)

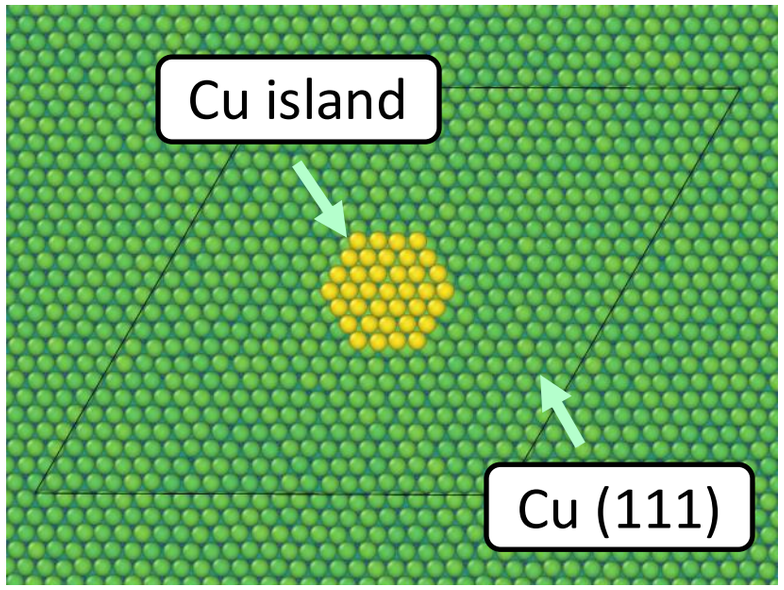

Top view

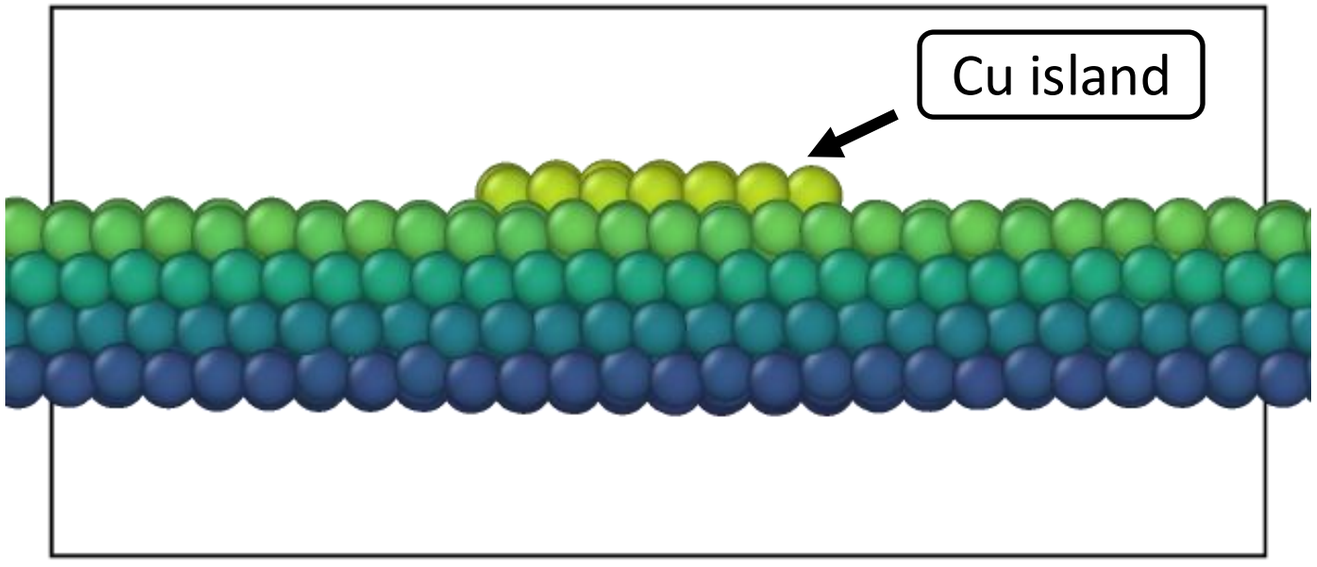

Side view

CO ($\theta = 0.5$) and Cu-island is deposited on Cu(111) (3485 atoms / unit cell)

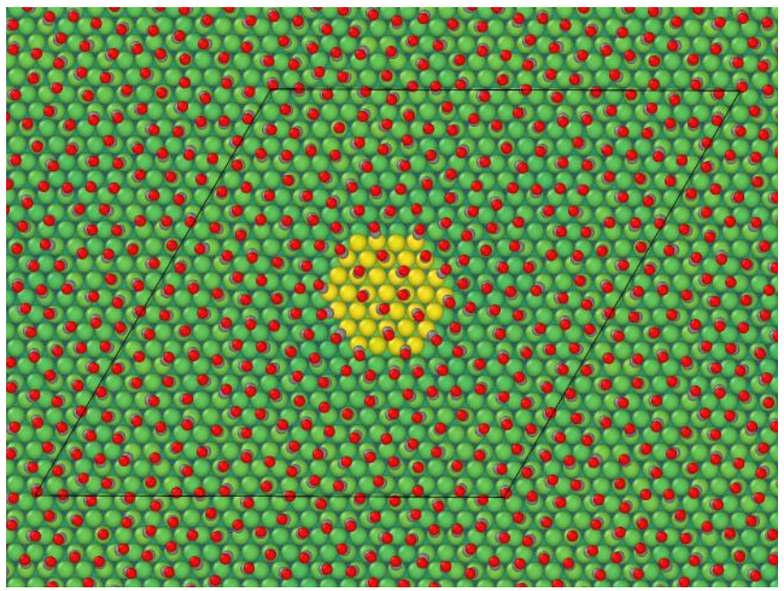

Top view

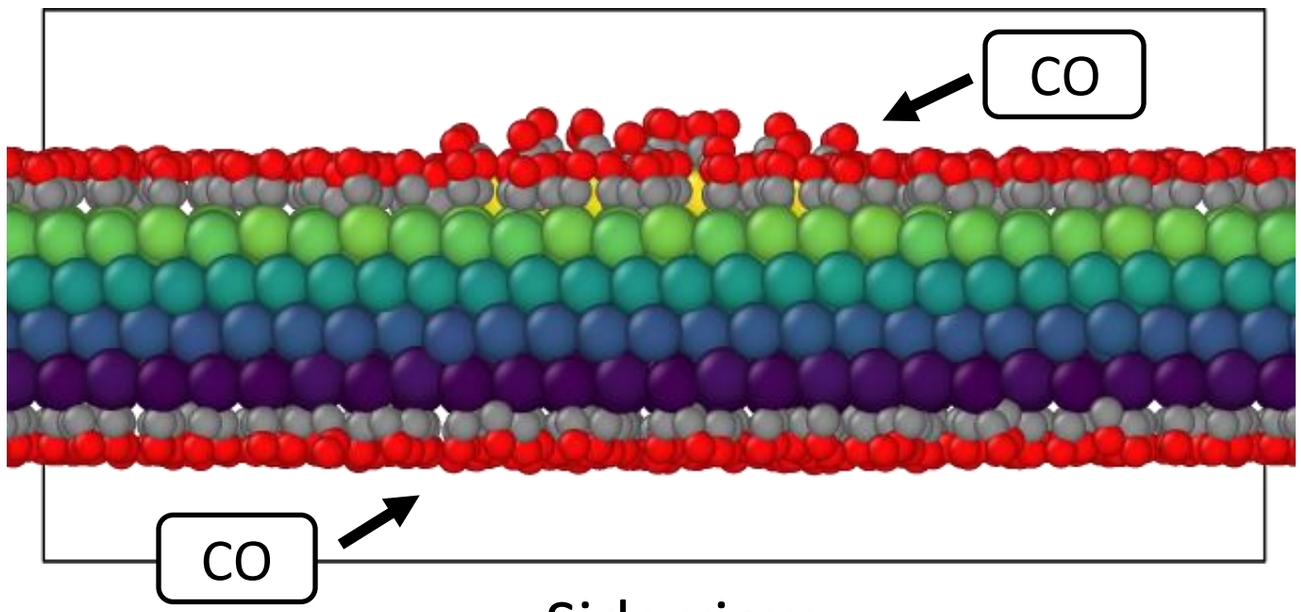

Side view

大阪大学

Results and discussion
Evolution of surface without CO (T = 550 K)

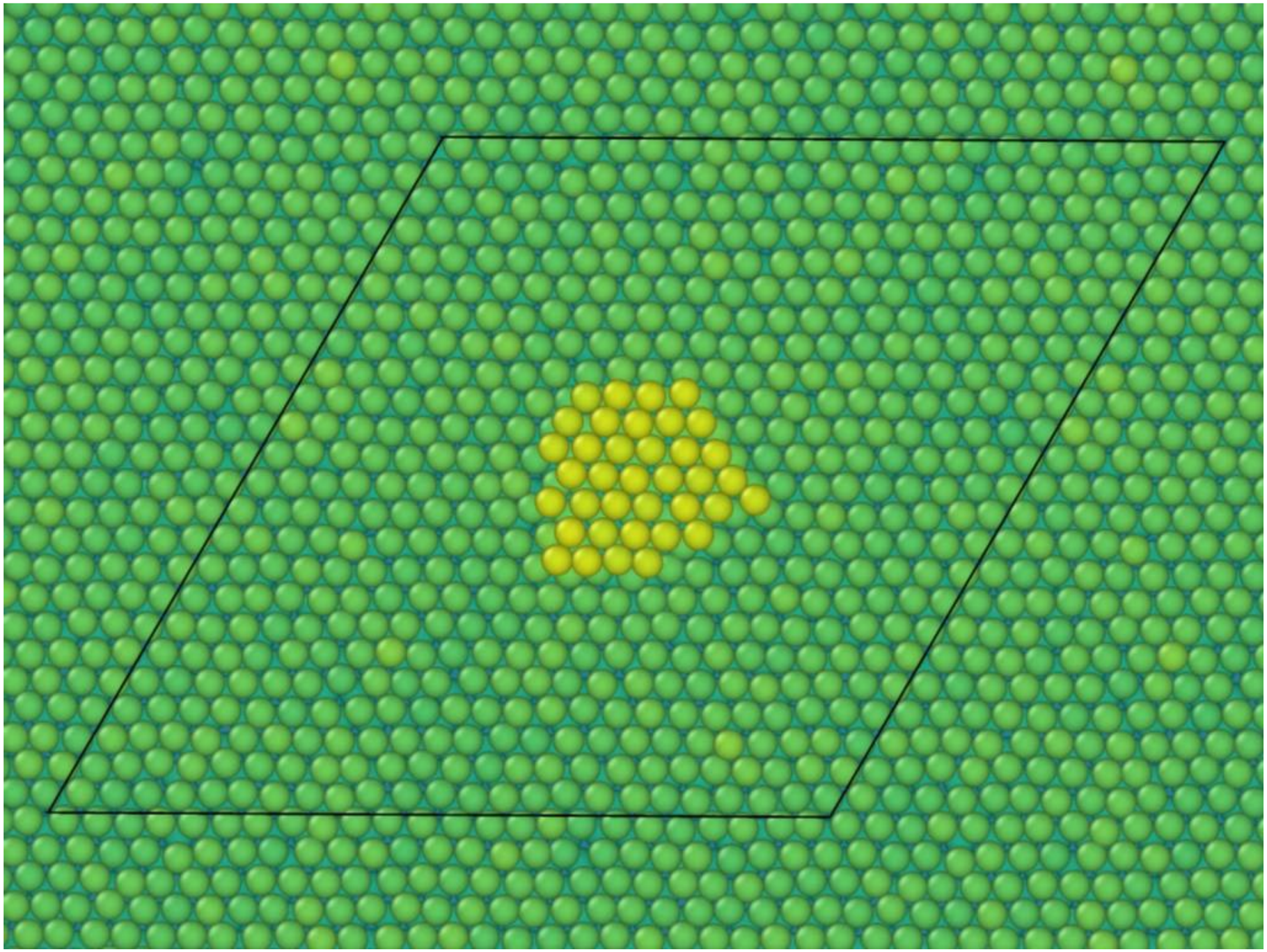

Without CO exposure, no cluster formation is observed event at 550 K

Results and discussion
Evolution of surface with CO (T = 550 K)

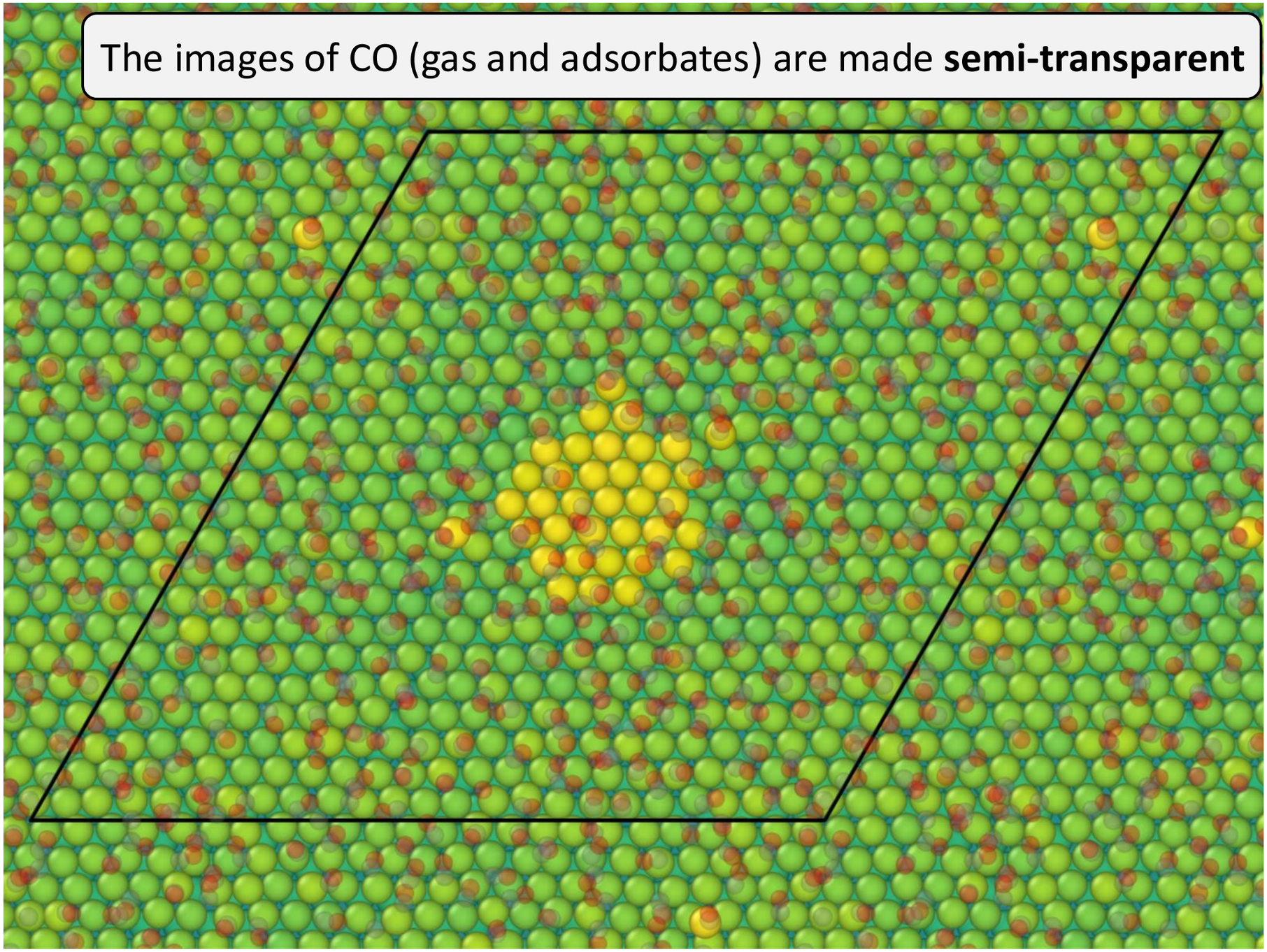

With CO exposure, nanoclusters is formed within tens of ns.

Results and Discussion

Evolution of Cu Surface at different temperatures

Cu only (550 K)

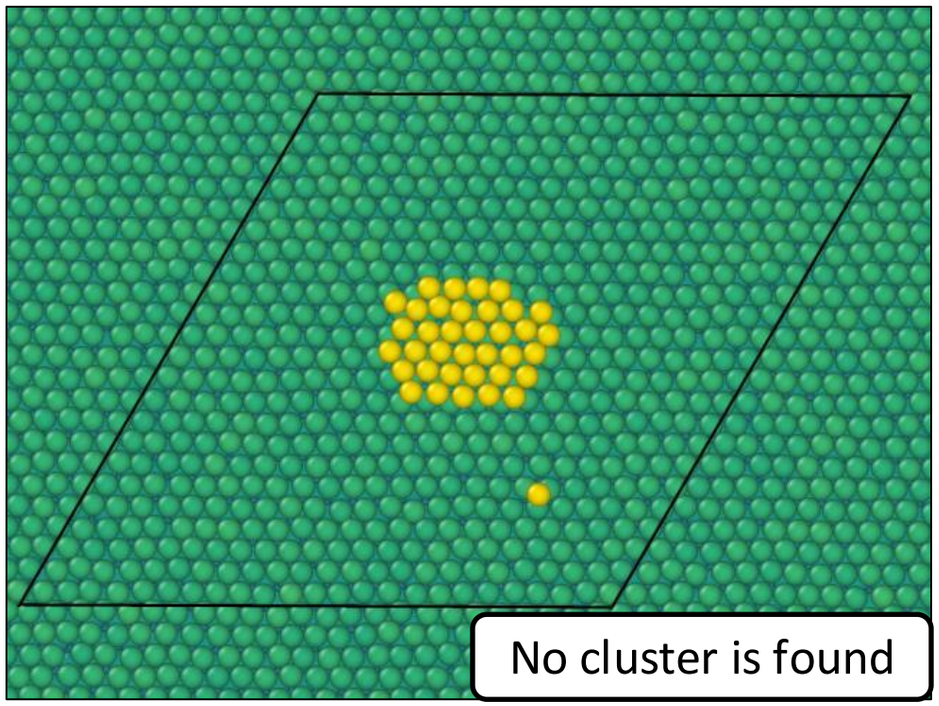

Cu + CO (350 K)

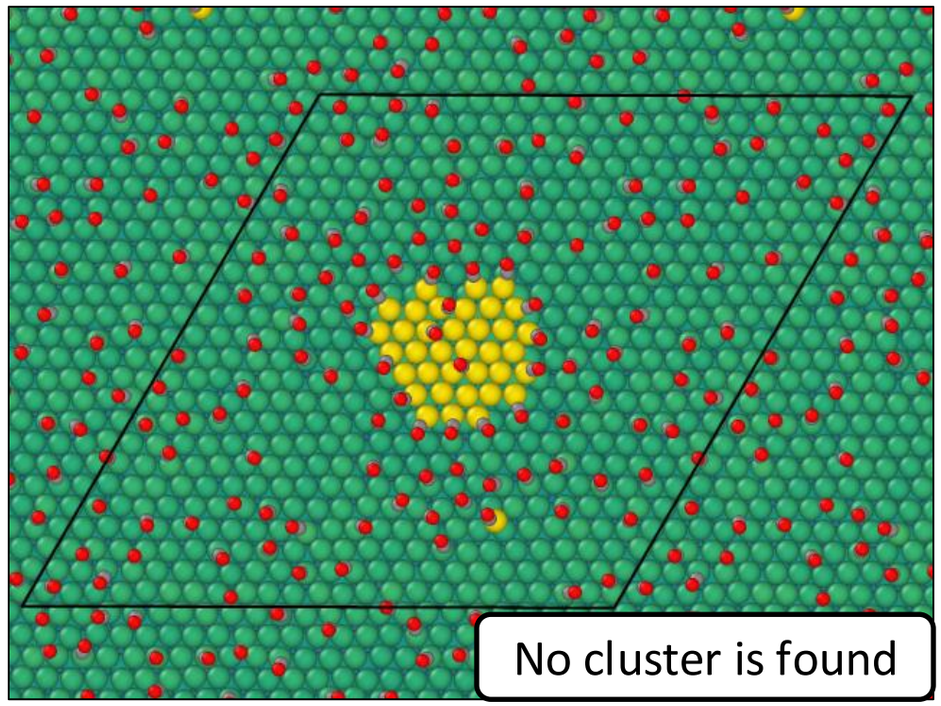

Cu + CO (450 K)

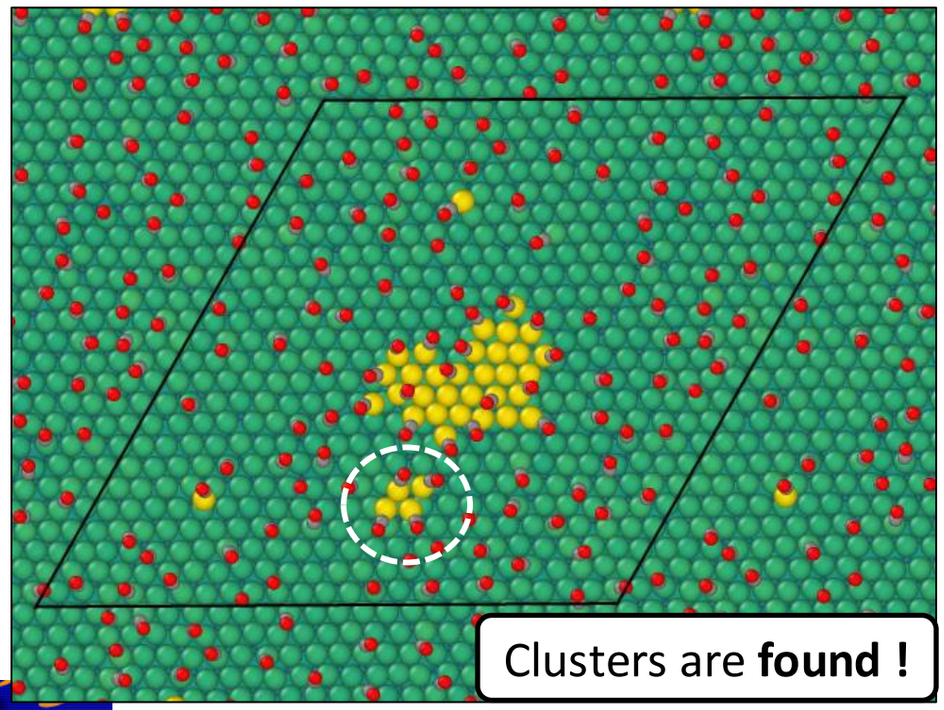

Cu + CO (550 K)

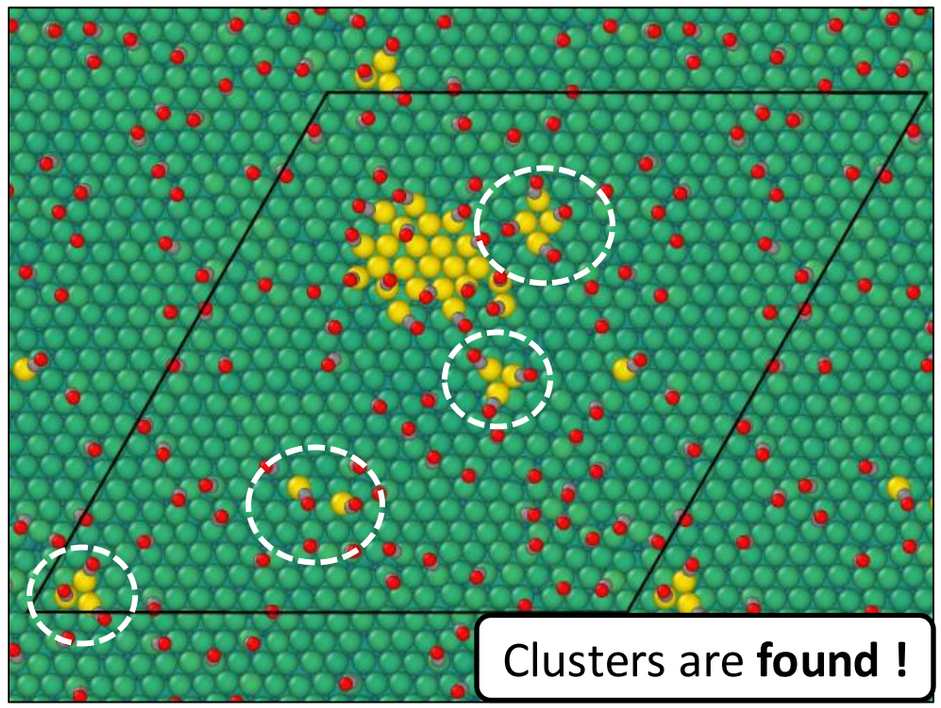

Number of clusters on Cu(111) without CO at T=550K

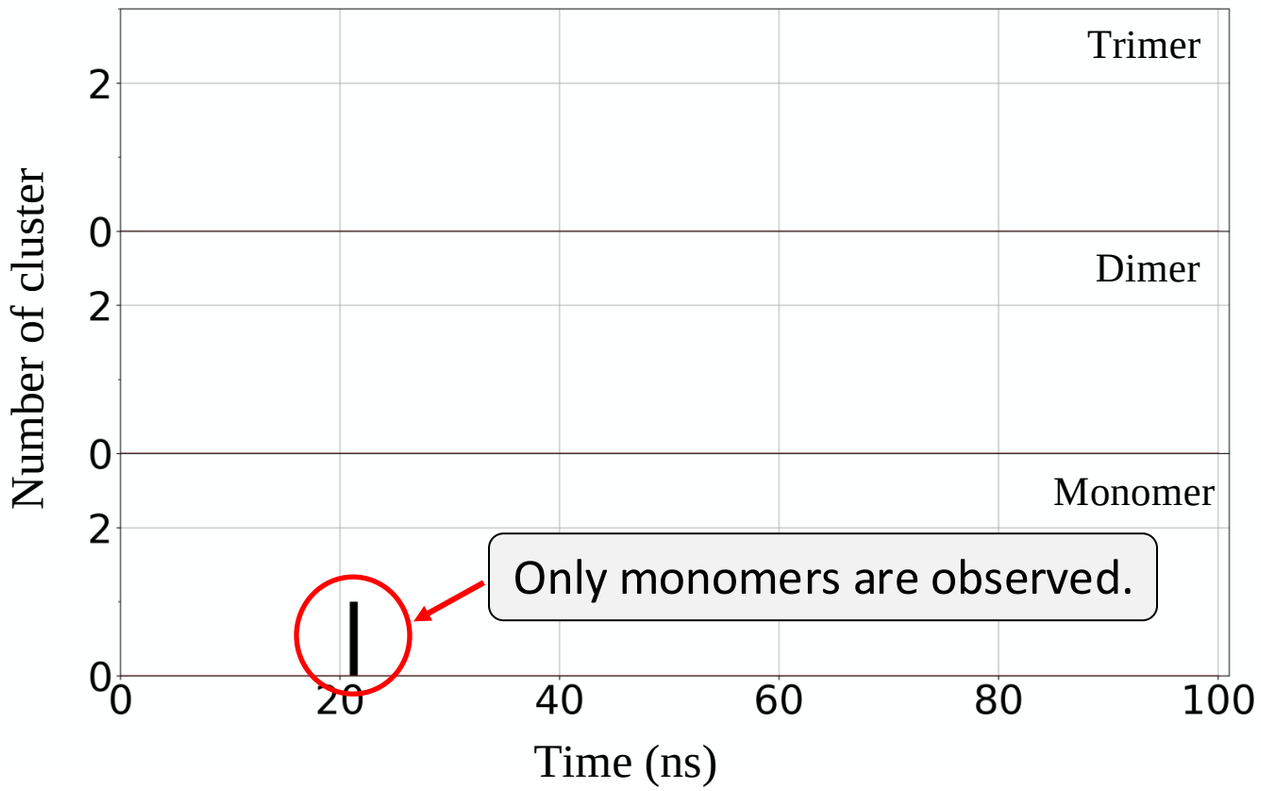

Number of clusters on CO-exposed Cu(111) at T=550K

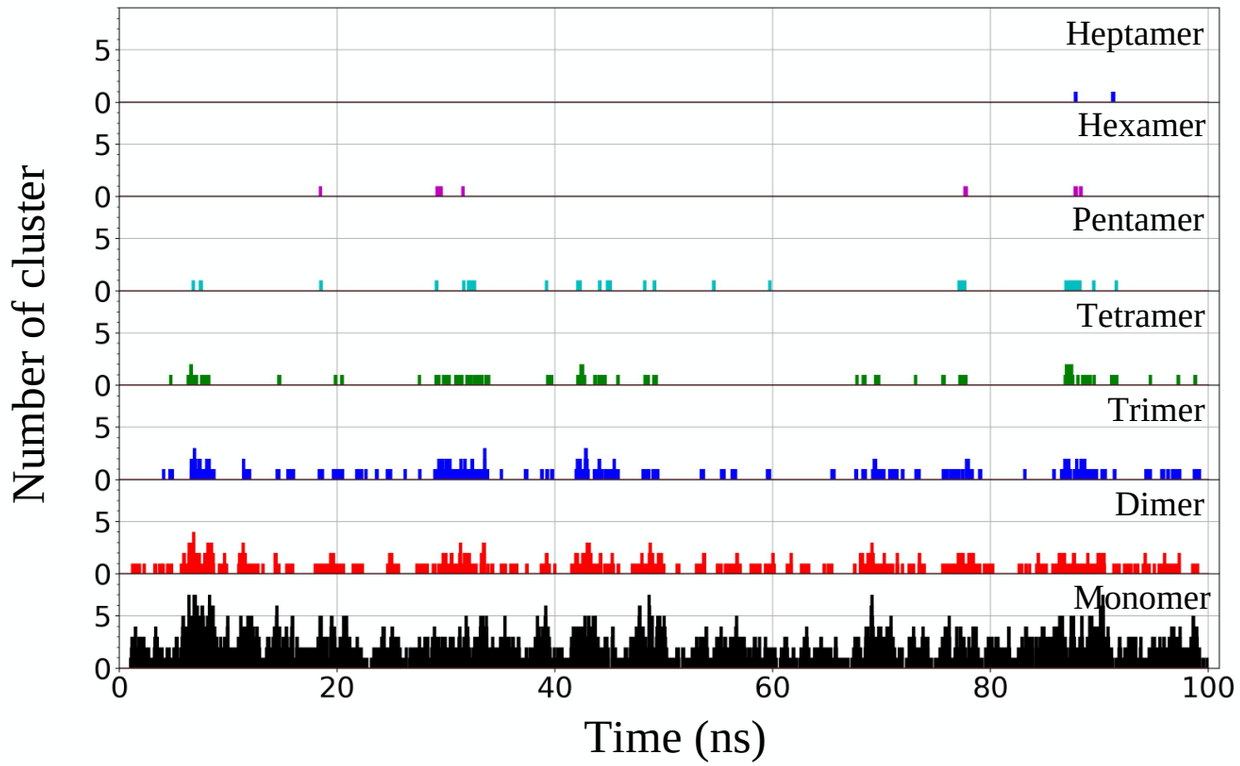

Clusters varying from dimer to heptamer are observed.

The shapes of Cu-CO clusters

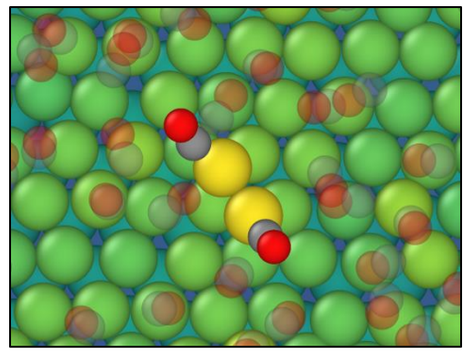

Dimer

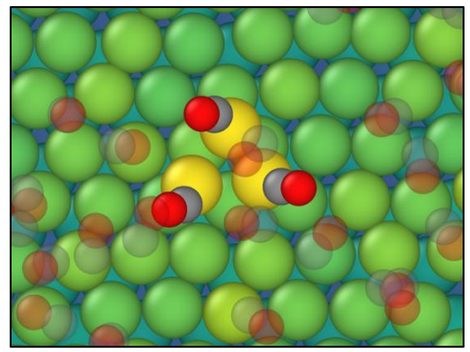

Trimer

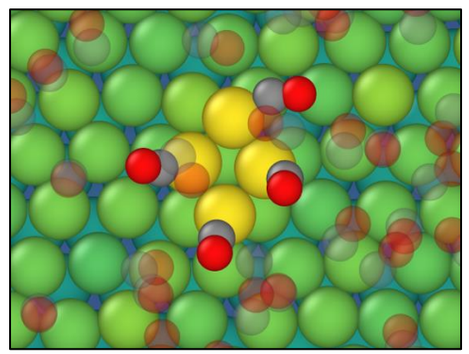

Tetramer

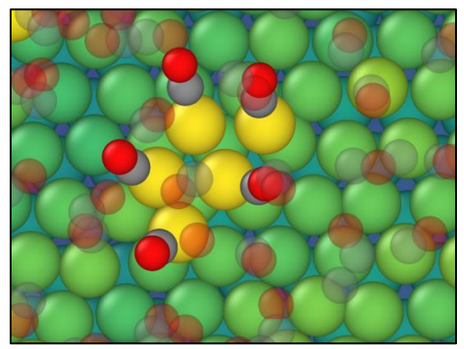

Pentamer

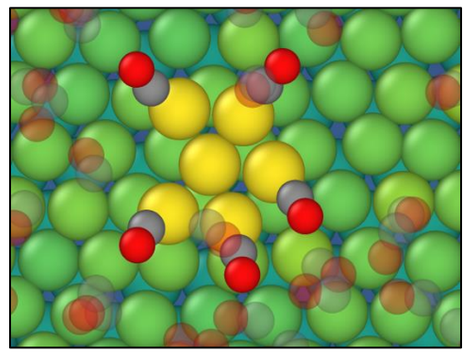

Hexamer

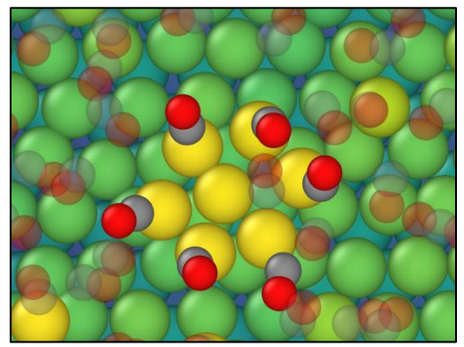

Heptamer

Cu-CO monomers dominate the surface.

The number of clusters reduces with the size.

Lifetime of the clusters

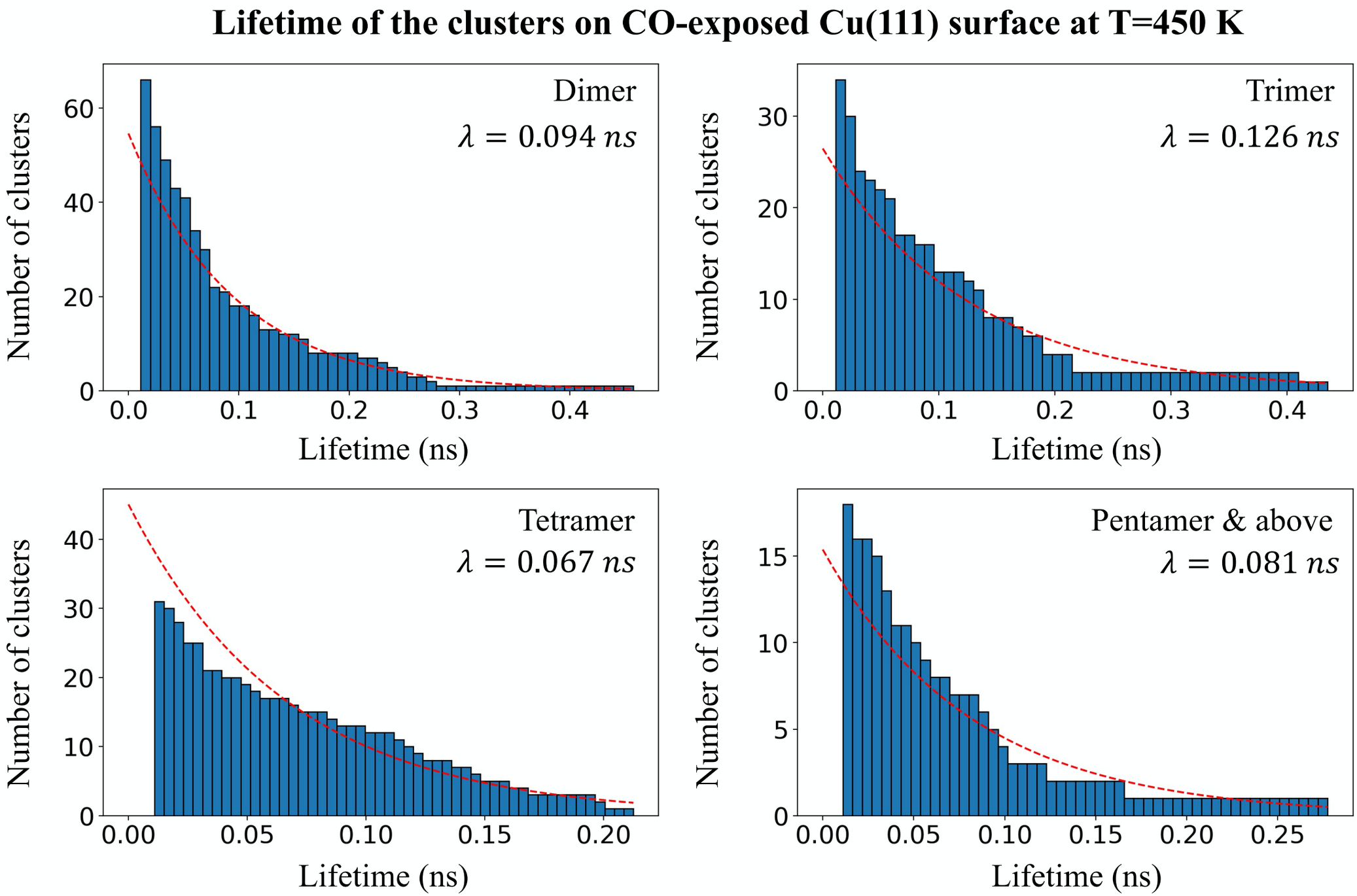

At 450 K, the average lifetime of the clusters ranges from 0.067 ns to 0.126 ns

Lifetime of the clusters

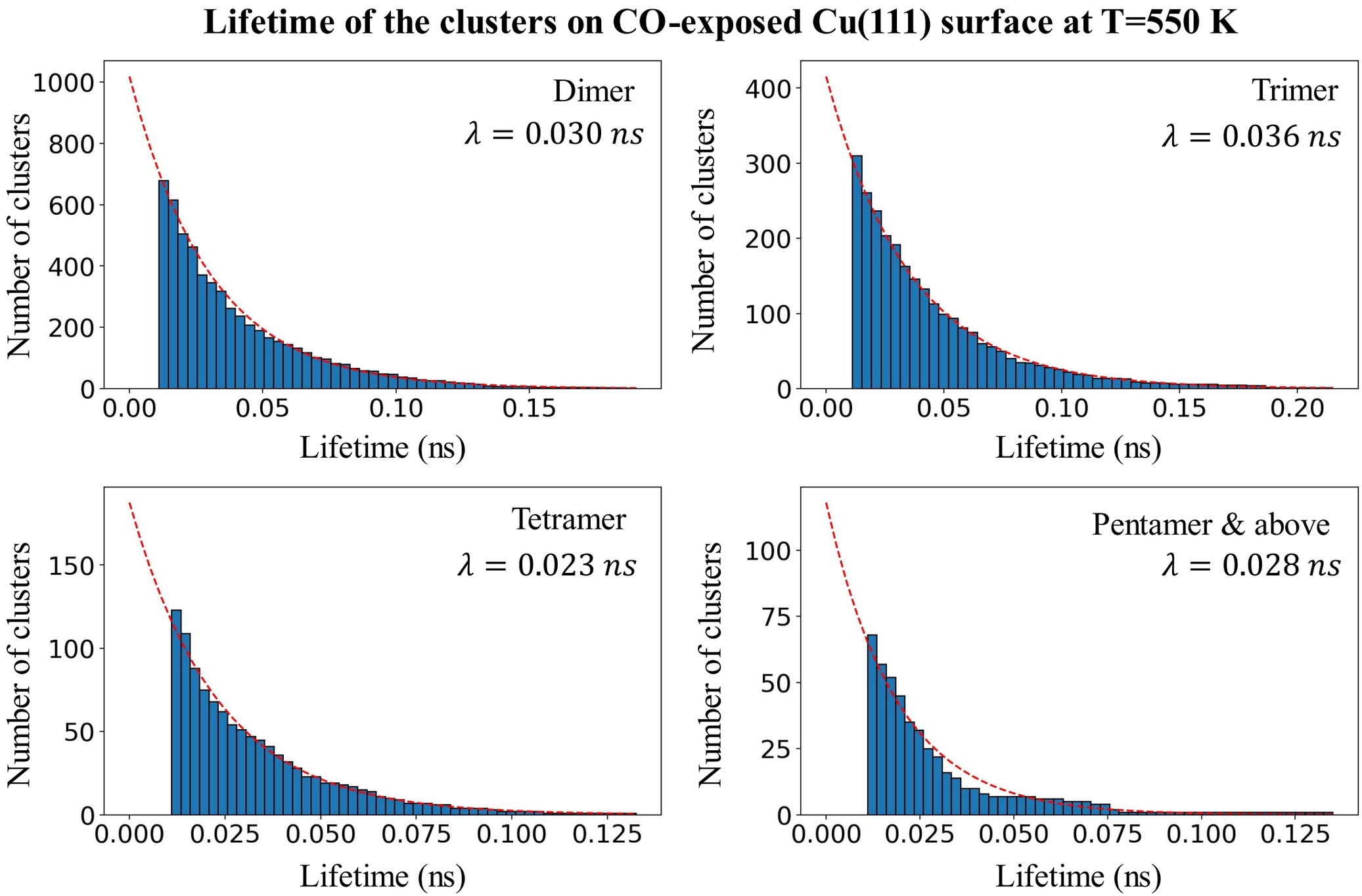

Raising the temperature to 550 K results in the shortening of the lifetime

Results and discussion
How are the clusters formed ?

A. Indirect formation of cluster

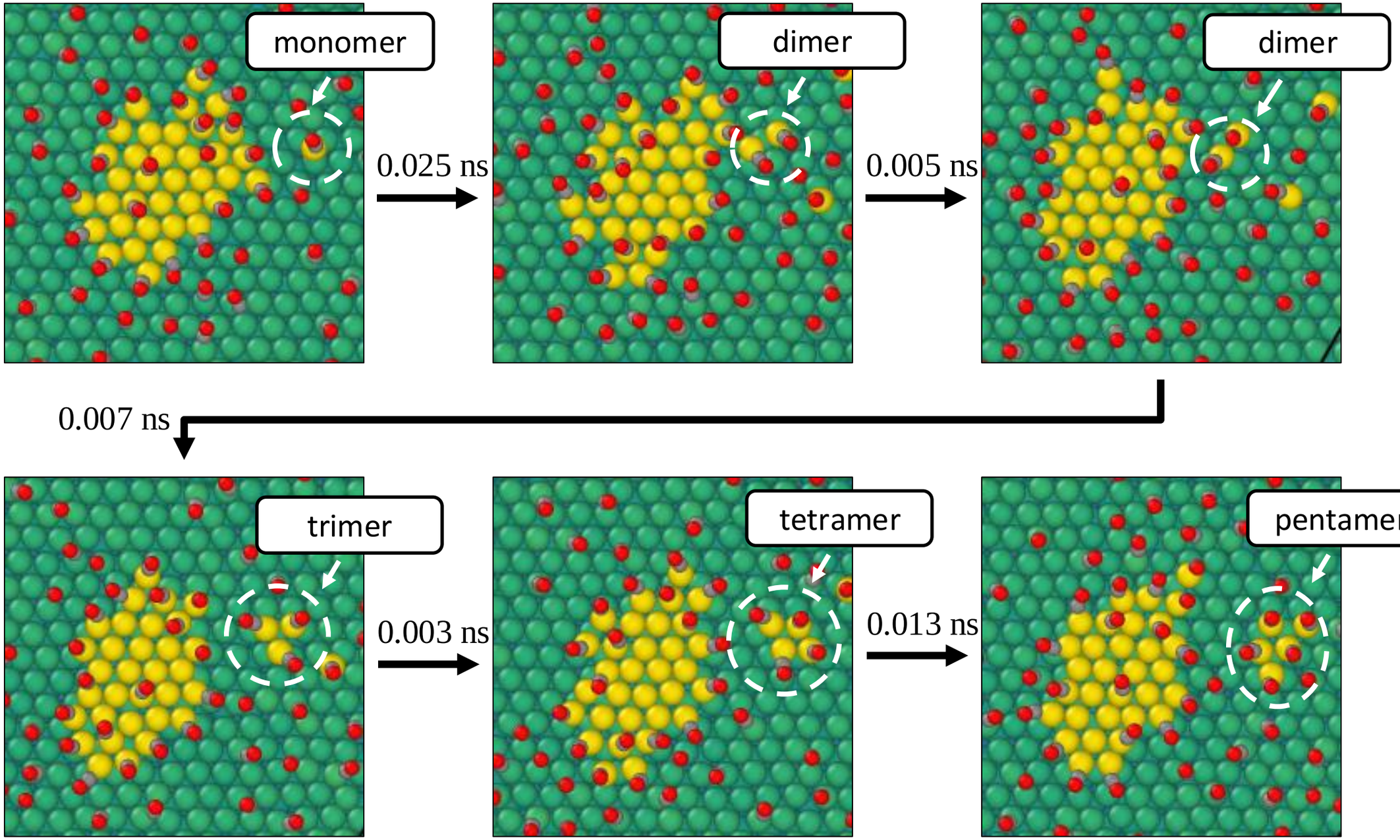

Clusters are formed by coalescence of smaller clusters, initiated by monomer.

Results and discussion
How are the clusters formed ?

B. Direct formation of cluster

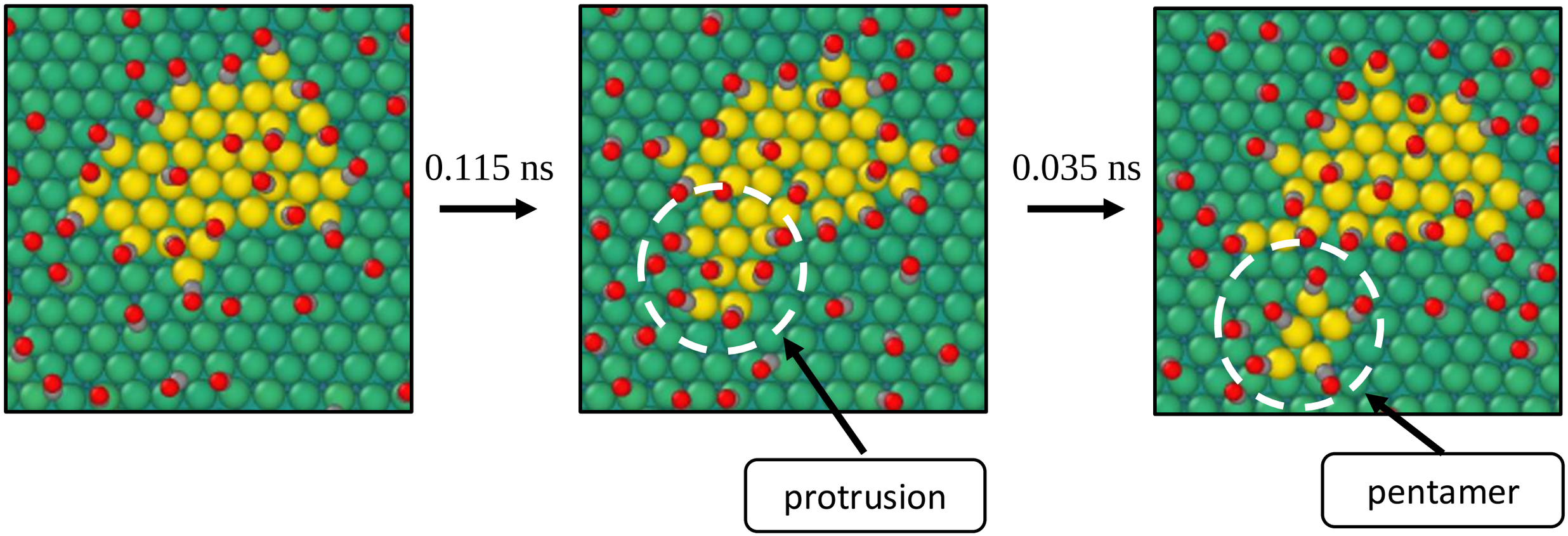

Clusters are formed directly by splitting from the island.

Results and discussion

Statistics of clusters' formation and decomposition

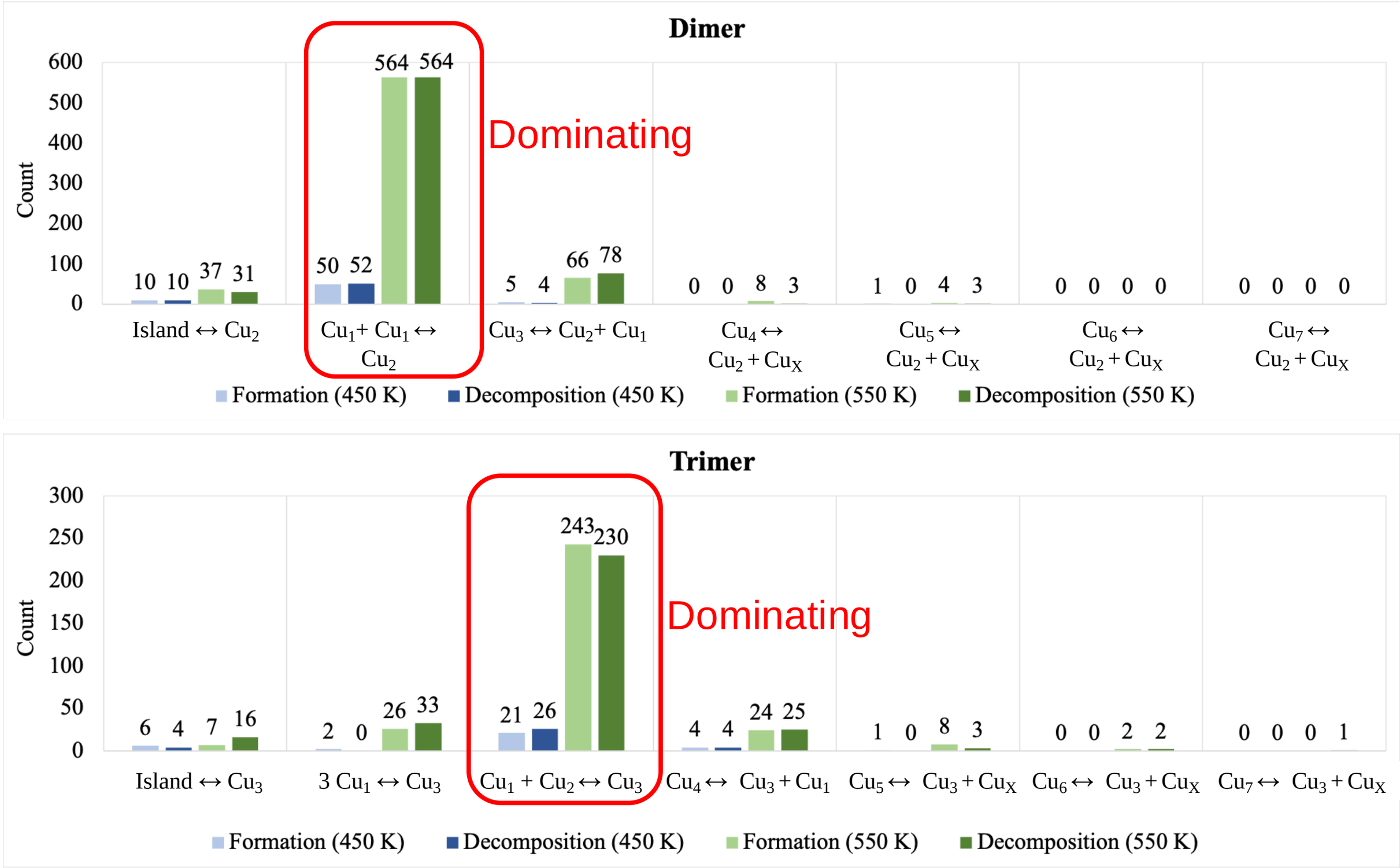

The indirect mechanisms are dominating.

Results and discussion

Statistics of clusters' formation and decomposition

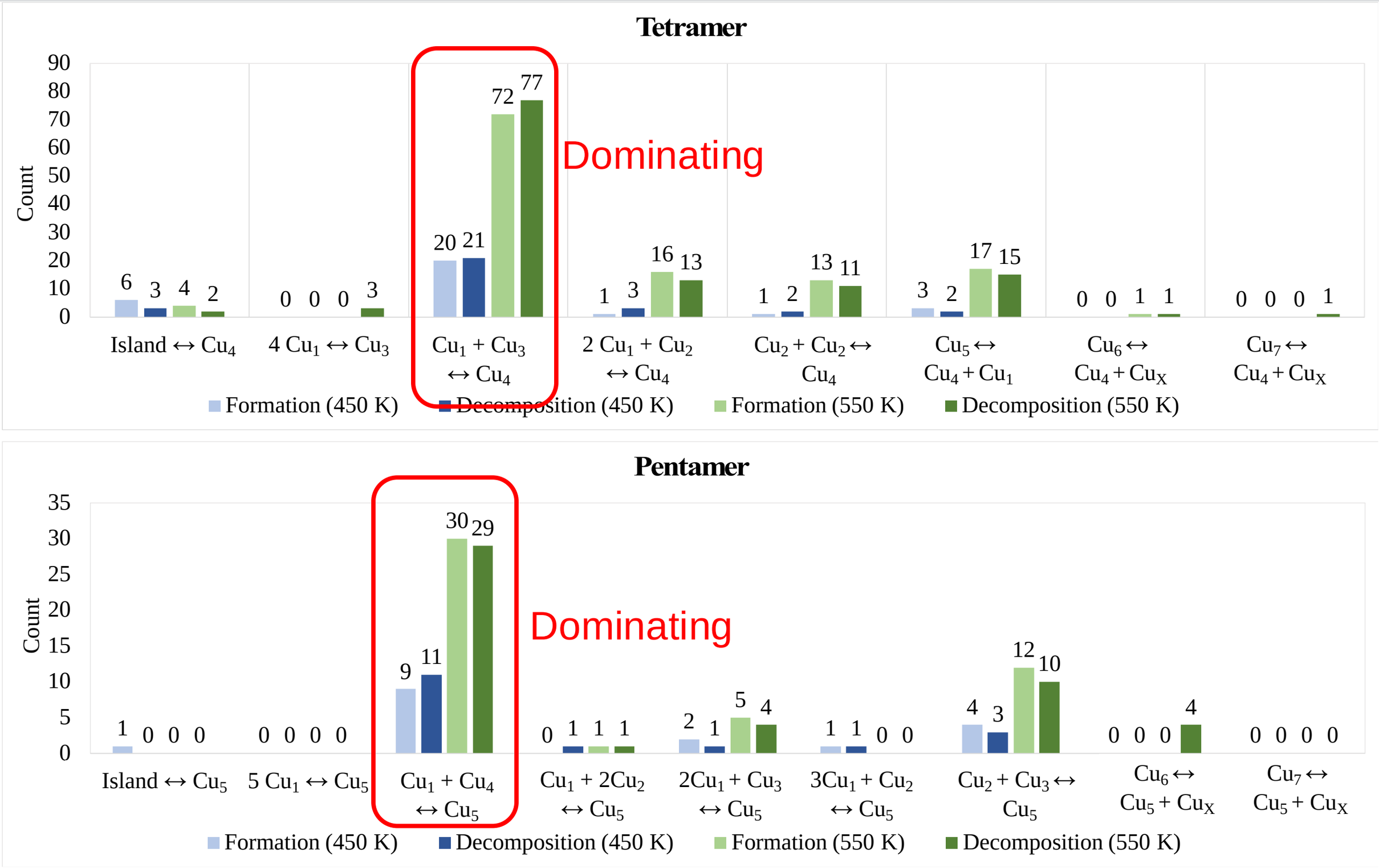

The indirect mechanisms are dominating.

Results and discussion
How does CO influence monomer detachment ?

Detachment / Attachment barriers at Cu(221)

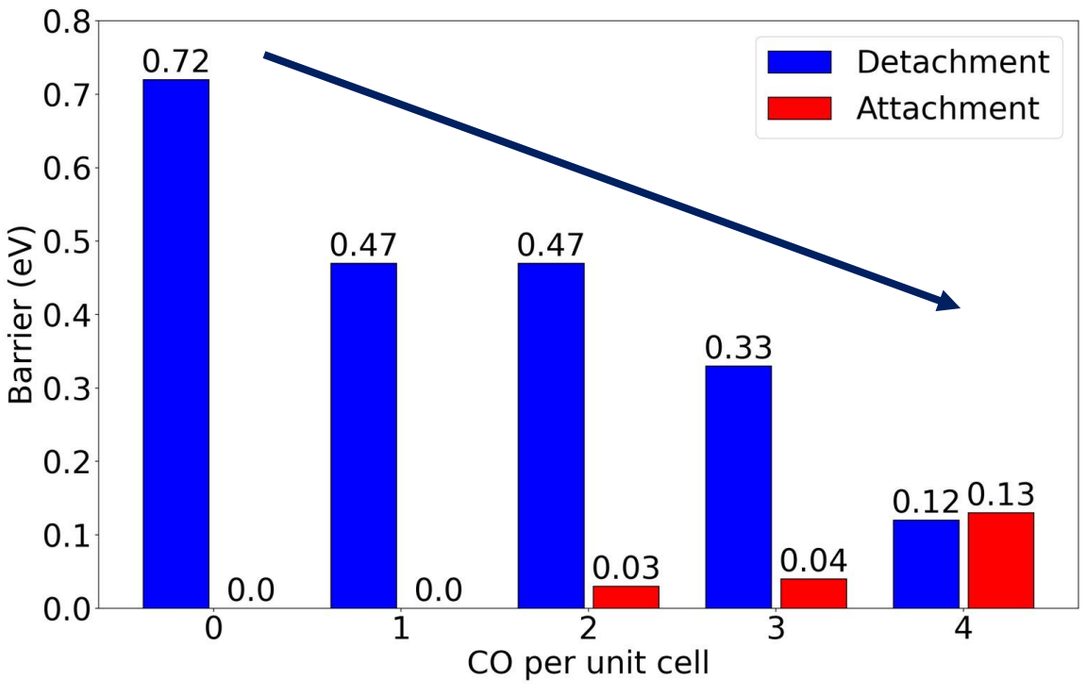

CO adsorptions **reduces** the barrier of detachment and **raises** the barrier of attachment.

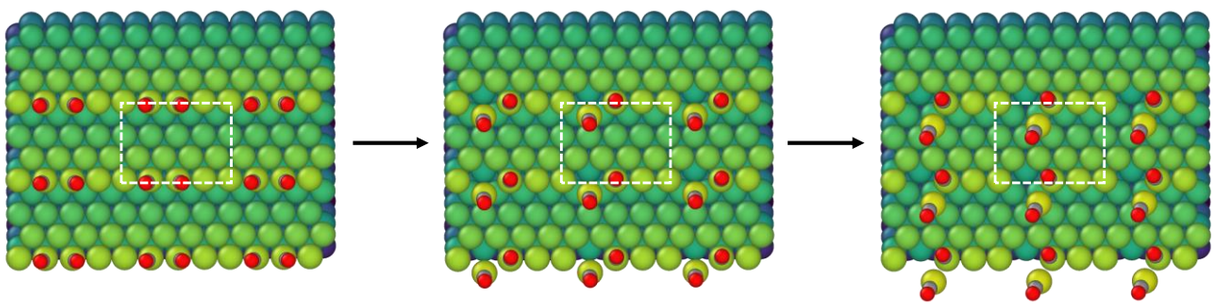

2 CO / unit cell

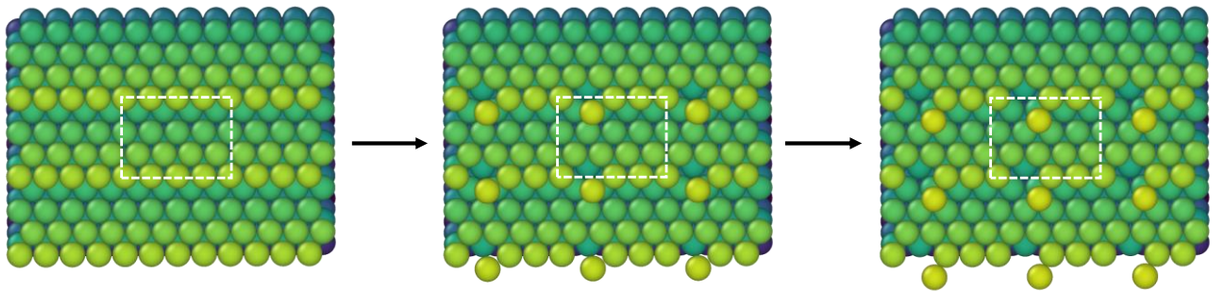

0 CO / unit cell

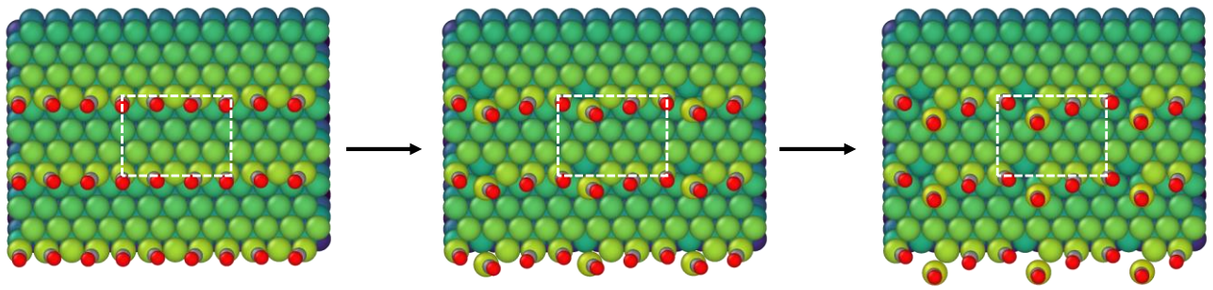

3 CO / unit cell

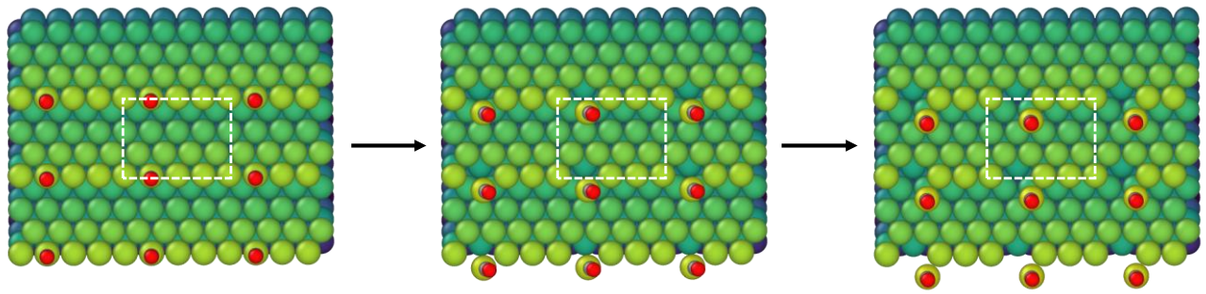

1 CO / unit cell

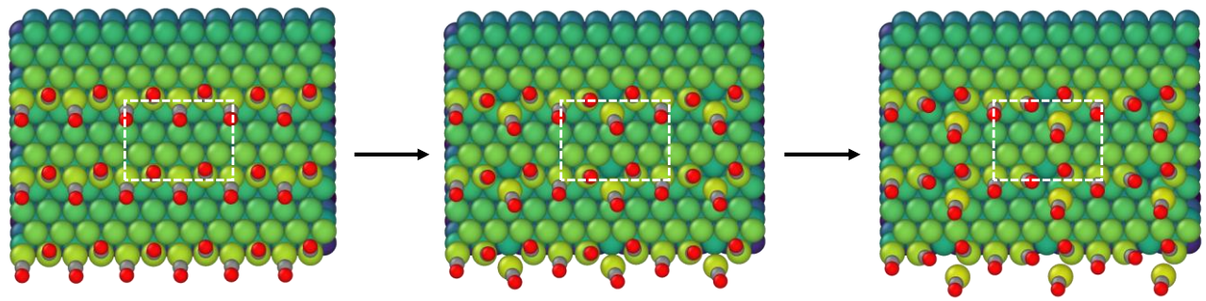

4 CO / unit cell

大阪大学

Conclusion

The cluster formation induced by CO adsorptions has been investigated by MLMD.

Exposure of Cu surface to CO results in formation of clusters with different sizes, varying from **dimer** to **heptamer**.

Raising the temperature increases the occurrence of the clusters but at the same time reduces their lifetime.

Clusters can be formed by **direct** and **indirect** mechanisms, of which the indirect mechanism dominates.

CO drives the formation of clusters by reducing the barrier of adatom detachment and raising the barrier of re-attachment.

H.H. Halim, R. Ueda and Y. Morikawa, ***J. Phys. Condensed Matter, Special Issue from the Speakers of Surface Science Discussions 2022and 2023*****, 35, 495001 (18pp) (2023).**

Acknowledgements

- CO_2 hydrogenation
  F. Muttaqien (OU → ITB)
  I. Hamada (OU)
  K. Inagaki (OU)
  Y. Hamamoto (OU)

- Harry Handoko Halim (OU, D3)

- Cu-Zn alloy with Machine Learning
  CO-driven Formation of Cu Clusters

Discussions with exp. groups:

- CO_2 hydrogenation
  J. Nakamura (Kyushu Univ.)
  T. Kondo (Univ. Tsukuba)
  J. Quan (Univ. Tsukuba)
  J. Yoshinobu (Univ. Tokyo)
  T. Koitaya (Univ. Tokyo)

Funding:

科研費 KAKENHI

Japan Society for the Promotion of Science • Founded 1932 •

the e-ASIA Joint Research Program

富岳

IMS

ESICB

大阪大学

Core-to-core

Outline

1. Vibrationally Enhanced Hydrogenation of CO_2 for Methanol Synthesis

   F. Muttaqien, et al., *J. Chem. Phys.*, 147, 094702 (2017).
   Chem. Comm., 53, 9222(2017),
   Nature Chem., 11, 722-729 (2019).

2. The Elucidation of Cu-Zn Surface Alloying on Cu(997) by Machine-Learning Molecular Dynamics

   H.H. Halim and Y. Morikawa, *ACS Phys. Chem. Au*, in press,
   DOI: 10.1021/acsphyschemau.2c00017

3. **Theoretical Study on the Dry Reforming of Methane**

   Y. J. Wong, et al., *ChemCatChem.*, 11, 5593-5605, (2019).
   ***J. Phys. Chem. C*, 125, 21902-21913 (2021).**
   ***J. Phys. Chem. C*, 125, 23657-23668 (2021).**

Theoretical Study on the Dry Reforming of Methane

Y. J. Wong[1,2], H. H. Halim[1], N. F. Khairudin[2], T.-N. Pham[1], S. E. M. Putra[1], Y. Hamamoto[1], K. Inagaki[1], I. Hamada[1], A. R. Mohamed[2], and Y. Morikawa[1]

[1]Osaka University, [2]University Sains Malaysia

1. Y. J. Wong, M. K. Koh, N. F. Khairudin, S. Ichikawa, Y. Morikawa, and A. R. Mohamed, ***ChemCatChem***., **11**, 5593-5605, (2019).
2. Y. J. Wong, H. H. Halim, N. F. Khairudin, T. N. Pham, S. E. M. Putra, Y. Hamamoto, K. Inagaki, I. Hamada, A. R. Mohamed, and Y. Morikawa, ***J. Phys. Chem. C*, 125**, 21902-21913 (2021).
3. Y. J. Wong, S. Tanaka, K. Mukai, Y.H. Choi, A.R. Mohamed, I. Hamada, J. Yoshinobu, Y. Morikawa, ***J. Phys. Chem. C*, 125**, 23657-23668 (2021).

Background of Study:
Global warming and the importance of CO_2 reforming of CH_4

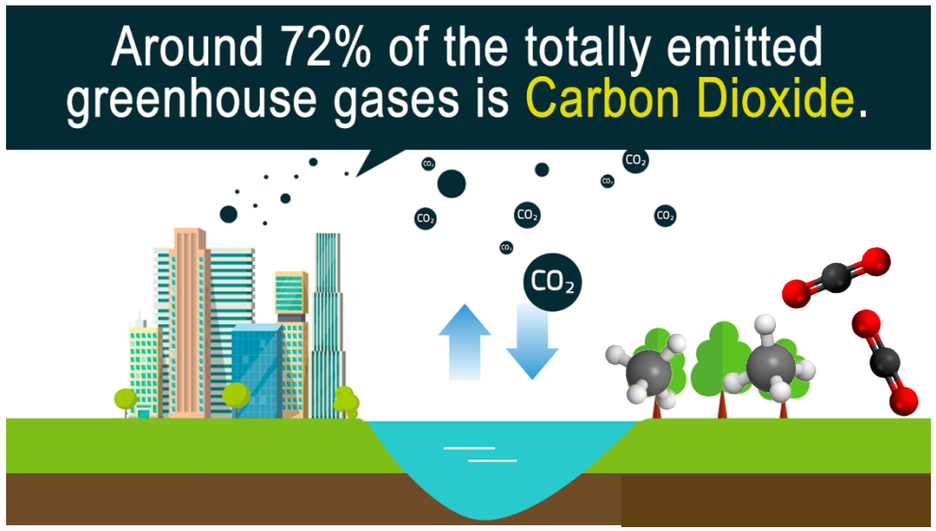

Particularly, in southeast Asian countries, the emission of biogas (CH_4 and CO_2) from palm oil industry (palm oil mill effluent, POME) is a serious problem.

- Malaysia currently accounts for 28% of world palm oil production and 33% of world palm oil exports.
- Research on CO_2 and CH_4 activation become importance to **recycle biogas into renewable energy**.

Due to human activities and higher demand of energy, the emission of greenhouse gases (CH_4 and CO_2) is increasing exponentially, leading towards global warming and climate changes.

Background of Study: Global warming and the importance of CO_2 reforming of CH_4

$$CH_4(g) + CO_2(g) \rightleftharpoons 2CO(g) + 2H_2(g)$$

- In industry, syngas is widely used as intermediate chemicals to produce higher quality hydrocarbon fuel via Fischer-Tropsch synthesis.
- Syngas can be purified to produce pure H_2 which is widely used for fuel cell application.

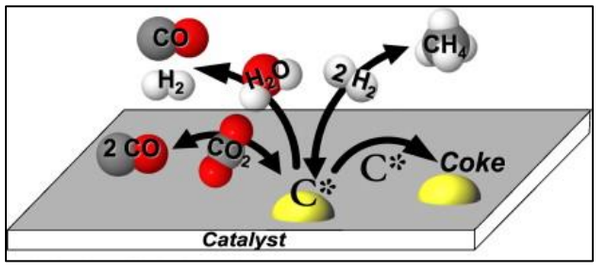

Dry reforming

Fischer-Tropsch synthesis

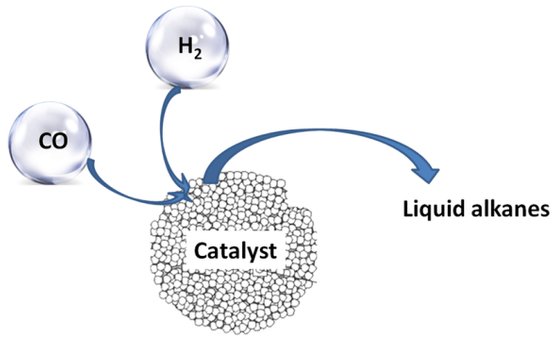

Problem:

- Ni is most well studied metal catalyst for DRM
- Carbon deposition and coking deactivate metal Catalyst.
- Co is more tolerant of carbon deposition compared with Ni catalyst

Co particle size dependence

Co-to-Al mol ratio

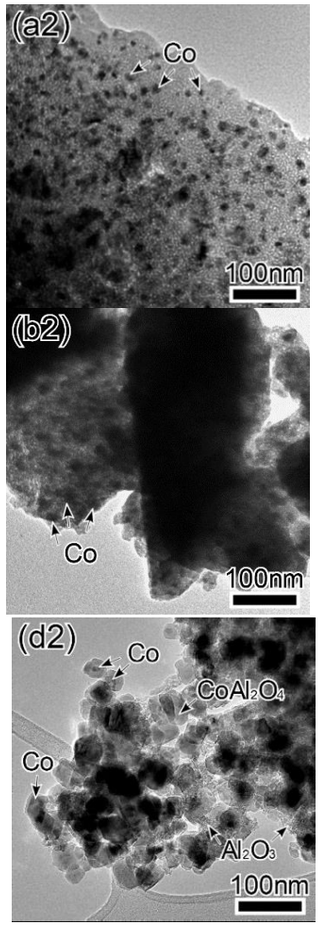

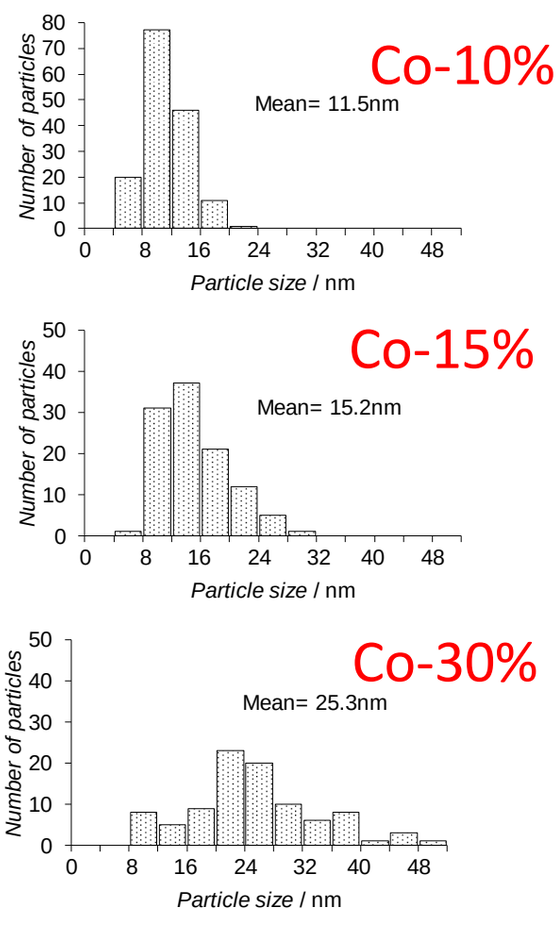

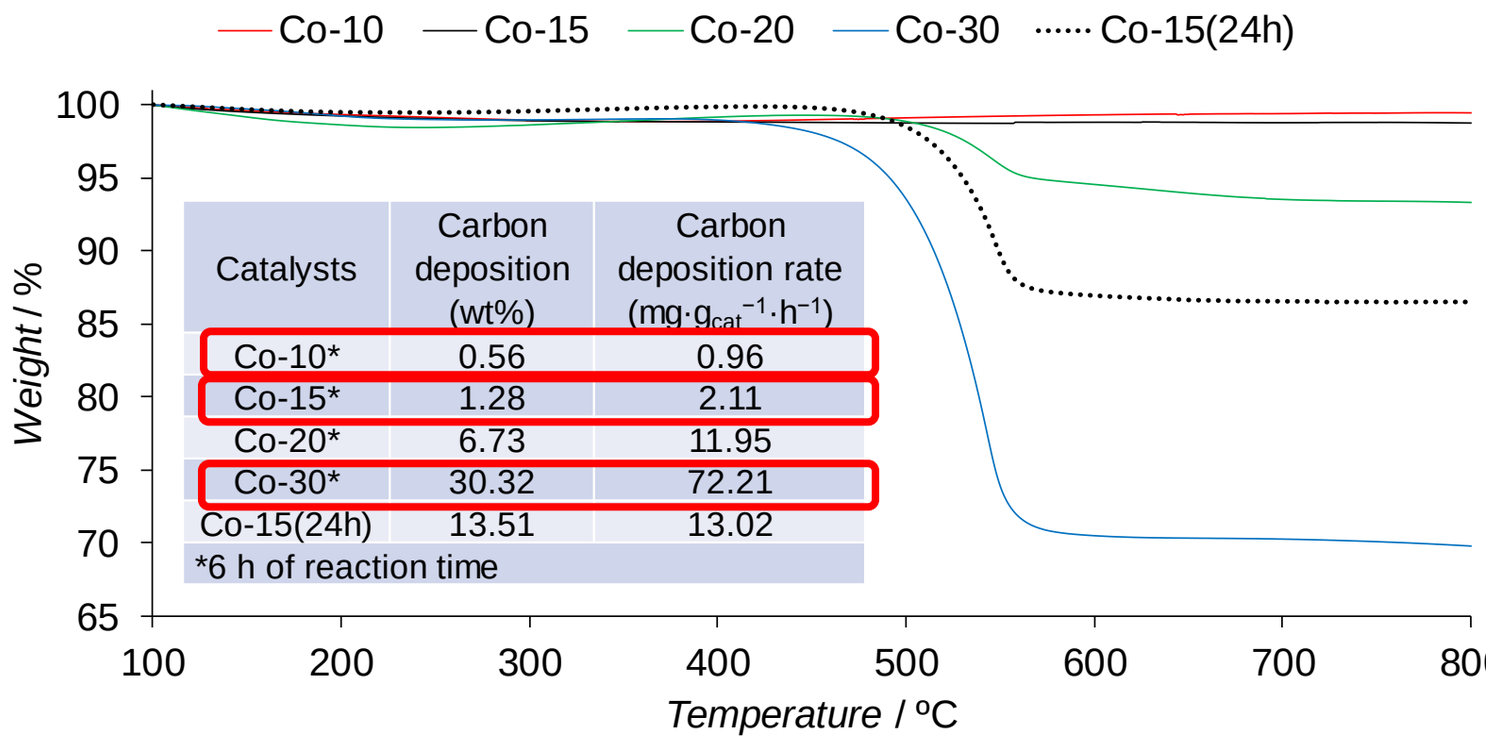

Catalysts	Carbon deposition (wt%)	Carbon deposition rate ($mg \cdot g_{cat}^{-1} \cdot h^{-1}$)
Co-10*	0.56	0.96
Co-15*	1.28	2.11
Co-20*	6.73	11.95
Co-30*	30.32	72.21
Co-15(24h)	13.51	13.02

*6 h of reaction time

As catalysts particle size increases, carbon deposition increases

1. Y. J. Wong, M. K. Koh, N. F. Khairudin, S. Ichikawa, Y. Morikawa, and A. R. Mohamed, ***ChemCatChem***., **11**, 5593-5605, (2019).

Dependence of reactivity on the particle size

Fractions of surface facets depends on the particle size.

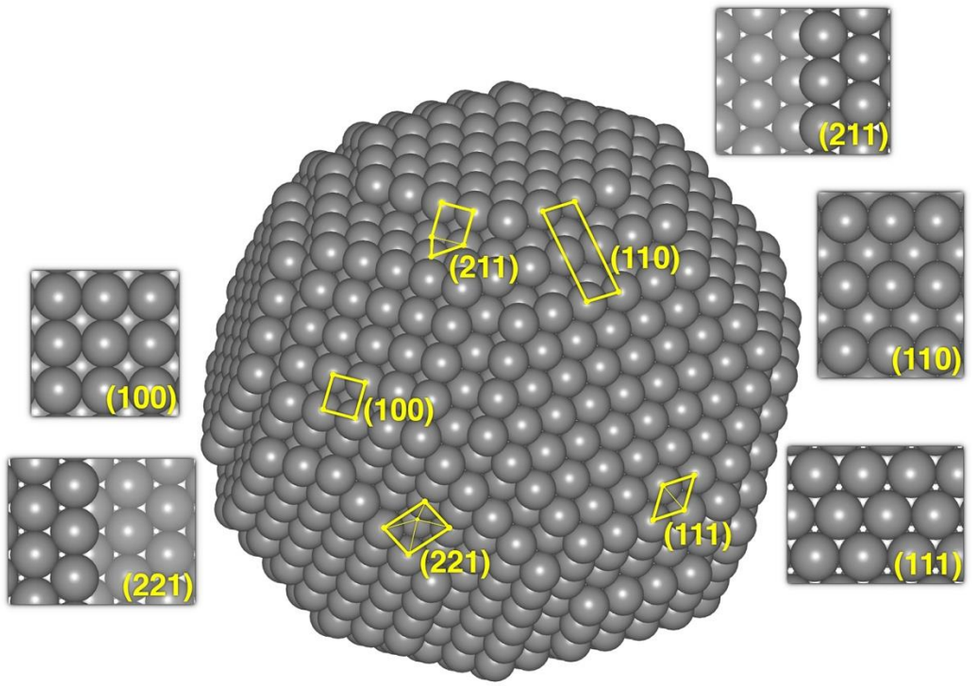

$$CH_4(g) + CO_2(g) \rightleftharpoons 2CO(g) + 2H_2(g)$$

Elementary steps:

$$CH_4(g) + * \rightleftharpoons CH_3^* + H^*$$
$$CH_3^* + * \rightleftharpoons CH_2^* + H^*$$
$$CH_2^* + * \rightleftharpoons CH^* + H^*$$
$$CH^* + * \rightleftharpoons C^* + H^*$$
$$CO_2(g) + * \rightleftharpoons CO_2^*$$
$$CO_2^* + * \rightleftharpoons CO^* + O^*$$
$$C^* + O^* \rightleftharpoons CO^* + *$$

Carbon deposition process:

$$C^* + C^* \rightleftharpoons C_2^* + *$$

Aim and Objectives of Study

Aim:

Understand the carbon deposition on Co surfaces during DRM and compare the results with that on Ni.

Objectives:

- Investigated the dependence of chemical reaction of CO_2 and C* on the structure of Co surfaces
- Clarify the origin for the higher tolerance of Co compared to Ni against carbon deposition.

Methodology

Total energy calculations:
Code : STATE[1]
Theory Level: DFT[2]
Basis : Plane Wave
Cutoff : 25 Ry (wave function),
400 Ry (charge density)
XC Functional : GGAPBE[3]
vdW Correction: DFT-D2[4]
K-Point Sampling : Monkhorst Pack Scheme[5]
Reaction Path Search: CINEB Method[6]
Spin-polarized

[1] STATE Code: https://state-tutorial.readthedocs.io/en/latest/
[2] Kohn and Sham (1965) Physical Review 140(4A):A1133-8
[3] Perdew et al. (1996) Physical Review Letters 77(18) 3865-8
[4] Grimme (2004) Journal of Computational Chemistry 26 1463
[5] Monkhorst and Pack (1976) Physical Review B 13(12) 5188-92
[6] Henkelman et al. (2000) Journal of Chemical Physics 113 9901

Overall reaction

- The overall energy diagram on all the investigated Co surfaces:
  - CO_2 activation (green region)
  - O* and C* diffusion (blue region),
  - CO* formation and C-C coupling (red region)

1. Carbon graphitization is dominant on (111) and possibly on (110).
2. Carbon graphitization is not favorable on (100), (211), and (221).

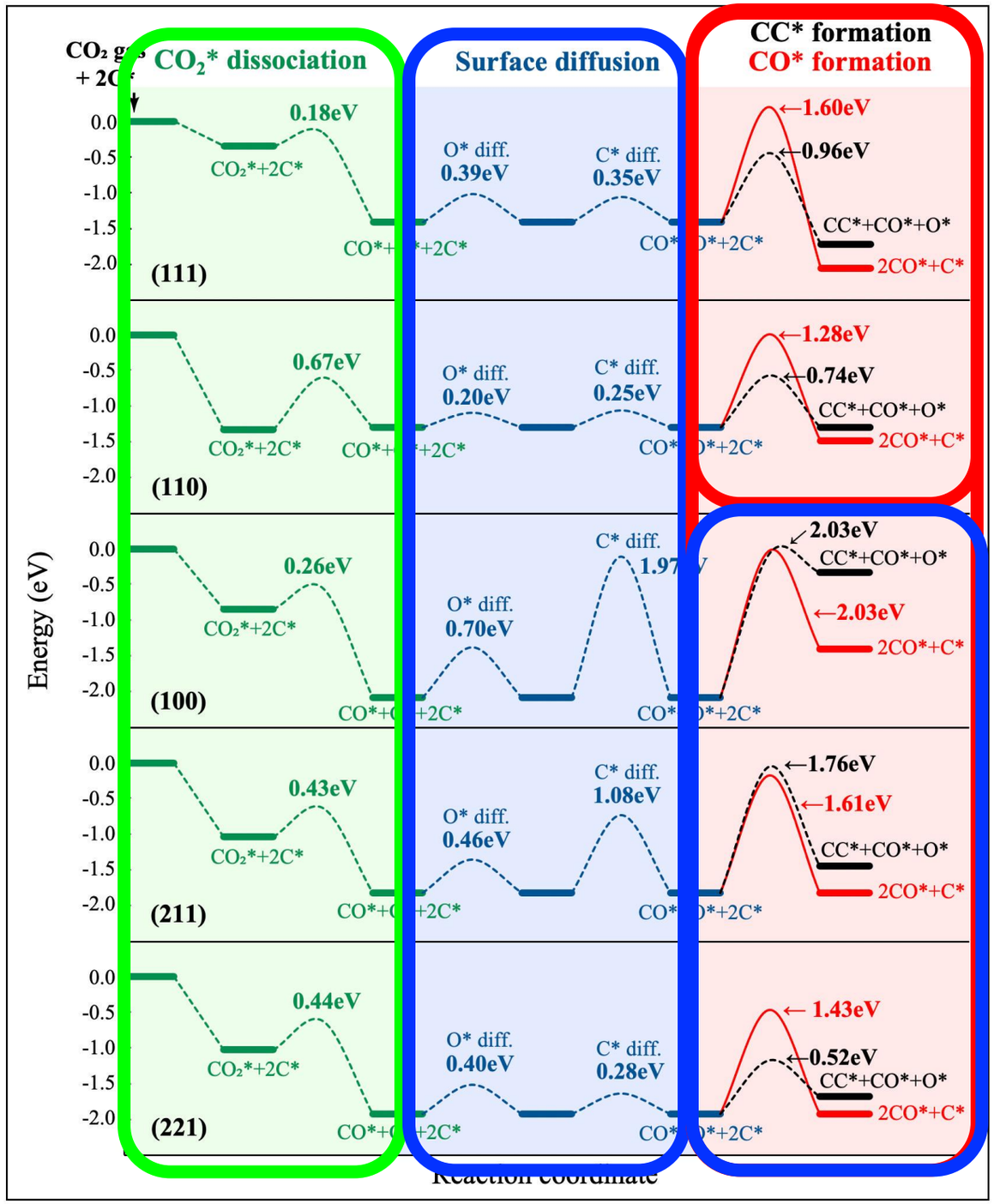

Comparison between Co and Ni

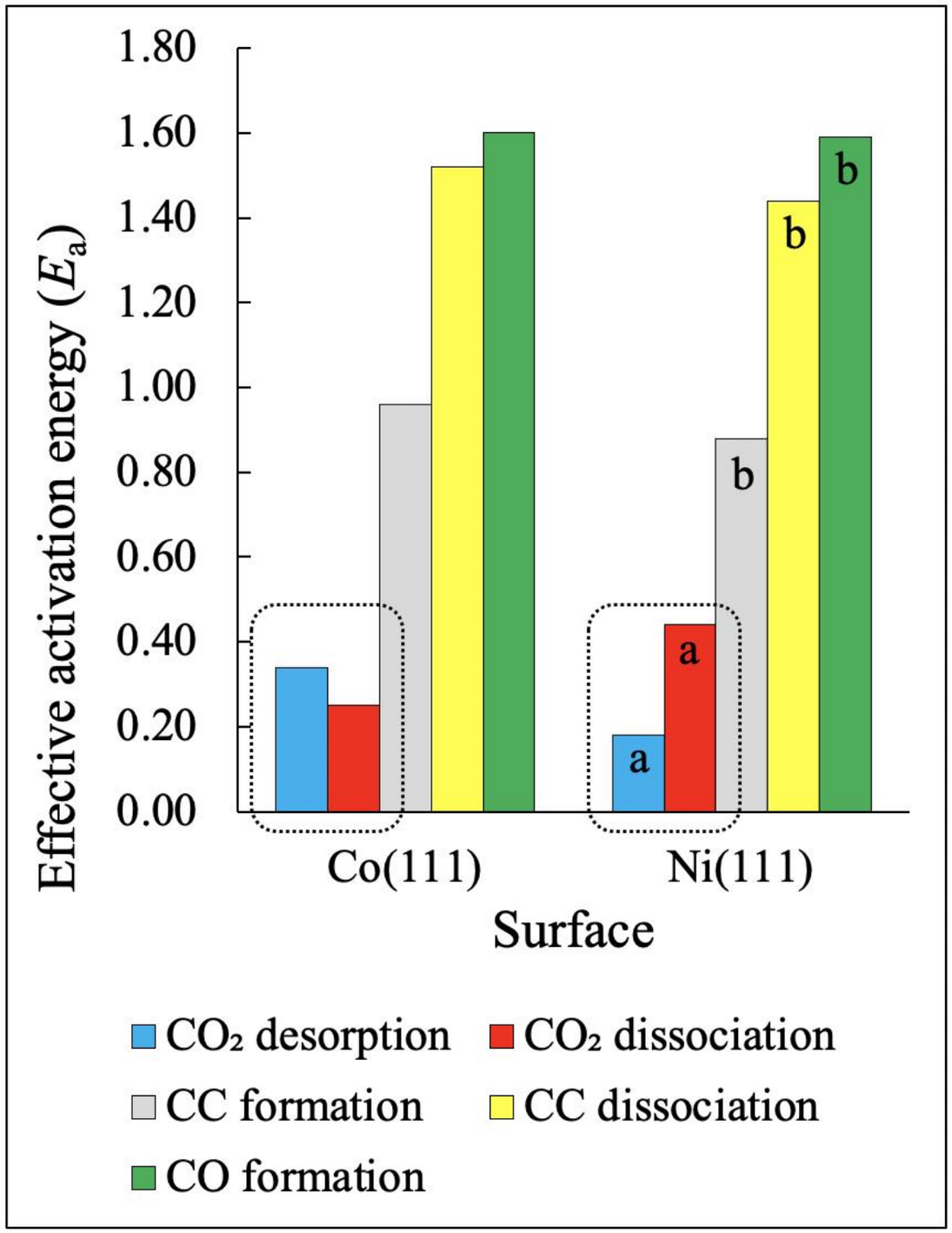

Compare the Co (111) results with Ni (111) to establish the origin for the difference in the potential of carbon graphitization and removal between Co and Ni.

1. On Ni (111), CO_2* desorption is more preferred to CO_2* dissociation
2. On Co (111), CO_2* dissociation is preferred to CO2 desorption

Summary

1. Reduce the exposure of (111) surface in Co nanoparticles might be effective to efficiently reduce the formation of graphitic carbon during DRM
2. Higher tolerance of Co compared with Ni against carbon deposition may come from the higher dissociation rate of CO_2 on Co surface.

Acknowledgements

- CO_2 hydrogenation
  F. Muttaqien (OU → ITB)
  I. Hamada (OU)
  K. Inagaki (OU)
  Y. Hamamoto (OU)

- Cu-Zn alloy with Machine Learning
  Harry Handoko Halim (OU, D2)

- Dry Reforming
  Y. J. Wong (OU-USM DDP → Malaysia)
  Abdul Rahman Mohamed (USM)

Discussions with exp. groups:

- CO_2 hydrogenation
  J. Nakamura (Kyushu Univ.)
  T. Kondo (Univ. Tsukuba)
  J. Quan (Univ. Tsukuba)
  J. Yoshinobu (Univ. Tokyo)
  T. Koitaya (Univ. Tokyo)

Funding:

科研費 KAKENHI

ESICB

e-ASIA (JST)

Enhancement of GaN crystal growth using Na flux method

Takahiro Kawamura
Mie Univ.
Minoru Kawahara
Shin-Etsu
Susumu Yanagisawa
Univ. Ryukyu's
Yusuke Mori, and Yoshitada Morikawa
Osaka University

J. Appl. Phys., **101**, 066106 (2007).
J. Cryst. Growth, **303**, 34 (2007).
Jpn. J. Appl. Phys., **52**, 08JA04 (2013).
Physica status solidi, **252**, 1084 (2015).
Appl. Phys. Express., **9** 015601 (2016).

大阪大学

GaN important material for opt/electronic devices.

- GaN is promissing material for opt-electronic and power devices.

Light Emitting Diode

Blue LED

BlueLD

（Laser Diode）

Reading/Writing of disks

Power device

Power Devices

携帯基地局

Nobel Prize for Physics was awarded to Professors Akasaki, Amano, and Nakamura in 2014

Problems in GaN crystal

- Large (16%) lattice mismatch between sapphire substrate and GaN

⇒ Dislocation defects in grown GaN crystal

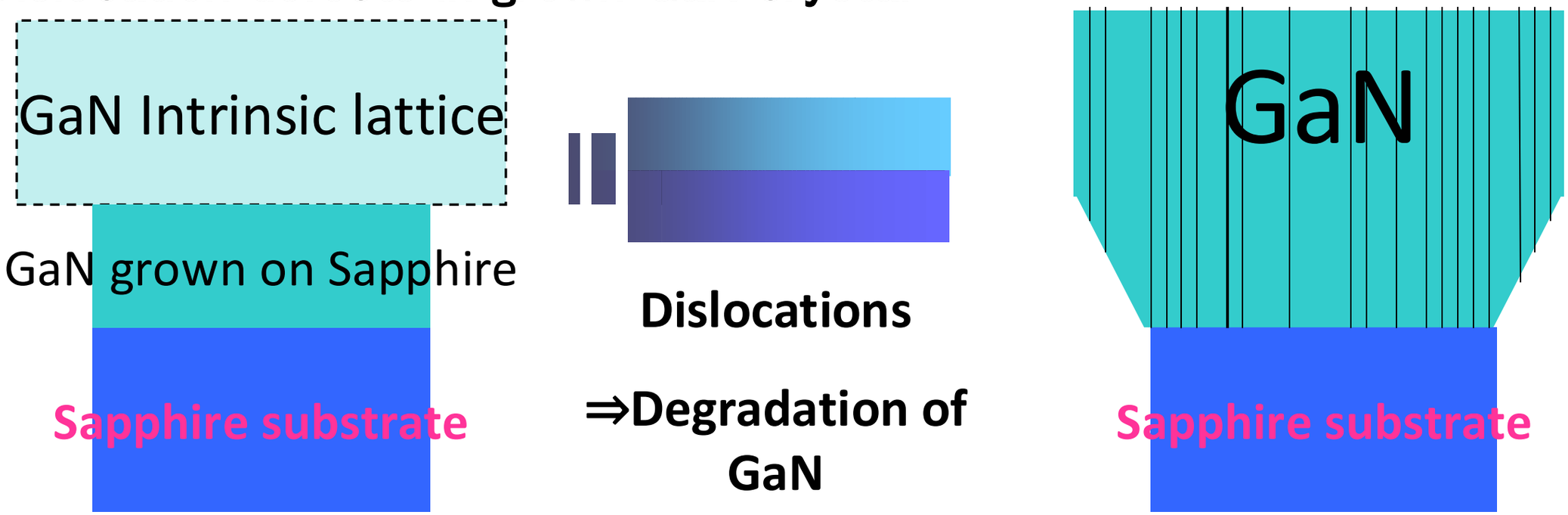

Ideally : GaN bulk substrate is desired.

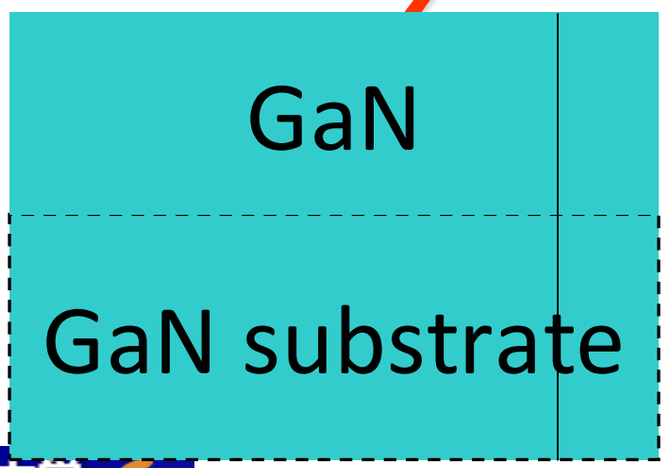

Na Flux Method is one of the most promising techniques used to grow bulk GaN single crystals.

Promissing Na flux method for bulk GaN growth

Figure 3. Photograph of the GaN crystal grown by Na flux LPE method on HVPE-GaN seed crystals. Both sides of the crystal were polished to the thickness of 750 μm to remove the seed crystals.

Y. Mori *et al.*, ECS J. Solid State Sci. Tech, 2, 3068 (2013).

GaN grown by Na flux LPE on HVPE-GaN seed crystal

Na flux method

- N is introduced into Ga–Na liquid alloy.

Na flux method

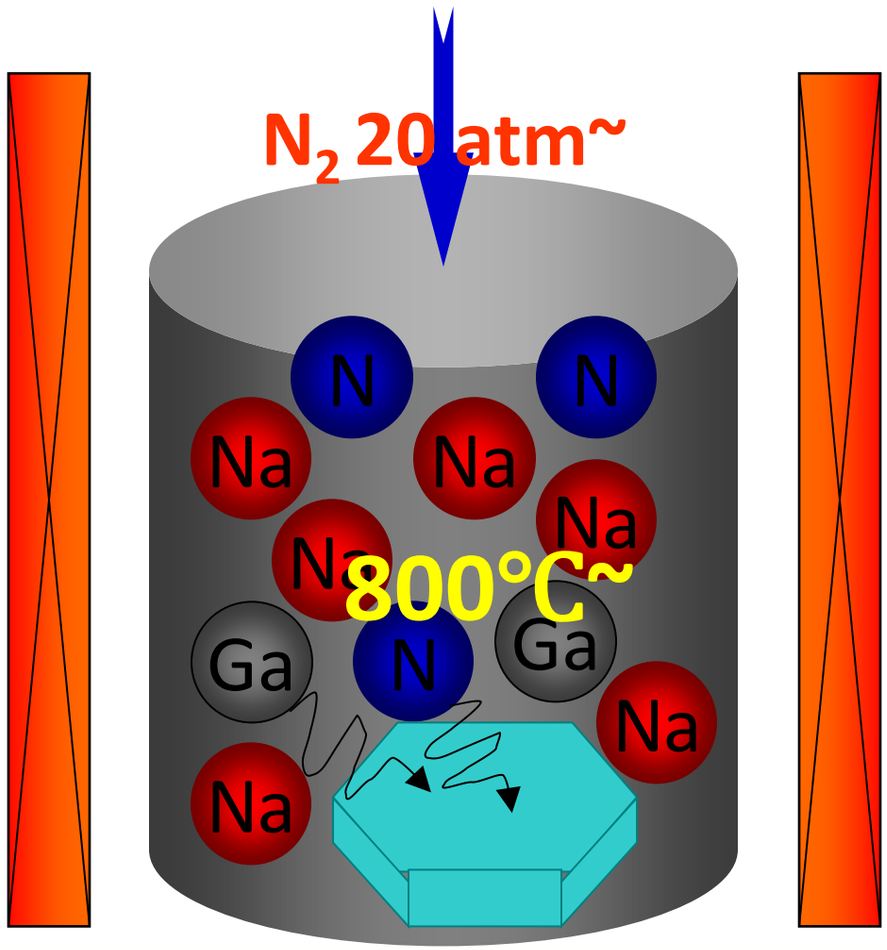

Cf. High pressure method.

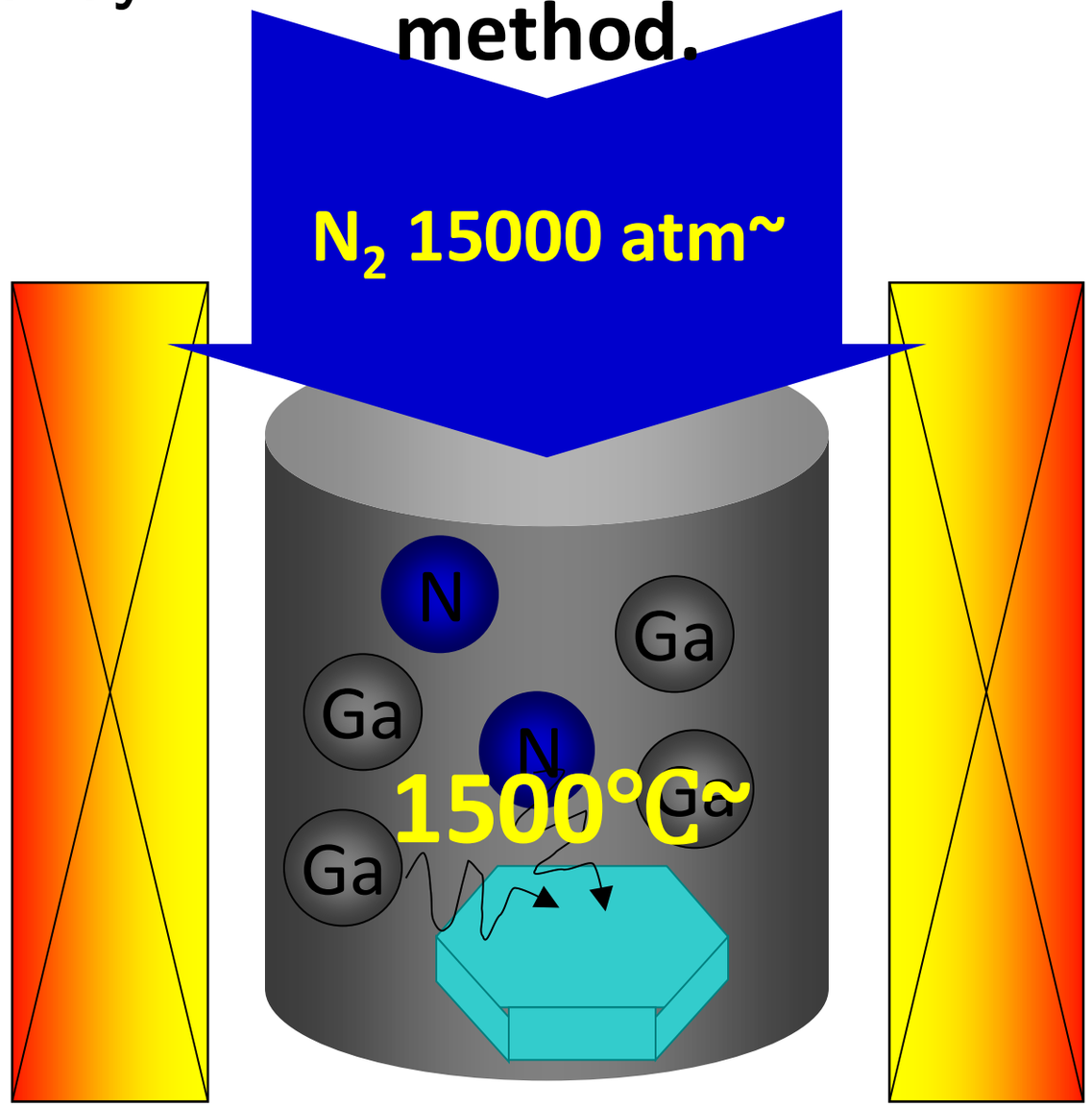

It is necessary to apply 10000atm and 1500℃ to dissolve N into pure Ga liquid. But if Ga is mixed with Na, the required pressure and temperature are reduced dramatically to 20atm and 800℃.

Comparison between Na-flux and pure Ga

	flux	T[K]	P[MPa]	N solubility
Pure Ga	**Ga**	＞1800K	1500	10^{-9}
Na flux	**Ga+Na**	**≒1100K**	**1−5**	**10^{-2}**

By alloying Ga with Na, the N solubility is dramatically enhanced.

However, N_2 solubility is as low as 10^{-9} at.% (1073K)

Pure Ga and Na liquids do not dissolve N_2. Why does the alloying of the two metals dramatically enhance the N_2 solubility?

First-principles simulation can clarify the microscopic origin of the puzzling phenomenon.

Puzzling phenomenon in Na flux method.

N_2 solubility into GaNa liquid alloys

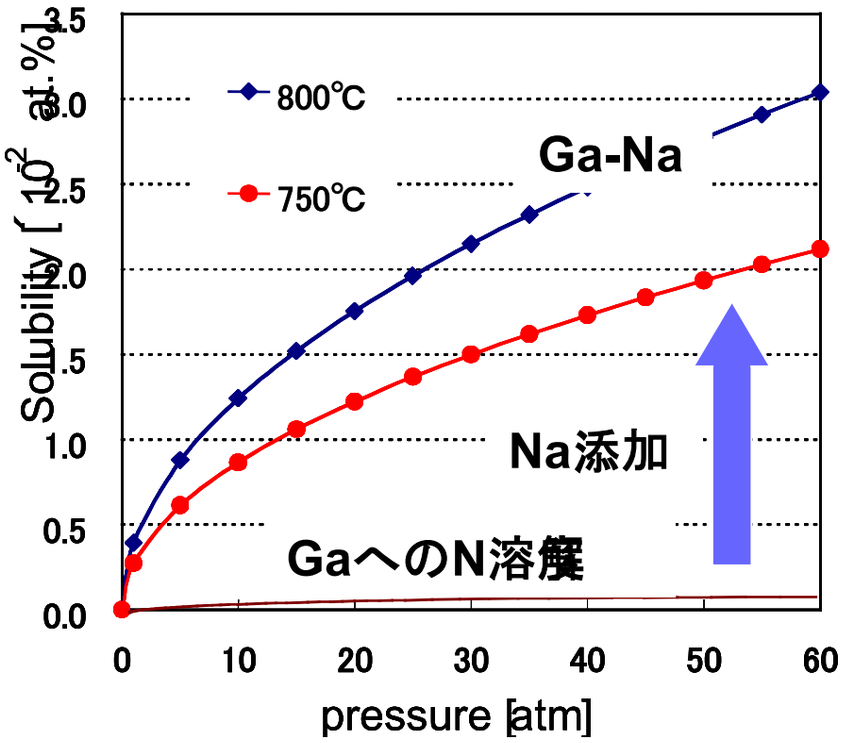

GaN Crystal Growth

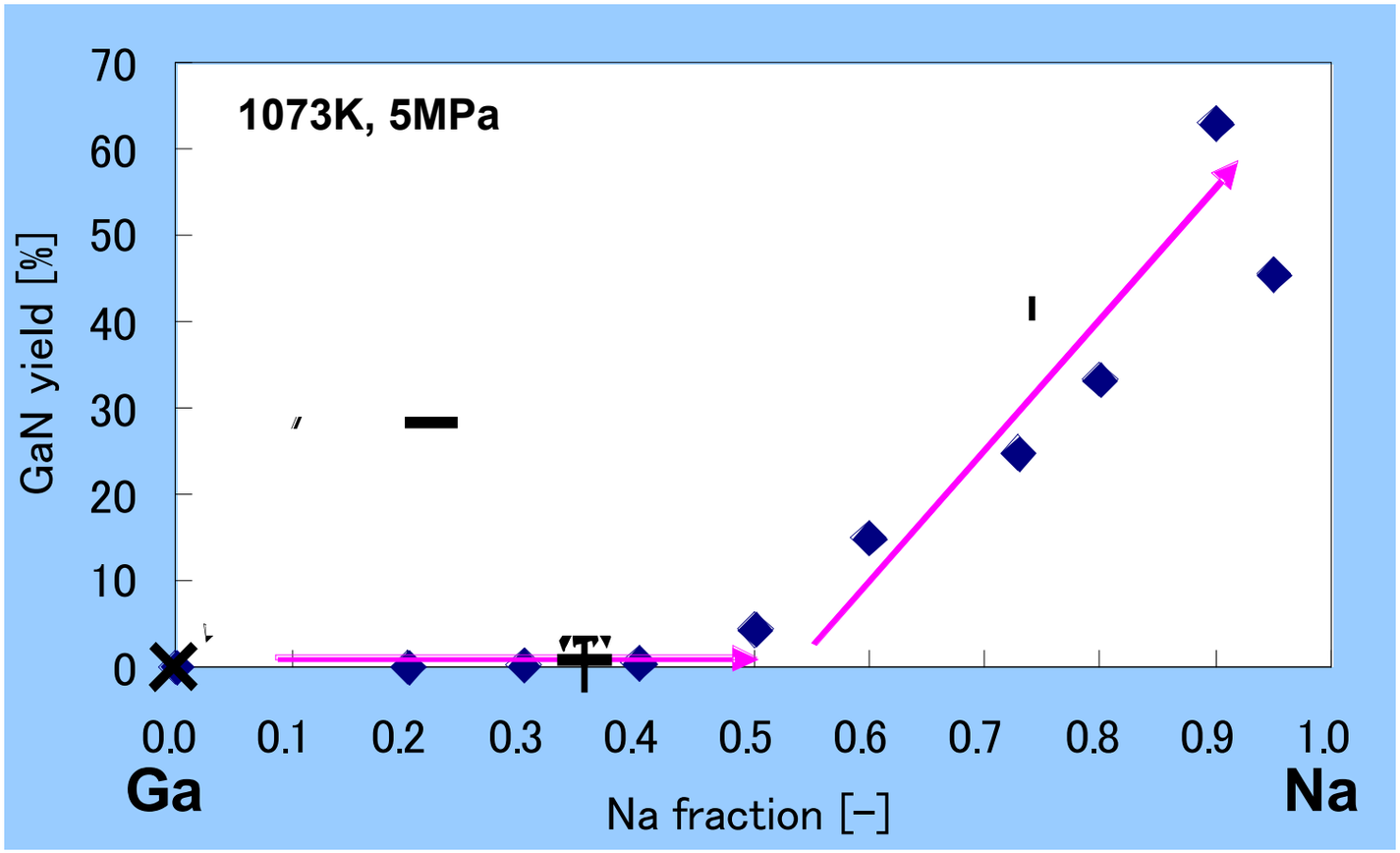

- Na < 50% : The N_2 solubility is quite low
- Na > 50% : It increases dramatically
- Na ～ 90%: It takes maximum value

Effect of a Carbon Additive

Suppression of polycrystals[6]

[6] F. Kawamura et al., J. Cryst. Growth 310 (2008) 3946.

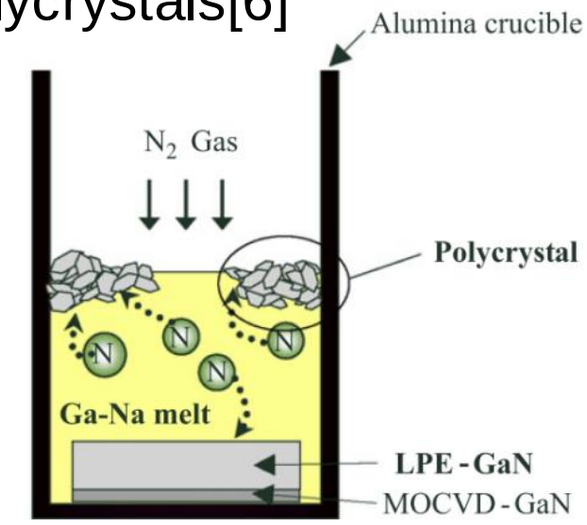

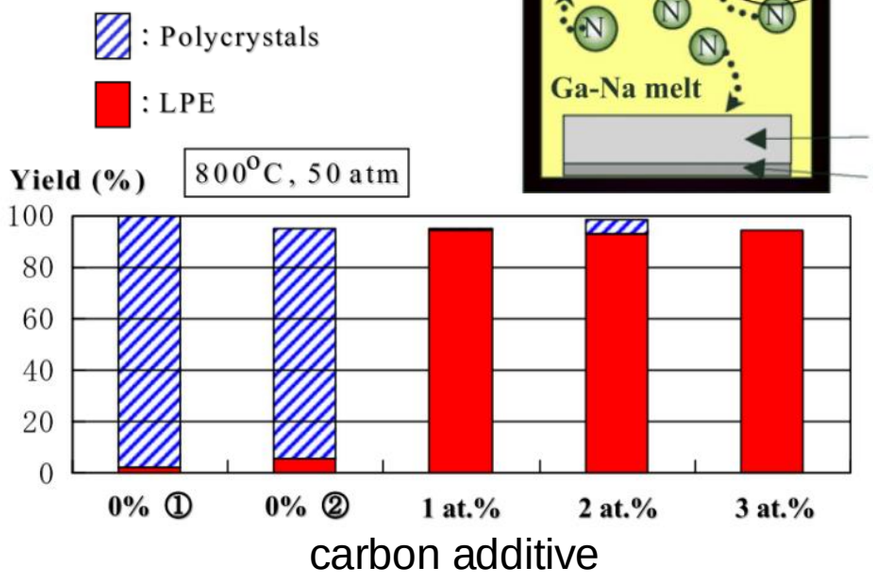

Enhancement of Growth Rate

[7] M. Imade et al., Applied Physics Express 3 (2010) 075501.

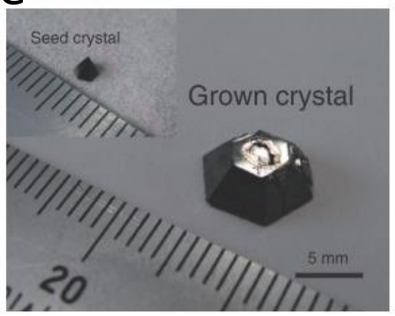

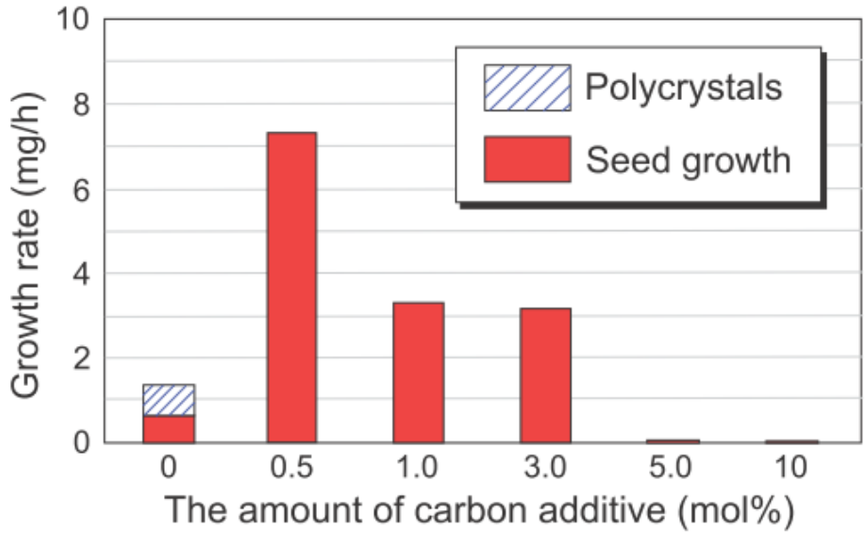

Addition of carbon into GaNa alloy dramatically suppresses the formation of poly-crystals and enhances GaN crystal growth.

⇩

What is the interaction between N and C atoms in GaNa liquid alloys?

Simulation Methods and Conditions

✓Simulation Tool for Atom TEchnology
(STATE-Senri)
✓DFT-GGA (PBE96)
✓Ultra-soft pseudopotential
✓Plane wave basis set:
25 Ry for wave function,
225 Ry for charge density

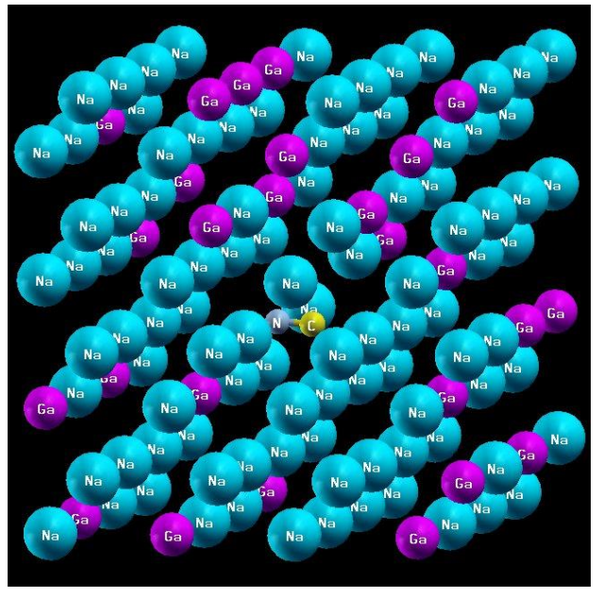

128 atoms in a cubic box of
16.8 × 16.8 × 16.8 [Å^3]
3D periodic b.c.

✓128 Atom Model
54 Atom Model
+ N (and C)
✓ 10 ps first-principles MD
～10,000 MD steps for each trajectory
✓ Blue Moon Ensemble method for free energy

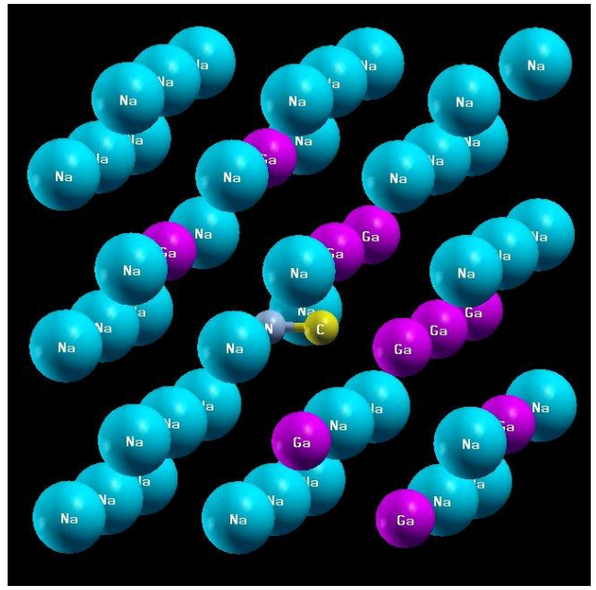

54 atoms
12.6 × 12.6 × 12.6 [Å^3]
3D periodic b.c.

First-principles Molecular Dynamics at 1073 K

Ga : Na 4 : 1 liquid alloy

Ga : Na 1 : 1 liquid alloy

Ga : Na 1 : 4 liquid alloy

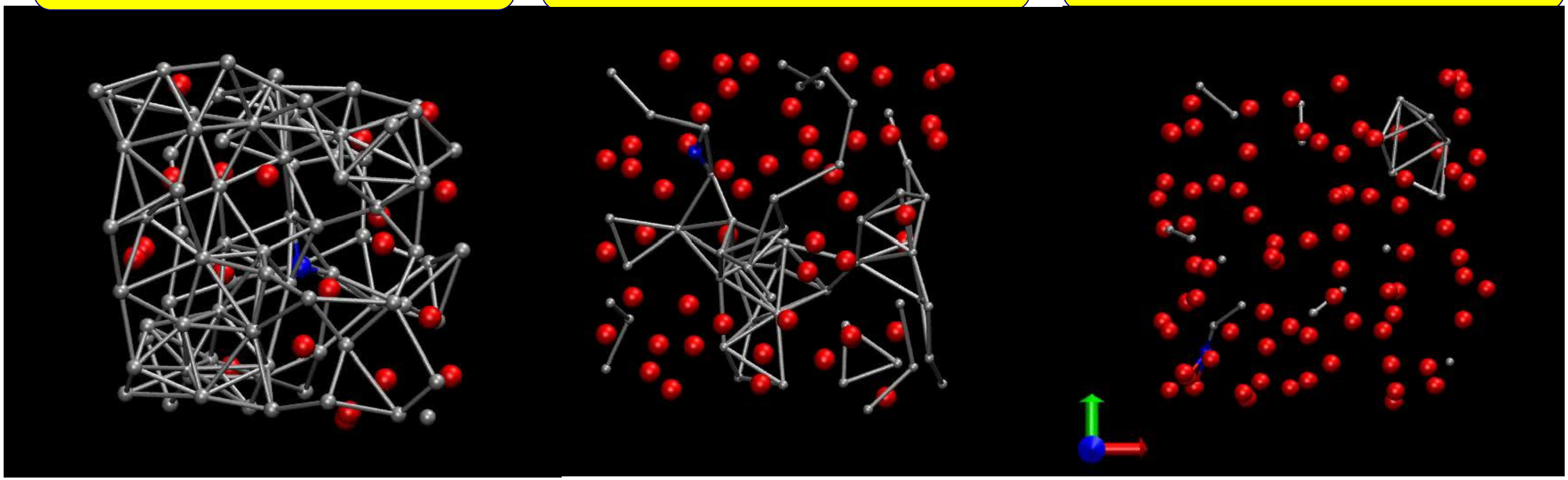

- In Ga-rich: Ga-rich region and Na-rich region are separated.
  N is located between Ga and Na regions.
- In Na-rich: Isolated Ga or small Ga clusters exist
  N is bound to those atoms or small clusters.

Microscopic origin becomes clear.

N dissolved in Ga–Na liquid alloys

Ga：Na 4：1 liquid alloys

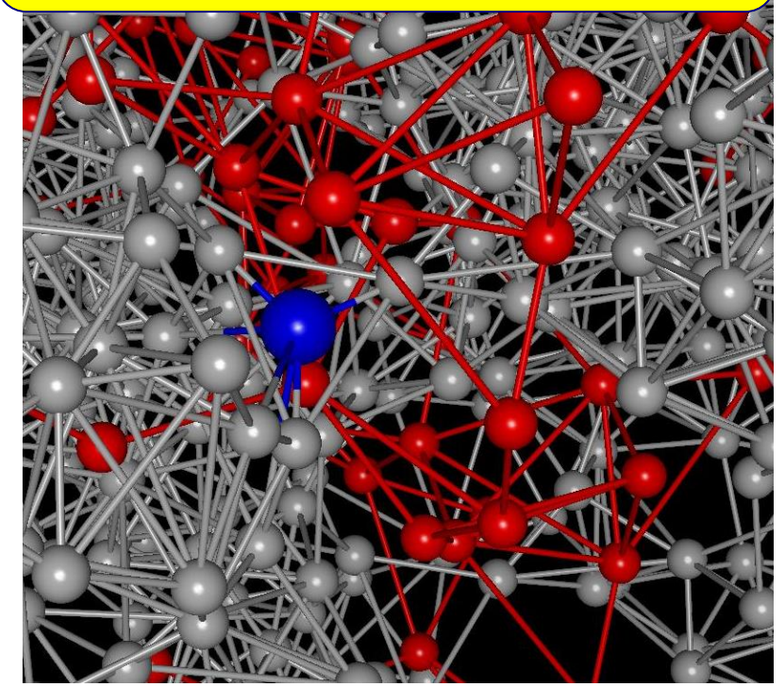

Ga：Na 1：1 liquid alloys

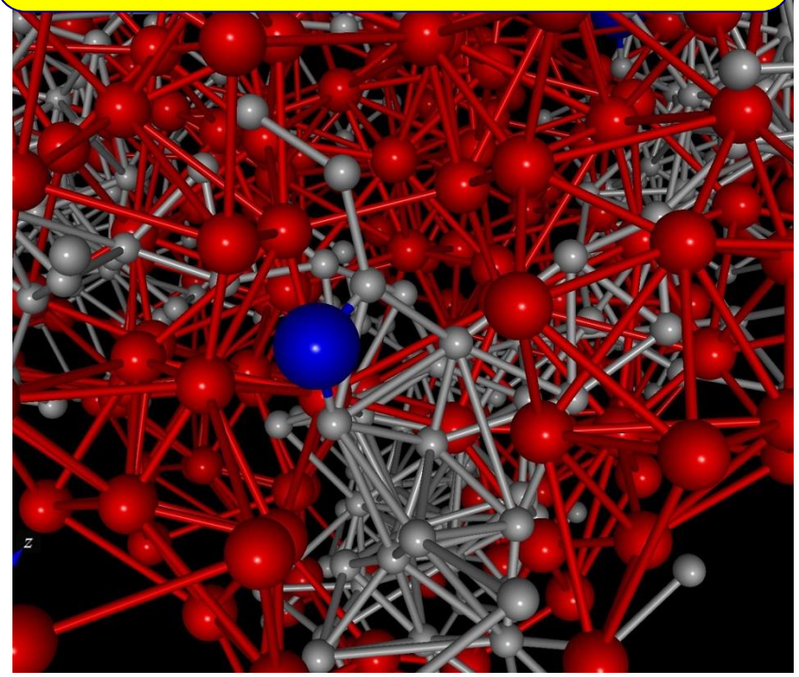

Ga：Na 1：4 liquid alloys

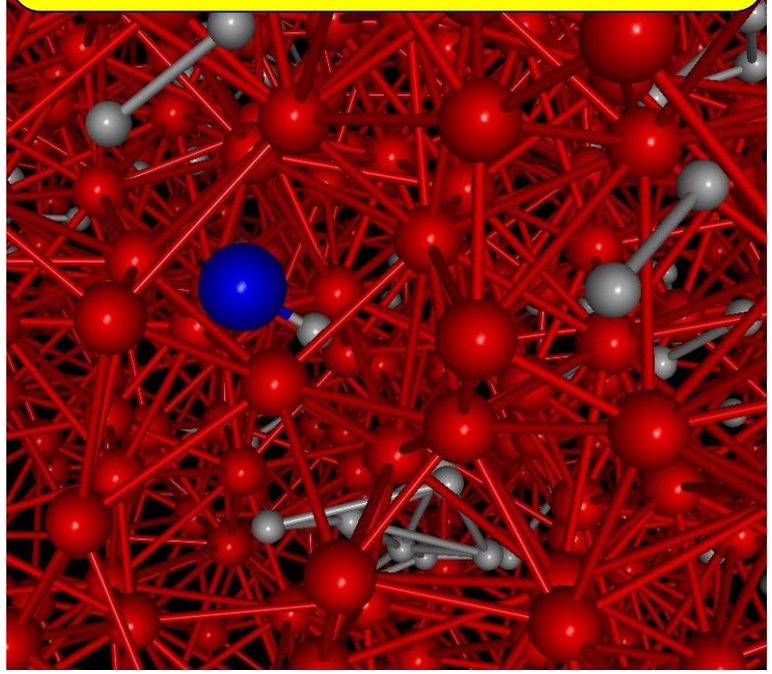

- In Ga-rich: Ga-rich region and Na-rich region are separated.
  N is located between Ga and Na regions.
- In Na-rich: Isolated Ga or small Ga clusters exist
  N is bound to those atoms or small clusters.

Microscopic origin becomes clear.

Calculated N_2 solubility into Ga–Na liquid alloys

- Formation enthalpy of N_2 dissolution into GaNa solid alloys（128−180粒子）are calculated as follows

E_{form}（N）＝ 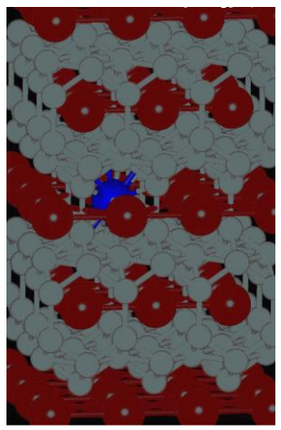 − { 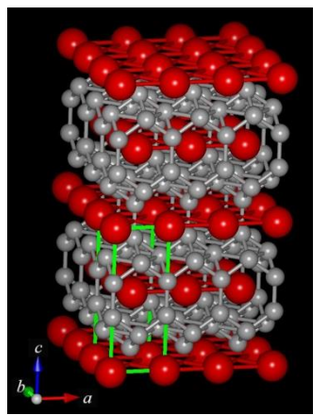 ＋ 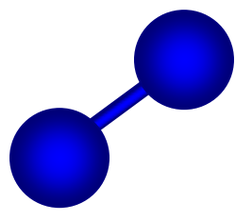 }

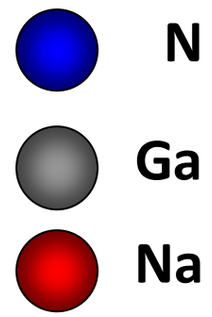

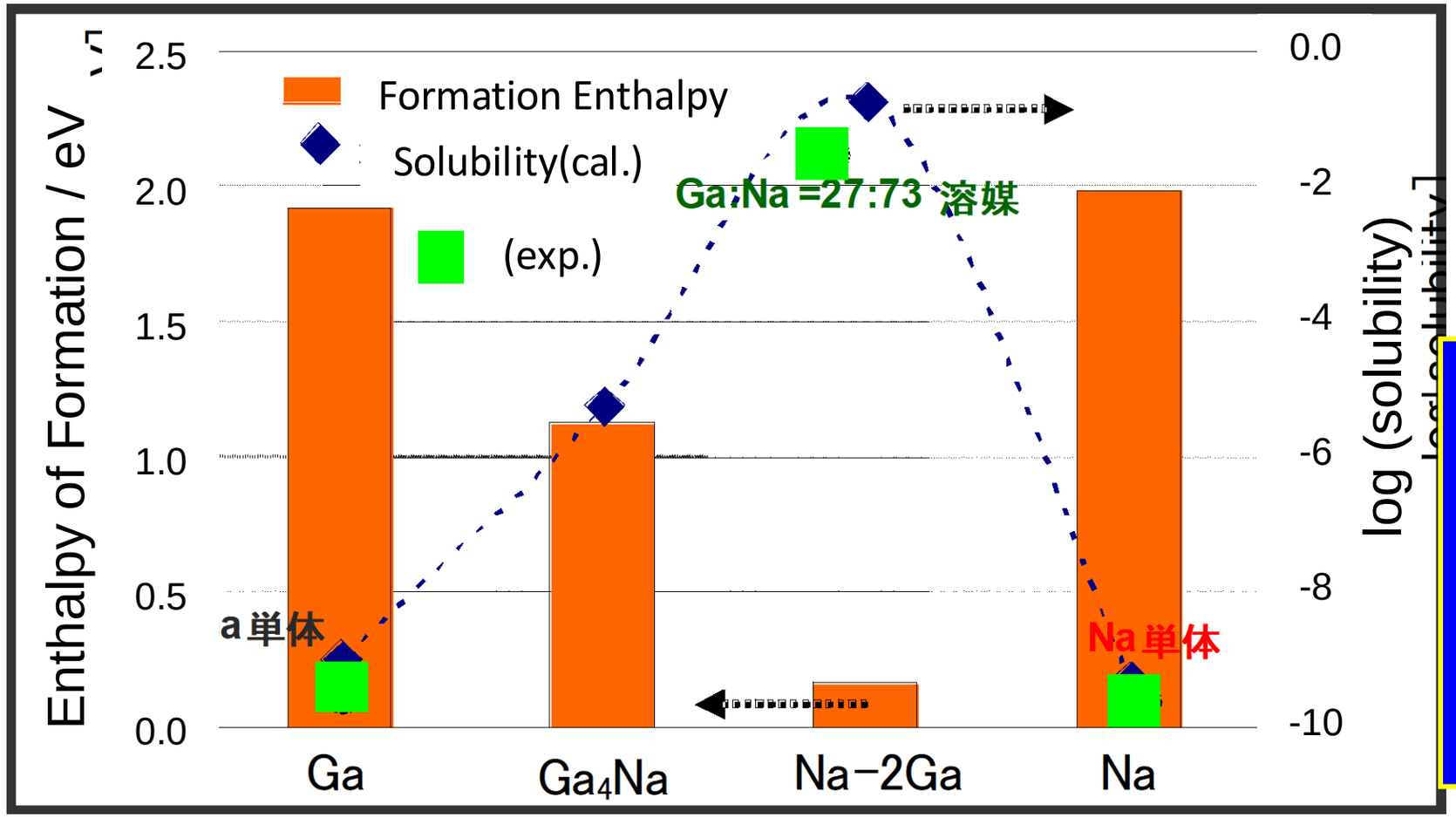

Experimental trend can be well reproduced.

Effect of a Carbon Additive

Suppression of polycrystals [6]

[6] F. Kawamura et al., J. Cryst. Growth 310 (2008) 3946.

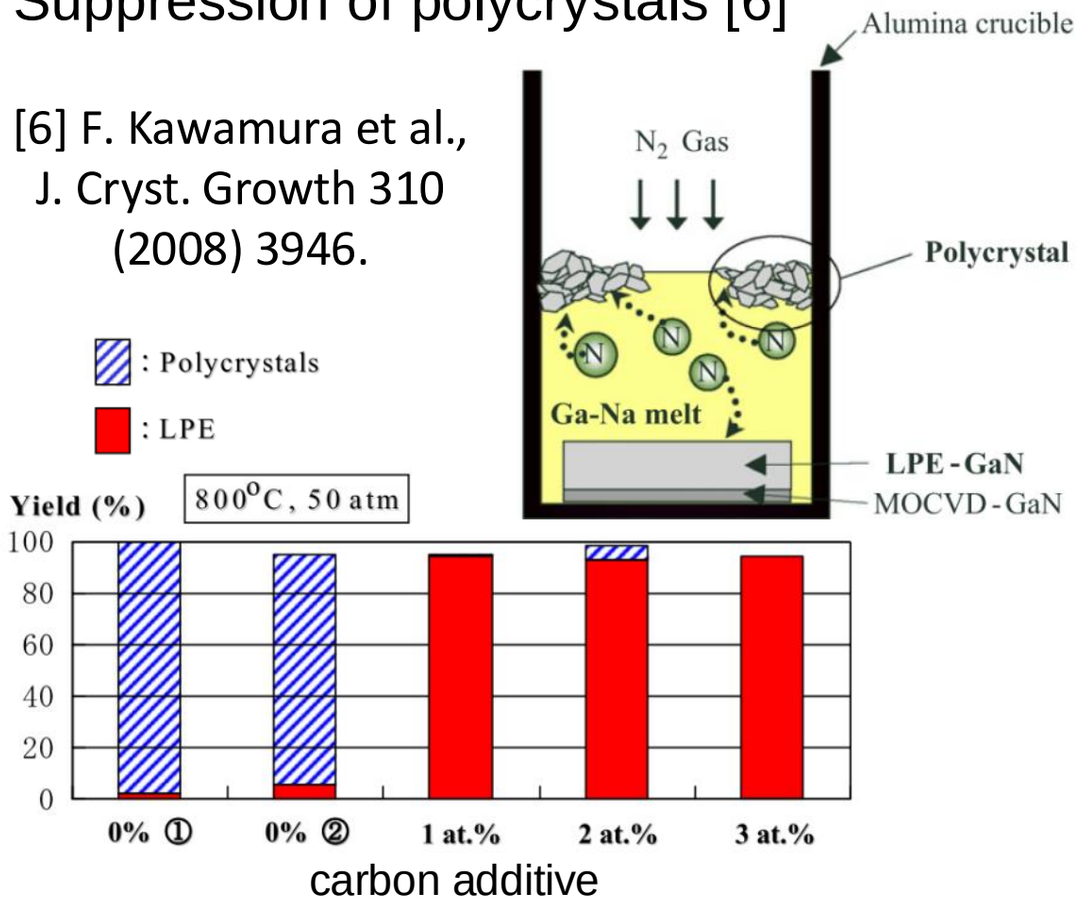

Enhancement of Growth Rate

[7] M. Imade et al., Applied Physics Express 3 (2010) 075501.

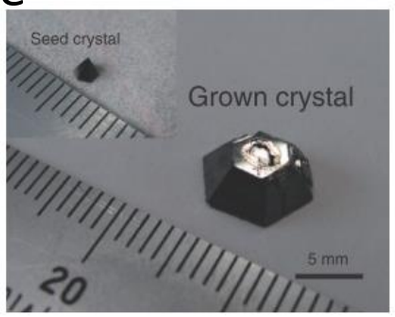

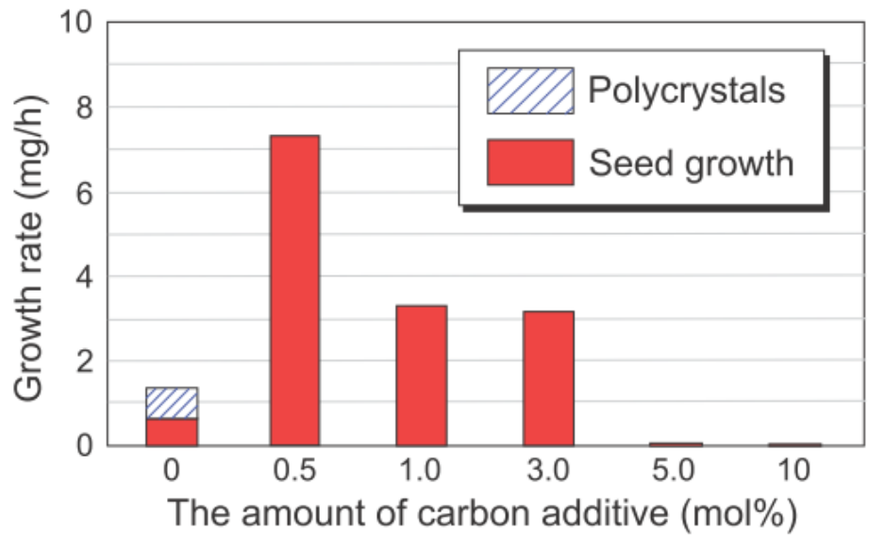

Addition of Carbon into GaNa alloy dramatically suppresses the formation of poly-crystals and enhances the GaN crystal growth.

⇩

What is the interaction between N and C atoms in GaNa liquid alloys?

First-principles MD : C and N in GaNa liquid alloys

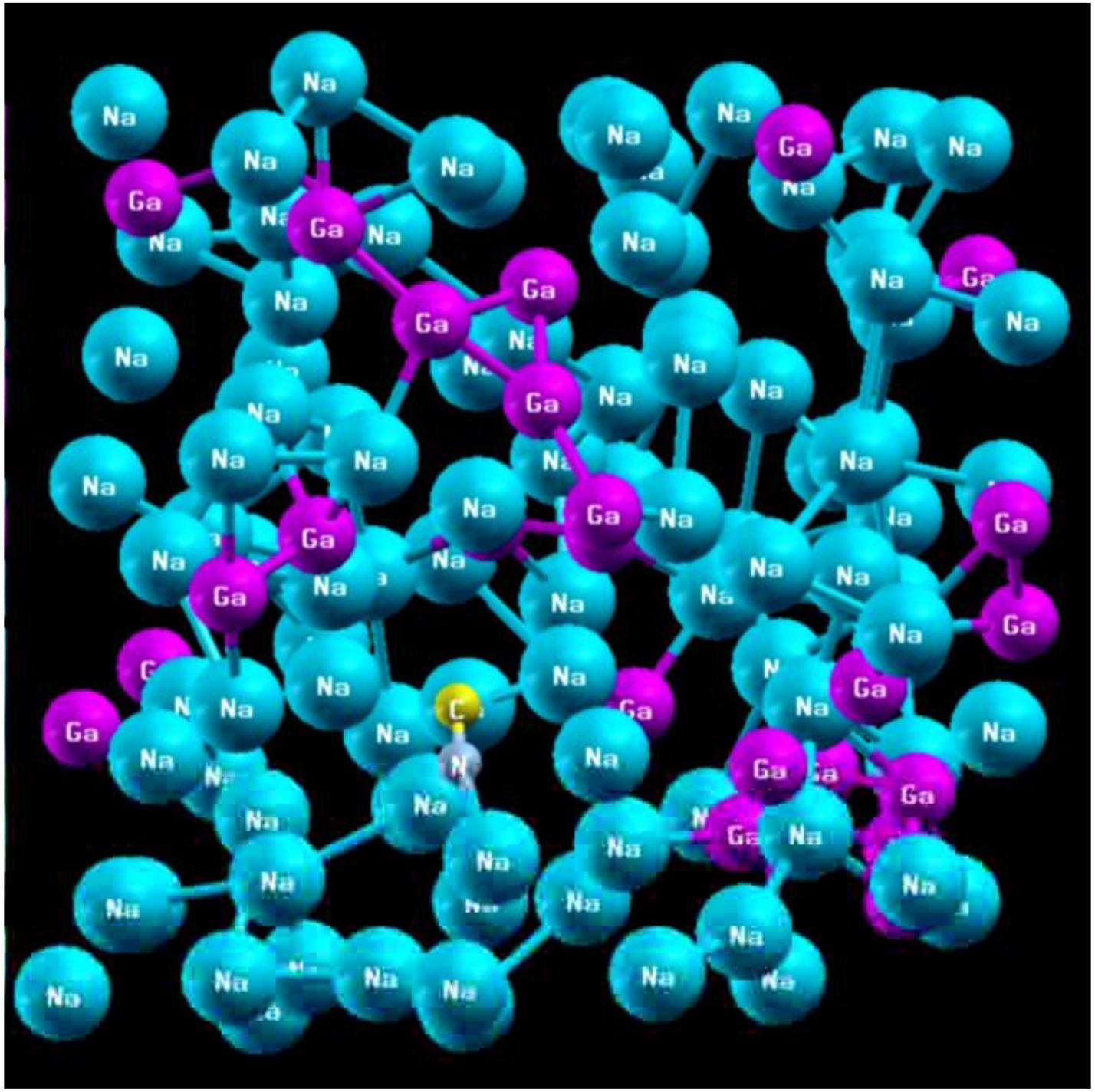

128 atoms（Ga26, Na100, N1, C1）, 1073K

C-N formation in GaNa liquid alloys

With C additive（Ga26, Na100, N1, C1）

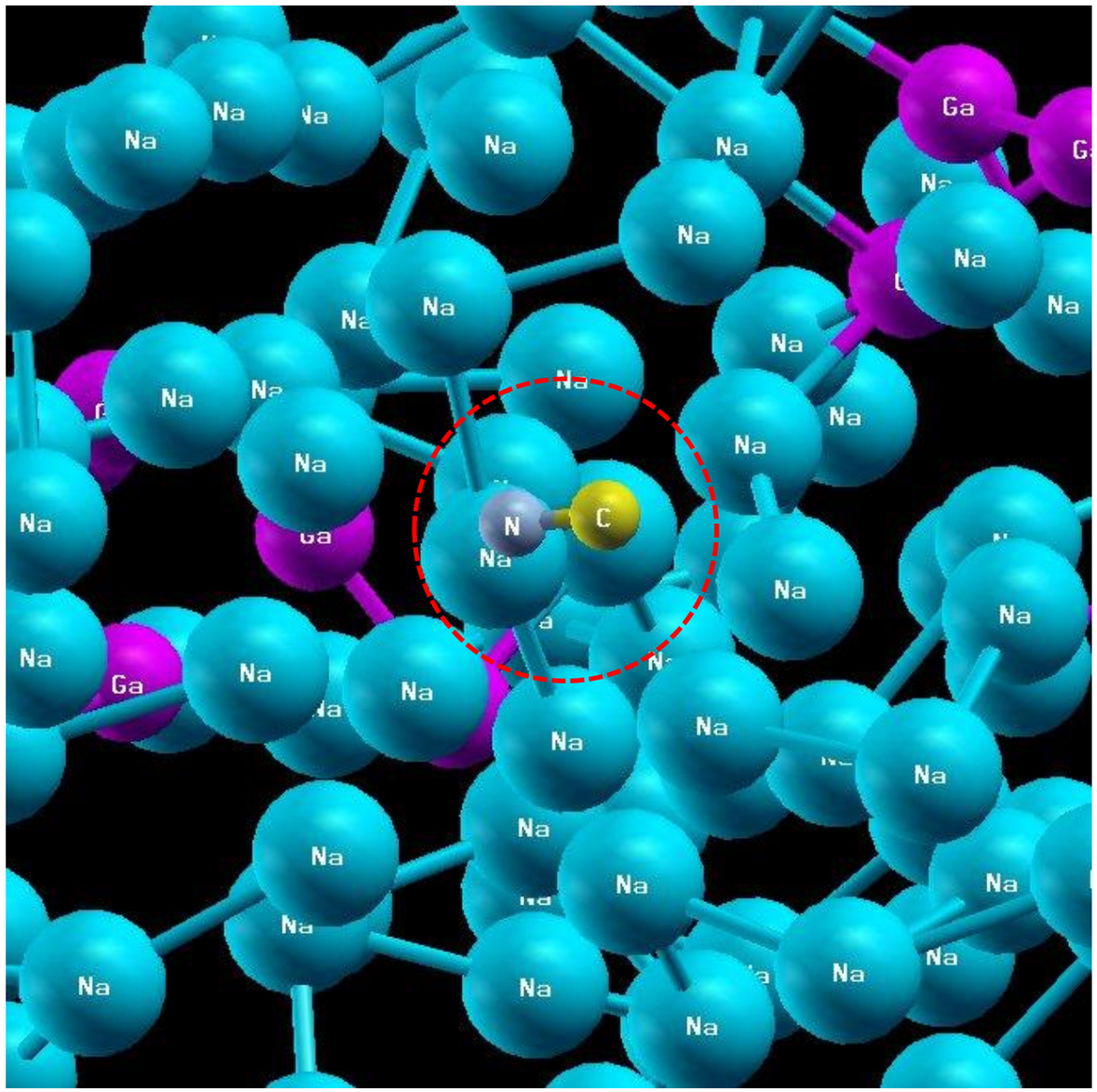

C-N bond is formed.
No N-Ga is formed

Without C additive（Ga27, Na100, N1）

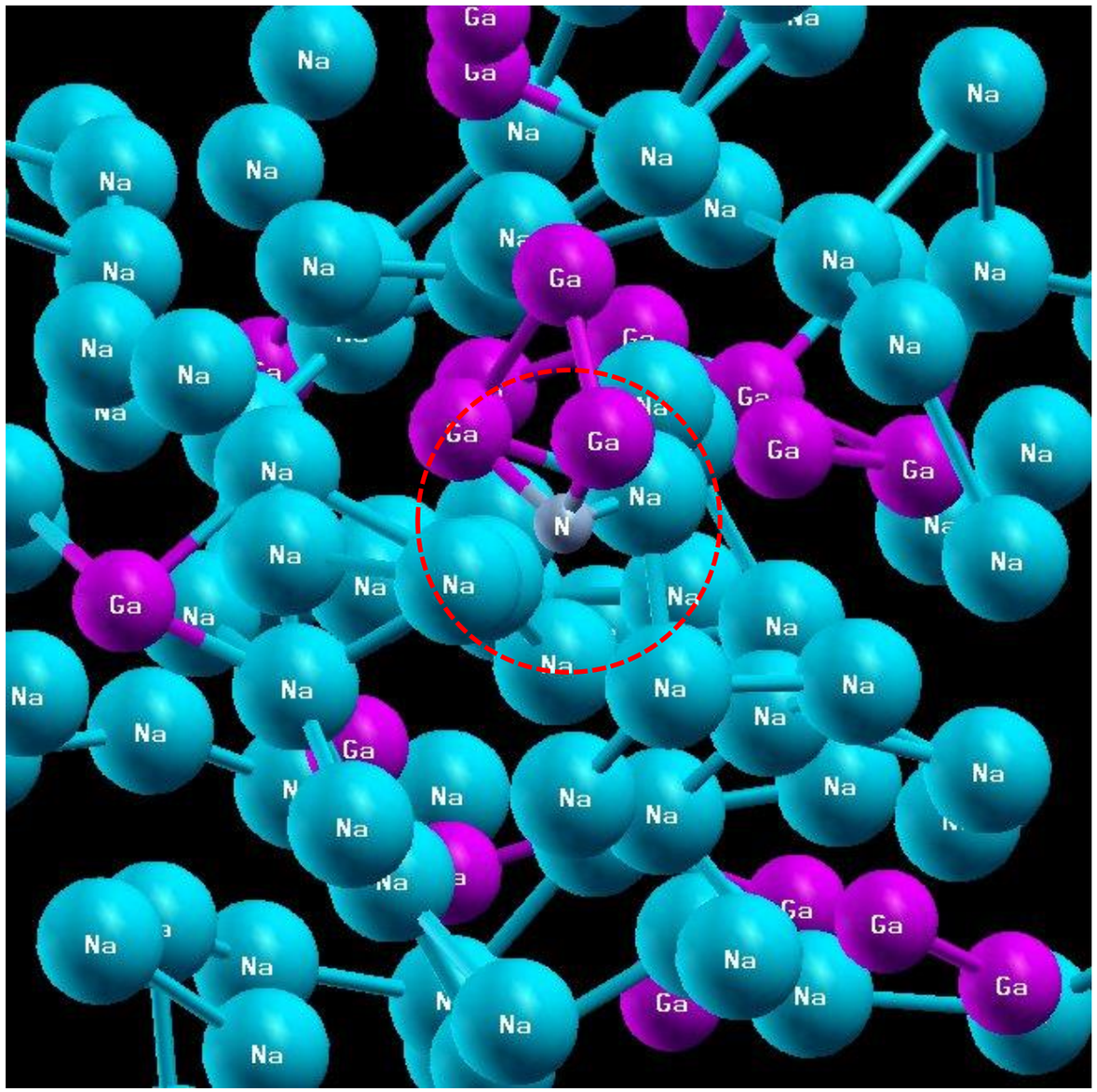

N-Ga bond is formed

Surface Model

CN adsorbed at kink-site on the GaN (001) surface

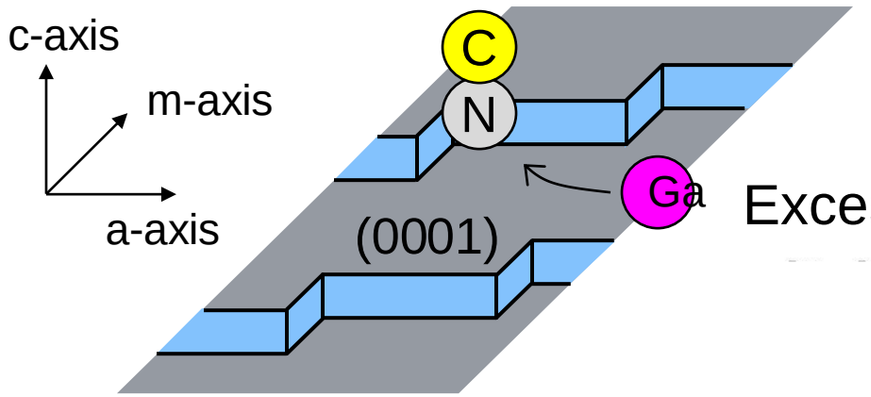

Excess Ga atoms included

Constraint on the C-N bond distance
1073 K, 10 ps First-principles MD.

Cell size $4.7 \times 9.8 \times 32$ Å^3
59 atoms

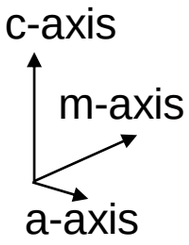

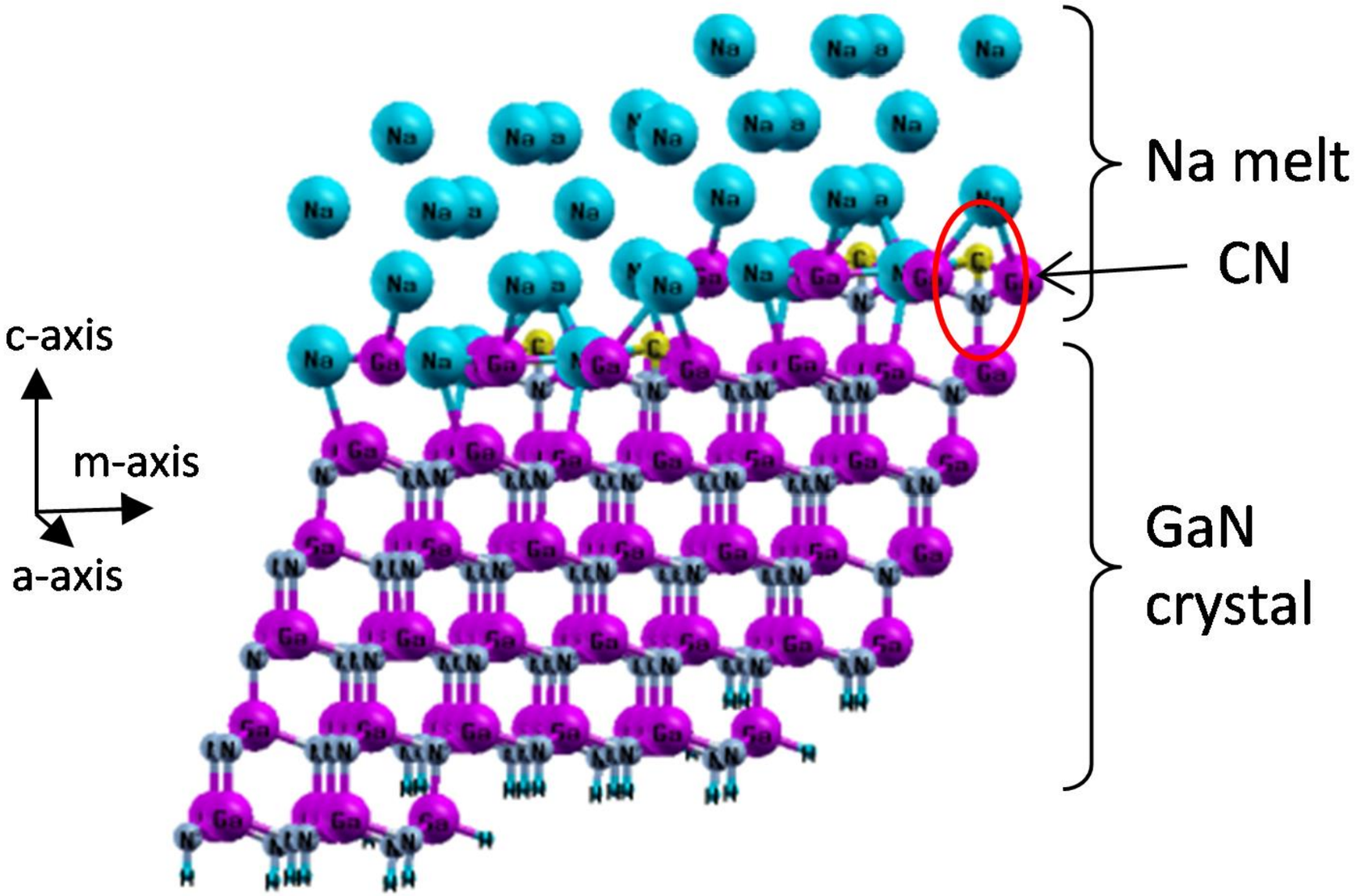

C–N bond length dependence

With excess Ga

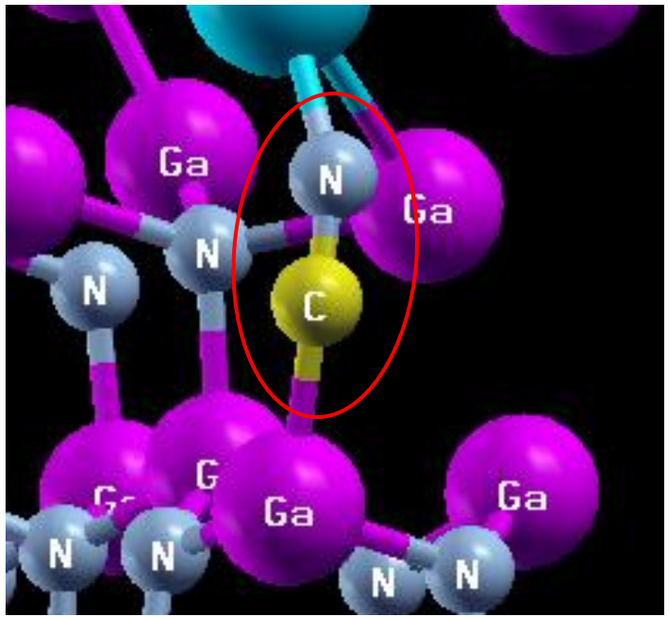

1.2 Å

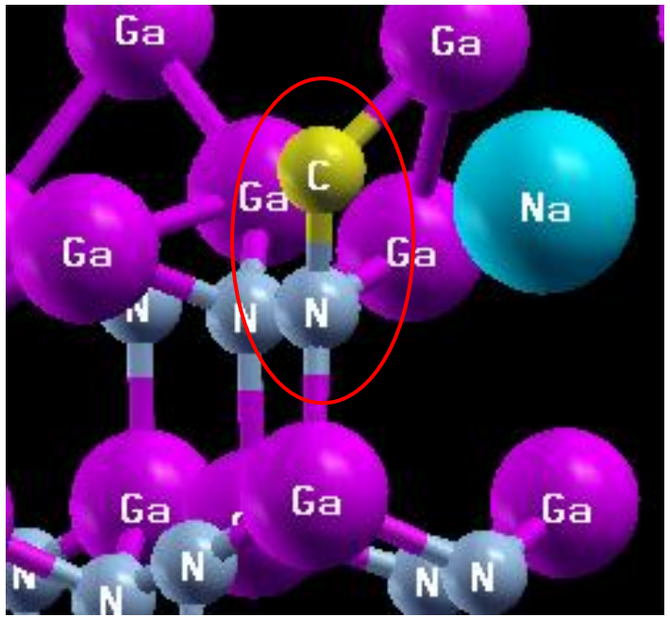

1.4 Å

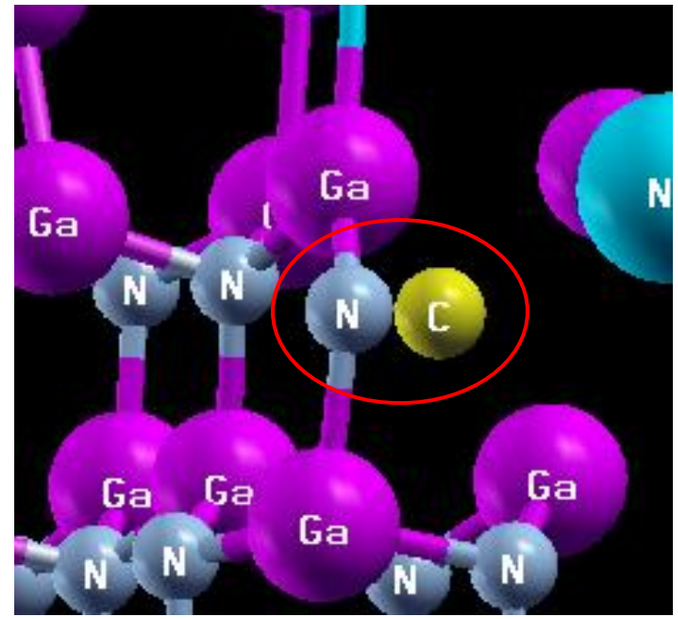

1.6 Å

Without excess Ga

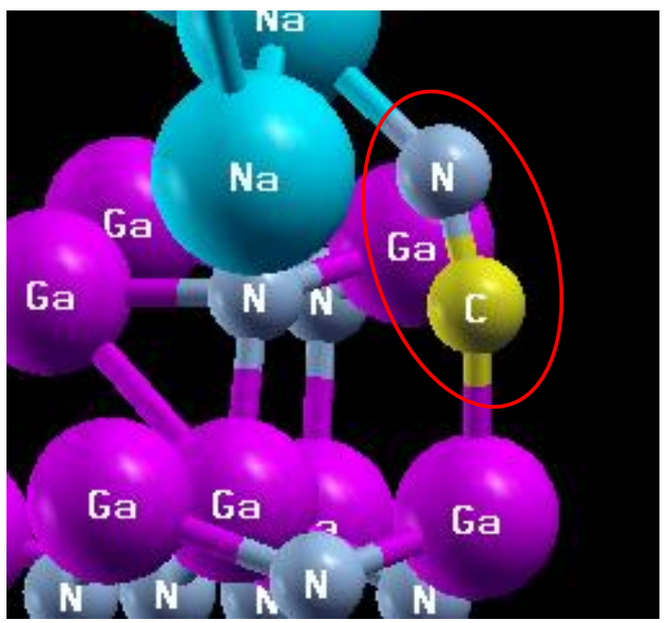

1.2 Å

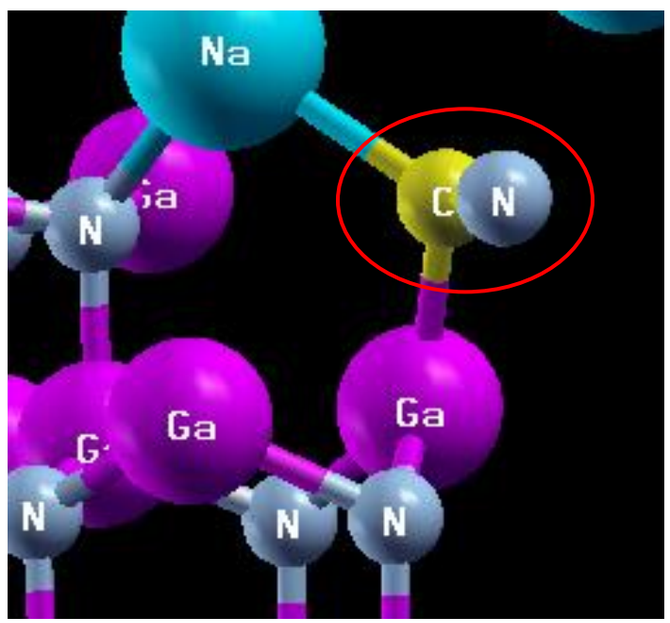

1.4 Å

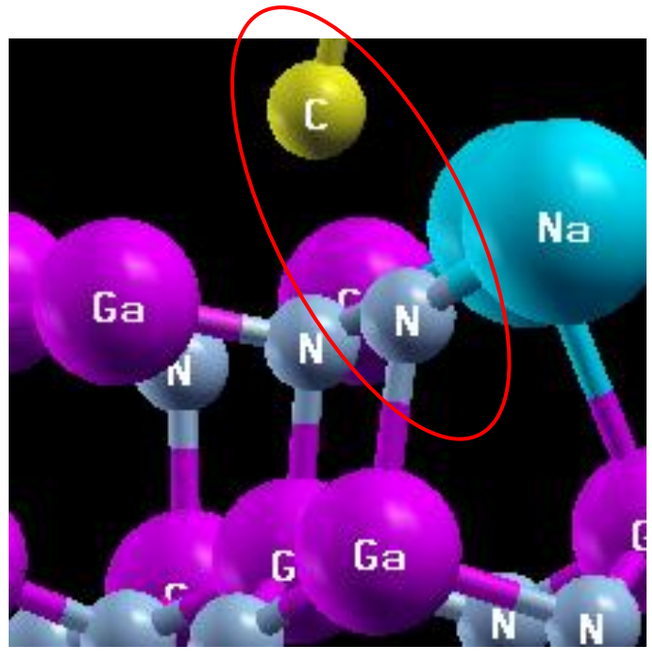

2.0 Å

Blue Moon Ensemble (BME) for Free Energy Evalulation

M. Sprik, JCP ('98)

Free Energy Difference

$$W(x_1) - W(x_2) = \int_{x_1}^{x_2} dx' \left\langle \frac{\partial H}{\partial x} \right\rangle_{x'}^{\text{cond}}$$

ξ: Reaction Coordinate

$W(\xi)$: Free Energy at ξ

$$-\left\langle \frac{\partial H}{\partial x} \right\rangle_{x'}^{\text{cond}}$$: Conditional Ensemble Average (Mean Force)

Free Energy Profile for C–N Bond Dissociation

In Na flux w/o Ga

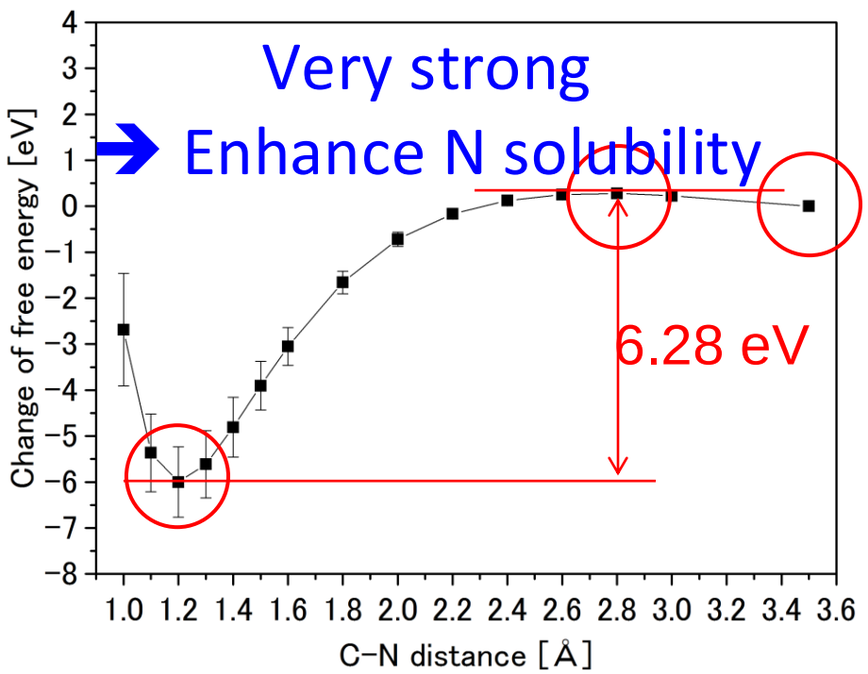

In GaNa flux

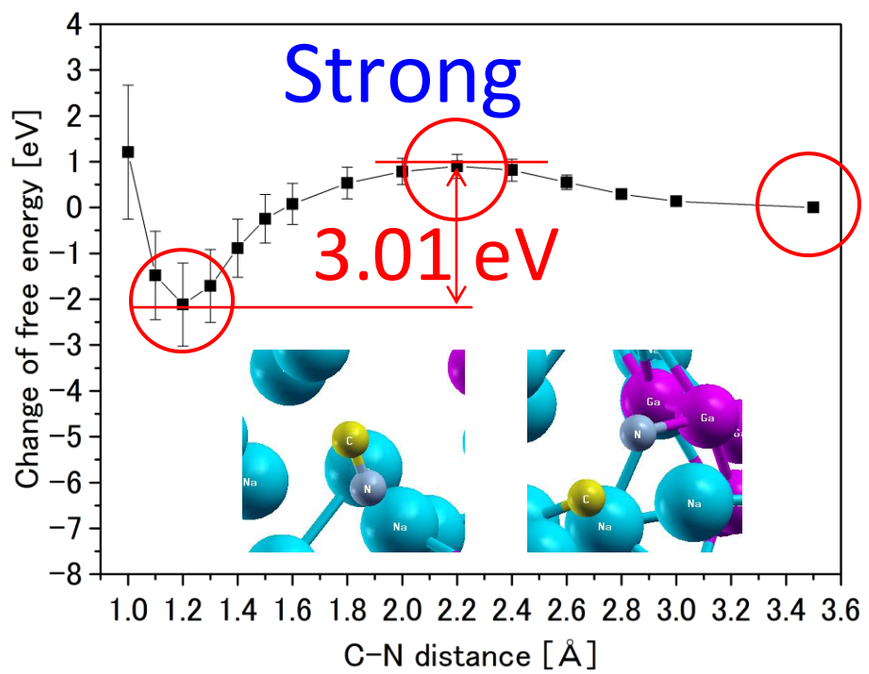

Suppress poly-crystal formation

On GaN(001) with excess Ga

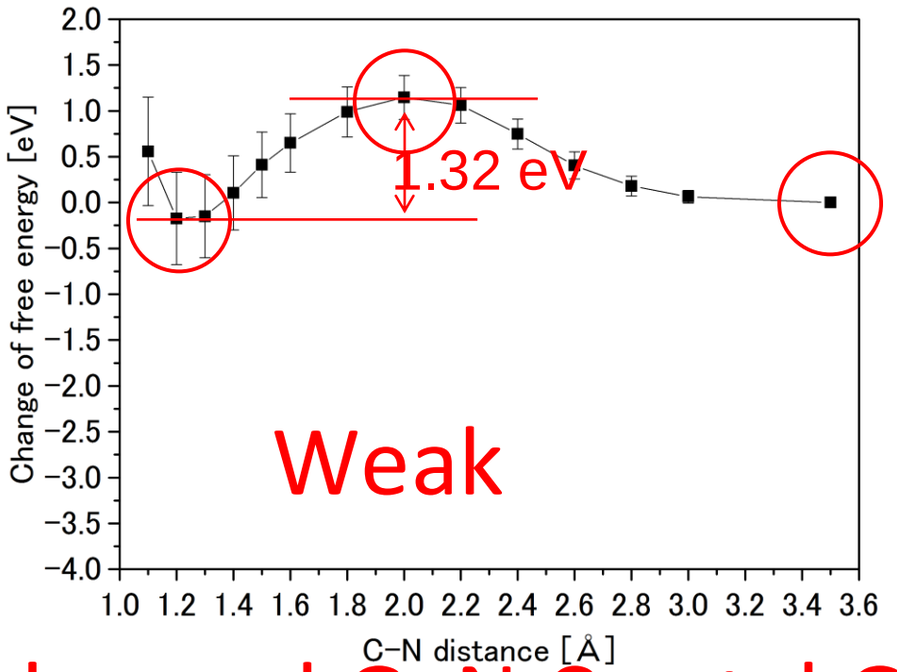

On GaN(001) without excess Ga

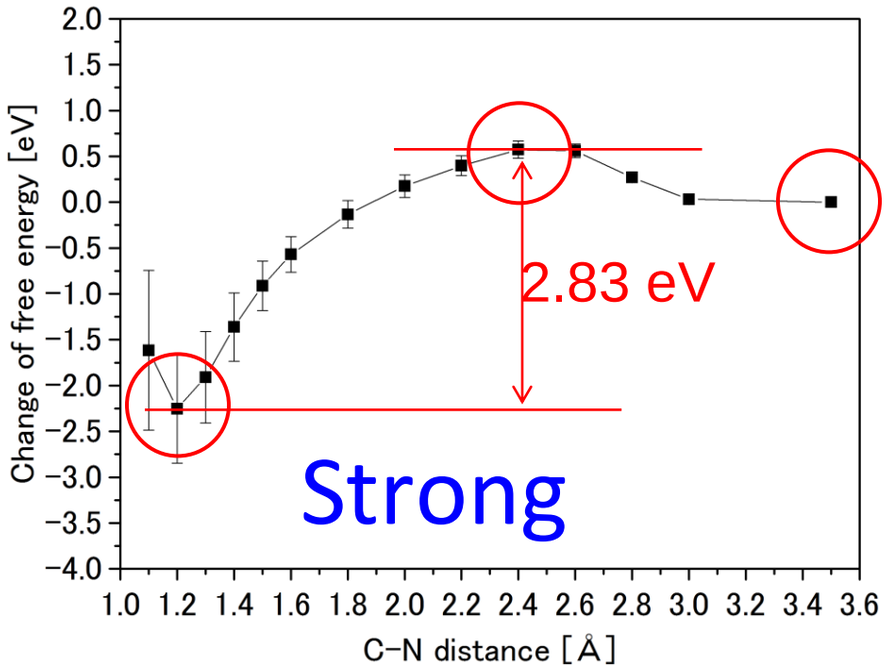

Enhanced GaN Crystal Growth

C-N VS N-N Bond Dissociation

N_2 dissociation

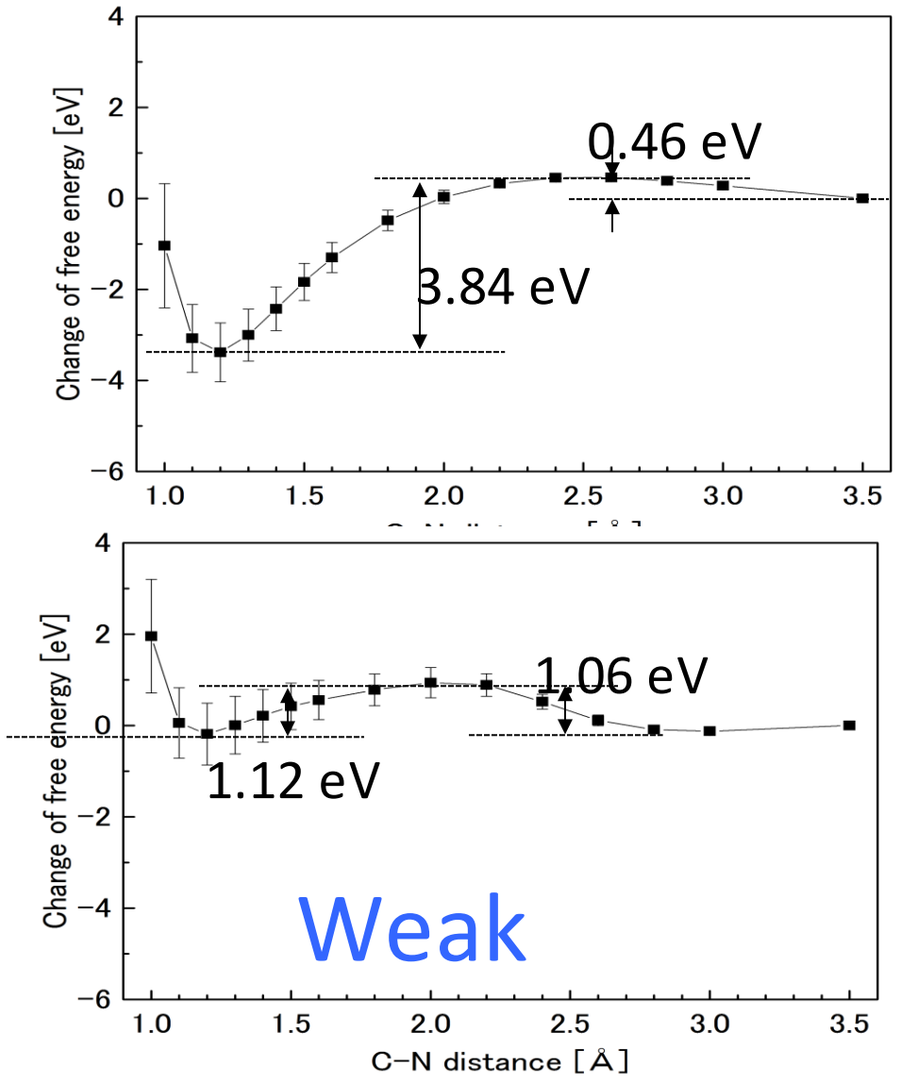

In pure Na

In Na+Ga

Na/GaN Interface

C-N dissociation

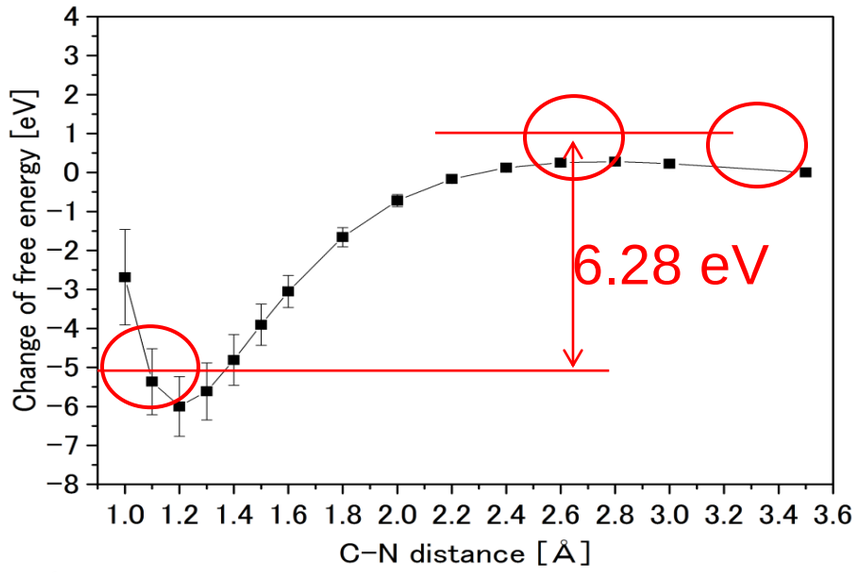

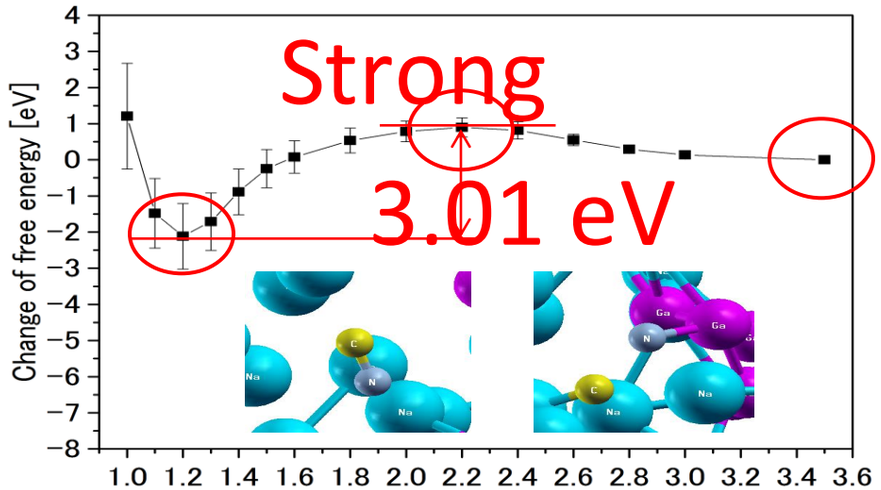

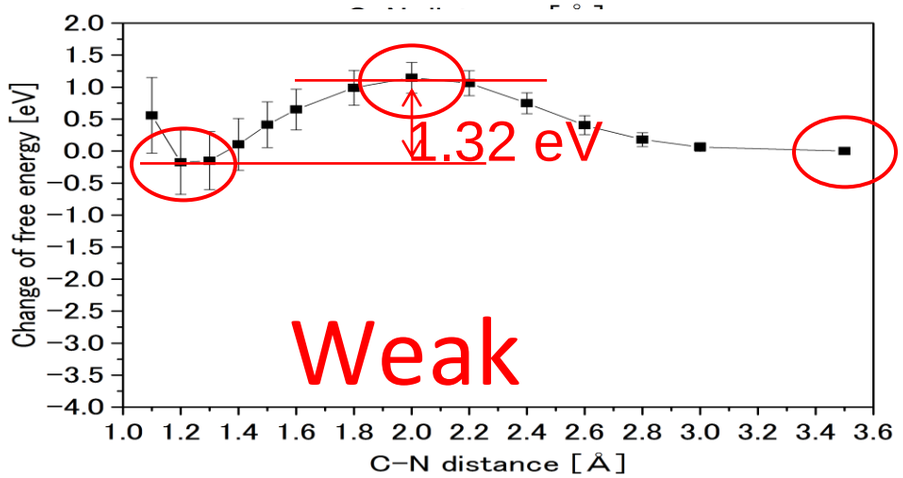

C-N VS N-N Bond Dissociation

In Gas Phase

N-N : 9.8 eV ← Stronger

C-N : 7.7 eV

Solvation Energy into Na-flux

N_2 : +1.0 eV

Destabilized owing to Pauli repulsion

CN : −3.3 eV

Stabilized by Formation of CN Anions

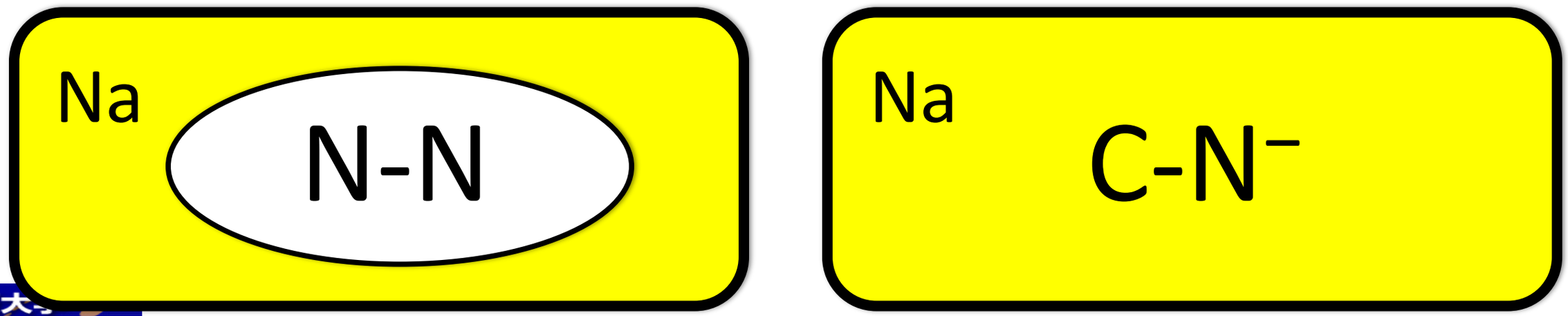

Summary

C additive in Na-flux

Form stable C-N

- C-N Bond Free Energy

In pure Na flux: 6.3 eV (Very strong)

Enhance N solubility ➔ Efficient N carrier

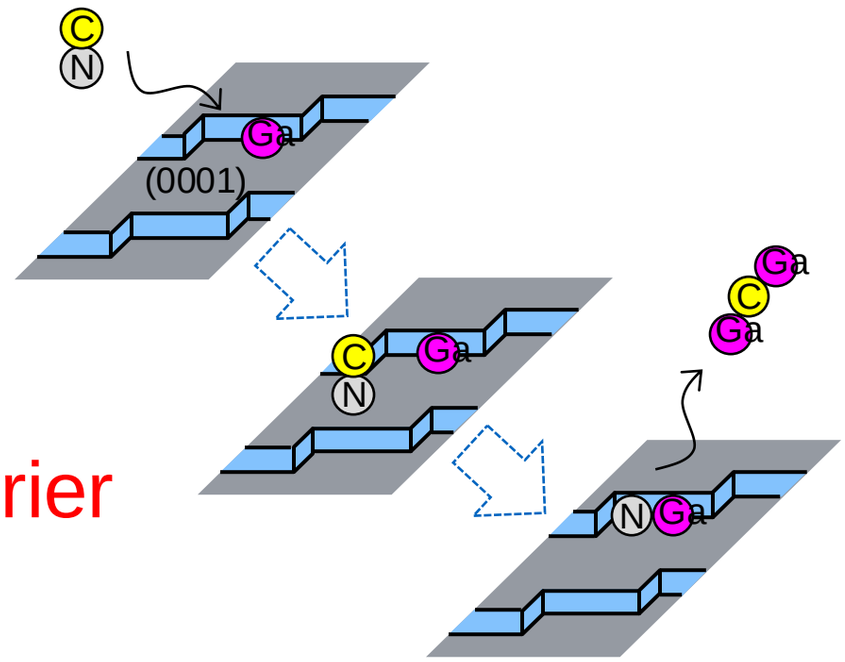

In Na-Ga flux: 3.0 eV (Still strong)

On Ga(001) w/o excess Ga: 2.8 eV (Still strong)

➔ Suppress poly-crystal formation

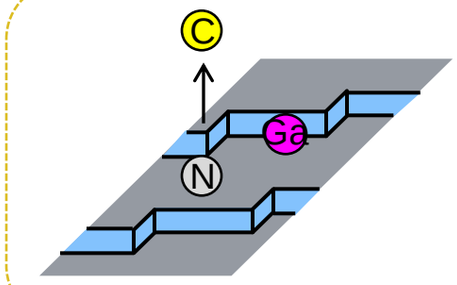

On Ga(001) with excess Ga: 1.3 eV (Easy to dissociate)

➔ Enhance GaN crystal growth

J. Appl. Phys., **101**, 066106 (2007).

J. Cryst. Growth, **303**, 34 (2007).

Jpn. J. Appl. Phys., **52**, 08JA04 (2013).

Physica status solidi, **252**, 1084 (2015).

Appl. Phys. Express., **9** 015601 (2016).

Acknowledgements

Discussions with experimental groups:

- **Univ. Tsukuba**
  J. Nakamura
  T. Kondo
  J. Quan
- **Univ. Tokyo, ISSP**
  J. Yoshinobu
  T. Koitaya
- **Mie Univ.**
  T. Kawamura
- **Osaka Univ.**
  Y. Mori
  M. Imade

Funding:

ACT-C
先導的物質変換領域

科研費
KAKENHI

ESICB

大阪大学